

**A KINETIC INSIGHT INTO TROPONIN T MUTATIONS RELATED  
TO DILATED AND HYPERTROPHIC CARDIOMYOPATHIES**

Thesis submitted for the degree of Doctor of Philosophy at the  
University of Leicester

by

Fatima Zimna Wazeer

BSc (Hons), University of Leicester

Department of Biochemistry

Faculty of Medicine and Biological Sciences

University of Leicester

August 2010

*To*

*Mom and Dad*

# Abstract

## A KINETIC INSIGHT INTO TROPONIN T MUTATIONS RELATED TO DILATED AND HYPERTROPHIC CARDIOMYOPATHIES

By Fatima Zimna Wazeer

Dilated and Hypertrophic Cardiomyopathy can be caused by mutations of genes encoding sarcomeric proteins. Mutations in cTnT are of particular interest since they are generally associated with mild or no ventricular hypertrophy but a high incidence of sudden death. Previous investigations have focused on steady state parameters such as maximal activation and inhibition of actomyosin ATPase and force and  $\text{Ca}^{2+}$  sensitivity. We have aimed to use transient kinetics to investigate the effects of 7 cTnT mutations on the dynamics of thin filament switching. We have studied two DCM mutations (R141W,  $\Delta$ K210) and five HCM ( $\Delta$ E160, S179F, K273E,  $\Delta$ 14,  $\Delta$ 28+7) mutations present in two functional domains of TnT (T1 and T2).

Overall circular dichroism studies showed that the structure of these mutant proteins is not grossly affected although minor changes in the  $\alpha$ -helical content were found for cTnT mutants K273E,  $\Delta$ 14,  $\Delta$ 28+7 and  $\Delta$ E160. Co-sedimentation with actin suggested that most of cTnT mutations do not interfere with the association between cTn and thin filament except for the truncated mutations.

Cooperativity along thin filament was changed for all deletion mutations ( $\Delta$ K210,  $\Delta$ E160,  $\Delta$ 14 and  $\Delta$ 28+7) but unchanged by the point mutations. In this study we also demonstrated that the equilibrium constant between the blocked and closed states ( $K_B$ ) for DCM mutations were unchanged but increased dramatically for HCM mutations suggesting loss of blocked state specifically for those in the T2 region.

We assessed  $\text{Ca}^{2+}$  binding of the regulatory site of cardiac TnC using IAANS attached to C35 and C84 of cTnC.  $\text{Ca}^{2+}$  binding affinity ( $\text{pCa}_{50} = 6.65$ ) of reconstituted Tn complex was unaffected by all mutations with the exception of  $\Delta$ 28+7 which caused a decrease ( $\text{pCa}_{50} 0.34$ ). In contrast when incorporated into thin filament, all HCM mutations and DCM  $\Delta$ K210 showed increased  $\text{Ca}^{2+}$  affinity. The observed rate constant of  $\text{Ca}^{2+}$  dissociation was unchanged for all mutations except for  $\Delta$ 28+7.

In conclusion, we have observed multiple structural and functional consequences from different TnT mutations that occur in different regions of the molecule. Overall the data suggests that it is the functional changes caused by mutations that are critical in developing the disease and not the specific location of the mutation.

# Acknowledgement

Breaking with tradition, I would like to thank first and very much foremost, my mom and dad, my bro and sis, Wazni and Hajara for all their support over the years. My dad in particular deserves most of the credit for his unfailing patience and continuous encouragement.

I would like to express my gratitude to the British Heart Foundation for funding this project.

For helping me directly in my attempts to complete my research, I wish to express my deepest gratitude to my supervisor, Dr.Mohammed El Mezgueldi for his expert guidance, trenchant critiques, valuable insights and expertise. I am also grateful for his helpful comments and critical reading of this thesis.

I would also like to express my profound appreciation to Prof.Clive Bagshaw and Dr.Mark Pfuhl for their helpful suggestions and discussions on the progress of my research.

The cDNAs encoding wild-type TnT, TnI and TnC were obtained as a gift from Dr. C. Redwood (University of Oxford, UK), Dr. N.Brand (Imperial college, UK) and Prof. K.Jacquet (Clinic of the Ruhr-University of Bochum, Germany). I am very grateful for their assistance with this.

I would like to extend my gratitude to Dr. Xiaowen Yang and Andrew Prescott at the Protein and Expression Laboratory (PROTEX) for carrying out my mutagenesis.

Special thanks to my colleagues and friends, Dr.Jaswir Basran, Dr.Sandip Badyal, Nina Bhanji, Dr.Harriet Seward, Sameeh Al-Sarayreh, for supporting, believing in me and making the lab an enjoyable place. I couldn't have got by without my close friends Suraiya and Sukraj. They have had to put up with three years of my stressing and obsessing over my PhD.

I would like to thank those that have helped me review my writings, for making neat sense of my wilder sentences and statements and made sure all the i's were dotted and the t's were crossed.

Finally, but in no means the least, I would like to thank Allah for his blessings and making this happen.

# Abbreviations

ADP	Adenosine diphosphate
AP	Atrial Pressure
ATP	Adenosine TriPhosphate
AV	Atrioventricular Valves
CD	Circular Dichroism
cTnC	cardiac Troponin C
cTnI	cardiac Troponin I
cTnT	cardiac Troponin T
DCM	Dilated Cardiomyopathy
DNA	Deoxyribonucleic Acid
DTT	Dithiothreitol
EDTA	Ethylene diamine tetra-acetic acid
EGTA	Ethylene glycol tetraacetic acid
F-actin	filamentous actin
fsTnI	fast skeletal Troponin I
G-actin	Globular actin
HCM	Hypertrophic Cardiomyopathy
IAANS	2-(4-(dimethylamino)styryl)-1-methylpyridinium
IPTG	IsoPropyl-beta-d-ThioGalactopyranoside
$K_B$	equilibrium between blocked and closed state
LAP	Left Atrial Pressure
LB	Luria-Bertani
L-type	long-lasting type
LV	Left Ventricle
LVP	Left Ventricular Pressure
MOPS	3-(n-Morpholino)Propanesulfonic Acid
$n$	size of the cooperative unit
$n_H$	Hills coefficient
NMR	Nuclear Magnetic Resonance
PCR	Polymerase Chain Reaction
$P_i$	inorganic phosphate

PIPES	Piperazine-1,4-Bis-2-Ethanesulfonic Acid
PKA	Protein Kinase A
PKC	Protein Kinase C
PMSF	Phenylmethanesulfonyl Fluoride
RyR	Ryanodine Receptors
S1	subfragment 1
SDS	Sodium Dodecyl Sulfate
SR	sarcoplasmic reticulum
ssTnl	slow skeletal troponin I
TAE	Tri Acetate EDTA
TCA	Tri chloroacetic acid
Tm	Tropomyosin
Tn	Troponin

## Units/Symbols

A	Absorption
Å	Angström ( $1\text{Å} = 1 \times 10^{-10} \text{ m}$ )
bp	base pairs
g	grams
h	hour
kb	kilobases
kDa	kilo daltons
l	litres
M	molar
min	minutes
mV	milliVolts
°C	degrees celcius
OD	optical density
rpm	revolutions per minute
s	seconds
v/v	volume to volume
w/v	weight per volume
$\epsilon$	Absorption coefficient
$\lambda$	wavelength

## Amino Acids

Amino Acids are abbreviated according to one and three-letter codes recommended by the I.U.P.A.C Joint Commission on Biochemical Nomenclature (1985).

Ala	A	Alanine
Arg	R	Arginine
Asn	N	Asparagine
Asp	D	Aspartic Acid
Cys	C	Cysteine
Gln	Q	Glutamine
Glu	E	Glutamic Acid
Gly	G	Glycine
His	H	Histidine
Ile	I	Isoleucine
Leu	L	Leucine
Lys	K	Lysine
Met	M	Methionine
Phe	F	Phenylalanine
Pro	P	Proline
Ser	S	Serine
Thr	T	Threonine
Trp	W	Tryptophan
Tyr	Y	Tyrosine
Val	V	Valine

# Table of Contents

<b>Abstract</b>	<b>iii</b>
<b>Acknowledgement</b>	<b>iv</b>
<b>Abbreviations</b>	<b>v</b>
<b>Table of Contents</b>	<b>viii</b>
<b>Chapter 1</b>	<b>1</b>
<hr/>	
<b>1.1 Human Heart- The Power of Life</b>	<b>3</b>
1.1.1 The Normal Heart	3
1.1.2 The Ventricular Cycle	4
1.1.3 Calcium Homeostasis	5
<b>1.2 The Diseased Heart – A Malfunctioning Pump</b>	<b>8</b>
<b>1.3 Classification of Inherited Heart Disease</b>	<b>10</b>
1.3.1 Hypertrophic Cardiomyopathy (HCM)	11
1.3.2 Dilated Cardiomyopathy	13
1.3.3 Pathophysiology of HCM and DCM	15
<b>1.4 Components of the Sarcomere</b>	<b>17</b>
1.4.1 Myosin Thick Filament	19
1.4.2 Actin Thin Filament	20
<b>1.5 Towards a Mechanism of Muscle Contraction</b>	<b>22</b>

<b>1.6</b>	<b>Regulatory Components of the Sarcomere</b>	<b>24</b>
1.6.1	Tropomyosin - The Link Between Actin and Troponin	24
1.6.2	The Tn Complex	26
<b>1.7</b>	<b>Regulation of Muscle Contraction</b>	<b>36</b>
1.7.1	Models of Regulation	36
1.7.2	Calcium Mediated Regulation of Myocardial Activities	38
<b>1.8</b>	<b>Troponin T Dysfunction</b>	<b>39</b>
1.8.1	Functional Studies	43
1.8.2	Transgenic Animal Models	45
<b>1.9</b>	<b>Programme of Research</b>	<b>49</b>

---

## **Chapter 2** **52**

<b>2.1</b>	<b>Buffers and Stock Solutions</b>	<b>54</b>
<b>2.1</b>	<b>Buffers and Stock Solutions</b>	<b>54</b>
<b>2.2</b>	<b>Preparation of Tissue Purified Proteins</b>	<b>54</b>
2.2.1	Preparation of Myosin Thick Filament	54
2.2.2	Preparation of Actin Thin Filament	56
2.2.3	Preparation of Regulatory Proteins of Thin Filament	58
<b>2.3</b>	<b>Preparation of Recombinant Proteins</b>	<b>60</b>
2.3.1	Preparation of Human Cardiac Troponin Subunits	60
2.3.2	Purification of Troponin Subunits	62
2.3.3	Formation of the Troponin Complex	63
<b>2.4</b>	<b>Fluorescent Protein Labeling</b>	<b>64</b>
2.4.1	Pyrene-labeled Actin Preparation	64
2.4.2	Pyrene-labelled Tropomyosin Preparation	65

2.4.3	Preparation and IAANS Labeling of Troponin C	65
<b>2.5</b>	<b>General Methods</b>	<b>66</b>
2.5.1	Plasmid Mini and Midi Preps	66
2.5.2	Transformation	66
2.5.3	Glycerol Stocks	67
2.5.4	Determination of Protein Concentration	67
2.5.5	Polyacrylamide Gel Electrophoresis	68
2.5.6	Agarose Gel Electrophoresis	68
2.5.7	Cosedimentation Assay	69
<b>2.6</b>	<b>Determination of Actomyosin Mg<sup>2+</sup>ATPase Activity</b>	<b>69</b>
2.6.1	Measurements of Acto-S1 ATPase	70
<b>2.7</b>	<b>Circular Dichroism</b>	<b>71</b>
<b>2.8</b>	<b>Enzyme Kinetics</b>	<b>72</b>
2.8.1	Transient State Kinetic Measurements	72
2.8.2	Equilibrium Kinetic Measurements	75
<b>Chapter 3</b>		<b>79</b>
<hr/>		
<b>3.1</b>	<b>Introduction</b>	<b>81</b>
<b>3.2</b>	<b>Results</b>	<b>84</b>
3.2.1	Cloning and Expression of TnT Mutations	84
3.2.2	Reconstitution of Troponin Complex	85
3.2.3	Acto-S1 ATPase Assays of TnT Mutations	87
3.2.4	Acto-S1 pCa Curves of TnT Mutations	90
3.2.5	Co-sedimentation of TnT Mutations with Thin Filament	93
3.2.6	Circular Dichroism of TnT Mutations	94
<b>3.3</b>	<b>Discussion</b>	<b>102</b>

3.3.1	Structural Effects of TnT Mutations	102
3.3.2	Functional Effects of TnT Mutations	103

## **Chapter 4** **106**

---

<b>4.1</b>	<b>Introduction</b>	<b>108</b>
<b>4.2</b>	<b>Results</b>	<b>111</b>
<b>4.2 (A)</b>	<b>Effect of TnT Mutations on the Size of the Cooperative Unit</b>	<b>111</b>
4.2.1	Characteristics of Pyrene Labelled Cardiac Tm	111
4.2.2	S1 Induced Switch between Closed and Open State of the Thin Filament	113
<b>4.2 (B)</b>	<b>Equilibrium Constant <math>K_B</math></b>	<b>127</b>
4.2.3	Comparison of Cardiac and Skeletal Muscle Thin Filaments	127
4.2.4	Effect of Troponin T Mutations on $K_B$ .	130
<b>4.3</b>	<b>Discussion</b>	<b>136</b>
4.3.1	Effect of Troponin T Mutations on the Size of the Cooperative Unit, $n$	137
4.3.2	Equilibrium Constant $K_B$	139

## **Chapter 5** **141**

---

<b>5.1</b>	<b>Introduction</b>	<b>143</b>
<b>5.2</b>	<b>Results</b>	<b>145</b>
<b>5.2 (A)</b>	<b>TnT Mutations on <math>Ca^{2+}</math> Binding Properties</b>	<b>145</b>
5.2.A.1	Fluorescence Properties of IAANS-Cys 35/84 Labelled TnC	145
5.2.A.2	Effect of cTnT Mutations on $Ca^{2+}$ Affinity of the Tn Complex	148
5.2.A.3	Effect of Mutations in cTnT on the $Ca^{2+}$ Affinity of Thin Filaments:	152
<b>5.2 (B)</b>	<b>Effect of TnT Mutations on the Kinetics of <math>Ca^{2+}</math> Dissociation</b>	<b>157</b>

5.2.B.1 Ca <sup>2+</sup> Dissociation Kinetics of cTnT Mutations using IAANS-Cys	35	157
5.2.B.2 Ca <sup>2+</sup> Dissociation Kinetics of cTnT Mutations using IAANS-Cys	84	169
5.2.B.3 Study of Ca <sup>2+</sup> Dissociation Kinetics of cTnT Mutations using Quin-2		180
<b>5.3 Discussion</b>		<b>191</b>

---

## **Chapter 6**

### **194**

---

<b>6.1 Summary of the Thesis</b>		<b>196</b>
6.1.1 Background		196
6.1.2. Main Findings in the Thesis		197
<b>6.2 Limitations of the Studies</b>		<b>206</b>
<b>6.3 Future Directions</b>		<b>207</b>

---

## **Appendices**

### **208**

---

<b>Appendix A</b>		<b>209</b>
<b>Appendix B</b>		<b>210</b>
<b>Appendix C</b>		<b>211</b>
<b>Appendix D</b>		<b>212</b>
<b>Appendix E</b>		<b>213</b>

---

## **References**

### **214**

---

# CHAPTER 1

Introduction

# Contents

1.1	Human Heart- The Power of Life	3
1.2	The Diseased Heart – A Malfunctioning Pump	8
1.3	Classification of Inherited Heart Disease	10
1.4	Components of the Sarcomere	17
1.5	Towards a Mechanism of Muscle Contraction	22
1.6	Regulatory Components of the Sarcomere	24
1.7	Regulation of Muscle Contraction	36
1.8	Troponin T Dysfunction	39
1.9	Programme of Research	49

# 1.1 Human Heart- The Power of Life

## 1.1.1 The Normal Heart

The normal heart is an exquisitely designed pump that works tirelessly from the moment the heart starts beating in utero. It is a roughly cone-shaped, hollow muscle comprised of four chambers: the right and left atria and the right and left ventricles. The two thin walled atria serve as contractile reservoirs for returning blood and the ventricles serve as pumps. The right ventricle pumps deoxygenated blood through the pulmonary artery to the lungs which returns oxygenated blood to the left atrium through the pulmonary veins which perfuse the pulmonary circulation. The left ventricle pumps out an equal volume of oxygenated blood to the rest of the body and deoxygenated blood returns through the venae cavae to the right atrium completing the systemic circulation.

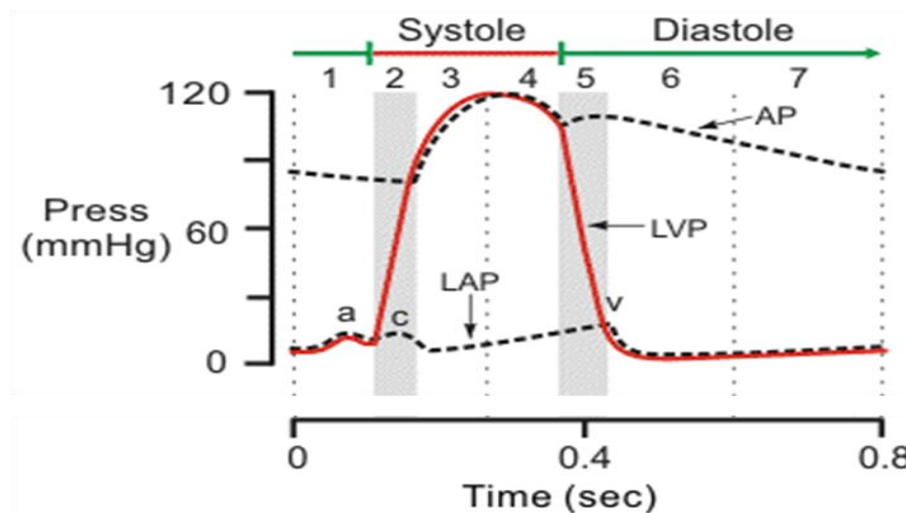


**Figure 1.1 Cardiac events occurring in a cardiac cycle**

*Pressure and volume changes in the ventricle: Phase (1) Atrial contraction (2) isovolumetric contraction (3) rapid ejection (4) reduced ejection (5) isovolumetric relaxation (6) rapid filling and (7) reduced filling. Press (mmHg)-pressure in millimeter mercury, AP-aortic pressure, LAP-left atrial pressure and LVP-left ventricular pressure (Klabunde 2005)*

### 1.1.2 The Ventricular Cycle

The cardiac cycle is divided into two phases: diastole and systole. Diastole refers to the period of time when the ventricles are undergoing relaxation and filling with blood from the atria. Systole, or ventricular contraction, is initiated by electrical depolarisation of the ventricles. The primary action of a cardiac myocyte is to contract and this is initiated by electrical changes within the cardiac cells. The relationship between electrical and mechanical events in the cardiac cycle is summarised in Figure 1.1. The atria and ventricles contract in sequence and is characterised by tracking changes in pressure and volume. The diagram has been divided into 7 phases where left ventricular pressure (LVP), left atrial pressure (LAP) and aortic pressure (AP) are plotted as a function of time.

Phase 1 begins with atrial contraction where the pressure within the atrial chambers increase forcing more blood to flow across the open atrioventricular (AV) valves leading to a rapid flow of blood into the ventricles. On completion of the contraction the AP begins to fall causing a pressure gradient reversal across the AV valves. At this point, the ventricular volumes are maximal. In Phase 2 the LVP rises to a value greater than the LAP closing the mitral and aortic valves. During this time period the ventricular volume does not change and the contraction is said to be isovolumetric. LVP slightly exceeds AP and the AV valve opens ejecting blood thus reducing the LV volume. During phase 3 the contraction process of the cardiac muscle reaches its maximum. Phase 4 is followed by slow ejection of blood ultimately relaxing the muscles. This results in a fall in LVP below AP and the AV closes. In the meantime, LAP gradually rises and the LV volume is at its minimum. The relaxation process continues as

indicated by the decline of LVP in Phase 5. The AV valves rapidly open up in and ventricular filling begins. The opening of the mitral valve in Phase 6 causes a rapid fall in LAP. In the final diastolic phase 7 the ventricles continue to fill with blood and expand causing the intraventricular pressures to rise.

The timings above refer to a human cycle of ~0.9 s duration and a heart rate of 67 beats per min. In normal resting hearts, the ventricle is about 90% filled by the end of this phase and has a cardiac output of 4-7 litres per minute.

### **1.1.3 Calcium Homeostasis**

In myocytes, calcium exerts diverse signalling events that include mediation of action potential shape by regulating calcium channels and cation exchangers, contraction of actomyosin myofilaments and apoptotic cell death to name a few (Bers 2008). A number of calcium regulated or dependent processes are interrelated and malfunction of one or the other signalling events leads to coordinated structural, mechanical and electrical cardiac dysfunctions. Most of the signalling is mediated through specific calcium-binding proteins, namely calmodulins and cardiac troponin C (cTnC). The graph below (Figure 1.2) exemplifies the shape of an action potential generated by the ventricular cardiomyocyte.

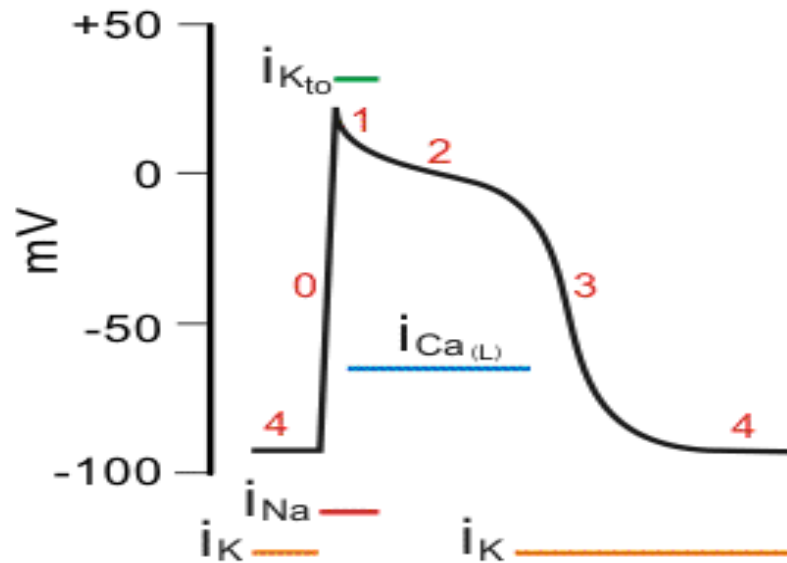


**Figure 1.2 Changes in action potential of the ventricular myocyte**

*The typical cardiac action potential has 5 phases: Phase (0) depolarisation, (1) partial repolarisation (2) plateau (3) repolarisation and (4) resting membrane potential. mV, units of membrane potential in milli volts,  $i_K$ -inwards potassium current,  $i_{Na}$ - inward sodium current,  $i_{Ca(L)}$ - L-type inward calcium current. (Klabunde 2005)*

Excitation-contraction coupling is a process in which electrical impulses are translated to mechanical activities in the muscle fibres. It begins with Phase 4, the period that the cell remains at rest until it is electrically stimulated. In mammalian heart, depolarization (Phase 0) results from a rapid inward pulse of  $Na^+$  ions to a positive potential of +20-30 mV. In response to this,  $K^+$  channels transiently open outwards causing early partial repolarisation (Phase 1). The myocyte then increases the cytoplasmic  $Ca^{2+}$  concentration by activating the L-type  $Ca^{2+}$  channels (also known as dihydropyridine receptors) present on sarcolemma membrane (Phase 2). This plateau lasts for 200-400 ms. The  $Ca^{2+}$  concentration is maintained by simultaneous expulsion of  $Ca^{2+}$  through  $Ca^{2+}$ -mediated activation of sarcoplasmic reticulum (SR)  $Ca^{2+}$  release channels or ryanodine receptors (RyR) by a process known as “calcium-induced calcium release”. SR is the calcium storehouse and upon RyR activation the  $Ca^{2+}$  starts

to release into the cytosol. During phase 3 of the action potential the L-type  $\text{Ca}^{2+}$  channels close, while the slow delayed rectifier  $\text{K}^+$  channels are still open. This ensures a net outward current, corresponding to negative change in membrane potential allowing more  $\text{K}^+$  dependent channels to open.

The cytoplasmic calcium builds up to a level sufficiently high to bind to the cTnC, and to activate the contractile activity of the myofilaments. The process of relaxation is accompanied by a reduction in cytoplasmic  $\text{Ca}^{2+}$  levels and dissociation of  $\text{Ca}^{2+}$  from cTnC. This is accomplished by two routes: (i) re-absorption of  $\text{Ca}^{2+}$  in SR by the  $\text{Ca}^{2+}$ -ATP-dependent pump facilitated by calcium-calmodulin-dependent protein kinase (CaMKII) which phosphorylates the phospholamban (ii) The release of  $\text{Ca}^{2+}$  from myocytes through RyR system for diastole that activates the expulsion of  $\text{Ca}^{2+}$  from sarcomeres through  $\text{Na}^+/\text{Ca}^{2+}$  exchangers. A minor fraction of  $\text{Ca}^{2+}$  is removed from cytosol using the sarcolemmal  $\text{Ca}^{2+}$  ATPase and mitochondrial transporters. It is therefore logical that an alteration in one or more of these proteins could have an effect on the  $\text{Ca}^{2+}$  handling of the myocyte. Many reports have been published on the changes in  $\text{Ca}^{2+}$  handling in failing myocytes (Hasenfuss, Mulieri et al. 1992).

## 1.2 The Diseased Heart – A Malfunctioning Pump

Any number of factors from viruses to birth defects can cause the heart to stop working efficiently. Figure 1.3 illustrates some of the events that are triggered by stress on the myocardium that may lead to cardiac dysfunction and failure. These include factors such as hypertension, myocardial infarction, ischemia and genetic diseases to name a few. In response to this stress, the heart undergoes morphological changes by a process called remodelling.

Remodelling can be described as physiological or pathological (Cohn, Ferrari et al. 2000) or alternatively adaptive or maladaptive (Dorn, Robbins et al. 2003).

Physiological remodelling is a compensatory change in the dimensions and function of the heart in response to physiological stimuli such as exercise and pregnancy. This type of remodelling is seen in athletes and has been referred to as "athlete's heart".

Pathologic remodelling has been described in three general patterns: as a consequence of i) pressure overload such as aortic stenosis and hypertension, ii) volume overload such as valvular regurgitation or iii) following cardiac injury such as myocardial infarction, myocarditis, or heart failure.

Initially, the heart instigates compensatory responses depending on the nature and severity of the inciting influence. In the above cases, it may transition from an apparently compensatory process to a maladaptive one (Opie, Commerford et al. 2006).

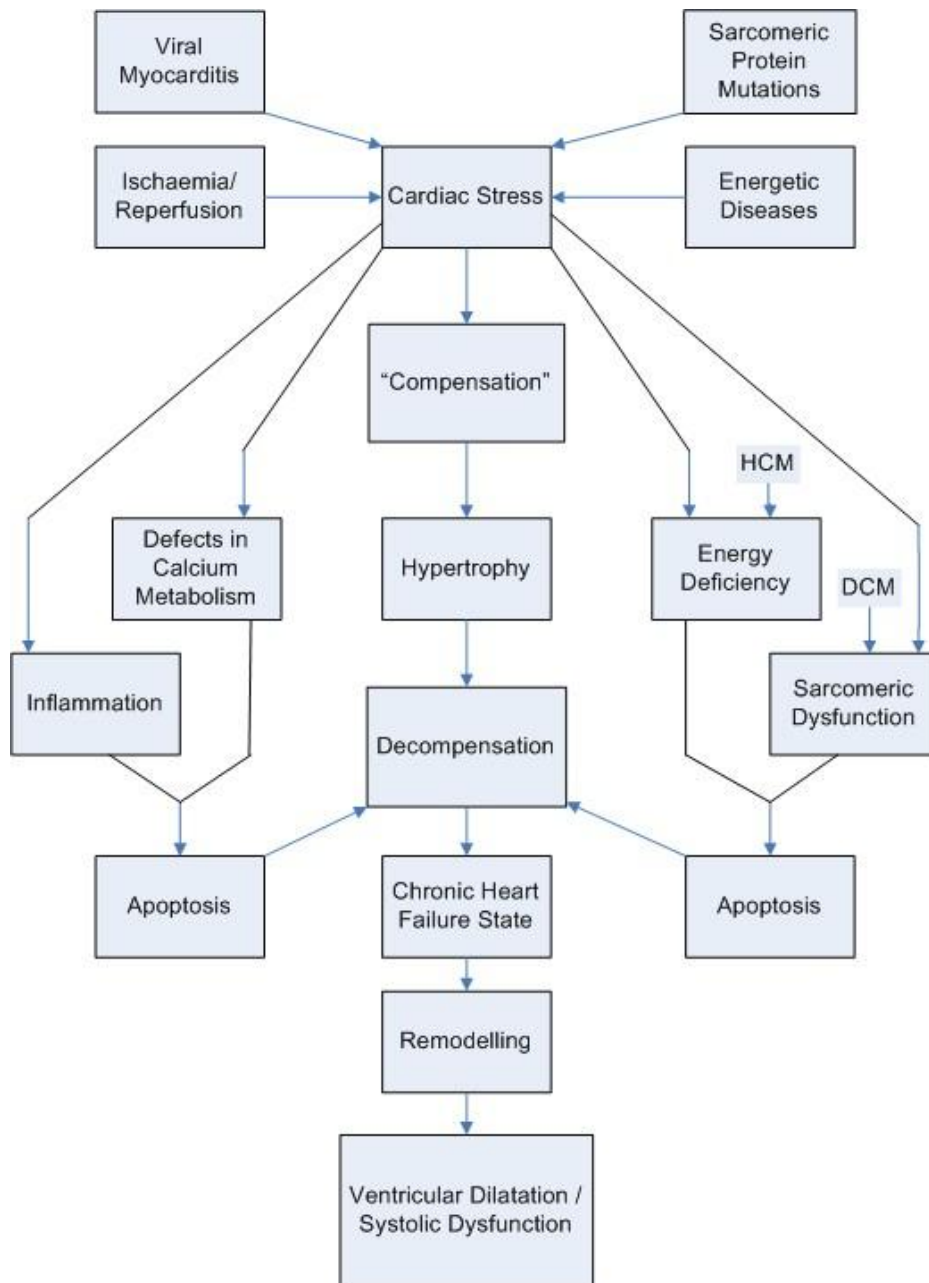


**Figure 1.3 Mechanism through which cardiac stresses incite cardiac dysfunction.**

*(An adaptation from Ashrafian and Watkins 2007)*

In this thesis we are interested in studying genetically related effects. Hypertrophy, failure and sudden death are known to begin with a primary defect in sarcomeric proteins. Linkage of mutations in genes controlling expression of sarcomeric proteins to cardiomyopathy supports this idea (Mogensen et al. 2003; Gomes and Potter 2004).

### 1.3 Classification of Inherited Heart Disease

Genetic cardiomyopathies are a complex, pathophysiological condition associated with myocardial dysfunction often leading to cardiovascular morbidity and mortality. They have been classified by the observations of morphologic-clinical studies into three main types: dilated, hypertrophic, or restrictive (Richardson, McKenna et al. 1996). The two most common forms of cardiomyopathies are dilated and hypertrophic cardiomyopathies (Figure 1.4). Recent genetic insights have reclassified them providing a more refined taxonomy which coupled with functional studies have identified novel potential therapeutic targets such as cardiac energetics, calcium handling and apoptosis (Ashrafian and Watkins 2007).

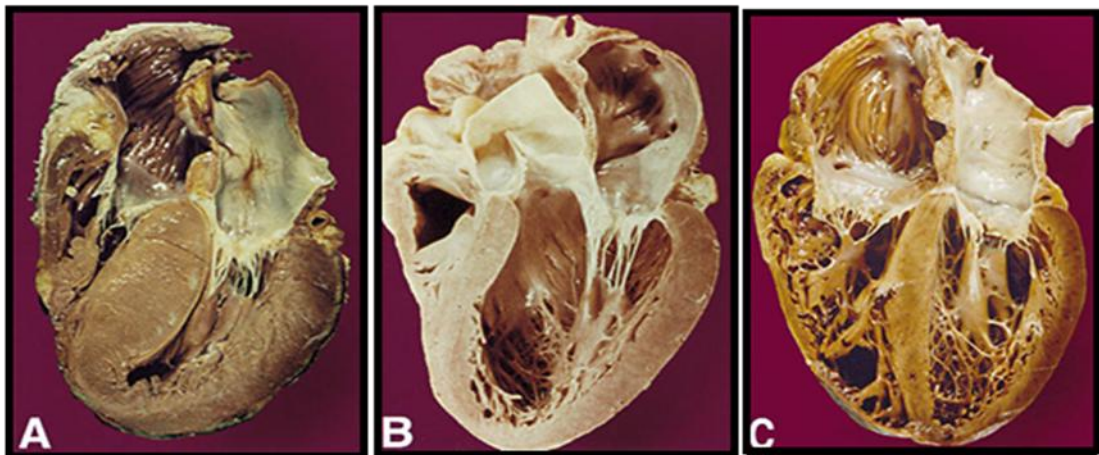


**Figure 1.4 Histopathology of normal left ventricular wall thickness and chamber volume**

*(B) the healthy heart in comparison to (A) HCM and (C) DCM (Seidman and Seidman 2001)*

### **1.3.1 Hypertrophic Cardiomyopathy (HCM)**

#### **A Disease of the Sarcomere and Energy Deficiency**

HCM is defined by the presence of unexplained ventricular hypertrophy and impaired diastolic function with a prevalence of one in five hundred (Teare 1958; Maron, Roberts et al. 1980; Bonne, Carrier et al. 1998). Typically the left ventricle volume is normal or reduced. Systolic function is variable with hyperdynamic, normal or impaired indices of contractile performance. Some patients showed left ventricular outflow obstruction in late systole whilst other findings included a fourth heart sound and abnormal electrocardiogram.

#### **Clinical Presentation**

The disease is clinically variable, ranging from benign to severe and is the commonest cause of sudden death in young individuals. The presenting symptoms among individuals with HCM include shortness of breath (dyspnea), angina, presyncope and/or syncope (McKenna and Camm 1989; Vikstrom and Leinwand 1996; Franz, Muller et al. 2001).

#### **Etiology**

Most cases of HCM exhibit an autosomal pattern of inheritance representative of genetic and allelic heterogeneity, with as many as 10 sarcomeric genes and over 400 predominantly missense mutations leading to the proposition that HCM is a 'disease of the sarcomere'. To date, a number of genetic loci have been identified as being causative agents of HCM (Table 1.1). The sarcomeric proteins affected include: i) thick filament proteins,  $\beta$ -myosin heavy chain (Geisterfer-Lowrance, Kass et al. 1990) and cardiac regulatory and essential myosin light chains (Poetter, Jiang et al. 1996), ii) thin filament proteins, cardiac

actin (Mogensen, Klausen et al. 1999),  $\alpha$ -tropomyosin (Thierfelder, Watkins et al. 1994; Watkins, McKenna et al. 1995), troponin T (Thierfelder, Watkins et al. 1994; Nakajima-Taniguchi, Matsui et al. 1995; Watkins, McKenna et al. 1995; Moolman, Corfield et al. 1997; Ho, Lever et al. 2000), TnI (Kimura, Harada et al. 1997) and TnC iii) myosin binding protein C (Bonne, Carrier et al. 1995) (Watkins, Conner et al. 1995) and titin (Sato, Takahashi et al. 1999). Each of these proteins is encoded by multigene families that show tissue specific, developmental and physiologically regulated patterns of expression.

### **Pathophysiological Mechanisms**

Despite over a decade of research, the stimulus for hypertrophy has not been definitively identified. Some dominant gene mutations could inactivate a single allele resulting in reduced functionality (haplo insufficiency) while others create a mutant protein that interferes with normal protein function and act as poison peptide (dominant negative). This poison peptide hypothesis is supported by a variety of results obtained by in vitro studies (Sweeney et al. 1994).

Watkins proposed that a stimulus for hypertrophy is an energetic compromise with  $Ca^{2+}$  constituting a sensor for cellular energy balance. This is supported by alterations in myocardial metabolism seen in patients with HCM suggesting that it may occur as a primary effect of mutant proteins.

Various studies have been carried out where patients have been diagnosed to have an increased carbohydrate utilisation and reduced phosphocreatine/ATP level leading to an increased energy demand (Cirilley et al. 2003). Most HCM mutations increase  $Ca^{2+}$  sensitivity, which would be expected to produce

hypercontractile phenotype, with increasing use of ATP (Montgomery et al. 2001).

The insight that HCM arises from perturbations of the sarcomere provided unheralded opportunities to explore its pathogenesis. The findings led to the suggestion that mutated, poorly functioning proteins may impair myocyte function triggering adaptive mechanisms resulting in a compensatory mechanism. However this hypothesis requires further consideration as some studies produced divergent results: reduced maximum force generation or enhanced contractility (Redwood et al. 1999). Enhanced contractility according to clinical studies is not in agreement with the “compensatory hypertrophy hypothesis” and was refuted. These studies underscore the importance of validating all findings with genetic, biochemical and clinical studies.

### **1.3.2 Dilated Cardiomyopathy**

#### **End Result of Diverse Pathways**

Dilated cardiomyopathy is a syndrome characterised by left ventricular dilation and systolic dysfunction leading to heart failure (Richardson, McKenna et al. 1996; Towbin and Bowles 2002). The prevalence of DCM was estimated to be 36.5 cases of 100,000. The failing heart triggers neurohormonal responses in order to maintain the cardiac output through increased circulatory volume. Only 50% of DCM patients survive more than 5 years since first been diagnosed. DCM is associated with many acquired characteristics like myocardial ischemia, inflammation, infection, pregnancy, alcohol, autoimmune disorder with 20-35% cases linked to familial DCM (Michels, Moll et al. 1992; Keeling, Gang et al. 1995; Grunig, Tasman et al. 1998; Mestroni, Rocco et al. 1999)

## **Clinical Representation**

DCM is diverse; making the assessment of individuals at risk of sudden death difficult. This includes common symptoms such as shortness of breath, fatigue, inability to tolerate physical exertion, faint, light headedness and sweating at rest.

## **Etiology**

Over the past decade, progress has been made in understanding the genetic aetiology of DCM. 20-35% of cases account for the familial form of the disease and autosomal dominance being the predominant pattern of transmission. No specific genotype-phenotype correlation is evident for familial DCM in part due to the nature of the genes identified and the relatively small number of mutations in any one gene. They carry poor prognostic information. Less frequently affected individuals present with involvement of other organ systems such as DCM with conduction system disease, skeletal myopathy and abnormal mitochondrial function (Ichida, Tsubata et al. 2001; Chen, Tsuji et al. 2002; Suomalainen, Paetau et al. 1992). The genetic loci for pure DCM identified are listed in Table 1.1. Mutations have been listed in gene loci encoding sarcomeric proteins : (i)  $\beta$ -myosin heavy chain (Kamisago, Sharma et al. 2000) (ii) thin filament proteins, cardiac actin (Olson, Michels et al. 1998),  $\alpha$ -Tm (Olson, Kishimoto et al. 2001), cTnT (Kamisago, Sharma et al. 2000; Li, Czernuszewicz et al. 2001; Mogensen, Murphy et al. 2004), cTnI and cTnC (Mogensen, Murphy et al. 2004) (iii) cardiac myosin binding protein C (Shimizu, Ino et al. 2005) and titin (Gerull, Gramlich et al. 2002).

## **Pathophysiological Mechanisms**

One of the proposed mechanisms of DCM causing mutations impairing cardiac function and resulting in increased chamber volume and dilation is called the 'defective force transmission' hypothesis (Kamisago, Sharma et al. 2000). This is based on the fact that the cytoskeleton provides intracellular scaffolding that is important for transmission of force from the sarcomere to the extracellular matrix and for the protection of myocyte from extrinsic mechanical stress. Defects in these cytoskeletal proteins are believed to cause DCM by reducing force transmission and/or resistance to mechanical stress. Identification of mutations in genes encoding cytoskeletal proteins cardiac actin, desmin and dystrophin has provided supportive evidence for this hypothesis (Franz, Muller et al. 2000). Significant quantitative differences in various aspects of the disease such as the risk of sudden death, length of survival, severity of hypertrophy have been identified. Several factors could account for the large variability of the phenotypic expression of the mutations such as the degree of functional impairment caused in the sarcomere (varied positional mutations and the type of protein involved) the role of environmental factors and acquired traits (differences in lifestyle, risk factors and exercise regime) and the existence of modifier genes and or polymorphism that could modulate the phenotypic expression of the disease.

### **1.3.3 Pathophysiology of HCM and DCM**

Mutations that cause HCM and DCM fall into 3 classes: i) missense mutations (one amino acid is replaced by another), ii) In-frame deletion mutations (deletion of one specific amino acid), iii) splice-donor-site mutations (removes the carboxyl terminal amino acids and forms a truncated mutant).

**Table 1.1 Disease genes in HCM and DCM phenotypes**

Chromosomal Loci	Gene	Protein	No. of Mutations	
			<i>HCM</i>	<i>DCM</i>
14q12	MYH7	$\beta$ -myosin heavy chain	196	13
11p11	MYBPC3	Myosin binding protein C	164	3
1q32	TNNT2	Troponin T	34	13
19q13	TNN13	Troponin I	29	1
3p21-p14	TNNC1	Troponin C	5	2
15q22	TPM1	$\alpha$ -tropomyosin	11	2
15q14	ACTC	$\alpha$ -cardiac actin	7	2
12q23-q24	MYL2	Regulatory myosin light chain	10	-
3p21	MYL3	Essential myosin light chain	5	-

See <http://www.hgmd.cf.ac.uk/ac/search.php>

This raises the question of the mechanism by which these seemingly minor changes result in disease pathogenesis. Increased calcium sensitivity means enhanced systolic contraction and delayed diastolic relaxation whereas a decrease in calcium sensitivity depresses systolic contraction which supports the importance of the change in calcium sensitivity of contraction in these two forms of cardiomyopathy leading to pathogenesis. Histological appearance of the HCM heart (myofibre disarray) is absent in DCM. In vitro the HCM and DCM

mutants behave antagonistically, e.g. DCM mutations depress myofibrillar function whereas HCM mutations enhance it.

The detailed mechanism by which these functional consequences of various mutations of the sarcomere converge into HCM and DCM are still unclear. Mutations in the same sarcomeric genes may lead to either DCM or HCM notwithstanding about 5% of HCM patients display DCM-like characteristics.

The finding that both HCM and DCM can be caused by sarcomere protein mutations has raised the question of whether these different morphologies reflect gradation of a single pathway. The extent of cardiac remodelling is dependent on the severity of the dysfunction; mild deficits could result in hypertrophy while more severe dysfunction might trigger myocyte death and eventually result in cardiac dilation. Transgenic mice model studies support a single progressive programme. Mice heterozygous for sarcomere mutations develop HCM (Geisterfer-Lowrance, Christe et al. 1996) whereas homozygous mice develop DCM (Fatkin, Christe et al. 1999; McConnell, Jones et al. 1999). However, clinical studies in humans are not consistently supportive of either a single or dual pathway model.

## **1.4 Components of the Sarcomere**

The cellular units of cardiac muscle fibres, myocytes (10-20  $\mu\text{m}$  diameters and 50-100  $\mu\text{m}$  length) are connected end-to-end in series by a network of interdigitating cell membrane called intercalated discs, comprising two units, the desmosomes and gap junctions. These intervening structures not only hold the fibres together, they also allow the action potential to run over the entire length of connecting fibres. Myocytes surrounded by cell membrane, sarcolemma,

possess, besides the usual cell inclusions, compact bundles of longitudinally arranged myofibrils. Each myofibril is composed of small repeated units called sarcomeres that are joined from the ends and are poised between two adjacent Z-lines. The myofilaments comprise approximately 45-60% of net cardiomyocyte's volume. The sarcomere gives striated appearance, and is composed of the muscle contractile structures categorized into thick and thin filament (Figure 1.5). The core of the thick filament is composed of the tails of myosin and other components including C-protein and titin. The myosin heads (S1) project out from the backbone at regular intervals and interact with actin in the thin filament. Thin filament consists of actin, tropomyosin and troponin twisted in a double string of pearls.

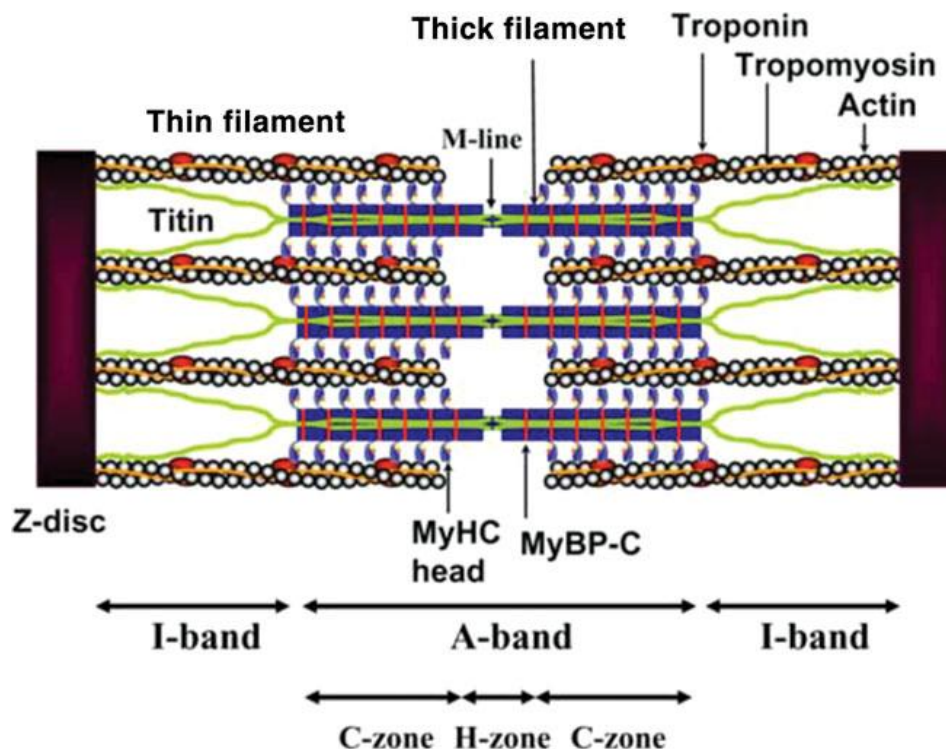


**Figure 1.5 Components of the sarcomere in the central region of the muscle.**

*(Morimoto 2008)*

### 1.4.1 Myosin Thick Filament

Myosins are motor proteins that interact with actin thin filament and hydrolyse ATP to generate movement. The myosin superfamily consists of more than 35 classes with diverse cellular activities (Foth, Goedecke et al. 2006). Myosin II (herein after referred to as myosin) is the most common class present in muscle tissue.

Myosin is a hexamer that consists of two heavy chains (220 kDa) and four light chains (~ 20 kDa each) paired into two regulatory light chains and two essential light chains. The heavy chain consists of three proteolitically defined domains (Weeds and Taylor 1975): subfragment 1 (S1) subfragment 2 (S2) and light meromyosin (LMM) of approximately 20, 50 and 100 nm in length. The globular head (S1) forms the actin binding site and the ATPase site and can be further divided into 3 subdomains: the N-terminal 25 kDa nucleotide binding domain, the central 50 kDa actin binding domain and the C-terminal 20 kDa actin binding domain (Figure 1.6). The crystal structure of the myosin head (Rayment et al. 1993) show the relative positions of the actin binding site, the ATP binding and hydrolysis pocket and a long helix stabilised by the binding of the light chains. It is thought that the position of this region changes during the contractile cycle (see section 1.5 below)

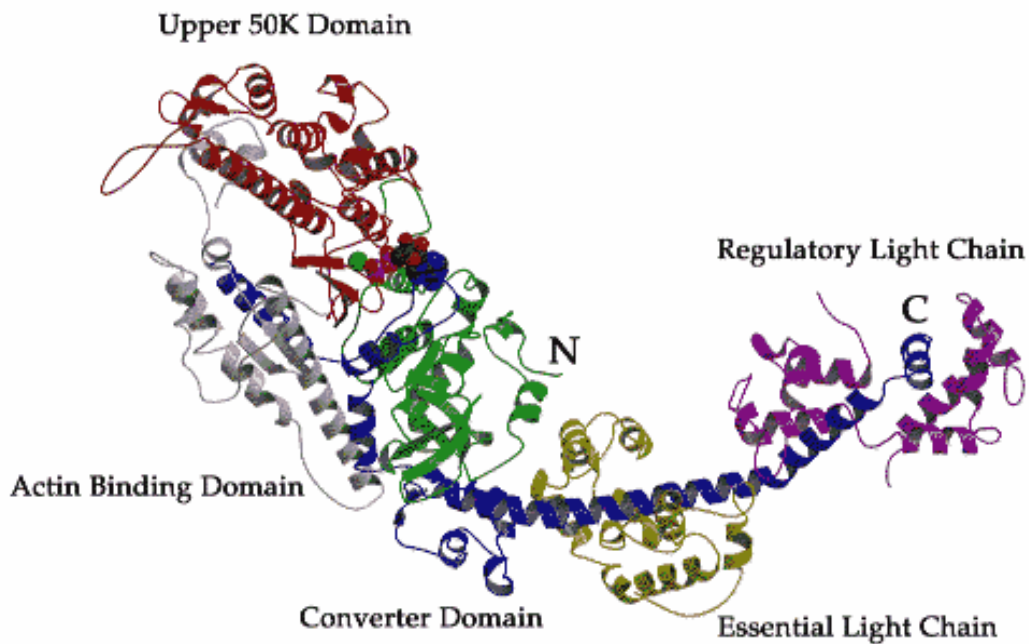


### Figure 1.6 Structure of myosin S1

*Ribbon diagram of the motor domain consisting of seven-stranded  $\beta$ -sheet and a C-terminal tail which carries the regulatory light chains (magenta) and the essential light chain (yellow). The 3 S1 proteolytic domains are: 25 kDa N-terminal (green), 20 kDa C-terminal (blue) and the 50 kDa fragments which span two domains: S1 head region showing the ATP binding site (red) and actin binding site (grey). (Rayment, Rypniewski et al. 1993)*

## 1.4.2 Actin Thin Filament

Actin is a scaffolding protein made up of 375 amino acids and is the most conserved of all proteins with only 5% divergence in different species (Pollard 1990). Much of the structural information available on actin myofilaments was obtained from X-ray crystallographic analysis, which shows the presence of four sub-domains per actin molecule (Figure 1.7). These sub-domains in the native states are separated by a cleft that contains either  $Mg^{2+}$  or  $Ca^{2+}$  and the bound ADP, thus providing a linker for stable association of the sub-domains (Kabsch, Mannherz et al. 1990). The crystal structure further indicates that the exterior

sub-domains 1 and 2 that interact with myosin constitute the surrounding structure of the filaments. The positions of sub-domains 3 and 4 are more centralized, projecting towards the helical axis, where they associate with identical sub-domains of adjacent actin monomers. The sub-domain 1 contains both the N-terminal and C-terminal ends of actin monomers and are more solvent exposed (Holmes, Popp et al. 1990). Because of its tendency to form filaments, actin has often been crystallised in the presence of other proteins and therefore it is still difficult to determine the intrinsic structural differences between actin isoforms.

In the presence of physiological salt concentrations it can spontaneously self assemble from its monomeric globular form (G-actin) prevailing at low salt concentrations, to a filamentous macromolecule of fibrous actin (F-actin).

F-actin is a twisted rope made up of G-actin monomer strands with a half pitch cross over every 35.5 nm, a thickness of 10 nm and average length of 1  $\mu\text{m}$ . In cardiac muscles, F-actin is always associated with accessory proteins, Tm and Tn.

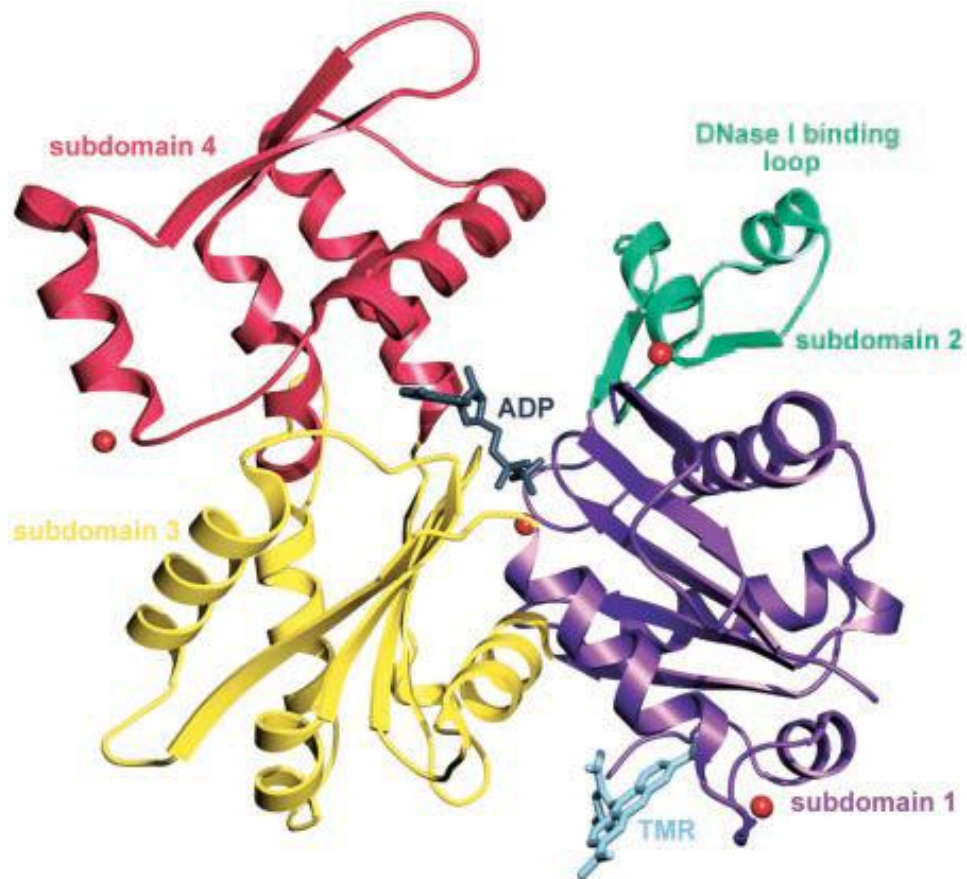


**Figure 1.7 Structure of Actin monomer**

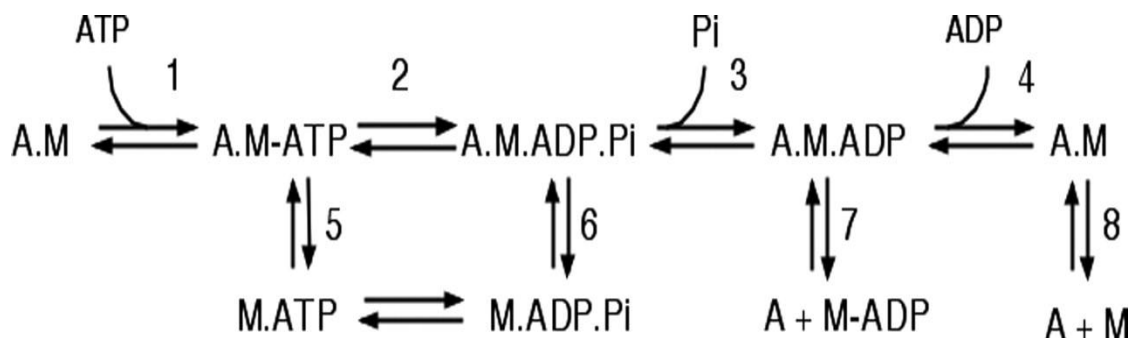
*Ribbon diagram of the actin monomer structure subdomains: 1, 2, 3 and 4 and divalent ions and nucleotide binding sites. The DNase loop is located towards the upper part of subdomain 2. ADP is bound in the centre of the molecule. 4 Ca<sup>2+</sup> ions bound to the actin monomer in crystals are represented as red spheres. (Otterbein, Graceffa et al. 2001)*

## 1.5 Towards a Mechanism of Muscle Contraction

Over the past half century several extensive investigations of the mechanism of muscle contraction led to the postulation of several theories to explain the molecular basis of muscle contraction. In the 1950's the popular sliding filament theory explained how sliding of actin filaments between myosin filaments can produce movement (Huxley 1958). In the 1970's this molecular mechanism of contraction was developed to have a role in hydrolysis of ATP by myosin alternating conformational changes in complementary actin sites relating to the

sliding of filaments (Taylor and Lymn 1972). Spudich and co-workers in the 1990's suggested that the conformational change in the cross bridge involves a swing of the myosin heads known as the "lever arm mechanism" (Spudich 1994).

The ATPase reaction mechanism that powers this swinging lever involves the reaction sequence shown in Scheme 1.1. This mechanism first involves rapid ATP binding to actomyosin (Step 1) followed by rapid dissociation to actin and myosin.ATP (Step 5). The ATP is then hydrolysed to ADP and  $P_i$ . ATP hydrolysis can also take place while actin is still bound to myosin (Step 2) (Sleep and Hutton 1978). The cleaved myosin.ADP. $P_i$  then rebinds to actin (Step 6) and this dynamic complex undergoes a slow transition to a stable high affinity actin-myosin complex by releasing  $P_i$  (the rate limiting step 3) at a rate of 75 and 20  $s^{-1}$  respectively for skeletal and cardiac muscles. The bound ADP then dissociates, leaving the actin.myosin complex (Step 4) at a much quicker pace, the maximum being  $\sim 400 s^{-1}$  for skeletal and  $100 s^{-1}$  for cardiac muscles. The cycle is repeated upon new ATP binding (El Mezgueldi and Bagshaw 2008).



**Scheme 1.1 ATP hydrolysis and the cross bridge cycle.**

*(1)ATP binding to actin bound myosin (2) ATP hydrolysis of actin bound myosin (3)  $P_i$  released (4) ADP released (5) Myosin ATP dissociates from actin (6) Myosin.ADP. $P_i$  binds actin (7) Actin dissociation from myosin.ADP (8) actomyosin dissociation*

## 1.6 Regulatory Components of the Sarcomere

### 1.6.1 Tropomyosin - The Link Between Actin and Troponin

Tropomyosin is a right-handed helical protein which forms a coiled dimer that cooperatively binds head to tail to actin thin filament. Each Tm chain is composed of 284 amino acids, and a tight hydrophobic interaction between two chains holds them together

The 7Å crystal structure of Tm revealed the periodicities in non-interface positions postulated to be seven quasi-equivalent actin binding sites along the length of one Tm that corresponds to the seven half turns of the supercoil (Whitby and Phillips 2000). Recently, 2.1 Å resolution crystal structure of Tm C- and N-terminal overhangs was examined (Murakami, Stewart et al. 2008). The model peptide structures at N and C termini (Figure 1.8) suggest that in solutions the chains are wound around, but upon crystallization the chains separate from each other into a slightly distorted form (Whitby and Phillips 2000; Li, Mui et al. 2002). Although isoform diversity with respect to the tissue of origin and functions exists, most of the Tm exhibit remarkable conserved phylogeny (Gunning, Schevzov et al. 2005). In human muscle at least two genes code for two variants of tropomyosin,  $\alpha$  and  $\beta$ . In fast skeletal muscles mixed  $\alpha$ -,  $\beta$ -chains, and in cardiac muscles only  $\alpha$ -,  $\alpha$ - chains are present (Tobacman 1996; Purcell, Bing et al. 1999).



**Figure 1.8 Model of Tm based on the 7A crystal structure**

*PDB entry 1C1G (Whitby and Phillips 2000)*

The Tm component of the thin filament is important for various interactions, like with actin filament by physically stiffening the filament as well as by inhibiting the activity of proteins that destabilise actin (Bharadwaj, Hitchcock-DeGregori et al. 2004). The other crucial function of Tm is in its role in regulation and its responsibility for the cooperative activation of the striated muscle thin filament by  $\text{Ca}^{2+}$  and myosin.

It has been shown in reconstituted skinned muscle fibres that once Tn is present, the affinity of Tm with actin is enhanced by about 80-130 fold (Hill, Mehegan et al. 1992). The possible binding sites of Tm with TnT subunit of Tn complex is distributed between two regions located at the N and C termini of Tm, which coincides with the head-to-tail overlapping regions. Tm supposedly

interacts with TnT at its N-terminus- a  $\text{Ca}^{2+}$  independent interaction while the interaction at the C-terminus region of TnT is  $\text{Ca}^{2+}$  dependent in nature. Tm also interacts with TnI and TnC (Potter, Sheng et al. 1995; Malnic, Farah et al. 1998).

A schematic representation of Tn-Tm-actin complex is shown Figure 1.9. As indicated, the presence of high  $\text{Ca}^{2+}$  perturbs the interaction between Tm and TnT at residues 159-259, whereas it strengthens the binding with TnT-TnC (Pearlstone and Smillie 1983). Conversely, when  $\text{Ca}^{2+}$  concentration falls, the interaction is reversed.

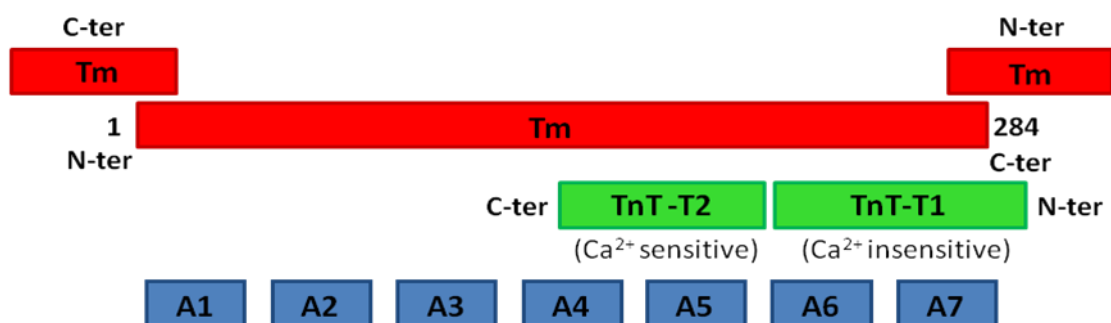


**Figure 1.9 Tm.TnT.Actin complex with their structural domains**

*The red block corresponds to Tm filament with the N and C termini interactions of neighbouring Tm molecules. The green bars represent Tm interactions with TnT and the grey blocks are actin monomers. N ter- N terminal, C-ter- C terminal, A(1-7)-Actin monomers (1-7).*

## 1.6.2 The Tn Complex

### 1.6.2.(A) Structure of the Tn Complex

For over 40 years Tn has been discovered to be the calcium regulated protein complex with unique regulatory properties in muscle contraction. It is a heterotrimeric-protein complex constituted by three interacting subunits, namely TnC (~18.3 kDa), TnI (~23.5 kDa) and TnT (~38 kDa). However, understanding the

mechanism of muscle contraction has been significantly slowed down because of insufficient structural information for Tn. After repeated trials, a high resolution crystal structure for human cardiac Tn was obtained under  $\text{Ca}^{2+}$  saturated conditions, which corresponds to the contractile state (systole) of the myofilaments (Takeda, Yamashita et al. 2003).

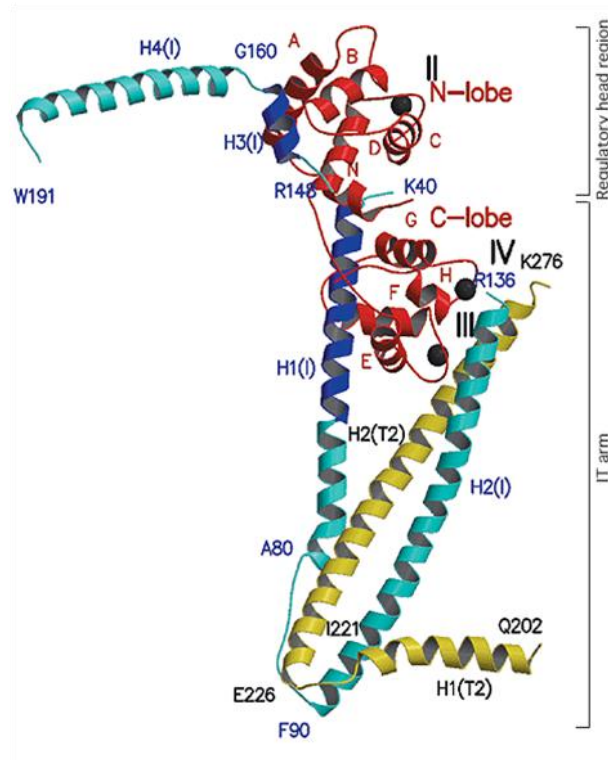


**Figure 1.10 Ribbon model of the crystal structure of cTn core domain**

*TnC (red); TnI (blue and cyan); TnT (yellow). Filled circles designate the three sites (II-IV) in the helix-loop-helix arrangement of TnC to which three  $\text{Ca}^{2+}$  cations bind to. Each helix within TnI and TnT is indicated by the helix number, whereas each helix of TnC is indicated by a capital letter (N, A-H) (Takeda et al 2003).*

The defining contribution in the Tn field has been the X-ray crystal structure of Tn core shown in Figure 1.10. This structure revealed that cardiac Tn is a highly flexible molecule dominated by  $\alpha$ -helices. The core domain can be divided into two sub-domains, the regulatory head (cTnC residues 3-84 and 150-159 of cTnI) and the IT region (cTnC residues 93-161, cTnI 42-136 and cTnT 203-271).

## **Regulatory Head**

The N-terminus of TnC and the C-terminal of TnI (switch region) are arranged in an anti-parallel orientation. The oppositely tuned interaction of TnI and TnC towards regulatory head involves the two EF hands (helix-loop-helix) of B and C helices of Ca<sup>2+</sup>-bound TnC in “open” conformation and the “switch region” of TnI (residues 116-131; helix H3). Ahead of this, the 150-159 residues of TnI also interact with the Ca<sup>2+</sup>-bound “open” hydrophobic patch of the N terminus of TnC. The inhibitory segment of TnI (residues 104-115) exists in an ordered loop that also interacts with TnC. TnI at the C-terminus protrudes as another  $\alpha$ -helix (residues 166-188; helix H4) and apparently in the crystalline state does not directly associate with the rest of the Tn complex although it contributes immensely towards inter-domain interactions and Ca<sup>2+</sup> sensitivity.

## **IT Arm**

In this region three parallel helical domains of TnI and TnT wind around each other and hold the C-terminus domain of TnC. These helices are the N-terminal helix of TnI (residues 8-48; H2, the TnI residues 90-135; H1, and TnT residues 226-271; H2(T2). TnT residues 203-220 upstream from the coiled coil form the  $\alpha$ -helix, represented as H1(T2). While one end of the H2(T2) helix make coiled-coil which interacts with TnI (H1), the other end of H2(T2) associates with the C-terminus EF hands (helix-loop-helix) of E and F helices of Ca<sup>2+</sup>-bound TnC.

The Tn complex displays unique signature amino acid sequences that constitute hydrophobic, acidic, and basic and Ca<sup>2+</sup> binding domains, dynamism in inter- and intra-domain interactions, and post-translational modifications like phosphorylation.

### 1.6.2.(B) Function of the Tn Subunits

Figure 1.11 is a cartoon representation of the conformational changes that occur during muscle contraction (Li, Wang et al. 2004). Recent work by Vinogradova's group revealed a noncompact structure using chicken skeletal muscle Tn complex that looked like two chopsticks holding a dumbbell. (Vinogradova, Stone et al. 2005).

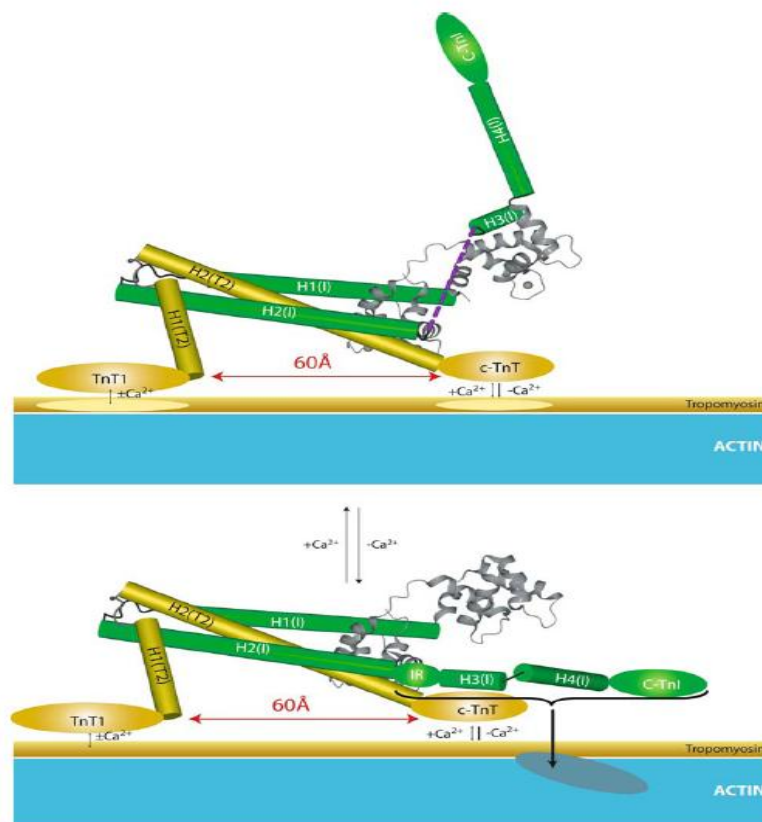


**Figure 1.11 Cartoon representation of the thin filament regulation**

*Top at high  $[Ca^{2+}]$  and Bottom at low  $[Ca^{2+}]$ . The ribbon representation is TnC and the grey sphere is the bound  $Ca^{2+}$ . (Blue bar) is actin, (gold bar) Tm, (green) TnI and (gold) TnT (Li, Wang et al. 2004)*

## **Troponin C: The Ca<sup>2+</sup> Sensor**

In sarcoplasm, TnC is one of the prominent Ca<sup>2+</sup>-binding proteins. Two relatively similar isoforms of TnC are expressed in vertebrate genome: the slow skeletal/cardiac muscle TnC (cTnC) and fast skeletal muscle TnC (sTnC), which exhibit low and high Ca<sup>2+</sup> affinities, respectively, due to alterations in calcium binding pockets. The structure of sTnC, as determined by X-ray crystallography (Herzberg and James 1988; Houdusse, Love et al. 1997) and NMR spectroscopy (Slupsky and Sykes 1995) reveals it to be 76 Å long and dumb bell shaped protein. The protein is considered to be highly acidic owing to the presence of a high number of glutamate and aspartate residues (Zot, Potter et al. 1987). Although cTnC and sTnC possess 161 and 160 amino acid residues respectively, about 54 residues are different, and this accounts for only 65% similarity between them. There exist two globular domains in the structure of both TnC's corresponding to the N- and C-termini of the proteins, separated by a long helical linker.

TnC belongs to the tetra EF class of helix-loop-helix proteins that are known to bind to Ca<sup>2+</sup>. Towards the N-termini, loops are found between helices A and B (site I) and C and D (site II), and at the C-terminus between E and F (site III) and G and H (site IV). A divalent cation, predominantly Mg<sup>2+</sup> or Ca<sup>2+</sup> non-specifically occupies sites III and IV with a high binding affinity ( $\sim 10^7$  M<sup>-1</sup>). The cations in this structural region maintain the integrity of Tn and prevent TnI and TnC dissociation (Sin, Fernandes et al. 1978). In contrast, sites I and II in the case of sTnC and only site II in cTnC bind to Ca<sup>2+</sup> at much weaker affinities ( $\sim 10^5$  M<sup>-1</sup>) (Gordon, Homsher et al. 2000).

In the apo-state the N-terminal domains in cTnC (site II), which contain hydrophobic amino acid residues, remain in a closed state, i.e. buried in the structure, whereas upon  $\text{Ca}^{2+}$  binding the corresponding domains dramatically open up, exposing the hidden hydrophobic residues. The hydrophobic region attracts the TnI, pulling the protein at the C-terminus away from actin, thus enabling the myosin S1 “heads” to bind to the actin for downstream contraction process.

A solution structure of the regulatory domain of human cardiac troponin C in complex with the switch region of cardiac troponin I was published recently explaining a 13-fold affinity reduction of cTnI<sub>147-163</sub> for cTnC• $\text{Ca}^{2+}$  providing a structural basis for the inhibitory effect. This generates molecular insight into structural features that are useful for the design of cTnC-specific  $\text{Ca}^{2+}$ -desensitizing drugs (Oleszczuk, Robertson et al. 2010).

### **Troponin I: Inhibitory Protein**

This subunit of Tn complex is shown in vitro to inhibit actomyosin ATPase activity, which is the driving force for sliding of muscle microfilaments. There exist three structural isoforms of TnI in vertebrates: cardiac TnI (cTnI), fast twitch skeletal TnI (fsTnI) and slow twitch skeletal TnI (ssTnI). The fundamental difference between the human cTnI and the skeletal isoforms of TnI's is an additional 27-33 amino acid residues towards the N-terminus tail, which composes the total 209 amino acid residues for cTnI, while for ssTnI it is 186 and for fsTnI only 181 (Li, Wang et al. 2004)

This extended region in cTnI includes a region rich in acidic residues and another extensive phosphorylation region that interacts with the C-domain of

cTnC. The common structures between skeletal and cardiac TnI isoforms are in the C-terminus of the protein. It has been unequivocally proven that TnC and TnI at 1:1 ratio are capable of alleviating the inhibitory action of  $Mg^{2+}$  actomyosin ATPase solely by TnI. TnI is also assumed to stabilize the entire troponin complex together by  $Ca^{2+}$  regulated binding with TnC and TnT, and it facilitates the  $Ca^{2+}$ -dependent binding of TnT with actin. In addition to the above functions, the residues 128-147 in cTnI are responsible to prevent binding of myosin S1 "head" with actin in presence of  $Ca^{2+}$ .

Sadayappan and co-workers (Sadayappan, Finley et al. 2008) segregated the N-terminus of cTnI into three regions: an acidic N region with a single turn of helix (1-10 residues), followed by a polyproline rich domain (11-20 residues) and another helix with property of extensive phosphorylation (21-30). With  $\beta$ -adrenergic signaling the Ser23/24 is phosphorylated with AMP dependent protein kinase A (PKA). This phosphorylation results in  $Ca^{2+}$  desensitization, i.e. reduced affinity of  $Ca^{2+}$  to the sole binding pocket in cTnC. This is executed by a conformational change in the phosphorylated cTnI. The NMR data reveal that residues 19-30 are the minimum required for a weak interaction of N-terminus of cTnI and N-terminus of cTnC in proximity to the inactive  $Ca^{2+}$ -binding site I. This interaction greatly affects the  $Ca^{2+}$  affinity at site II in N-terminus region of TnC. In the non-phosphorylated state, the N-extension of cTnI contacts the N-terminus site I of cTnC and influence the site II  $Ca^{2+}$  binding. Upon PKA-mediated Ser23/24 phosphorylation, the above affinity weakens and N-terminal of cTnI bends such that the acidic region makes electrostatic interaction with the inhibitory region of cTnI. Consequently,  $Ca^{2+}$  affinity of cTnC also decreases. In a cTnI protein construct in which 2-11 residues were deleted, the remaining

cTnI was neither capable of interacting with N-terminal of cTnC, nor was it able to block the inhibitory site of cTnI.

An overall manifestation of phosphorylation on cTnI-cTnC interaction reaffirmed the prevalence of PKA-mediated Ser23/24 phosphorylation as overall modulator of cTnC-Ca<sup>2+</sup> binding affinity, follow-up signal transduction to cTnT and overall cardiac contractility (Solaro, Rosevear et al. 2008). Accordingly, with phosphorylation, the affinity of N-terminus of cTnI is further weakened the N-terminal site I of cTnC causing Ca<sup>2+</sup> desensitization or greater Ca<sup>2+</sup> release from cTnC. Consequently, cTnI folds in such a way that the acidic domain lying at N-terminus of cTnI bends, and due to electrostatic interactions binds with the inhibitory region of cTnI lying towards C-terminus. In normal course this inhibitory region is expected to bind with actin, but due to this conformational change within cTnI, this affinity subsides, which affects the actomyosin cross-bridge reaction. Phosphorylation of Ser-42/44 towards N-domain and Thr-143 in the inhibitory region in cTnI is achieved by protein kinase C (PKC). A larger implication of this modification can be seen on decreased maximal actomyosin Mg<sup>2+</sup>-ATPase. Overall, the PKA and PKC mediated phosphorylation at the respective positions in cTnI have quite an opposite response on cross-bridge formation. Figure 1.12 describes the structural domains of extended cTnI N terminus.

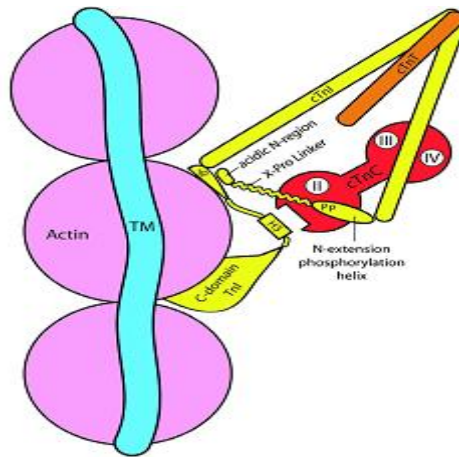


**Figure 1.12 Assembly of cTnI and cTnC.**

*Extended N-terminus region of cTnI, where phosphorylation of Ser-23/Ser-24 residues within a phosphorylation helix, a polyproline rich region and an acidic region, determines the Ca<sup>2+</sup> binding efficiency of site II in cTnC governing the exposure of myosin binding sites in actin. (Solaro, Rosevear et al. 2008)*

**Troponin T- The Glue That Holds It All together**

TnT is an elongated highly symmetrical rod shaped protein of approximately 18 nm in length responsible for binding with TnI, TnC and Tm. In vertebrates, TnT is expressed in three isoforms – cardiac (cTnT), fast twitch skeletal (fsTnT) and slow twitch skeletal (ssTnT). The main cTnT isoform in normal adult heart is composed of 298 amino acids, and upon proteolytic cleavage it can be separated in two fragments - an extended amino-terminal T1 domain (cTnT1, residues 1–181) and a globular carboxy terminal T2 domain (cTnT2, residues 182–298).

Essentially, the N-terminus of TnT binds to the C-terminus of Tm, especially at the overlapping region of head-to-tail association of C- and N-terminus overlapping region of Tm. The C-terminus of TnT interacts with TnI, TnC and Tm (Figure 1.12). The variation within the cTnT even in one individual is expected even though there is only one gene, TNNT2, expressing all the variants. This happens because alternate splicing sites present in pre-mRNA

get processed into several cTnT mRNA species (Mesnard, Logeart et al. 1995). Interestingly, cTnT is recognized as highly charged protein; the N-terminus region comprises ~30% acidic residues whereas the C-terminus has predominantly 20% basic residues (Pearlstone, Carpenter et al. 1976). At physiological pH and low ionic strength this highly polar protein hardly stays in soluble form. The fragment responsible for Tm binding towards the N-terminus, also called the TnT1, is vested by a patch of amino acid residues 71-151, and this binding is considered  $\text{Ca}^{2+}$ -insensitive and deleting 45 residues does not change cTnT's response towards  $\text{Ca}^{2+}$ . On the other hand, the  $\text{Ca}^{2+}$ -sensitive binding of TnT with Tm is attributed to the fragment in the C-terminal fragment, also known as TnT2.

In a recent 2.9 Å resolution crystal analysis of the skeletal Tn:Tm complex (Murakami et al. 2008), residues 66-99 in TnT were found to be crucial for binding with the overlapping region of Tm. The residues 58 to 112 in TnT are highly conserved. The binding partially unfolds the Tm, but rotation angles vary in N- and C-termini in presence of  $\text{Ca}^{2+}$ . Tm covers 7 actin monomers in F-actin. The N-terminus region of Tm covering actin monomers 5-7 moves deeper into the actin grooves yielding a “closed” state, to which myosin heads bind weakly. Conversely, C-terminus of Tm covering actin monomers 1-4 fail to slide much resulting in the generation of an “open” state of actin, to which myosin heads bind strongly. Surprisingly, TnT has practically no influence on the inhibitory action of Tnl on actomyosin ATPase, but as shown above, does influence the numbers of open and closed states of cross bridges between actin and myosin, and this regulates overall contractibility in presence of  $\text{Ca}^{2+}$ .

# 1.7 Regulation of Muscle Contraction

## 1.7.1 Models of Regulation

### The Two-State Model of Regulation

Hill proposed a theoretical model based on each of the 7 actin regions of the thin filament existing in equilibrium between two states: strong myosin binding and weak myosin binding (Hill, Eisenberg et al. 1980). This model states that the equilibrium between these states is not only influenced by local binding of  $Ca^{2+}$  and myosin but also other interactions such as between adjacent Tm-Tm is essential for thin filament assembly. Although the model was consistent with several important features of thin filament structure and was used successfully to describe the effect of troponin-tropomyosin on the equilibrium binding of myosin head to actin but was unable to account for their effect on the kinetics of myosin binding.

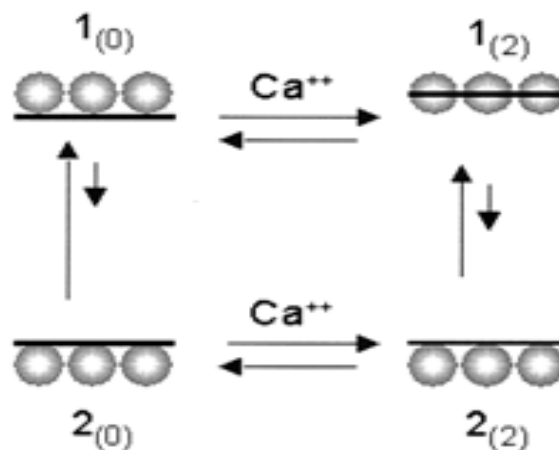


**Figure 1.13 Relationship of key actin filament states of the Hill model with known structural states.**

$Ca^{2+}$  and the occupancy of binding sites on actin with S1 control the state probability and the rate of ATP hydrolysis. The numbers refer to the major states of the actin filament and the subscripts define the number bound  $Ca^{2+}$  (Hill, Eisenberg et al. 1980)

### **An Alternative Three-State Model of Regulation**

To explain the discrepancies between the effect of troponin- $\text{Ca}^{2+}$  on the equilibrium binding and the kinetics of myosin head binding to actin McKillop and Geeves (McKillop and Geeves 1993) proposed a three state model:

- The blocked state – dominates in absence of  $\text{Ca}^{2+}$  when myosin cross-bridges do not interact with actin lowering ATPase activity.
- The closed state – dominates in presence of  $\text{Ca}^{2+}$ . Here the cross-bridges weakly bind to actin. In this state myosin is unable to bind strongly to actin and the actomyosin ATPase is still inhibited.
- The open state – dominates in the presence of myosin heads, cross-bridges bound to actin isomerises to form the strong bound state. In this state the actomyosin ATPase is active.

In addition they suggested that  $\text{Ca}^{2+}$  control the transition from the blocked to the closed state while myosin heads binding to actin is needed for the transition from the closed to the open state.

The three binding state transitions are cooperative in nature, determined by the size of the cooperative unit 'n' (Geeves and Lehrer 1994), equilibrium between blocked and closed states " $K_B$ ", and equilibrium between closed and open states " $K_T$ " (Maytum, Lehrer et al. 1999).

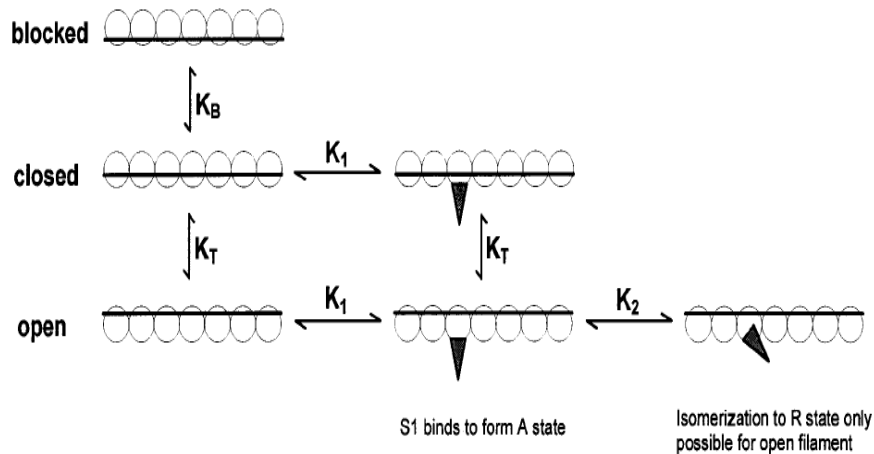


**Figure 1.14 Three state model of thin filament.**

(Open circles) actin linked by a (line) Tm.  $K_B$  is the equilibrium constant between blocked and closed states controlled by  $Ca^{2+}$ .  $K_T$  is the equilibrium constant between the closed and open states controlled by myosin strong binding to actin (Maytum, Lehrer et al. 1999)

### 1.7.2 Calcium Mediated Regulation of Myocardial Activities

The calcium regulation of Tn complex dynamics and eventual Tm.actin interaction has been reviewed by Stehle's group (Stehle, Iorga et al. 2007). Accordingly, an increase in cytosolic  $Ca^{2+}$  makes the site II of cTnC fill with  $Ca^{2+}$  and this, in turn, activates the contraction process. The calcium binding sites take an "open" configuration, thereby attracting cTnI, in particular the "switch region". Consequently, cTnI C-terminus is pulled away from its actin binding sites, and Tn-Tm complex rolls deeper into the grooved positions of actin polymer (Lehman, Hatch et al. 2000). This enables myosin heads to sit on the positions in actin and cross-bridge is formed (Farah and Reinach 1995; Solaro and Rarick 1998; Squire and Morris 1998; Gordon, Homsher et al. 2000). A cross-bridge further deepens the positioning of Tn-Tm in actin grooves and in a co-operative manner helps cross-bridge formation in adjoining actin sites, and  $Ca^{2+}$  binding to more apo-cTnC proteins. Figure 1.15 shows the individual protein component movements in cardiac sarcomere.

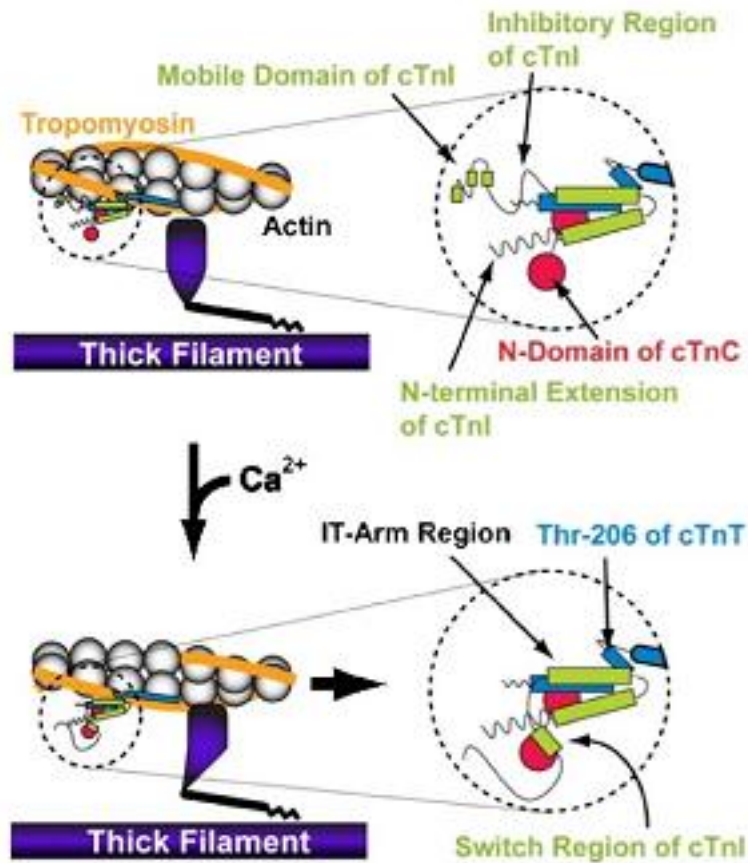


**Figure 1.15 Schematic diagram illustrating protein components of the cardiac sarcomere**

*Top panel- in resting condition in absence of  $Ca^{2+}$  in apo-state of cTnC. Bottom panel- Binding of  $Ca^{2+}$  to cTnC moves the cTnI away from actin thus exposing myosin binding sites on actin(Kobayashi, Jin et al. 2008)*

## 1.8 Troponin T Dysfunction

Since the first troponin T mutations were reported in 1993 (Thierfelder, MacRae et al. 1993; Thierfelder, Watkins et al. 1994), it has been shown that nearly 100 mutations in genes of the three subunits of human cTn alone has been discovered. To date there are 34 TnT HCM mutations and 13 TnT DCM mutations.

Figure 1.16 below is the primary structure of the TnT isoform used in our studies and Table 1.2 lists all of the mutations of cTnT relative to their functional domains. The HCM and DCM mutations investigated in this thesis are highlighted and underlined respectively.

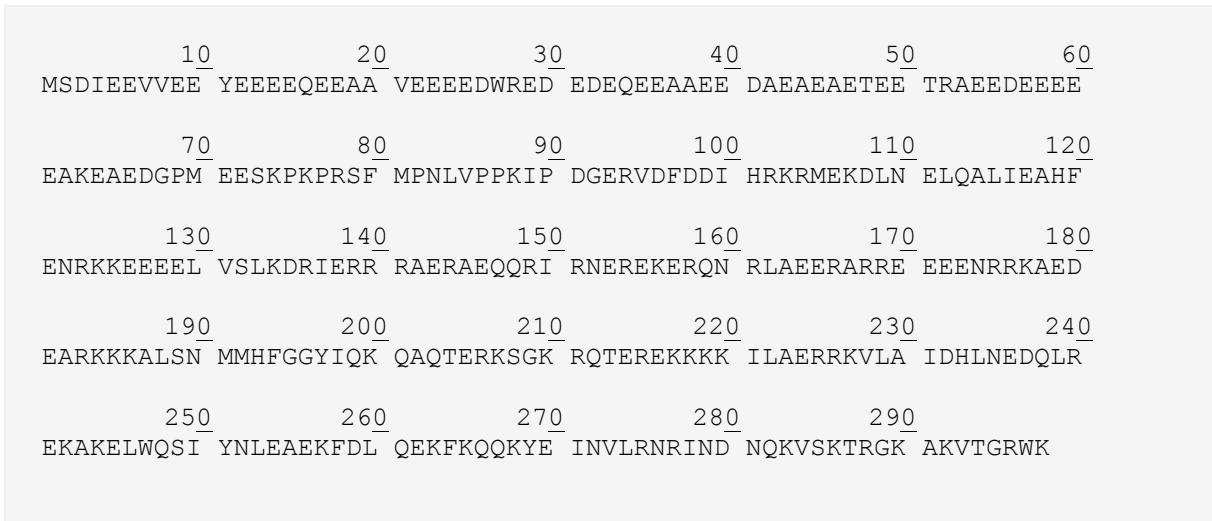


**Figure 1.16. Human cTnT sequence**

In the past few decades the number of disease causing genes identified has increased exponentially. It has remained a challenge to determine if a sequence variation identified in a clinically affected individual is a true disease causing mutation or merely a benign polymorphism. In order to answer this question various information is needed about the sequence variation and one means of substantiating this is to look at the potential functional impact of the sequence variation based on in vivo/vitro studies.

**Table 1.2 TnT mutations relative to the functional domains**

Functional domain in TnT	Mutation
<p><b>Tropomyosin binding domain</b></p>	<p>A28V,S69F<sup>1</sup>,P70L<sup>1,2</sup>,P77L<sup>1</sup>,I79N<sup>1,3,4</sup>,E83K,V85L,D86A<sup>7</sup>,R92W<sup>1,4,5</sup>/Q<sup>3</sup>/L<sup>1,2,8</sup>,R94L<sup>1</sup>/C<sup>9</sup>,K97N, A104V, F110I<sup>3,4,10</sup>/L<sup>11</sup>/V,R113W<sup>15</sup>,K124N,R130C<sup>5</sup>,R131W,R134G<sup>14</sup>, <u>R141W</u>, R151C<sup>14</sup>,</p>
<p><b>TnI-TnC interacting-T1 domain</b></p>	<p>R159Q<sup>14</sup>, <b>ΔE160</b><sup>5</sup>, E163K<sup>3</sup>/R<sup>5</sup>, A172S, A173Q, <b>S179F</b><sup>12</sup>, R205L<sup>15</sup>/W<sup>14</sup>, <u>ΔK210</u><sup>15,17,18</sup></p>
<p><b>TnI-TnC interacting-T2 domain</b></p>	<p>E244D<sup>3,14</sup>,K247R/E,D270N<sup>15</sup>,N271I<sup>2</sup>, <b>K273E</b><sup>16</sup>,R278C<sup>2</sup>/P,R286C<sup>2</sup>/H<sup>7</sup>, W287ter<sup>2</sup>, <b>Δ14, Δ28+7</b><sup>1,2,13</sup></p>

\* HCM and DCM mutations investigated in this thesis are highlighted and underlined respectively

1.(Knollmann, Kirchhof et al. 2003)2. (Ashrafian, Redwood et al. 2003);3. (Varnava, Elliott et al. 2001);4. (Thierfelder, Watkins et al. 1994);5. (Watkins, McKenna et al. 1995);6. (Richard, Charron et al. 2003);7.(Sheng, Shan et al. 2008);8. (Mogensen, Bahl et al. 2003); 9. (Cheng 2005);10. (Doolan, Tebo et al. 2005);11. (Varnava, Baboonian et al. 1999);12.(Van Driest, Vasile et al. 2004);13.(Hoffmann, Schmidt-Traub et al. 2001);14.(Elliott, D'Cruz et al. 1999);15.(Fujino, Shimizu et al. 2002);16.(Torricelli, Girolami et al. 2003);17.(Hershberger, Parks et al. 2008);18. (Li, Czernuszewicz et al. 2001)

Mutations for arginine residues account for more than 25% of known HCM and 60% of known DCM mutations. Typically a 3-D structure would allow us to evaluate the potential structural effects of Tn mutations and possible disruption of key protein-protein interactions. However, publications of both the skeletal and cardiac Tn structures lack critical regions namely residues sTnT(1-30) and cTnT (1-182) and a large number of cardiac mutations were unresolved within this structure (Takeda et al. 2003).

Reconstruction of the crystal structure of the core domain (C.I.T2 complex) from human cardiac Tn complex is shown in Figure 1.17. Most mutations were found to be localised to a non-crystallizing mobile functional domain of cTnT, such as the Tm-actin, cTnI or cTnC binding sites located outside the core domain. Biochemical, physiological and transgenic animal models are crucial tools in eliciting details about the way in which these mutations disrupt the function of thin filaments.

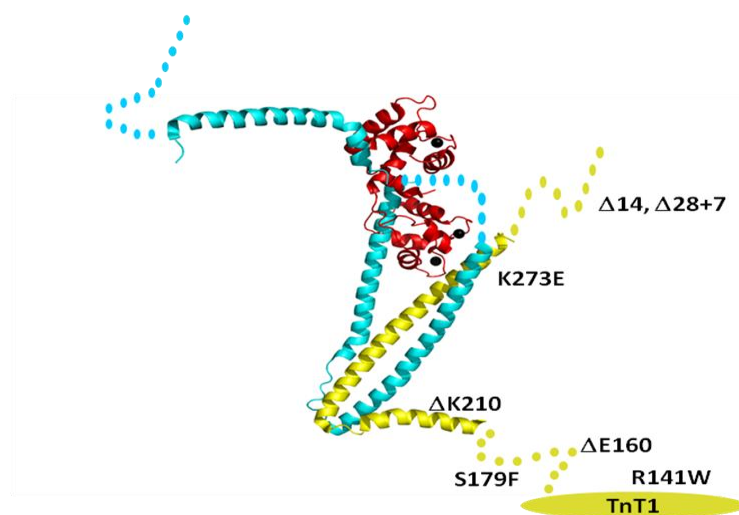


**Figure 1.17 Ribbon model of the cardiac Tn crystal structure.**

*The loci of the mutations in this study that cause cardiomyopathy; TnC, red, TnI, cyan and TnT yellow. The dotted lines indicate the segments that were included in the crystals but lacked defined electron densities. (Takeda et al. 2003)*

### 1.8.1 Functional Studies

Physiological studies using cultured myocytes transfected with mutant cTnT have been reported to impair the cardiac muscle contractility which may lead to causing a compensatory hypertrophy (Watkins, Seidman et al. 1996; Marian, Zhao et al. 1997; Sweeney, Feng et al. 1998; Rust, Albayya et al. 1999). Using rabbit or rat skinned myofibrils composed with human cTnT mutations- S179F and R92Q/W/L different investigators reported elevated myofilament  $Ca^{2+}$  sensitivity, without any changes in maximum force generation and myosin ATPase activity (Morimoto, Yanaga et al. 1998; Yanaga, Morimoto et al. 1999). Szczesna and Harada and Potter (Szczesna, Zhang et al. 2000; Harada and Potter 2004) reported similar results for I79N, R92Q/W/L using nearly the same experimental systems as Yanaga's group.

The approach of mimicking the human genome mutations using reconstituted animal skinned myofibril led to some erroneous conclusions. This issue was raised by Chang et al. (Chang, Parvatiyar et al. 2008) in cTnT S179F mutation, known for HCM phenotype. This mutation had induced ventricular tachycardia (abnormal pulse) even in the absence of hypertrophy. Thus, more than anatomical changes in heart the arrhythmias were the cause for sudden cardiac deaths. (Fiset and Giles 2008) attempted to relate  $Ca^{2+}$  sensitivity and ventricular electrophysiology in relation to such cTnT mutations, and concluded that  $Ca^{2+}$  desensitization is positively correlated to ventricular tachycardia.

The two splice donor site mutations,  $\Delta 14$  and  $\Delta 28+7$  increase the calcium sensitivity and decrease the cooperativity in the force generation of cardiac muscle.  $\Delta 28+7$  further decrease the maximum force when the mutation is

exchanged into rabbit cardiac skinned muscle fibres by ~50% and a decrease in the slope of force-pCa relationships (Nakaura, Morimoto et al. 1999).

Investigations using the in situ troponin exchange technique revealed that the most examined mutations (I79N, R92W/L/Q, A104V, R130C,  $\Delta$ E160, S179F, K273E, R287C,  $\Delta$ 14 and  $\Delta$ 28+7) had the Ca<sup>2+</sup> sensitising effect on skinned fibre force development, while the maximum force level was not significantly affected by these mutations (Morimoto, Nakaura et al. 1999);(Szczesna, Zhang et al. 2000) (Morimoto, Lu et al. 2002); (Lu, Morimoto et al. 2003); (Venkatraman, Harada et al. 2003); (Harada and Potter 2004). These findings strongly indicate that the main functional consequence of HCM mutations are increased Ca<sup>2+</sup> sensitivity of force generation.

The first cTnT mutant,  $\Delta$ K210 in TNNT2 gene, was identified to be responsible for two distinct familial DCM (Kamisago, Sharma et al. 2000). Decrease in Ca<sup>2+</sup> sensitivity for force generation and ATPase activity in cardiac myofibrils were the primary pathogenic response in skinned cardiac fibres (Morimoto, Lu et al. 2002). Similar findings were reported by other groups (Robinson, Mirza et al. 2002; Venkatraman, Harada et al. 2003). Other mutations, R131W, R141W, R205L and  $\Delta$ 270N, also caused subdued Ca<sup>2+</sup> sensitivity without affecting maximum force generation, besides enhancing the cTnC-Tm affinity.

A172S and R141W occur within a critical region of TnT tail required for the determination of the position of Tn-Tm complex on thin filament. Whilst A172S does not result in a charge change since both amino acids are neutral the serine residue if it gets phosphorylated may further alter the TnT-Tm interaction.

## 1.8.2 Transgenic Animal Models

Although it would be ideal to investigate cardiac tissue extracted directly from the affected individuals, this is rarely obtainable. However, a fairly new scientific discipline has developed studying transgenic animals to assess the effects of mutations in vivo. Several mutations have been successfully expressed in animals developing a similar phenotype to the clinical disease expression seen in HCM and DCM patients.

Changes in intracellular  $\text{Ca}^{2+}$  concentration would affect outward transport of  $\text{Ca}^{2+}$  using  $\text{Na}^+/\text{Ca}^{2+}$  exchangers and this electrogenic transporter, in turn, can modulate ventricular excitability. A comprehensive assessment of  $\text{Ca}^{2+}$  sensitization and arrhythmias in HCM-linked cTnT transgenic mice was carried out by Baudenbacher et al. (Baudenbacher, Schober et al. 2008), who used three human missense mutants, S179F, F110I and R278C, which also exhibited decreasing trend in  $\text{Ca}^{2+}$  sensitization in human cardiac myofibres. There was no evidence of fibrosis or hypertrophy in transgenic mice, but in skinned fibre preparations the  $\text{Ca}^{2+}$  sensitivity was in order of S179N>F110I>R278C. It was concluded that, independent of any anatomical changes in the heart, cTnT mutations in the same graded order caused risk of ventricular tachycardia by changing the ventricular action potential shape, shortening refractory periods between action potentials, beat to beat T wave shape and amplitude alterations, and faster than normal dispersal of ventricular conduction.

In a similar investigation on cTnT  $\Delta\text{K}210$  mice, which should show DCM phenotype, the death was quite rapid due to arrhythmias and induction of long

QT (QT gap increases due to delayed repolarisation), associated with increased phosphorylation of RyR and PLB (Solaro 2007).

A knock-in mouse model with K210 codon deletion analogous to human DCM conditions displayed swollen heart, reduced  $\text{Ca}^{2+}$  sensitivity, and premature deaths. Administration of a  $\text{Ca}^{2+}$  sensitizer, pimobendan, completely reversed all the DCM characteristics. Lombardi et al. (Lombardi, Bell et al. 2008) constructed two mouse models with cTnT mutations, R92Q and R141W, which are prevalent in HCM and DCM patients, respectively. A transgenic mouse expressing human R29Q cTnT mutation exhibited enhanced contractility, and diastolic abnormalities, with myocytes displaying shortened sarcomere lengths, increased sarcometric activation and reduced relaxation, suggestive of increased  $\text{Ca}^{2+}$  sensitivity. Indeed the mice phenotypes resembled human cardiomyopathy. Upon autopsy, a R141W mouse showed a dilated heart with lower diastole. Conversely, constricted heart and high systole were characteristics of R92Q mice.  $\text{Ca}^{2+}$  sensitivity of myofibril and myosin ATPase responded opposite in the two transgenic animals. The binding properties of cTnT with other thin filament proteins were examined in two mutated mice and it was revealed that R141W displayed higher affinity for cTnC,  $\alpha$ -Tm and  $\alpha$ -actin, whereas cTnI binding was more with cTnT R92Q. Such contrasting affinities among the thin filament proteins could be one of the reasons for HCM and DCM phenotypes.

Yet another group (Miller, Szczesna et al. 2001) created a transgenic mouse model expressing I79N and confirmed that skinned cardiac muscle fibres showed an increase in  $\text{Ca}^{2+}$  sensitivity of force generation and ATPase activity. Tardiff and workers created a transgenic mouse expressing R92Q that exhibited

hypercontractility and diastolic dysfunction (Tardiff, Hewett et al. 1999). Isolated cardiac myocyte displayed increased basal sarcomeric activation, impaired relaxation which is indicative of increased  $\text{Ca}^{2+}$  sensitivity of myofilaments. Further work by Chandra and co-workers demonstrated that  $\text{Ca}^{2+}$  sensitivity of myofilaments was increased even in skinned cardiac muscle fibres from these transgenic mice (Chandra, Rundell et al. 2001).

Another cTnT mutant in animal model,  $\Delta\text{E160}$  with HCM characteristics, was also found to alter the  $\text{Ca}^{2+}$  fluxes and induced ventricular arrhythmic action potential. Again, the maximum force or ATPase and cooperativity were unaffected; however it exhibited an increase in the  $\text{Ca}^{2+}$  sensitivity of cardiac muscle contraction in skinned muscle fibre preparation (Morimoto, Lu et al. 2002).

The nature of replacing amino acids in single point mutation also profoundly affects the type and severity of the disease. For example, R92W develop negligible or mild hypertrophy but such patients experience sudden cardiac deaths and the disease progressed from HCM to DCM; upon replacement with Leu the carriers developed acute hypertrophy but no sudden deaths, and if the substitution was with a Glu then the response is similar to that of S179F patients and ventricular beats and rhythms got perturbed leading to sudden cardiac deaths (Chang, Parvatiyar et al. 2008).

Functional consequences of cTnT mutations have been intensively examined at different levels from molecules to animal models, revealing heterogeneity in the functional and structural consequences of a variety of mutations spreading over the entire molecule. Mutations in the region of 92-110 have been shown to

impair the T<sub>m</sub>-dependent function of cTnT but mutations outside the region (I79N, ΔE160 and E163K) do not. Nevertheless they are all responsible for the same disease pathogenesis implying a common mechanism. Most cTnT mutations investigated: S179F, R92Q/W/L, F110I, R278C, R141W, R131W, R205L, Δ270N, ΔK210, ΔE160, Δ14 and Δ28+7 mutations have produced inconsistent results and sometimes the in vivo implications of such mutations could not be explained from results of reconstituted skinned microfibre studies. Potential environment surrounding ventricular sarcomere is different from the isolated muscle fibres, the constitution of cTnT isoform under given diseased condition might be different, the interaction with other thin filament proteins may vary and the electrogenic stimulation may exert its own impact. There is still no clear understanding as to why cTnT mutations alter Ca<sup>2+</sup> sensitivity to maximum force generation and ATPase activity. It is likely that binding of cTnT with actin, T<sub>m</sub> and cTnC/cTnI may be affected. Possibly cTnI phosphorylation gets modified and this affects Ca<sup>2+</sup> sensitivity of cTnC and/or movement of the inhibitory arm away or close to actin and other cTnC configurational changes. T<sub>m</sub> affinity with actin can be jeopardized such that actin.myosin can not transit from “closed” to “open” state and thus ATPase activity and the maximum force generation may get perturbed.

Overall these studies led to the suggestions that mutations in TnT could alter the regulation of cardiac muscle contraction at several levels: alteration of crossbridge cycling rate because of its interaction with TnI, alteration of Ca<sup>2+</sup> binding to thin filaments through its interaction with TnC, alteration of thin filament cooperativity through its interaction with T<sub>m</sub>, altered stoichiometry of TnT incorporation into Tn complex or various combinations of these effects.

## 1.9 Programme of Research

Hypertrophic and dilated cardiomyopathies are autosomal dominant diseases of the myocardium that have been linked to mutations in the genes of almost all sarcomeric proteins including TnT. Patients carrying mutations in TnT have been shown to be at high risk of sudden death yet they display only moderate hypertrophy and fibrosis unlike patients carrying mutations in other genes. The absence of gross histologic or anatomic abnormalities led to the suggestion that functional changes are likely to occur at the level of the sarcomere. Over the last 20 years extensive biochemical investigations using steady state methods including in vitro motility, actomyosin ATPase, and mechanical studies have tried to unravel this molecular dysfunction but have not been able to provide a molecular mechanism linking the effect of mutations to the onset and progression of the disease. In this study we aimed to use transient kinetics methods to assess in depth the effect of cTnT mutations on the  $\text{Ca}^{2+}$  mediated thin filament regulation. Overall this thesis has three objectives:

**(1) To produce and characterise seven selected cTnT mutations causing DCM and HCM.**

Our first aim was to generate mutations in troponin T in sufficient amount and characterise them by steady state methods including ATPase assays, co-sedimentation assays and circular dichroism to study the functional and structural effects of the mutations. We selected seven mutations that were previously characterised by steady state methods. Among the 37 known TnT mutations, we selected mutations in the 2 functional domains of TnT (T1 and T2) that were linked to both HCM and DCM. These mutations are grouped in 3:

Group 1: DCM mutations R141W and  $\Delta$ K210 in the T1 and T2 domain respectively.

Group 2: HCM mutations  $\Delta$ E160 and S179F in the T1 domain

Group 3: HCM mutations K273E, truncated  $\Delta$ 14 and  $\Delta$ 28+7 in the T2 domain

**(2) To investigate thoroughly the effects of these mutations on the kinetics of thin filament switching.**

Thin filaments in cardiac muscle behave as a classical cooperative-allosteric system in which a number of actin monomers are simultaneously switched between a blocked state, a closed state and an open state. We aimed to use two techniques to measure the impact of TnT mutations on the cooperativity along the thin filament (defined by the size of the cooperative unit  $n$ ) and on the proportion of thin filaments in the blocked state (defined by  $K_B$ ) as illustrated in Figure 1.18.

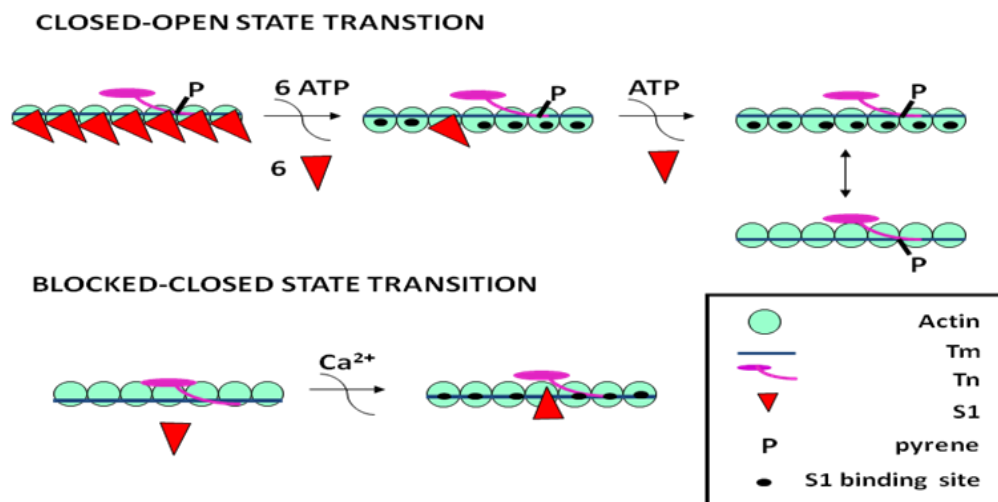


**Figure 1.18 Schematic models of thin filament switching states**

(A) size of cooperative unit ' $n$ ' (B) equilibrium constant  $K_B$ .

**(3) To investigate thoroughly the effects of these mutations on the kinetics of Ca<sup>2+</sup> dissociation.**

Transient changes in the concentration of Ca<sup>2+</sup> ions are believed to be the trigger for a cascade of protein-protein interaction alterations which lead to muscle contraction. It is known that the presence of DCM mutations decrease calcium sensitivity and HCM increases it. The objective of this chapter is to assess whether this functional phenomenon was a direct result of altered Ca<sup>2+</sup> affinity or was caused by altered Tn-Tm switching.

We aimed at investigating the effect of TnT mutations on the Ca<sup>2+</sup> affinity and dissociation kinetics using mutant cTnT reconstituted into Tn, thin filament and thin filament in the presence of myosin heads.

**Overall Aim**

The ultimate goal of the studies described above is to understand, at the molecular level, how mutations that cause cardiomyopathies alter the regulation of the cardiac contractile cycle.

# CHAPTER 2

Materials and Methods

# Contents

<b>2.1</b>	<b>Buffers and Stock Solutions</b>	<b>54</b>
<b>2.2</b>	<b>Preparation of Tissue Purified Proteins</b>	<b>54</b>
<b>2.3</b>	<b>Preparation of Recombinant Proteins</b>	<b>60</b>
<b>2.4</b>	<b>Fluorescent Protein Labelling</b>	<b>64</b>
<b>2.5</b>	<b>General Methods</b>	<b>66</b>
<b>2.6</b>	<b>Determination of Actomyosin Mg<sup>2+</sup>ATPase Activity</b>	<b>69</b>
<b>2.7</b>	<b>Circular Dichroism</b>	<b>71</b>
<b>2.8</b>	<b>Enzyme Kinetics</b>	<b>72</b>

## **2.1 Buffers and Stock Solutions**

Unless otherwise specified, all chemicals were obtained from commercial sources and used without further purification. All buffers and solutions were made up using double deionised water drawn from an Elga Purelab option (DV35) water purification system and are listed in Appendix A.

## **2.2 Preparation of Tissue Purified Proteins**

Myosin subfragment-1 (S1) was prepared from rabbit skeletal muscle. F-actin was prepared from both rabbit skeletal and sheep cardiac muscle.  $\alpha\alpha$ -tropomyosin was prepared from sheep cardiac muscle. Human cardiac troponin was expressed in *Escherichia coli* system. All procedures were carried out at 4°C unless otherwise stated.

### **2.2.1 Preparation of Myosin Thick Filament**

#### **Preparation of Skeletal Muscle Myosin**

Myosin was prepared from rabbit skeletal muscle based on the method of Margossian and Lowey (Margossian and Lowey 1982; Potter 1982). The euthanized white New Zealand rabbits (7-8kg) were skinned, the back and leg muscles removed and packed in iced water. The muscle was minced and weighed before being extracted in 3 volumes of Guba-Straub buffer (0.3M KCl, 0.15M  $KP_i$ , pH 6.5) for 20 minutes using an overhead stirrer. The suspension was then filtered through layers of fine mesh cloth and the residue was retained for acetone powder preparation. The extract was subsequently precipitated by addition of 14 volumes of cold deionised water over a 10 minute period while stirring in a 25 litre bucket. The crude myosin was allowed to settle for 4 hours,

the supernatant siphoned off and sedimented by re-centrifugation at 8,000 rpm for 15 minutes on a SLC 6000 rotor. The resulting pellet was dissolved overnight in 250 ml of 0.6 M KCl, 5 mM imidazole at pH 7.0. After dialysis against the same buffer, contaminant acto-myosin was precipitated by slow addition of 1.14 volumes of cold deionised water and centrifuged at 8,000 rpm, SLC 6000 rotor for 15 minutes. To further clarify the myosin, the supernatant was diluted 6 volumes with deionised water, left to stand for 15min and centrifuged at 8,000 rpm on a SLC 6000 rotor for 15 minutes. The fluffy myosin precipitate was re-suspended in a further 250 ml of 0.6M KCl and 5 mM imidazole at pH 7.0 and the dilution step repeated. The final pellet was taken into 150 ml of 1.2 M KCl, 10 mM NaP<sub>i</sub>, 3 mM MgCl<sub>2</sub>, 0.2 mM EGTA and 3 mM NaN<sub>3</sub> at pH 7 to give a final concentration of ~ 40 mg/ml. The protein concentration was determined by Lowry assay and the myosin stored at -20°C in 50% glycerol.

### **Preparation of Skeletal Myosin Subfragment 1**

Preparation of subfragment 1 from skeletal muscle myosin was based on Weeds and Taylor (Weeds and Taylor 1975). Myosin in 50% glycerol was washed free of glycerol by dilution in 15 volumes of cold water. The cloudy precipitate was then centrifuged at 13,000 rpm, Sorvall RC-5B, SLA 1500 rotor for 10 minutes. The myosin was re-suspended in 0.6 M NaCl and dialysed against 0.12 M NaCl, 20 mM NaH<sub>2</sub>PO<sub>4</sub>, 1mM EDTA and pH 7.0 to give a fine suspension of approximately 20 mg/ml. Digestion was started by addition of chymotrypsin (Sigma type VII) to a final concentration of 0.05 mg/ml with incubation in a water bath at 25 °C for 10 minutes. The reaction was stopped by adding PMSF to a final concentration of 0.1mM. After further incubation for 5

minutes, the myosin was dialysed against 5 mM PIPES pH 7.0, 5 mM MgCl<sub>2</sub>, 1 mM DTT, and 0.1mM PMSF overnight at 4°C. The solution was centrifuged at 20,000 rpm, Sorvall RC-5B, SS-34 rotor for 30 minutes, the S1 being present in the supernatant.

S1 was further purified over a Q-Sepharose column (1.6x 20 cm) against 5 mM Pipes pH 7.0, 5mM MgCl<sub>2</sub>, 1mM DTT, and 0.1mM PMSF with a gradient of 0-200 mM NaCl. Fractions were collected every 8 minutes at 60ml/ hr. The S1 containing fractions were monitored at absorbance of 280nm and checked for purity on a 15% SDS gel. The pooled fractions were then subjected to 70% ammonium sulfate precipitation. The suspension was centrifuged at 13000 rpm for 10min at 4°C and the pellet re-suspended and dialysed in minimal ATPase buffer (10 mM PIPES pH 7.0, 140 mM KCl, 3.5 mM MgCl<sub>2</sub>, 1mM DTT and 1mM NaN<sub>3</sub>). The concentration of S1 was determined, frozen in liquid nitrogen and stored at -80 °C.

## **2.2.2 Preparation of Actin Thin Filament**

### **Preparation of Skeletal Muscle Acetone Powder**

The residue following myosin extraction was stirred into 5 volumes of 0.4% NaHCO<sub>3</sub>, 0.1 mM CaCl<sub>2</sub> for 30 minutes. It was then filtered through a fine nylon mesh and the filtrate discarded. The pellet was then re-extracted in 1 volume of pre-chilled 10 mM NaHCO<sub>3</sub>, 10 mM Na<sub>2</sub>CO<sub>3</sub> and 0.1 mM CaCl<sub>2</sub> for 10 minutes. The suspension was poured into 5 l of deionised water at room temperature, extracted by filtering immediately through nylon mesh at 4°C and squeezed to dryness. The wash procedure was carried out in the fume hood twice in 1l of cold acetone with stirring for 15 minutes before being filtered. The final residue

was placed on a tray with filter paper and dried overnight in the hood. The resulting acetone powder was stored at  $-80^{\circ}\text{C}$ .

### **Preparation of Cardiac Muscle Acetone Powder**

Cardiac muscle acetone powder was prepared from sheep heart using the same method as for skeletal acetone powder.

### **F-actin Preparation**

This method is a modification of the classic method of Spudich and Watt (Spudich and Watt 1971) for both skeletal and cardiac acetone powder. Each 2.5g of acetone powder was extracted for 30 min on ice with 50 ml of G-actin buffer (2 mM Tris-HCl pH 8.0, 0.2 mM ATP, 0.5 mM DTT, 0.1 mM  $\text{CaCl}_2$  and 1 mM  $\text{NaN}_3$ ). Insoluble material was pelleted by centrifugation at 18,000 rpm using a Sorvall RC5C, SS34 rotor at  $4^{\circ}\text{C}$  for 20 minutes. The supernatant was filtered through glass wool and the pellet was re-extracted in the same volume of G actin buffer and centrifugation repeated. Both supernatants were combined, and actin was polymerized by the addition of 0.1V of 10X KME buffer (100mM Tris-HCl, 500 mM KCl, 25 mM  $\text{MgCl}_2$ , 10 mM EGTA and 10 mM  $\text{NaN}_3$  pH 8.0, at  $25^{\circ}\text{C}$ ). The now viscous, well-polymerised F-actin solution incubated at  $30^{\circ}\text{C}$  for 45 minutes was brought to 0.8 M KCl. The actin filaments were pelleted by ultracentrifugation using a T1250 rotor at 42,000 rpm at  $4^{\circ}\text{C}$  for 2 hours. The filaments were re-suspended in 10 ml of G-actin buffer (~ 5-5.5 mg/ml) and depolymerised by dialysis against two times 1 l changes of G-actin buffer over 2 days at  $4^{\circ}\text{C}$  and any remaining filaments were pelleted by ultracentrifugation. The supernatant was gel filtered on a 1.6x95cm column of Sephacryl S-300 pre-equilibrated with G-actin buffer to remove minor

contaminants (MacLean-Fletcher and Pollard 1980). Fractions of 4 ml were collected, monitored at absorbance at 290 nm and run on 12% SDS gel to check for purity. The peak and following fractions were pooled and polymerised using 0.1V of 10xKME buffer at 30°C for 45 minutes followed by ultracentrifugation using a T1250 rotor at 42K rpm at 4°C for 2 hours. Purified actin was stored at 4°C as pellet. At the time of use it was re-suspended in ATPase buffer prior to use in experiments.

### **2.2.3 Preparation of Regulatory Proteins of Thin Filament**

#### **Sheep Cardiac Muscle Ether Powder**

To isolate cardiac Tm and Tn from sheep heart, we needed to prepare ether powder according to the method adapted from Potter (Potter 1982). Left ventricle tissue was trimmed of fat, valves and connective tissue before mincing on a meat grinder. 3kg of minced muscle was homogenised for 30 seconds using a Polytron homogeniser in 15 l of wash buffer containing 1% Triton X-100, 50 mM KCl, 5 mM Tris-HCl pH 8.0 and 0.5 mM PMSF and 0.5 mM benzamidine protease inhibitors. The homogenate was then filtered through cheese cloth and the tissue re-suspended in equal volume of wash buffer. This procedure was repeated 8 times or until the residue turned yellow to white in colour. The following steps were carried out in a fume hood at room temperature and the final pellet was then transferred into a 25 l bucket on a cheese cloth and washed with 3 V of pre-chilled 95% ethanol. The filtrate was discarded and this step was repeated a further 2 times. The pellet obtained from the ethanol washes was then re-suspended in 3 V of diethyl ether with the supernatant

discarded. After two further diethyl ether washes, the powder was allowed to dry overnight on a filter paper in a fume hood. The dry powder was stored at  $-80^{\circ}\text{C}$ .

### **Cardiac Troponin Preparation**

Tn was extracted from sheep heart ether powder according to the method described by Potter (Potter 1982). 30g of ether powder was extracted in 20 V of 1M KCl, 20 mM TES pH 7 and 15mM  $\beta$ -mercaptoethanol which was homogenised with an overhead stirrer overnight at  $4^{\circ}\text{C}$ . The suspension was centrifuged at 10,000 rpm for 20 minutes at  $4^{\circ}\text{C}$  using a SLA 3000 rotor and the pellet discarded. The supernatant was adjusted to pH 8.0 with 1M potassium hydroxide and the solution brought to 30% ammonium sulphate saturation (167g/l added). The pH was maintained between 7 and 8 during addition. The solution was stirred for a further 30 minutes to ensure that ammonium sulphate was completely dissolved and centrifugation was carried out at 12,000 rpm for 20 minutes at  $4^{\circ}\text{C}$  using an SLA 1500 rotor, the pellet suspended in 15 ml of ATPase buffer (10 mM PIPES pH 7.0, 50 mM KCl, 3.5 mM  $\text{MgCl}_2$ , 1mM DTT and 1mM  $\text{NaN}_3$ ) and left to dialyse overnight in same buffer. The supernatant from the previous step was brought to 42.5% ammonium sulphate saturation (73g/l added) to precipitate Tn and left stirred for a further 30 minutes. Centrifugation was carried out at 12,000 rpm for 20 minutes at  $4^{\circ}\text{C}$  using a SLA 1500 rotor. The pellet was suspended in 15 ml of ATPase buffer and dialysis was carried out with the buffer changed at least four times in 250 ml. The supernatant from this fractionation was kept for tropomyosin preparation. The crude Tn was loaded onto a DEAE Sephadex column which was pre-equilibrated with 2 l of column buffer. The  $\text{OD}_{280}$  was checked until the baseline reading was zero before column was eluted stepwise with column buffer

containing increasing concentration of 0.1, 0.2, 0.3, .0.4, 0.5 and 0.6 M KCl. Fractions were collected 1ml/min at 6 minutes per fraction, monitored at  $A_{280}$  and run on a SDS gel to check for purity. The fractions with pure cardiac Tn were pooled, concentrated and stored at  $-80^{\circ}\text{C}$ .

### **Cardiac Tropomyosin Preparation**

The pooled 42.5% ammonium sulfate supernatant from previous ether powder extractions were brought to 65% ammonium sulphate saturation (140g/l added) to precipitate the tropomyosin which was pelleted thereafter by centrifugation at 12000 rpm using an SS-34 rotor for 20 minutes. The pellet was re-suspended and dialysed overnight against ATPase buffer to remove any remaining ammonium sulphate. The dialysate was then centrifuged at 20,000 rpm, SS-34 rotor for 10 minutes and the supernatant loaded onto a DEAE Sephadex column with linear gradient of 50 mM to 500 mM KCl in medium (50 mM KCl) ATPase buffer. Fractions were collected every 6 minutes, monitored at absorbance of 280 nm and run on a SDS gel to check for purity. The fractions with pure cardiac tropomyosin were pooled, concentrated and stored at  $-80^{\circ}\text{C}$ .

## **2.3 Preparation of Recombinant Proteins**

### **2.3.1 Preparation of Human Cardiac Troponin Subunits**

The cDNAs encoding wild-type TnT, TnI and TnC were obtained as a gift from Dr. C. Redwood (University of Oxford, UK), Dr. N.Brand (Imperial college, UK) and Prof. K. Jacquet (Clinic of the Ruhr-University of Bochum, Germany) respectively. Recombinant mutant TnT subunits were cloned by the Protein expression lab at the University of Leicester. Using hcTnT as a template the

cDNA was subcloned into pLEIC05 expression vector by overlap extension PCR. The primers for the construction of TnT mutations were designed based on the human cardiac TNNT2 sequence with a minimum of 15 base pairs on either side of the mutation.

A single colony was picked up from the LB agar plate and placed into a 5ml starter culture (LB media) containing appropriate antibiotics (see Appendix A) and the cells were grown in a shaker at 200 rpm at 37°C for 8 hours. 1ml of the day culture was used to inoculate a 100ml night culture (100 ml LB media and 100 µl antibiotics) and grown in a shaker at 200 rpm at 37°C overnight. 10 ml of the overnight culture were subsequently inoculated into LB broth containing 1ml/L antibiotics at 37°C until OD at 600 reached 0.6. Expression of the target protein was induced by adding 1ml/l of 0.4 M IPTG stock solution keeping the cultures shaking at 37°C and 220 rpm. The expression of the subunits by *E. coli* is critically dependent on the incubation time and the above described conditions consistently gave good expression levels. The cells were harvested by centrifugation on Sorvall SLC 6000 rotor at 5000 rpm for 15 min at 4°C. The pellets were frozen at -80°C until further purification.

The pellets were re-suspended in ice-cold 25 mM Tris- HCl, 1 mM EDTA, 20% sucrose, 200 mM NaCl, 5 M urea, 0.1% Triton X100, pH 7.5 lysis buffer at 10 ml/l of cell culture. A single protease inhibitor tablet constituting serine, cysteine and metalloproteases inhibitors was added per 50 ml extraction. Additionally, 0.5 mM PMSF and 0.5 mM benzamidine inhibitors were added followed by incubation on ice for 20 minutes. The suspension was subsequently French pressed at least twice at 110 MPa using a pre-chilled cell. After further incubated on ice, the cell lysate was centrifuged on a SS34 rotor at 20,000 rpm

for 20 minutes at 4°C. The soluble crude bacterial lysate supernatant was dialysed overnight against column buffer to be purified by ion exchange chromatography.

### **2.3.2 Purification of Troponin Subunits**

#### **TnT Wildtype, Mutants and TnC Wildtype**

The lysis supernatant was diluted with an equal volume of Q buffer A (50 mM Tris-HCl, 1mM EDTA, 1mM  $\beta$ -mercaptoethanol and 6 M urea, pH 7.5, 4°C) and dialysed 2 times against litre of the same buffer overnight. The protein was loaded onto an anion exchange column (Q-Sepharose 16/10) previously equilibrated with column buffer. The proteins bound to the column were selectively eluted by increasing the ionic strength of the column buffer to 2 M NaCl. The flow rate was set at 1ml/min and the fractions collected every 6 minutes. TnT/TnC containing fractions were pooled and identified by SDS-PAGE. Frequently TnC will not completely bind to the first column as it can be saturated with nucleotide material and often a second run was carried out using the previous runs flow through. The protein concentration was determined and stored at -80°C.

#### **TnI**

The lysis supernatant was diluted with an equal volume of SP buffer A (20 mM MOPS, 1 mM EDTA, 1 mM  $\beta$ -mercaptoethanol and 6 M urea, pH 6.5, 4°C) and dialysed two times against 1 litre of the same buffer. The protein was loaded onto a cation exchange column (SP-Sepharose 26/20) and eluted using a gradient of 0-2 M NaCl. TnI containing fractions was identified by SDS-PAGE and pooled. Protein was frozen and stored at -80°C. A fresh solution of Tn is

fluid and transparent but it becomes highly viscous and frequently turbid during the course of storage.

### **2.3.3 Formation of the Troponin Complex**

Initially we purified each troponin subunit before reconstitution as described above. This method takes about 4 weeks and is laborious. After few months we rationalised that since all troponin subunits were expressed in *E.coli*, the contaminant proteins (*E.coli* proteins) were the same and decided to shorten the method by reconstituting the complex before a single purification.

Bacterially expressed recombinant human cardiac TnT, TnI and TnC were reconstituted by mixing the Tn subunit *E.coli* culture pellets stored at -80°C from section 2.3.1 in a 3:2:1 (T:I:C culture volume ratio). The mixture was left in ice for 15 minutes before successively dialysing out urea and KCl in reconstitution buffer composed of 6 M urea, 1 M KCl, 0.2 mM CaCl<sub>2</sub>, 10 mM MOPS, pH 7.0, 1mM DTT 0.01% NaN<sub>3</sub> and protease inhibitor tablets. The mixture was dialysed for 3-4 hours and the reconstitution buffer changed to one with 2 M urea and 1M KCl, followed by no urea, 0.75 M KCl and finally 0.5 M KCl at 4 hour intervals. The final dialysate was then spun down at 14000 rpm, Sorvall RC-5B, SLA 1500 rotor for 10 minutes. The supernatant was brought to 30% ammonium sulphate precipitation and spun down at 14000 rpm for 20 min. The subsequent supernatant was then brought to 50% ammonium sulphate and spun down at 20000 rpm for 20min. The crude Tn precipitate found in the 30-50% pellet was then re-suspended in column buffer ( 10 mM MOPS, pH 7, 1mM DTT, 0.01% NaN<sub>3</sub>, 0.2 mM CaCl<sub>2</sub> and 0.15 M KCl) and dialysed overnight. The excess precipitate (TnT and TnI) were removed by centrifugation at 20000 rpm, 20 min.

The intact protein was purified by gel filtration using a Sephacryl 300 column (1.6x100 cm). The flow rate was 1ml/min and fractions of 3ml were collected. The purified proteins were checked on 15% SDS-PAGE for purity, pooled, 0-45% ammonium sulphate precipitated, re-suspended and dialysed against ATPase buffer (10 mM MOPS, pH 7.0, 140 mM KCl, 4 mM MgCl<sub>2</sub>, 1 mM DTT, 1 mM NaN<sub>3</sub>). The purity of proteins was checked by SDS/PAGE and estimated to be at least 90% and a final yield of ~10-12 mg per preparation was obtained.

## 2.4 Fluorescent Protein Labeling

### 2.4.1 Pyrene-labeled Actin Preparation

Actin was labelled with *N*-(1-pyrene) iodoacetamide on the Cys-374 as described previously by Criddle (Criddle, Geeves et al. 1985). Following the protocol for actin preparation up to the first high speed spin, the pellet was re-suspended in 5ml of pyrene labelling buffer at 1 mg/ml (25 mM Tris-HCl pH 7.5, 100 mM KCl, 2 mM MgCl<sub>2</sub>, 3 mM NaN<sub>3</sub> and 0.3 mM ATP). After determination of concentration using literature data: 38.5 μM actin / A<sub>280</sub>, the actin was diluted to 1mg/ml before incubating at room temperature for 4 hours with a 7-fold molar excess of pyrene iodoacetamide (dissolved in dimethyl formamide). The labelled reaction was spun down at 10000 rpm for 10 minutes on a SS34 rotor at 4°C to remove excess dye. The supernatant was ultracentrifuged at 42000 rpm for 2 hours on a T1250 rotor at 4°C, the pellet resuspended in 8 ml of G-buffer (5.5-6 mg/ml), and then dialysed for 48 hours. The labeled G-actin was further ultracentrifuged at 42,000 rpm for 90 minutes and the supernatant was loaded onto a S300 gel filtration column. The degree of pyrene labeling was determined by comparing the actin concentration at 290 ((A<sub>290</sub>-(A<sub>344</sub>\*0.127))\*

38.5  $\mu\text{M}/\text{OD}$  with the concentration of pyrene label at 344 ( $A_{344} \cdot 45.5 \mu\text{M}/\text{OD}$ ). The labeling ratio was between 85-95%.

#### **2.4.2 Pyrene-labelled Tropomyosin Preparation**

Pyrene labelled cardiac tropomyosin was prepared using the method described by Ishcii and Lehrer (Ischii and Lehrer 1987). This involved reducing tropomyosin at 3mg/ml with 20 mM DTT for 20 minutes at 40°C followed by exhaustive dialysis in 5 M Guanadine chloride, 30 mM MES pH 7 and 0.6 mM DTT. The reduced Tm was then reacted with 5 time molar excess of *N*-(1-pyrene) iodoacetamide for 2 hours at room temperature with rocking. The reaction was quenched with 20 mM DTT and centrifuged at 13,000 rpm for 5 min at room temperature. The sample was then exhaustively dialysed against renaturing buffer 5 mM MOPS pH 7.5, 1 M NaCl, 1 mM EDTA. The sample was then further dialysed against medium ATPase buffer. The solution was spun down at 12,000 rpm for 10 minutes at 4°C using a SS34 rotor. The concentration of Tm was determined by the Lowry method and pyrene was determined by using 45.5 $\mu\text{M}$  /OD at 344nm (Kouyama and Mihashi 1981). The degree of labeling should typically be in the range 1.8-2.2 pyrene to Tm.

#### **2.4.3 Preparation and IAANS Labeling of Troponin C**

A 5 fold excess of IAANS was added to purified C35S or C84S of cTnC (2 mg/ml) in 6 M urea, 150 mM KCl, 50 mM Tris-HCl pH 7.5 and 0.2 mM DTT and incubated in the dark at 25°C for 5 hours. The reaction was quenched with 10 mM L-cysteine and free label was removed by extensive dialysis into first reconstitution buffer prior to reconstitution of Tn as previously described in section 2.3.3. The amount of label incorporated was determined by the

absorbance at 325 nm using an extinction coefficient of 24900 adjusting for the absorbance of unlabeled TnC. The labeling ratio was between 90-95%.

## **2.5 General Methods**

### **2.5.1 Plasmid Mini and Midi Preps**

The cDNA encoding the troponin subunits and mutants were purified from JM109 competent cells using a Wizard<sup>®</sup> *Plus* Miniprep kit (Promega). Cells from a 5 ml overnight culture were pelleted (3x1.5 ml) in a micro-centrifuge for 5 minutes at 13000 rpm discarding the supernatant each time. The pellet was then re-suspended in the various buffers as described in the protocol provided in the kit with the exception of the elution step which was performed using sterile TE buffer. The DNA sample obtained was stored at -80°C.

### **2.5.2 Transformation**

1 µl of the desired expression construct DNA was transformed into 50 µl of calcium competent BL21(DE3)pLysS cells. The cells were mixed gently by flicking the tubes few times and with incubation on ice for 30 min. The cells were then heat shocked for 1 min without shaking in a water bath at exactly 42°C. The tubes were placed back in ice immediately for 2 min. The transformed cells were diluted into 400 µl of LB media and incubated at 37°C with shaking at 220 rpm for 90 minutes. The cell culture is thereafter spun down at 13,000 rpm for 15 s at room temperature and the pellet re-suspended in fresh 100 µl of LB media. The total culture was then spread on LB agar plates with appropriate antibiotics (Appendix A) and incubated at 37°C overnight.

### 2.5.3 Glycerol Stocks

A single colony was picked up from a transformation plate and placed into 5 ml LB containing the appropriate antibiotics. The cells were incubated for 5-6 hours at 37°C at 200 rpm. The 5 ml day culture was diluted into 5 ml of 20% glycerol-80% LB solution. The culture was distributed into 1ml aliquots and stored at -80°C.

### 2.5.4 Determination of Protein Concentration

Protein concentrations were routinely measured spectrophotometrically using a Varian Cary 50 spectrophotometer. Samples were scanned from 340 nm to 220 nm so that a correction for turbidity could be made. The table below (Table 2.1) gives the absorption coefficients used for each proteins used in this project.

**Table 2.1 Absorption coefficients of sarcomere proteins**

Protein	Absorbance at 280nm (1 mg/ml)
Myosin	0.54
Subfragment 1	0.79
Actin	1.15
Tropomyosin	0.33
Troponin	1.3

For fluorescently labelled proteins the concentration was determined by the Lowry method (Lowry, Rosebrough et al. 1951). Small aliquots (1-100 µl) of the test protein solution or dilutions of it were added to 1 M NaOH to give a final volume of 0.5 ml. 5 ml of solution A (1 ml 0.5% CuSO<sub>4</sub> + 1 ml K<sup>+</sup>Na<sup>+</sup>tartrate + 48 ml 2% Na<sub>2</sub>CO<sub>3</sub>) was added to each tube and the solution mixed. After 10 minutes, 0.5 ml of solution B (Folin and Cioculteau's phenol reagent in water,

1:1 (v / v)) was added, the solution was mixed and then left for 30 minutes. Protein was detected by the development of a blue colour. The quantity of protein was determined by measurement of the absorbance at 700 nm using a spectrophotometer..

### **2.5.5 Polyacrylamide Gel Electrophoresis**

Proteins were resolved by electrophoresis comprising a 12% separating gel with a 4% stacking gel (see Appendix C) and run under the same conditions described by Laemmli (Laemmli 1970). Samples were diluted with an equal volume of 2x SDS sample buffer and boiled for 3-5 minutes prior loading. The gels were run using the Biorad minigel system at 25 mA and 200 V until the dye front reached the end of the gel. The gels were removed, washed immediately in deionised water before immersing in Coomassie blue staining solution for 30 minutes. The gel was then destained in several changes of Coomassie destain solution until the background was clear.

### **2.5.6 Agarose Gel Electrophoresis**

0.6g of agarose was dissolved in TAE buffer (60 ml) using a microwave until completely dissolved. After cooling to about 50°C, ethidium bromide solution to a final concentration of 0.5 µg/ml was added. The gel was poured into a casting tray with a well comb and allowed to set at room temperature. The set gel is then inserted into the electrophoretic chamber and covered in 1XTAE buffer. Samples were diluted in DNA loading buffer and electrophoretically resolved, by comparison with a DNA size standard (1kb plus ladder, Invitrogen). The gel was run at 100mA and the DNA visualised under UV light.

### **2.5.7 Cosedimentation Assay**

The assay was performed by mixing 6  $\mu$ M actin with 1  $\mu$ M tropomyosin in the presence of 1  $\mu$ M troponin complex in a final volume of 1 ml of ATPase buffer. The samples were then incubated for at least 30 minutes at room temperature before pelleting by centrifugation at 85,000 rpm for 20 minutes on a Beckman TLA110 rotor. Equivalent samples of the pellets and supernatants were then analysed on a 12% SDS-PAGE gel (Laemmli 1970) which was then stained with Coomassie Blue R250.

## **2.6 Determination of Actomyosin $Mg^{2+}$ ATPase Activity**

ATPase measurements were carried out on actomyosin reconstituted with actin, tropomyosin and troponin. The above mixtures were incubated in a final volume of 100  $\mu$ l with ATPase buffer. Assay blanks contained S1 only. The reaction was started by the addition of 5  $\mu$ L of 100mM MgATP at timed intervals and the mixtures were incubated for 10-20 minutes at 25°C. The assay was stopped by addition of 0.5 ml of 10% TCA. Precipitated protein was sedimented by centrifuging for 3 minute at 13,000 rpm after which 0.5 ml of the supernatant was withdrawn and placed in a test tube for determination of free inorganic phosphate ( $P_i$ ) by the method of Taussky and Schorr (Taussky and Schorr 1953). For each 500  $\mu$ l aliquot to be analysed, 1ml of 1% ammonium molybdate in 0.5 M  $H_2SO_4$  was added and vortexed, followed by 0.5 ml of freshly prepared 10 g  $FeSO_4 \cdot 7H_2O$  dissolved in 25 ml 0.5M  $H_2SO_4$  and left for 5 minutes for the

blue coloration to develop. Standards containing 0, 65 and 130 nmoles of inorganic phosphate were processed in the same way.

### 2.6.1 Measurements of Acto-S1 ATPase

By calibrating the spectrophotometer at 700nm to zero using buffer without inorganic phosphate to blank, and the standard phosphate solution (0.65mmol/l Pi) to read the 65 and 130 nmole, the amount of phosphate in each assay tube could be measured. The equations below were used to work out the optical density per nmole of Pi.

$$\text{Average OD per nmoles of Pi} = \left[ \left( \text{OD}_{700} \text{ for } 100\mu\text{L of Pi} / 65\text{nmoles of Pi} \right) + \left( \text{OD}_{700} \text{ for } 200\mu\text{L of Pi} / 130\text{nmoles of Pi} \right) \right] / 2 \quad (1)$$

The OD measured for S1 only and its contribution to the total  $P_i$  release should be subtracted from the acto-S1 OD. This difference divided by the average OD per nmole of Pi determines the amount of Pi produced from the acto-S1 ATPase. A volume correction had to be made since the OD measured was for a 0.5 ml reaction as opposed to the actual total quenching volume of 0.6 ml. To work out the rate at which ATP hydrolysis occurs we must divide the amount of nmoles produced by the total reaction time in seconds. The ATPase rate was expressed as nmoles of Pi per second.

$$\text{ATPase rate} = \text{nmoles of Pi produced} \times \left( \frac{6}{5} \times \frac{1}{\text{reaction time}} \right) \quad (2)$$

## 2.7 Circular Dichroism

CD measurements were recorded on a Jasco –J715 spectropolarimeter using a cell path length of 0.1cm at 4°C and 25°C in a 10 mM sodium phosphate, pH 7.0 and 0.3 M NaF solution. Spectra were recorded at 190-250 nm in the far UV region with a bandwidth of 1nm at a speed of 50 nm per min at a resolution of 1 nm. 10 scans were averaged, baseline corrected and no numerical smoothing was applied. The concentration of human cardiac wild type TnT and mutants were determined by Qubit kit at 5 μM. The mean residue ellipticity ( $[\theta]_{\text{MRE}}$ , degrees.cm<sup>2</sup>/dmol) for spectra were calculated utilising the same Jasco system software using the following equation:

$$[\theta]_{\text{MRE}} = [\theta]_{222} = -30300 f_{\text{H}} - 2340 \quad (3)$$

where  $f_{\text{H}}$  is the fraction of  $\alpha$ -helical content ( $f_{\text{H}} \times 100$  expressed in %). Spectra are presented as the mean residue ellipticity.

Thermal stability measurements were made by following the molar ellipticity of troponin T and complex at 222 nm as a function of temperature in buffer containing 0.3 M NaF, 10 mM sodium phosphate, pH 7.0. Data were obtained at 1.0 °C intervals from 5 to 90 °C using a protein concentration of 0.1 mg/ml. The molar ellipticity was normalized (10°C = 1, 90°C = 0) to give fraction folded.

## **2.8 Enzyme Kinetics**

### **2.8.1 Transient State Kinetic Measurements**

The Hi-tech Scientific SF61 stopped flow apparatus equipped with a 100 watt Xe/Hg lamp was used for all transient kinetic measurements. KinetAsyst software package was used for the analysis of the data. The apparatus can be used in single or double mixing modes. Upon initialisation of the system, the default condition of single mixing was selected for most of the experiments. The desired excitation wavelength was selected using the 'manual set up' option. The Live Display was used to maximise the signal by adjusting the photomultiplier voltage. Once the excitation wavelength is set up and the signal optimised, the run time and the channel used could be adjusted from the Acquire Control Panel.

#### **ATP Induced Myosin S1 Dissociation from Actin Thin Filament – Switch between Closed to Open State**

Lehrer and Geeves used the excimer fluorescence of pyrene labelled tropomyosin ( $Tm^*$ ) to monitor the kinetics of the ON/OFF state change of actin. $Tm^*$  filaments (Lehrer and Geeves 1998). The measurement of the excimer fluorescence signal was carried out at excitation wavelength of 364 nm and was detected after passing through a GG455 nm cut off filter to remove the light scattering and monomer fluorescence. Light scattering was observed at  $90^\circ$  to the incident beam using excitation wavelength of 364nm and UG-5 filter (light over 400 nm was cut off). The measurements were carried out in ATPase buffer at  $20^\circ\text{C}$  (10 mM PIPES, pH 7.2, 140 mM KCl, 5 mM  $\text{MgCl}_2$ , 1 mM DTT, 1

mM NaN<sub>3</sub>) unless otherwise stated. The temperature of the stopped flow machine was maintained within 0.1°C during the course of the experiment. All buffers were filtered and all proteins were clarified by centrifugation in a refrigerated bench top centrifuge for 10 minutes at 16000 rpm just before use. Usually between 4 and 10 transients were collected and averaged. The average data was then fitted to one or two exponential equations by a non linear least square curve fit using the 'Fit control Panel' of the Fit Asystant. The concentrations of the reactants stated are those in the stopped flow observation cell after mixing. On mixing actin.Tm\* with excess S1 the observed rate constant for light scattering  $k_{LS}$  which monitors S1 binding to actin and the observed rate constant for excimer fluorescence  $k_{FL}$  differs by 'n'. A good estimate of the value of 'n' can be obtained by super-imposing computer generated curves at the various different values of 'n' on the experimental curve and using the equation:

$$f_{on} = 1 - \left(1 - \exp(-k_{LS}t)\right)^n \quad (4)$$

### **Kinetics of S1 Binding to Thin Filament**

For 'n' actin subunits in a cooperative unit, the rate of S1 binding is slower than the rate of transition from the OFF state to the ON state by a factor of 'n' and the  $k_{obs}$  of the fluorescence (monitoring the switch) will be n times the  $k_{obs}$  of the light scattering (monitoring S1 binding). The rate constant of S1 binding monitored by light scattering was compared to the rate constant of change in state between closed and open which was monitored by excimer fluorescence of pyrene labeled Tm at 2.1 mol pyrene/Tm.

The reaction was pseudo first order with respect to S1 and  $k_{\text{obs}}$  for light scattering were linearly dependent upon S1 concentration. The fluorescence signal was fitted to two kinetic components that were fit by two exponentials.  $k_{\text{obs}}$  were linearly dependant on S1 concentration.

### **Myosin S1 Binding to Actin Thin Filament – Switch between Blocked and Closed States**

In the simplest experiment, a large excess of actin is rapidly mixed with a small amount of S1 (1/10<sup>th</sup>) and the kinetics of binding of S1 to pyrene labelled actin in the presence and absence of Ca<sup>2+</sup> (Head, Ritchie et al. 1995) was followed. The exponential change in fluorescence is observed which allows us to determine  $K_B$  from the relationship:

$$k_{\text{obs}}(-\text{Ca}^{2+})/k_{\text{obs}}(+\text{Ca}^{2+}) = K_B/(1+K_B) \quad (5)$$

$$k_{\text{obs}}(-\text{Ca}^{2+})/k_{\text{obs}}(\text{actin}) = K_B/(1+K_B) \quad (6)$$

### **Calcium Dissociation Kinetics Measurements**

For measurements of IAANS fluorescence, the excitation monochromator was set at 334 nm and the emitted light was isolated at right angle by a cut off filter GG400. In this typical binding experiment, one syringe contained Actin.Tm.Tn<sub>IAANS</sub>.S1 in the ratio of 21:4:4:8  $\mu\text{M}$  in the standard buffer (140 mM KCl, 4 mM MgCl<sub>2</sub>, 50 mM MOPS pH 7.2) containing 50  $\mu\text{M}$  CaCl<sub>2</sub>. The other

syringe contained the same solution without the proteins and added 1 mM EGTA. These conditions ensured that the two C-terminal high affinity Ca/Mg sites were presaturated with  $Mg^{2+}$  while the single low affinity  $Ca^{2+}$  specific site was saturated with  $Ca^{2+}$ .

To directly measure the  $Ca^{2+}$  dissociation the experiments were repeated using Quin-2 fluorescence. The excitation wavelength was 334nm and the emission was measured with a GG455 cut-off filter. In these measurements the  $Ca^{2+}$  dissociation was monitored by the increase of Quin-2 fluorescence. The same buffer conditions as for the IAANS labelled Tn experiment were used except the other syringe contained 150  $\mu M$  Quin-2 instead of 1mM EGTA. The traces obtained were an average of 6-8 shots and the resulting tracing was fitted to a sum of exponentials by a non-linear least-squares method.

## **2.8.2 Equilibrium Kinetic Measurements**

### **S1 Binding to Thin Filament Titration**

Simultaneous measurements of fluorescence and light scattering were carried out by titration of actin.Tm with increasing concentration of S1. In this experiment, we premixed actin.Tm at a molar ratio of (6:1) and titrated by step wise addition of a stock solution of 100  $\mu M$  S1 to a 2 ml volume at 1 minute intervals. Fluorescence intensities and protein concentrations were corrected for the volume change (< 10%) due to addition of S1. Light scattering for S1 alone was measured and subtracted from the thin filament data. All data were normalised with zero being the start of the titration and 1 the plateau point.

The cooperative unit size was determined by the fractional change in the excimer fluorescence ( $F_{open} = \Delta F_{excimer} / \Delta F_{excimer \text{ maximum}}$ ) plotted against the amount of S1 bound to actin as determined from the light scattering data. The data was fitted to the equation:

$$F_{on} = 1 - (1 - F_{bound})^n \quad (7)$$

### **Ca<sup>2+</sup> Binding Measurements**

For WT and mutant Tn measurements cTnC was labelled with IAANS at Cys 35 and Cys 84 as described in section 2.4.3. TnI, TnT and labelled TnC were then reconstituted as described above in section 2.3.3. However, the complex underwent final dialysis in experimental buffer (50 mM MOPS, 140 mM KCl, 4 mM MgCl<sub>2</sub> and 1 mM EGTA at pH 7.2). To obtain reconstituted thin filament we used two methods: 1) mixed 21  $\mu$ M actin, 3  $\mu$ M Tm and 3  $\mu$ M labelled troponin or 2) 21  $\mu$ M actin mixed in with excess Tm·Tn was cosedimented and resuspended to desired volume in experimental buffer. The free Ca<sup>2+</sup> concentration was calculated using Maxchelator programme WINMAXC version 2.0. The titrations were carried out by the addition of a concentrated stock solution of 20 mM CaCl<sub>2</sub> into a 2 ml volume cuvette which is constantly stirred by a magnetic stirrer. The change in fluorescence was monitored with the final  $\Delta F$  values adjusted for the difference in assay mix volume following each incremental addition. The adjusted and normalised  $\Delta F$  was plotted as a function of Ca<sup>2+</sup> concentration and the following equation was used to analyse the titration curve:

$$\Delta F_i = \sum \Delta F_{max} X \left( (X^{nH}_i) / (K^{nH}) \right) / 1 + \left( (X^{nH}_i) / (K^{nH}) \right) \quad (8)$$

where  $\Delta F_i$  is the total fluorescence signal change after  $i$ th addition of stock of  $\text{Ca}^{2+}$  solution,  $X_i$  is the free  $\text{Ca}^{2+}$  concentration after  $i$ th addition and  $n_H$  and  $K$  are the Hill coefficient and association constant for a  $\text{Ca}^{2+}$  binding site respectively.  $\Delta F_{\max}$  is the maximum fluorescence change.

**Table 2.2 Ca<sup>2+</sup>EGTA buffer**

[Ca] mM	[Ca] <sub>free</sub>	pCa	Volume of 40mM CaCl <sub>2</sub> μL	Volume Added μL	Volume Correction μL
0.05000	4.82E-09M	8.32	2.5	2.5	2002.5
0.10000	9.89E-09M	8.00	5	2.5	2005
0.20000	2.09E-08M	7.68	10	5	2010
0.30000	3.32E-08M	7.48	15	5	2015
0.40000	4.71E-08M	7.33	20	5	2020
0.50000	6.28E-08M	7.20	25	5	2025
0.60000	8.08E-08M	7.09	30	5	2030
0.70000	1.01E-07M	7.00	35	5	2035
0.80000	1.26E-07M	6.90	40	5	2040
0.90000	1.55E-07M	6.81	45	5	2045
1.00000	1.89E-07M	6.72	50	5	2050
1.10000	2.31E-07M	6.64	55	5	2055
1.20000	2.86E-07M	6.54	60	5	2060
1.30000	3.54E-07M	6.45	65	5	2065
1.40000	4.45E-07M	6.35	70	5	2070
1.50000	5.72E-07M	6.24	75	5	2075
1.60000	7.63E-07M	6.12	80	5	2080
1.70000	1.07E-06M	5.97	85	5	2085
1.80000	1.71E-06M	5.77	90	5	2090
1.90000	3.52E-06M	5.45	95	5	2095
1.95000	1.20E-05M	4.92	97.5	2.5	2097.5
2	1.99E-05M	4.70	100	2.5	2100
2.05	5.75E-05M	4.24	102.5	2.5	2102.5
2.1	1.04E-04M	3.98	105	2.5	2105

Buffer conditions: 140mM KCl, 4mM MgCl<sub>2</sub>, 50mM MOPS, 1mM EGTA at pH 7.2

# **CHAPTER 3**

Production and Characterisation of TnT  
Mutations

# Contents

<b>3.1</b>	<b>Introduction</b>	<b>81</b>
<b>3.2</b>	<b>Results</b>	<b>84</b>
<b>3.3</b>	<b>Discussion</b>	<b>102</b>

### 3.1 Introduction

Troponin subunits were first isolated by Greaser and Gergely in the late 1960s from rabbit skeletal muscle and separated into TnT, TnI and TnC. The first clue as to the involvement of  $\text{Ca}^{2+}$  and Tn in regulation of muscle contraction came from studies on activation of actomyosin ATPase (Weber and Winicur 1961). Shortly after their discovery it was established that Tn subunits played an obvious role in the  $\text{Ca}^{2+}$  regulation of muscle contraction and the nature of these interactions as well as the factors that influence them were critical to understanding the mechanism of muscle contraction (Ebashi and Ebashi 1965).

Regulation of muscle contraction requires the participation of Tm and Tn components with TnT being the most enigmatic of the components. TnT has 3 main roles: (i) it anchors the Tn complex to thin filament via Tm. (ii) it increases the cooperativity of actin-Tm interaction and (iii) it sensitises the actin-activated myosin-S1 ATPase in a calcium dependent fashion. Because of its interaction with TnI, TnC, Tm and actin, TnT has been extensively studied (Potter, Sheng et al. 1995; Perry 1998; Tobacman, Nihli et al. 2002). Furthermore mutations in TnT result in familial HCM (Thierfelder, Watkins et al. 1994; Watkins, McKenna et al. 1995) and DCM (Fujino, Shimizu et al. 2002; Robinson, Mirza et al. 2002)). In order to investigate the functional implications of these TnT mutations, expression of sufficient amount of TnT mutants and reconstitution with TnI and TnC into a fully functional trimeric Tn complex is necessary. Successful sub-cloning of the isolated Tn subunits into an inducible expression vector had been reported and expression was found to generate a Tn complex

essentially indistinguishable from the native tissue purified protein (Bottinelli, Coviello et al. 1998).

In our initial studies we adopted the previously established expression and isolation procedure for Tn as described in Chapter 2.3. This is based on expressing and purifying each subunit individually before reconstituting into a trimeric complex. However this procedure is not only time consuming but also generated Tn which often failed to remain stable. We then established a shortened method that allowed successful purification and characterisation of the chosen 7 mutations.

The first step was to determine the functional and structural effects of the recombinant TnT mutations causing HCM and DCM that have not been fully addressed. In order to answer these questions, we performed reconstituted ATPase activity, co sedimentation and spectroscopy assays.

In the presence of 100% HCM and DCM TnT mutations, we evaluated the ability of Tn to activate and inhibit the ATPase activity measured in the presence or absence of  $Ca^{2+}$  in an actomyosin.Tm.Tn reconstituted complex. We also evaluated the effect of TnT mutations on the  $Ca^{2+}$  sensitivity of actomyosin ATPase.

In addition we used co-sedimentation assay to assess the the effect of these mutations on the binding of the Tn complex to actin.

Finally we used circular dichroism to analyse the effect of mutations on the structure of troponin T alone and within the whole troponin complex.

Overall the results from this chapter show that we can obtain sufficient quantities of all seven troponin T mutants and the wild type. Co-sedimentation assay and circular dichroism measurements suggest that the overall folding is preserved and that interaction of actin is not substantially compromised.

## 3.2 Results

### 3.2.1 Cloning and Expression of TnT Mutations

The construct DNAs in pET expression vectors for wild type human cardiac TnT, TnI and TnC were obtained as a gift from Dr. C. Redwood (University of Oxford, UK), Dr. N. Brand (Imperial college, UK) and Prof. K. Jacquet (Clinic of the Ruhr-University of Bochum, Germany) respectively. Our initial expression trials showed that the expression levels were very low as has been reported previously (Lohmann, K et al 2001). In order to achieve expression at higher levels, we subcloned the cDNA into pLEIC05 expression vector (see Appendix C). Overlap extension PCR was then carried out by Dr. Xiaowen at the University of Leicester. We have designed the primers for the construction of several TnT mutations using the human cardiac troponin T (TNNT2) sequence with a minimum of 15 base pairs on either side of the mutation to ensure coding of the protein is in frame (Appendix D). The identities of the TnT mutations were verified by DNA sequencing.

Initially we tested the level of expression of the seven mutations (as described in Chapter 2). We monitored the protein expression levels for wildtype and mutant TnT at 25°C and 37°C. Cell lysates were analysed by SDS-gels and we monitored the time dependent increase in intensity of the troponin T band at 37 kDa molecular weight. Figure 3.1 shows the comparison of expression levels at both temperatures. No band is visible at 37kDa in Lane 1 before induction. Lanes 2-7 are cell lysates taken every hour between the 2<sup>nd</sup> and the 6<sup>th</sup> hour and then overnight. The highest expression was seen after 4 hours at 25°C and 2 hours at 37°C. However at 37°C substantial degradation of troponin T

occurred even after 2 hours of incubation (indicated by the lower arrow in Figure 3.1). After 3-4 hours of expression more than half the troponin T was degraded. In contrast degradation was minimal at 25°C and after 6 hours only minute amount of degradation was observed at 25°C. We therefore decided to use .6 hours of expression at 25°C as our standard method for expression of troponin T wild type and mutants. Test expression for Troponin I and C were also performed in our lab (By Sameeh Al-Sarayreh) and the best expression was found to occur at 37°C and 3-4 hours.

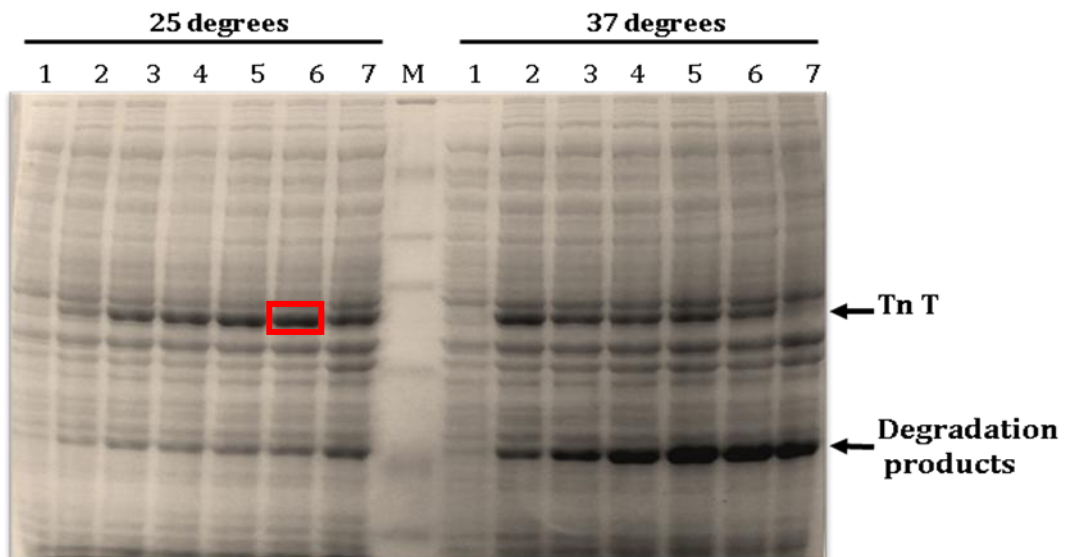


**Figure 3.1 Test expression of TnT subunit**

*Lanes: 1, non-induced; 2,3,4,5,6 induced and expression after 2,3,4,5 and 6<sup>th</sup> hour and 7, overnight. Left and right panel show expression of cells grown at 25°C and 37°C respectively. The arrow indicates TnT band and the red box the highest expression. M: marker: 250,148,98,64,50,36,22,16,6 and 4 in kDa*

### 3.2.2 Reconstitution of Troponin Complex

Following previously described techniques of purification of individual Tn subunits before reconstitution, was not only time consuming (4 weeks to obtain the purified troponin complex) but the obtained troponin complex was only

stable for a day or two (Redwood, Lohmann et al. 2000; Robinson, Mirza et al. 2002). As our studies involved producing 7 TnT mutations, this strategy was not viable.

We employed a methodology that involved reconstitution of the subunits following cell disruption and clarification by centrifugation. We reasoned that since all three subunits (T, I and C) were expressed in *E. coli*, the contaminants are likely to be the same in their *E.coli* cultures. Hence purifying each one of the Tn subunits separately before reconstitution has limited benefit while lengthening the procedure substantially. Instead we reconstituted the Tn subunits before purification using a ratio of 3I TnT: 2I Tn I: 1I TnC and subsequently purified the troponin complex (Lanes 1, 2 and 3 corresponding to TnT, TnI and TnC respectively in Figure 3.2. Successive stepwise dialysis was carried out as described in literature (Redwood *et al.* 2000). The supernatant from the last dialysis step was then precipitated using 0-30% ammonium sulphate. The subsequent supernatant (Figure 3.2, Lane 4) was then further precipitated to 50% using ammonium sulphate which contained Tn in the pellet (Figure 3.2, Lane 5). Due to large quantities of other bacterial proteins and traces of nucleic acid, we purified Tn by gel filtration (Figure 3.2, Lane 6). A yield of 10-15 mg was obtained from a typical purification.

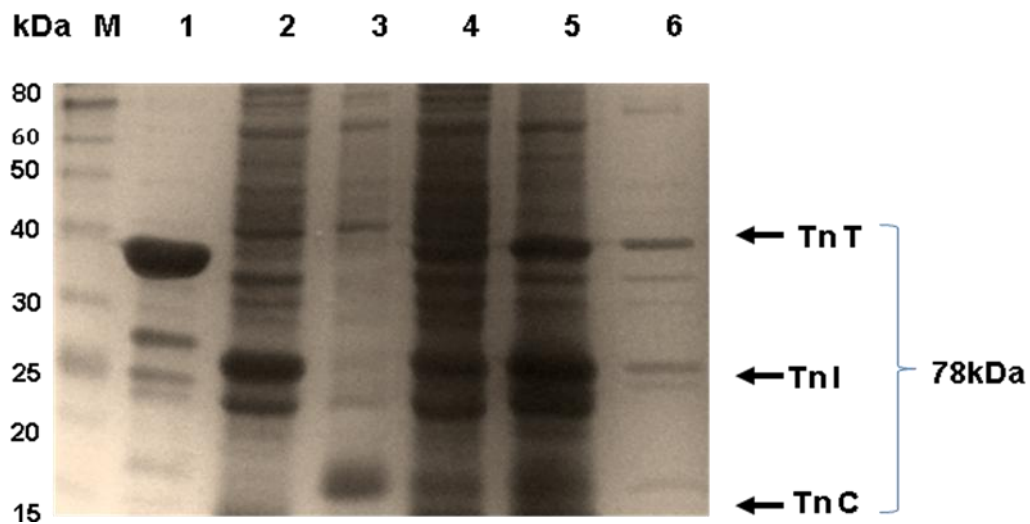


**Figure 3.2 Purification of cTn from *E. coli*.**

12% SDS showing the stages of purification are presented. For comparison Lanes 1, 2 and 3 are aliquots of the soluble fractions of T, I and C after cell lysis. Lanes 4 and 5 are aliquots of the 0-30% ammonium sulphate supernatant and 30-50% pellet (crude Tn) Lane 6 is the purified Tn after gel filtration.

### 3.2.3 Acto-S1 ATPase Assays of TnT Mutations

We aimed to check the activities of all the proteins and to show the capacity of the cTn complex to activate or inhibit actomyosin ATPase activity in the presence or absence of calcium respectively. In this study we used pre-formed, WT and 100% TnT mutants in an actin.Tm.Tn.S1 reconstituted system with Tn concentrations ranging between 0.25-3  $\mu\text{M}$ . Maximum activation was seen at the expected functional unit ratio of 7:1:1 suggesting that our purification procedure did not affect Tn ability to inhibit and activate the actomyosin ATPase. The actomyosin ATPase activity in the absence of Tn (actin.Tm.S1) was taken to be the basal activity level for both activation and inhibition and was set at 100%. The basal activity for S1 alone was found to be at 0.06  $\text{s}^{-1}$ . Under the standard ATPase assay conditions the reported assay activity measured for

recombinant wild type Tn was about 180-200% activation and 70-80% inhibition (Venkatraman, Harada et al. 2003; Mirza, Marston et al. 2005).

Figure 3.3 shows the ATPase activity of (A) DCM (B) T1-HCM and (C) T2-HCM mutations in the presence and absence of calcium. DCM mutations R141W and  $\Delta$ K210 reduced the activation of the reconstituted thin filament to 165 and 132% respectively. Previous work carried out on  $\Delta$ K210 showed similar results (Robinson et al. 2002). The activation values for Tn containing S179F,  $\Delta$ 14 and  $\Delta$ 28+7 were 171%, 170%.and 139% respectively.  $\Delta$ E160 and K273E on the other hand increased  $\text{Ca}^{2+}$  activation to 215% and 255% respectively. The inhibition of ATPase activity as a function of Tn concentration in the absence of  $\text{Ca}^{2+}$  did not show any significant changes for R141W,  $\Delta$ K210,  $\Delta$ E160 and S179F complexes compared to WT but was reduced substantially for HCM-T2 mutations- K273E,  $\Delta$ 14 and  $\Delta$ 28+7. Table 3.1 summarises the maximal ATPase rates as a percentage of total activation and inhibition.

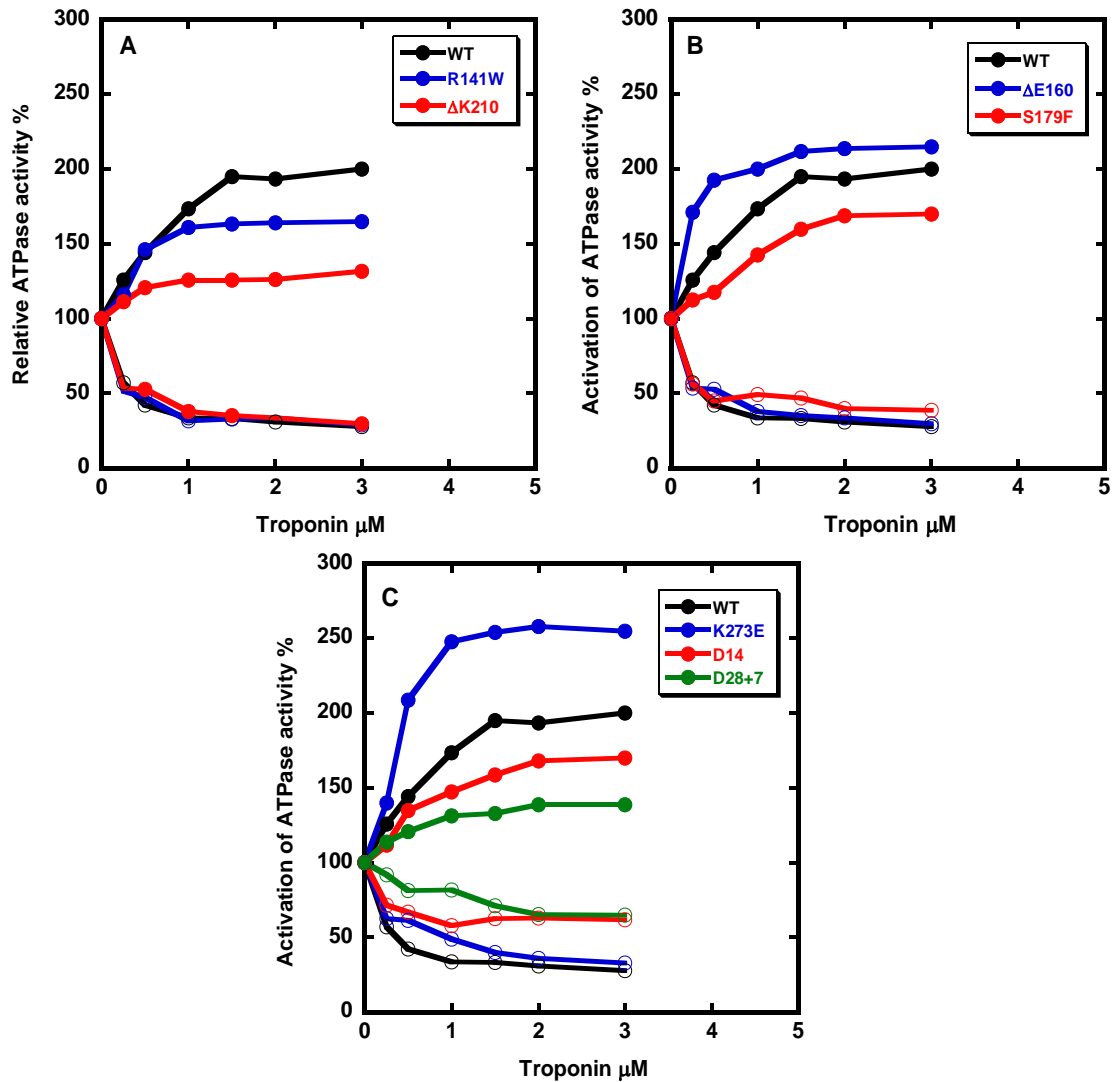


**Figure 3.3 Actin-Tm activated Myosin-S1 ATPase by cTnT mutants in the presence and absence of calcium.**

Activation and Inhibition of acto-S1 ATPase for (A) DCM (B) T1-region HCM and (C) T2-region HCM mutations reconstituted in thin filament at increasing ratios of Tn complex. The assay conditions are as follows: 14 μM actin, 2 μM Tm, 1 μM S1 were dissolved in 22 mM KCl, 4 mM MgCl<sub>2</sub>, 0.2 mM CaCl<sub>2</sub> (for activation assay) and 1 mM EGTA (for inhibition assay), 5 mM ATP, 1 mM DTT, 10 mM MOPS, pH 7.2. The myosin ATPase that occurs in the absence of Tn complex is considered 100% ATPase activity. The specific ATPase activity, in the absence of Tn was measured as 0.66 nmoles Pi/S1/s<sup>-1</sup>. 3 experiments were performed and are expressed as an average.

**Table 3.1 Summary of maximal ATPase activity by Tn complexes**

<b>TnT complex</b>	<b>Activation %</b>	<b>Inhibition %</b>
WT	198±7	72±8
TnT1-R141W	165±19	71±3.5
TnT2-ΔK210	132±9	70±14
TnT1-ΔE160	215±13	70±7
TnT1-S179F	171±38	59±8.5
TnT2-K273E	255±31	67±15
TnT2-Δ14	170±7	38±11
TnT2-Δ28+7	139±20	35±5

### **3.2.4 Acto-S1 pCa Curves of TnT Mutations**

The effect of DCM and HCM mutations on the  $\text{Ca}^{2+}$  concentration dependence of Tn regulation of actomyosin ATPase was determined. Figure 3.4 shows a representative normalised pCa-ATPase curve comparing thin filaments containing wildtype and mutant Tn. The data were fitted to the Hill equation and the  $\text{pCa}_{50}$  and  $n_H$  were determined (Table 3.2).

For WT thin filament the  $pCa_{50}$  obtained was 5.86 compared to literature values ( $pCa_{50}$  was 6.44 for ATPase, 6.69 for fraction of thin filaments motile, and 6.35 for filament velocity).

DCM mutations demonstrated opposite effects in the shift of the  $pCa$  curve compared to WT. The  $pCa_{50}$  was 5.81 for R141W and 5.92 for  $\Delta$ K210. All HCM mutations caused a leftward shift of the  $pCa$  curve. The increase in  $pCa_{50}$  was in the range 0.1-0.15 (HCM-T1 mutants) to 0.25-0.65 (HCM-T2 mutants). The largest increase in  $Ca^{2+}$  sensitivity was seen for S179F with a leftward shift to  $pCa_{50}$  5.93. The Hill coefficient  $n_H$ , which is a measure of cooperativity of activation by  $Ca^{2+}$  did not change noticeably except for in K273E which showed a higher degree of cooperativity.

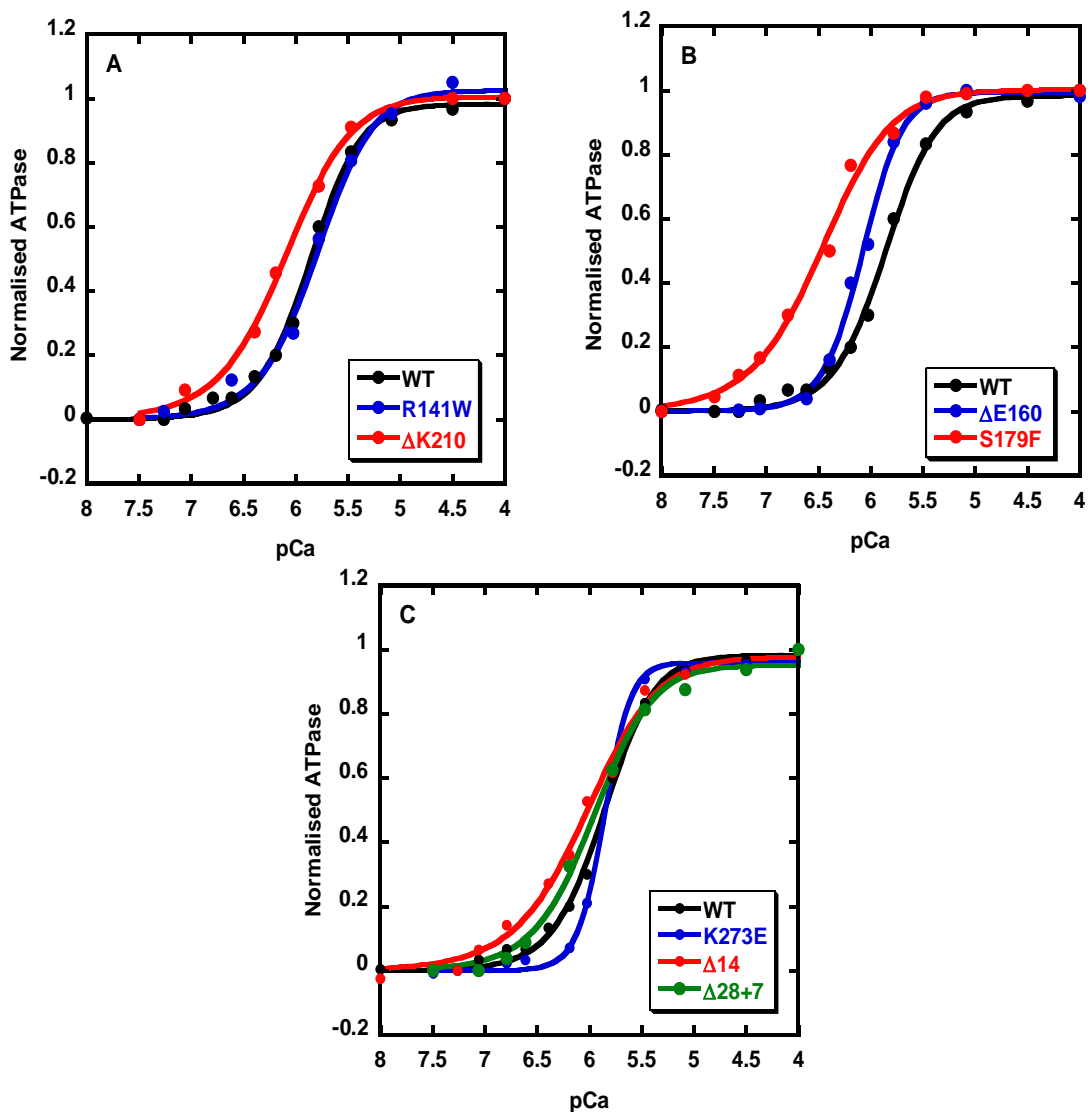


**Figure 3.4 Effect of HCM-T1 mutants on  $\text{Ca}^{2+}$  dependent Actin.Tm activated S1 ATPase activity**

Normalised ATPase as a function of pCa (A) DCM (B) T1-region HCM and (C) T2-region HCM mutations reconstituted in thin filament. The experiments were performed using  $14\mu\text{M}$  actin,  $2\mu\text{M}$  Tm,  $4\mu\text{M}$  Tn and  $1\mu\text{M}$  S1 and  $5\text{mM}$  ATP in  $50\text{mM}$  MOPS,  $10\text{mM}$  KCl,  $4\text{mM}$   $\text{MgCl}_2$ ,  $1\text{mM}$  DTT,  $0.2\text{mM}$   $\text{NaN}_3$  and  $2\text{mM}$  EGTA pH 7.2,  $25^\circ\text{C}$ . The basal ATPase activity at pCa 8 was considered 0% and the maximal ATPase activity at pCa 4 to be 100%. The rate of S1 alone was subtracted from the measured rates.

**Table 3.2 Summary of the effect of cTnT mutations on the Ca<sup>2+</sup> binding dependent actin-activated acto-S1 ATPase activity**

cTnT	pCa <sub>50</sub>	n <sub>H</sub>	ATPase Rate s <sup>-1</sup> pCa 4.0	ATPase Rate s <sup>-1</sup> pCa 7.5
WT	5.85	1.4	0.44	0.14
TnT1-R141W	5.8	1.3	0.31	0.1
TnT2-ΔK210	6.1	1.3	0.22	0.11
TnT1-ΔE160	6.1	1.5	0.43	0.19
TnT1-S179F	6.5	1.3	0.31	0.22
TnT2-K273E	5.9	1.7	0.4	0.18
TnT2-Δ14	6.0	1.2	0.32	0.24
TnT2-Δ28+7	6.0	1.3	0.35	0.26

The numbers are expressed as a single experiment

### 3.2.5 Co-sedimentation of TnT Mutations with Thin Filament

Since the ATPase assays showed that some TnT mutations affected the activatory and inhibitory effects of Tn in ATPase, we aimed to assess the effects of cTnT mutations on the ability of Tn to interact with actin.Tm. The thin filament proteins were premixed at a ratio of 7:2:2 Actin:Tm:Tn and ultra-centrifuged as detailed in section 2.5.7. 15% SDS-PAGE analysis of WT and mutant filaments showed no discernible changes in the ability of the Tn complexes to bind to actin.Tm and TnT co-migrated with actin. No changes were seen in the protein

content in the pellet (P) and supernatant (S) between Tn complexes containing CTnT in WT and mutants (Figure 3.5).

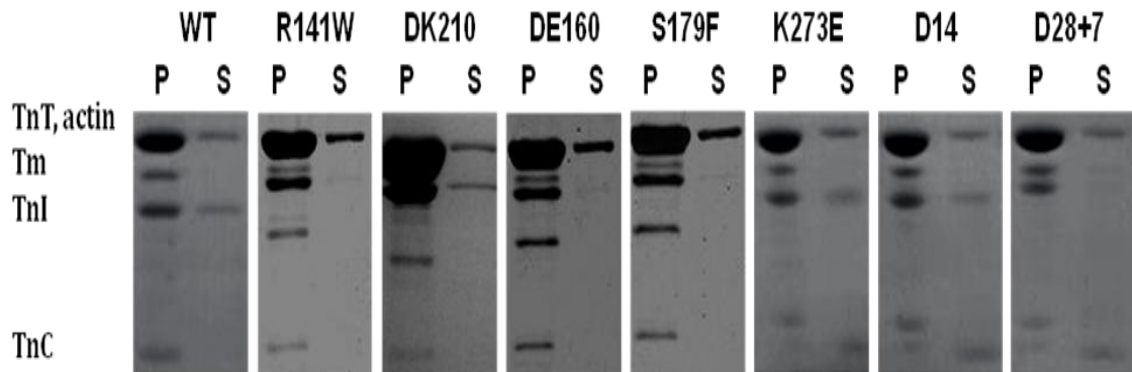


**Figure 3.5 Co-sedimentation of WT and mutant Tn to Actin-Tm.**

*From left to right pellets(P) and supernatants (S) are shown: Lanes 1-2 wild type;3-4 R141W;5-6  $\Delta$ K210; 7-8  $\Delta$ E160; 9-10 S179F; 11-12 K273E; 13-14  $\Delta$ 14; 15-16  $\Delta$ 28+7. Conditions: Thin filaments reconstituted using 7 $\mu$ M actin, 1 $\mu$ M Tm, and 1 $\mu$ M Tn in 20mM MOPS, 140mM KCl, 3.87mM MgCl<sub>2</sub>,0.1mM CaCl<sub>2</sub> and 1mM DTT (pH 7.2) for 30mins and ultracentrifuged at 85,000rpm for 30mins at 20 °C. Samples were run on 15% SDS-PAGE.*

### 3.2.6 Circular Dichroism of TnT Mutations

In this set of experiments we addressed whether the DCM and HCM mutations affected the secondary structure and the overall characteristics of the folding of protein for TnT subunit alone and in its complex with TnI and TnC.

The secondary structure was determined by CD spectroscopy as described in section 2.7 of Chapter 2. In the far UV spectral region (190-250nm) the chromophore is the peptide bond, and the signal arises when it is located in a regular, folded environment.

Alpha-helix, beta-sheet, and random coil structures each give rise to a characteristic shape and magnitude of the CD spectrum as illustrated in the graph below (Figure 3.6).

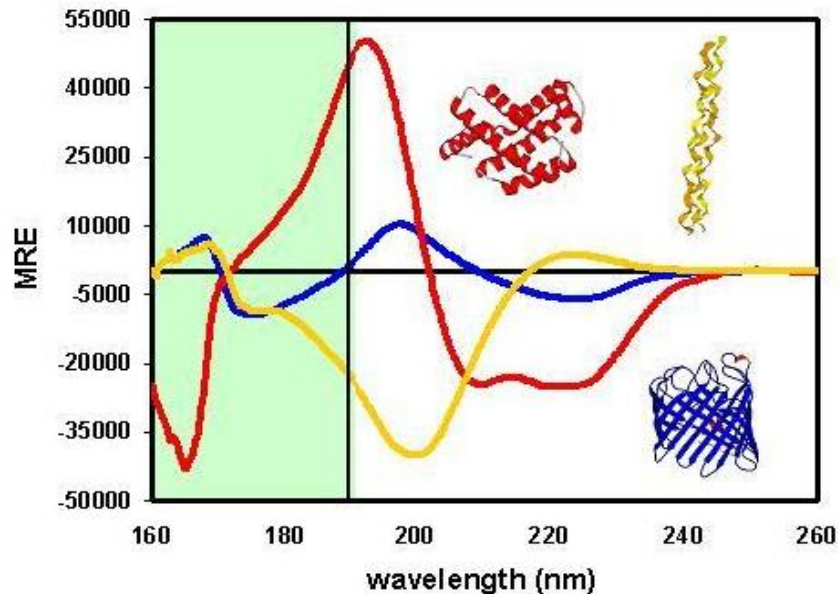


**Figure 3.6 CD spectra of proteins with different types of secondary structures**

*Red=alpha-helical, blue=beta-sheet, yellow=polyprotein-helical. The area shaded green to the left of the vertical black bar is only accessible by synchrotron radiation CD spectroscopy. Adapted from (Miles and Wallace 2006)*

The mean residue ellipticity (MRE) at 222nm in isolated TnT for WT showed an estimated  $\alpha$ -helical content of ~37%. Both the DCM mutants R141W and  $\Delta$ K210 and HCM mutant S179F showed  $\alpha$ -helical content almost identical to that of WT. Previous CD structural studies also confirmed no significant difference in  $\alpha$ -helical content for S179F (Harada and Potter 2004).

K273E,  $\Delta$ 14 and  $\Delta$ 28+7 resulted in an increased  $\alpha$ -helical content to ~42, 49 and 48%. The  $\Delta$ E160 spectrum on the other hand, showed a broad minimum around 208nm and lacked a well defined minimum around 222nm (Figure 3.7). When TnT was reconstituted in Tn complex all of the mutants showed little or no structural differences from WT except for K273E which showed slightly reduced  $\alpha$ -helical content (Figure 3.8). Secondary structure estimates are summarised in Table 3.3. The ratio of the ellipticities  $\theta_{222}:\theta_{208}$  with a value of ~1 is diagnostic of a stable coiled coil formation. The  $\theta_{222}:\theta_{208}$  ratio of isolated TnT

was  $\sim 0.8$  for WT and all mutants of study except for  $\Delta E160$  showed marked reduction in the stability of the coiled-coil region with a ratio of 0.3. This deletion mutation has interfered with the region expected to have helix stabilising capacity. However, upon reconstitution into Tn complex all WT and mutants showed ratios close to the ratio expected for stable coiled coil ( $\sim 0.95$ -1.2).

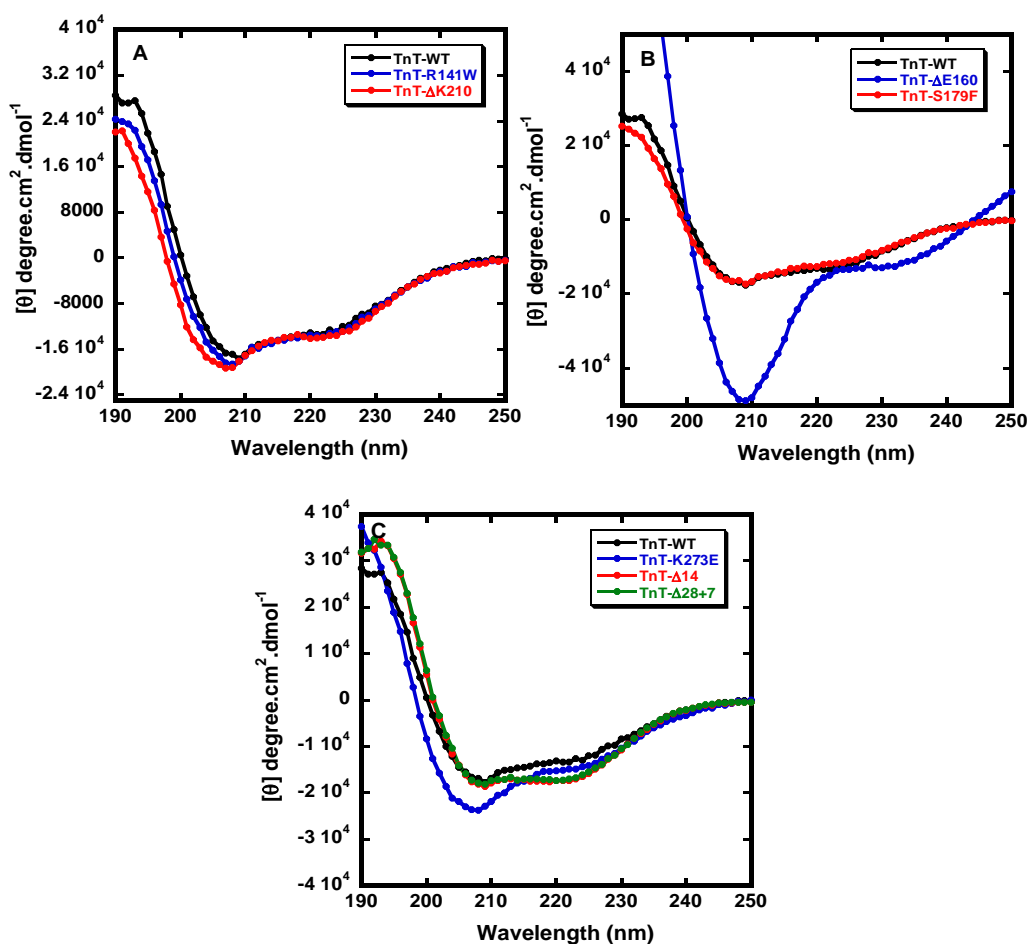


**Figure 3.7 Circular Dichroism spectra of WT and mutant cTnT.**

The secondary structure of the WT and TnT mutants were measured in the presence of 10mM  $\text{NaH}_2\text{PO}_4$ , pH 7.0 and 0.3M NaF. All samples were used at a concentration of 0.2mg/ml. Each data point is an average of two experiments at 5°C and 25°C and each experiment consisted of an average of 10 scans and is expressed as the mean.

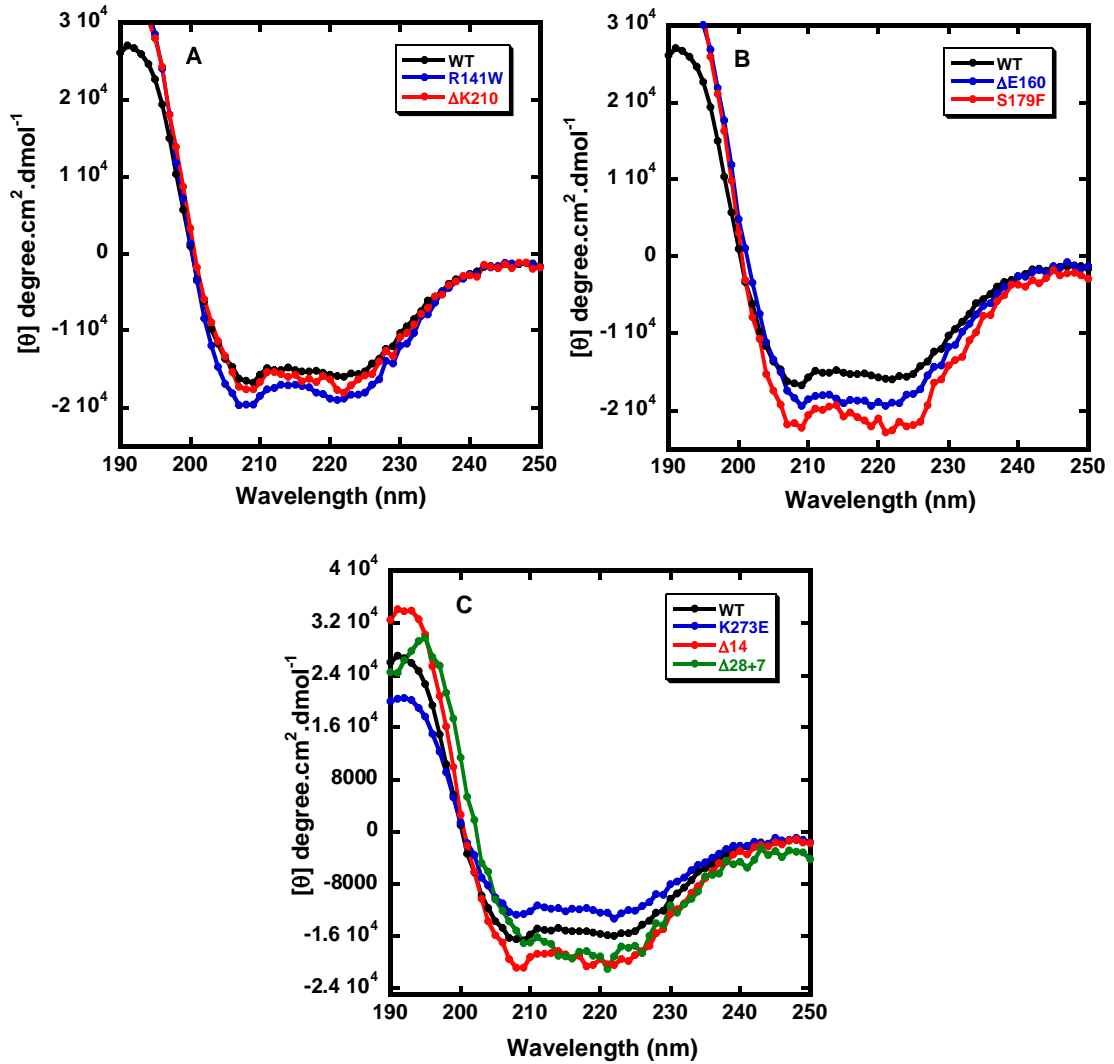


**Figure 3.8 Circular Dichroism spectra of WT Tn complex and mutants.**

The secondary structure of the WT and TnT mutants were measured in the presence of 10mM  $\text{NaH}_2\text{PO}_4$ , pH 7.0 and 0.3M NaF. All samples were used at a concentration of 0.2mg/ml. Each data point is an average of two experiments at 5°C and 25°C and each experiment consisted of an average of 10 scans and is expressed as the mean.

**Table 3.3 Secondary structural properties and stability of TnT and complex**

Species	$\alpha$ -helix- TnT % <sup>a</sup>	$\theta_{222}:\theta_{208}$ <sup>b</sup>	$\alpha$ -helix-Tn complex % <sub>a</sub>	$\theta_{222}:\theta_{208}$ <sup>b</sup>
Wildtype	37±1.6	0.79	45±2.1	0.97
TnT1-R141W	38±1.8	0.75	55±6	0.96
TnT2-ΔK210	38±2.8	0.73	52±9	1.02
TnT1-ΔE160	(42)±1.2	0.3	55±3	1.03
TnT1-S179F	38±2	0.72	67±12	1.04
TnT2-K273E	42±1.7	0.62	36±2.4	1.05
TnT2-Δ14	49±2.4	0.96	60±4.7	0.98
TnT2-Δ28+7	48±2.1	0.95	56±3.8	1.2

<sup>a</sup> Secondary structure for each protein was calculated using the equation for  $[\theta]$  at 222nm  $[\theta] = -30300f_H - 2340$  where  $f_H$  is the fraction of  $\alpha$ -helical content ( $f_H \times 100$  expressed in %).

<sup>b</sup>  $\theta_{222}:\theta_{208}$  value is an indicator of the coiled-coil state of interacting peptides.

Thermal stability is assessed using CD by following the changes in the spectrum with increasing temperature. The melting point of wild type and mutants were measured in the presence of 0.3M NaF at neutral pH using the change in ellipticity at 222nm with increasing temperature.

The graphs in Figure 3.9 illustrate the normalised plots of ellipticity versus temperature and the mid-point temperatures are shown in Table 3.4 for the Tn complex. The thermal stability of the troponin complex is clearly a multistep process with two melting transitions. At lower temperatures the protein had only partially lost its secondary structure whilst at higher temperatures we observed complete denaturation of the protein. At pH 7 the melting temperatures were 45°C and 78°C respectively for wildtype Tn. The temperature of the unfolding curve midpoint ( $T_{m1}$ ) was similar to WT for R141W, S179F,  $\Delta$ K210,  $\Delta$ 14 and  $\Delta$ 28+7  $\pm$ 2°C. Interestingly  $\Delta$ E160 had the opposite consequence and shifted the circular dichroism results in the direction expected for a stabilising mutation by 6°C. In contrast, K273E exhibited destabilising effect with a  $T_m$  lowered by 6°C. The CD data overall showed no trend, demonstrating that these mutations had strikingly disparate effects on the folding of TnT. However, no difference in  $T_{m2}$  values were seen across the whole range of mutations studied compared to WT. The effects of the mutations on the apparent stability were similar.

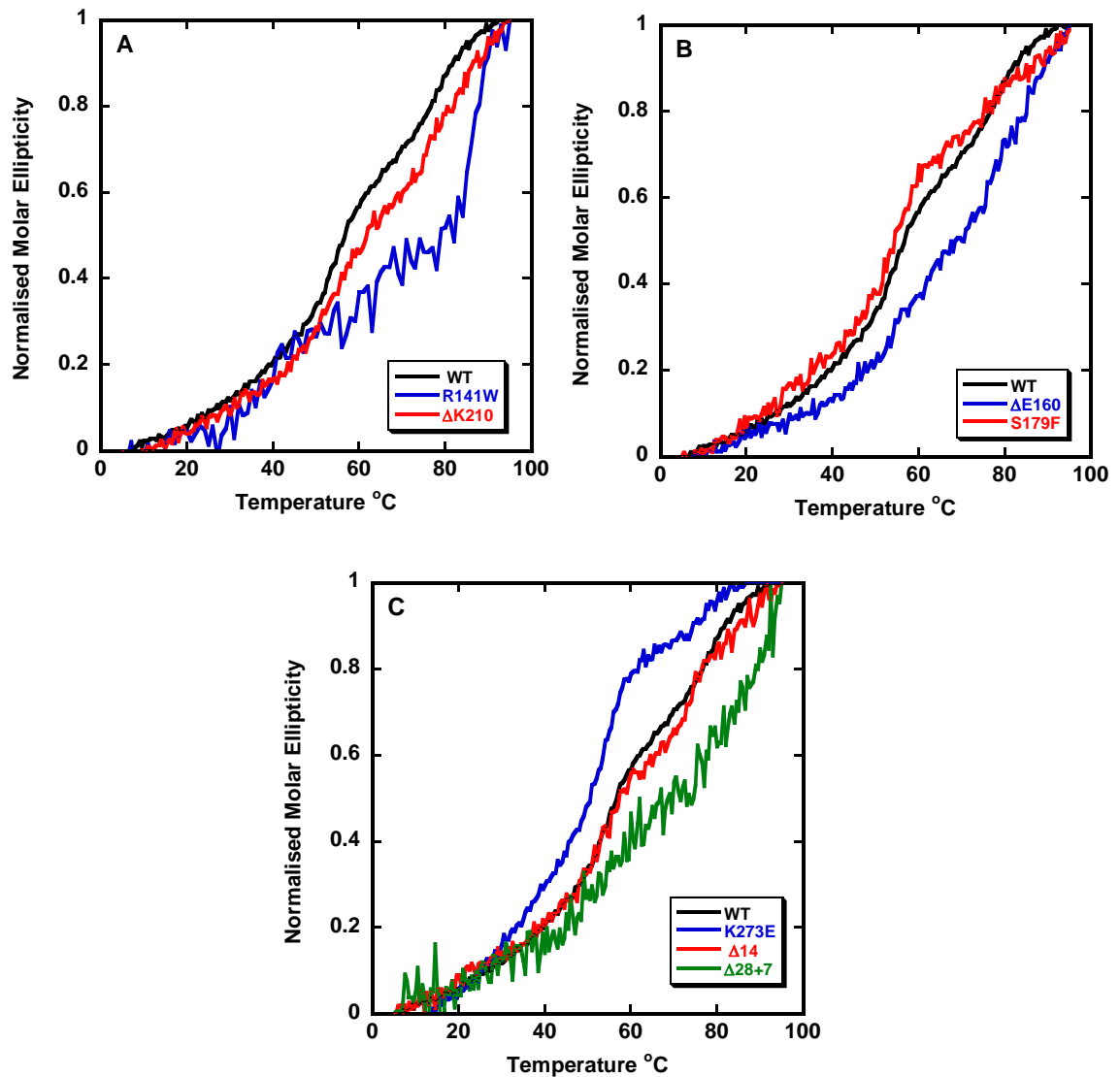


**Figure 3.9 Thermal denaturation of cTn complex.**

Thermal denaturation spectra of (A) DCM (B) T1-region HCM and (C) T2-region HCM mutations in complex. It was monitored at 222nm between 5-95°C at a rate of 1°C/min. All samples were in 10mM NaH<sub>2</sub>PO<sub>4</sub>, pH 7.0 and 0.3M NaF.

**Table 3.4 Mid-point melting temperatures of TnT complexes**

<b>Species</b>	<b>T<sub>m1</sub> (°C)</b>	<b>T<sub>m2</sub> (°C)</b>
<b>Wildtype</b>	45±0.9	78±0.5
<b>TnT1-R141W</b>	46±1.3	77±1.1
<b>TnT2-ΔK210</b>	47±1.1	81±0.6
<b>TnT1-ΔE160</b>	51±2.2	83±3
<b>TnT1-S179F</b>	43±4.9	80±2.1
<b>TnT2-K273E</b>	39±2.1	79±2
<b>TnT2-Δ14</b>	46±0.7	78±0.3
<b>TnT2-Δ28+7</b>	47±1.4	82±0.6

## 3.3 Discussion

In this chapter we have isolated recombinant WT and 7 cardiomyopathy linked cTnT mutants (R141W,  $\Delta$ K210,  $\Delta$ E160, S179F, K273E,  $\Delta$ 14 and  $\Delta$ 28+7) in considerably good yields, typically 10-15mg per preparation using a shortened procedure. This facilitated the detailed characterisation of Tn by a number of different techniques.

### 3.3.1 Structural Effects of TnT Mutations

To assess whether cTnT secondary structure was perturbed by the presence of mutations, CD was performed to determine the extent that the mutants changed the  $\alpha$ -helical content ( $\theta=222$ ) and  $\beta$ -sheet ( $\theta=208$ ). The spectra were collected both as TnT subunit alone and in complex. Generally, the isolated TnT subunit spectra showed similar conformations for both DCM mutations and S179F mutant of HCM. However,  $\Delta$ E160 in particular showed striking difference in the shape of the graph. This may be due to two reasons: 1) perhaps the local fold around  $\Delta$ E160 has been changed by the deletion of Glu or 2) its absence has caused the protein to misfold. However the results obtained in ATPase and co-sedimentation suggest that the Tn complex obtained with this mutant is still folded and at least partially functional. K273E and the truncated mutations ( $\Delta$ 14 and  $\Delta$ 28+7) also showed increased  $\alpha$ -helicity in the isolated forms.

The  $T_{m1}$  melting mutants analysed here was above body temperature (45 °C vs. 39°C) which means they are stable under physiological conditions.

For DCM mutations R141W and  $\Delta$ K210 no effect was observed in both  $\alpha$ -helical content and thermal stability in comparison to WT which is in strong agreement with previous studies (Venkatraman, Harada et al. 2003).

Our studies demonstrate  $\Delta$ E160 to be slightly more stable than WT (Figure 3.9B). This means  $\Delta$ E160 would be expected to negatively affect the cooperativity which would be the subject of further study in Chapter 4.

On the contrary, a destabilising effect seen for K273E (Figure 3.9C) is the result of a charge change which could interfere with salt bridges. Since the pathology has been detected in patients carrying K273E to have had 7 histories of sudden cardiac deaths (Fujino, Shimizu et al. 2002) this hypothesis supports the fact that mutations that cause the greatest loss in stability also causes pathology at a young age.

Overall, circular dichroism measurements suggest that significant structural changes exist in the secondary structure of TnT mutants for K273E,  $\Delta$ 14,  $\Delta$ 28+7 and  $\Delta$ E160. However, in TnT mutations in the presence of TnI and TnC the differences observed were less prominent and masked to a large extent by wildtype TnI and TnC subunits.

### **3.3.2 Functional Effects of TnT Mutations**

We assessed the functional and biochemical properties of 2 DCM (R141W,  $\Delta$ K210) and 5 HCM ( $\Delta$ E160, S179F, K273E,  $\Delta$ 14 and  $\Delta$ 28+7) TnT mutations using steady state methods including ATPase and co-sedimentation.

In our ATPase studies we observed that all 7 mutations examined showed no consistent trend between the acto-S1 ATPase and  $\text{Ca}^{2+}$  sensitivity. In general,

DCM associated mutants of TnT showed strikingly reduced activation whereas for HCM associated mutants activation was either unchanged or slightly increased. Mutations in the T1 region ( $\Delta$ K210,  $\Delta$ E160 and S179F) and to a lesser extent T2 region (K273E,  $\Delta$ 14 and  $\Delta$ 28+7) exhibited similar leftward shift in  $\text{Ca}^{2+}$  sensitivity.

In general, HCM TnT mutations showed higher levels of ATPase activation while both DCM TnT mutations lowered activation. Similar results were previously published using skinned fiber studies (Mukherjea, Tong et al. 1999; Tobacman, Lin et al. 1999; Ohtsuki and Morimoto 2008).

Co-sedimentation analysis using Actin.Tm.Tn was performed to determine whether any of the HCM cTnT mutations had altered the affinity of cTn for the thin filaments. The results in Figure 3.5 suggest that most of the cTnT mutations do not interfere with the association between cTn and thin filament except for the truncated mutations. This method however is not sensitive enough to detect small affinity changes. Changes caused by the TnT mutations could be locally at the level of TnT-TnI, TnT-TnC or TnT-TnI-TnC. Therefore the physiological changes measured are not a direct alteration in the affinity of cTn for thin filament. Further studies are required to elucidate which modifications of the thin filament occur in the presence of HCM and DCM mutations.

Nevertheless, all of the above studies for HCM in broad terms gave us reason to believe that HCM mutations act by similar mechanisms. Firstly, they all had increased  $\text{Ca}^{2+}$  activation and reduced inhibition for mutations in the T2 region in particular. Secondly, the  $\alpha$ -helical content and thermal stability was similar or increased compared to WT (except for K273E). Thirdly, they all raised the

calcium sensitivity of thin filament activation. The validity of this generalisation has been supported by the findings in other groups (Morimoto, Yanaga et al. 1998, Tobacman, Lin et al. 1999, Yanaga, Morimoto et al. 1999, Chandra, Rundell et al 2001).

Both the calcium sensitising and T<sub>m</sub> binding ability of TnT2 are greatly diminished when C-terminal residues are removed as seen for  $\Delta 14$  and  $\Delta 28+7$  in the ATPase and co-sedimentations assays. Therefore the calcium sensitising action and T<sub>m</sub> binding stability are correlated through this C-terminal region of TnT2. All other mutants showed essentially the same Ca<sup>2+</sup> inhibitory action as for the WT indicating that the H1-T1 and H1-T2 domain residues are not critical for Ca<sup>2+</sup> inhibition regulatory function.

In conclusion, we have observed multiple structural and functional consequences from different TnT mutations that occur in different regions of hcTnT molecule. We have demonstrated that the various Tn complexes obtained with different TnT mutations are fully functional allowing us to conduct kinetic experiments to provide further information on the impact of the mutations on the regulatory mechanism.

# CHAPTER 4

Effect of TnT mutations on Thin Filament  
Dynamics

## **Contents**

<b>4.1</b>	<b>Introduction</b>	<b>108</b>
<b>4.2</b>	<b>Results</b>	<b>111</b>
<b>4.2(A)</b>	<b>Effect of TnT Mutations on the Size of the Cooperative Unit</b>	<b>111</b>
<b>4.2(B)</b>	<b>Equilibrium Constant <math>K_B</math></b>	<b>127</b>
<b>4.3</b>	<b>Discussion</b>	<b>136</b>

## 4.1 Introduction

The current view on the molecular mechanism of how Tm-Tn controls the productive interaction of actin and myosin postulates coupled structural rearrangements in all components of the thin filament. The molecular mechanism of regulation is generally believed to be via steric blocking in which the position of Tm on actin directly obstructs the binding of myosin to actin (Gordon, Homsher et al., 2000). Herein we use a variant of this model, the three-state model of McKillop and Geeves described in detail in Section 1.7.1 (McKillop and Geeves, 1993). This model stipulates that muscle thin filaments act as a cooperative-allosteric system switching between three states (Lehrer & Geeves, 1998). According to this model, myosin-S1-ATP is the substrate while actin is the catalytic subunit (capable of activating the substrate), Tm is the regulatory subunit (which produces equilibrium between ON state and OFF state), Tn in the absence or presence of  $\text{Ca}^{2+}$  is the allosteric inhibitor or activator respectively.

Thin filament dynamics has been intensively studied using various approaches including structural methods (Li, Gagne et al., 1995; Craig and Lehman, 2001; Takeda, Yamashita et al., 2003; Vinogradova, Stone et al., 2005), fluorescent probes attached to proteins (Ishii and Lehrer, 1990; Bacchiocchi, Graceffa et al., 2004; Miki, Hai et al., 2004), ATPase assays (Hill, Eisenberg et al., 1981; Gomes, Liang et al., 2005) and motility assays (Fraser and Marston, 1995; Homsher, Kim et al., 1996).

A range of techniques have been developed to study the detailed equilibria and dynamics of thin filament regulation in skeletal muscle. The aim of this chapter

is to look at two parameters that describe thin filament dynamics: (A) ' $n$ ' -the size of the cooperative unit and (B)  $K_B$ , the equilibrium constant between the blocked and the closed states.

(A) The size of the cooperative unit,  $n$ : Cooperativity, in broad terms has been defined as the interaction process by which binding of a ligand to one site on a multimeric macromolecule influences binding at subsequent sites. In muscle thin filaments, cooperative switching between inhibited and activated states results in characteristic sigmoidal myosin-S1 binding curves. The cooperative unit is the number of actin monomers switched simultaneously between the ON and OFF states by the binding of an allosteric inhibitor (such as Tn in the absence of  $Ca^{2+}$ ) or activator (such as S1 myosin head). To accurately measure the size of the cooperative unit we used methods developed by Lehrer and Geeves for the study of striated muscle Tm. These methods are based on monitoring simultaneously the ON-OFF transition and myosin-S1 association/dissociation to thin filaments. Tm is labelled with *N*-(1-pyrenyl)-iodoacetamide covalently attached to Cys-190 of Tm. Pyrene labelled Tm dimers exhibit excimer fluorescence which increases noticeably when the thin filament switches from the OFF state to the ON state due to S1 binding (Geeves and Lehrer, 1994). For skeletal muscle actin-Tm filaments,  $n$  was estimated at 6-7 and is roughly equal to the number of actin monomers physically covered by a single Tm (structural unit). However in the presence of Tn and  $Ca^{2+}$  it was increased to about 14, significantly greater than the structural unit (Maytum, Konrad et al., 2001; Maytum, Westerdorf et al., 2003). Schaertl and co workers have reported that TnT influences Tm-Tm communication along the thin filament via its interaction at the Tm-Tm overlap region (Schaertl, Lehrer et al.,

1995). Hence we anticipated that mutations in T1 region of TnT may affect the size of the cooperative unit.

(B) The equilibrium constant between the blocked and the closed states  $K_B$ : In the absence of  $Ca^{2+}$  and when Tn is tightly bound, thin filaments are predominantly in the blocked state and  $K_B$  (ratio of thin filaments in the closed state over thin filaments in the blocked state) is expected to be substantially less than 1. In the presence of Tn - $Ca^{2+}$  there is little or no occupancy of the B-state and  $K_B$  is expected to be much larger than 1.

Head et al. (1995) have shown that the large fluorescence change of pyrene – iodoacetamide labelled actin allows the monitoring of the transition between blocked and closed states (Head, Ritchie et al., 1995; Alahyan, Webb et al., 2006).

Here we have assessed the effect of 7 mutations of TnT on the regulatory parameters 'n' and ' $K_B$ '. Some of the mutations studied in this project have shown to produce striking changes in regulatory function when studied in reconstituted thin filament by ATPase assay and CD spectroscopy (Chapter 3).

## 4.2 Results

### 4.2(A) Effect of TnT Mutations on the Size of the Cooperative Unit

#### 4.2.1 Characteristics of Pyrene Labelled Cardiac Tm

Previous studies have shown Tm labelled with pyrene iodoacetamide to report conformational changes associated with the closed to open transition (Ishii and Lehrer, 1990). Cardiac Tm consist mainly of  $\alpha\alpha$ -molecules where each  $\alpha$  contains a single cysteine at residue 190. Therefore the degree of labelling should typically be a value of two pyrenes per mole of Tm and we consistently obtained ratio of 1.8-2.1 of pyrene: Tm. During this project a total of five cardiac Tm purifications were carried out fresh prior to covalently labelling with pyrene.

Prior to carrying out kinetic experimentations, the effect of actin, S1 binding to actin and ATP induced dissociation of acto-S1 on the fluorescence of Tm were checked. The fluorescence emission spectra of pyrene labelled Tm on excitation at 343nm is shown in Figure 4.1. They are composed of monomer peaks at 385nm and 410nm and an excimer peak centred at 480nm (black curve). When actin was added, the monomer fluorescence was unchanged while the excimer fluorescence decreased slightly (blue curve). When S1 was added in quantities sufficient to turn the filament to the fully switched ON state, the excimer fluorescence level increased 70% (red curve). On addition of  $Mg^{2+}$ -ATP, the effect of S1 was reversed, and the excimer fluorescence returned to the level observed with actin alone (green curve).

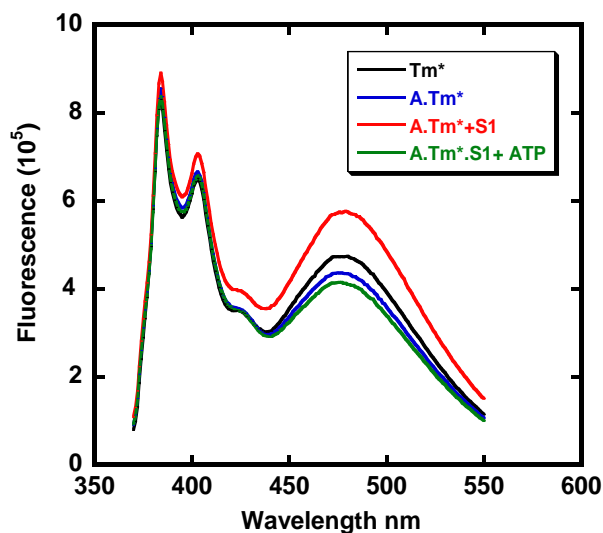


**Figure 4.1 Fluorescence emission spectra of pyrene labelled Tm.**

*Conditions: 6 $\mu$ M actin, 1 $\mu$ M Tm, 3 $\mu$ M S1, 1mM Mg<sup>2+</sup>-ATP in 10mM MOPS, 140mM KCl, 4mM MgCl<sub>2</sub>, and 1mM DTT 0.2mM NaN<sub>3</sub>, pH 7.2, 25°C.*

Figure 4.2 is the spectra of actin.Tm\* in the presence of Tn. On addition of Tn only a small change in monomer and excimer fluorescence was caused by the binding to actin.Tm (black curve). In the presence of calcium no significant change was observed for excimer peak (blue curve) and further addition of S1 induced an average increase of 6.6% in excimer fluorescence (red curve). The effect was reversed by the addition of ATP (green curve). Therefore change in the level of the excimer fluorescence is also capable of monitoring the transition to the ON state in the presence of troponin however the amplitude of this signal is much smaller in the presence of troponin in comparison to actin-Tm alone.

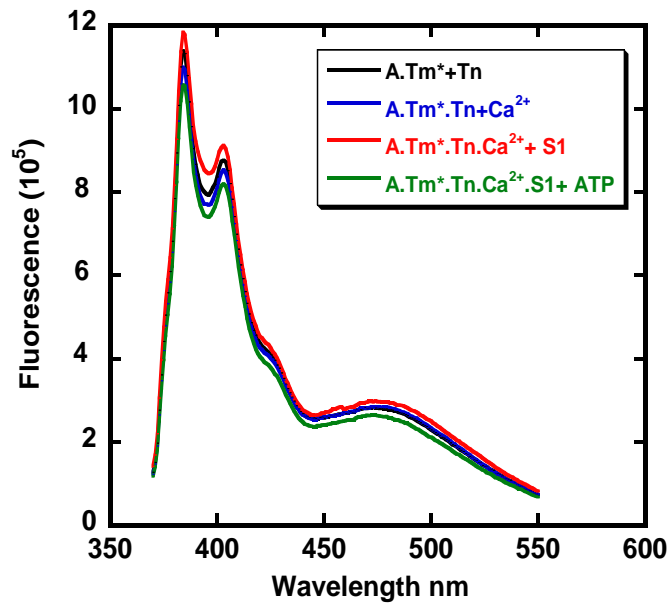


**Figure 4.2 Fluorescence emission spectra of pyrene labelled Tm.**

*Conditions: 6 $\mu$ M actin, 1 $\mu$ M Tm, 1 $\mu$ M Tn, 3 $\mu$ M S1, 1mM Mg<sup>2+</sup>-ATP and 0.2mM CaCl<sub>2</sub> in 10mM MOPS, 140mM KCl, 4mM MgCl<sub>2</sub>, and 1mM DTT 0.2mM NaN<sub>3</sub>, pH 7.2, 25°C.*

#### **4.2.2 S1 Induced Switch between Closed and Open State of the Thin Filament**

During the contractile cycle the number of actin monomers available for strong binding of cycling crossbridges is an important determinant of the amount of force produced. The cooperative unit is the number of actin monomers switched simultaneously between the ON-OFF states by the binding of an activator such as S1 myosin head.

Pyrene-iodoacetamide labelled Tm was used to monitor the transition between these states using two methods (Geeves and Lehrer, 1994); (1) equilibrium titration of actin thin filament with increasing concentration of S1. (2) Kinetic studies of ATP induced S1 dissociation from thin filament and subsequent transition to the closed state.

## Equilibrium Titration Method

Based on the fact that excimer fluorescence of pyrene iodoacetamide labelled Tm can directly report the conformational changes associated with the ON-OFF transition, the work carried out here aims at directly monitoring this transition in thin filament in the anticipation that the mutations in TnT will change the size of cooperative unit specifically mutants in the TnT-T1 region.

In this experiment, we premixed actin.Tm\* at a molar ratio of (6:1) and titrated by step wise addition of a stock solution of 100 $\mu$ M S1 to a 2 ml volume at 30 s intervals. Fluorescence intensities and protein concentrations were corrected for the volume change (< 10%) due to addition of S1. Figure 4.3 represents a plot of the excimer fluorescence (Red curve) and light scattering (blue curve) against the S1 concentration. We also measured light scattering for S1 alone (black curve) to assess the background light scattering due to S1 alone.

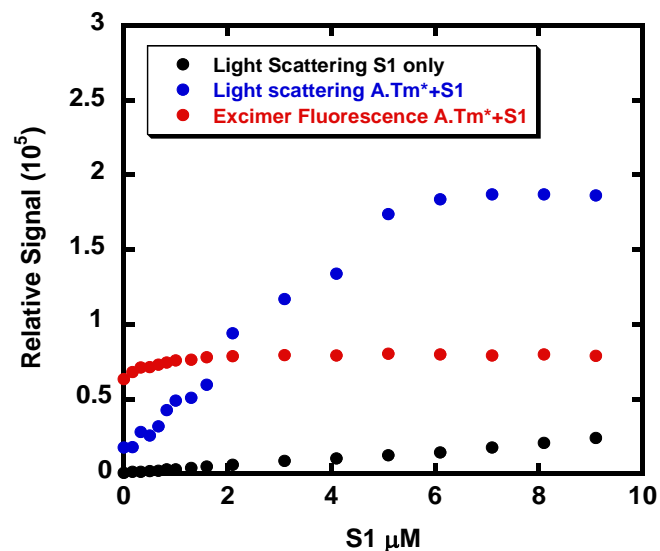


**Figure 4.3 Steady state S1 titration of cardiac actin.Tm thin filament.**

The pyrene excimer fluorescence monitors the fraction in the open state (Red curve) and the light scattering monitors the fraction of S1 bound (Blue curve). The contribution from light scattering with S1 only is represented (black curve). Conditions: 6  $\mu$ M actin, 1  $\mu$ M Tm, 0-10  $\mu$ M S1 in 10 mM MOPS, 140 mM KCl, 4 mM MgCl<sub>2</sub>, and 1 mM DTT 0.2 mM NaN<sub>3</sub>, pH 7.2, 25°C.

The excimer fluorescence reached a plateau at much lower S1 concentration than the stoichiometric binding of S1 to actin.Tm\* monitored by light scattering. The data were normalised to zero at the start of the experiment and at 1.0 for the plateau as shown in Figure 4.4. The fraction of thin filament in the ON state determined from the excimer fluorescence ( $F_{\text{open}} = \Delta FL / \Delta FL_{\text{max}}$ ) is plotted against the amount of S1 bound to actin ( $F_{\text{bound}}$ ) as determined from the light scattering data ( $F_{\text{bound}} = \Delta LS / \Delta LS_{\text{max}}$ ) (Figure 4.5). Using this method and fitting the data to equation  $F_{\text{open}} = 1 - (1 - F_{\text{bound}})^n$ , we found the size of the cooperative unit for cardiac Tm to be 8 in this experiment. An average value of  $9.2 \pm 1$  was obtained from three experiments, in agreement with a value of between 8-10 determined by Lehrer and co-workers using the same method (Lehrer et al., 1997).

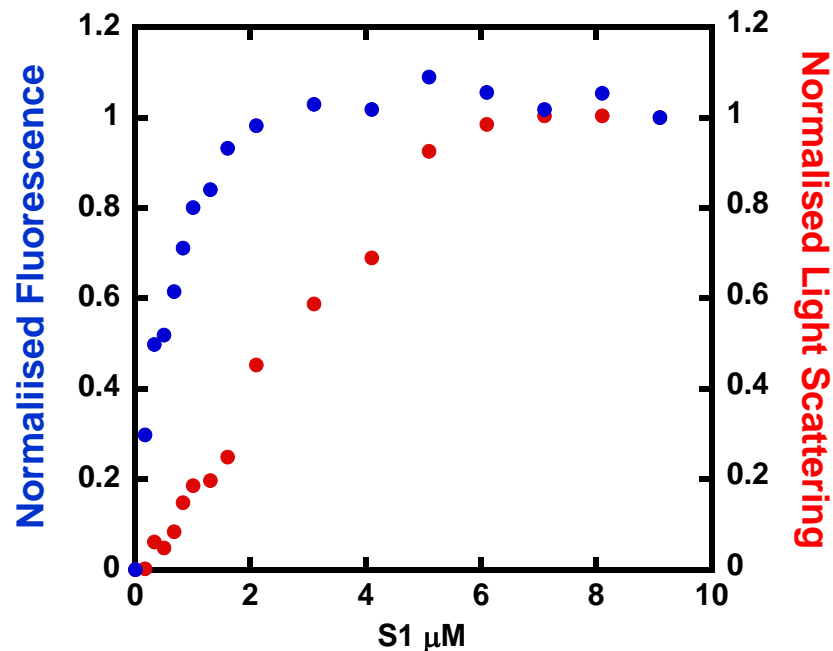


**Figure 4.4 Normalised Fluorescence and Light scattering.**

*The plot of pyrene excimer fluorescence and corrected light scattering against S1 concentration.*

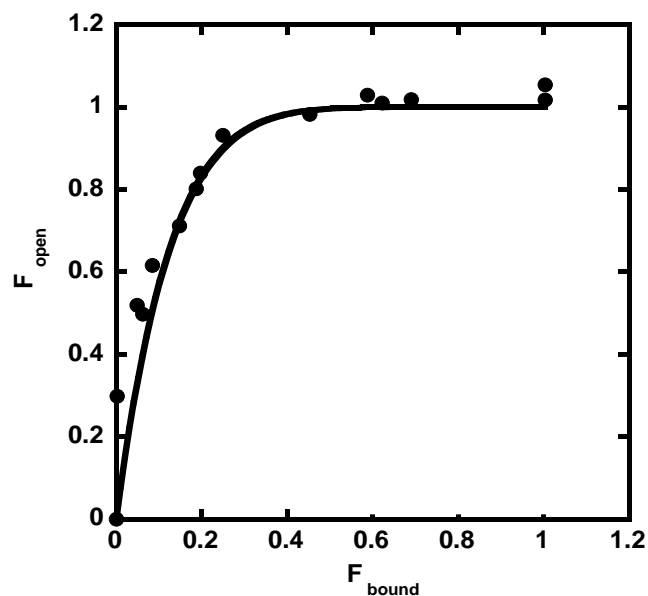


**Figure 4.5 Size of the cooperative unit of cardiac actin.Tm thin filament**  
*The plot of fraction of thin filament in the open state ( $F_{open}$ ) against the fraction of S1 bound to thin filament ( $F_{bound}$ )*

In order to determine the effect of Tn on the size of the cooperative unit we repeated the experiment in the presence of  $1\mu\text{M}$  wild type Tn and  $0.2\text{mM}$   $\text{CaCl}_2$ .

S1 titrations were performed using the exact conditions as for actin.Tm in a total volume of 2 ml. The solution was constantly stirred in the cuvette at a low speed as S1 was added. Figure 4.6 shows the fluorescence and light scattering changes versus S1 for actin.Tm.Tn thin filament. The shape of the light scattering (blue curve) was similar to that obtained with actin-Tm. However, the total change in excimer fluorescence in the presence of Tn on adding S1 is too small to see a measurable incremental change (red curve). Normalised data (Figure 4.7) clearly show that the data are too scattered due to the small amplitude of the excimer fluorescence signal obtained in the presence of Tn. It was therefore not possible to use this method to determine the effect of TnT mutations on the size of the cooperative unit.

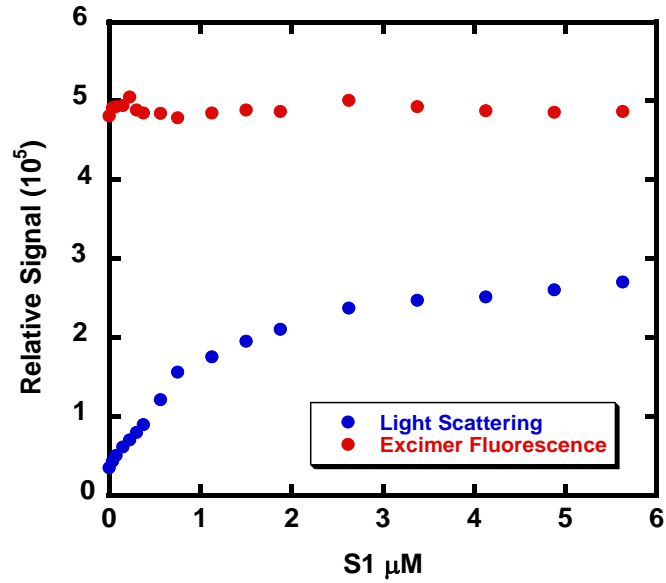


**Figure 4.6 Titration of cardiac actin.Tm.Tn thin filament.**

The pyrene excimer fluorescence monitors the fraction in the open state (Red curve) and the light scattering monitors the fraction of S1 bound (Blue curve). Conditions: 6 μM actin, 1 μM Tm, 1 μM Tn, 0-10 μM S1 in 10 mM MOPS, 140 mM KCl, 4 mM MgCl<sub>2</sub>, 0.2 mM CaCl<sub>2</sub>, 1 mM DTT 0.2 mM NaN<sub>3</sub>, pH 7.2, 25°C.

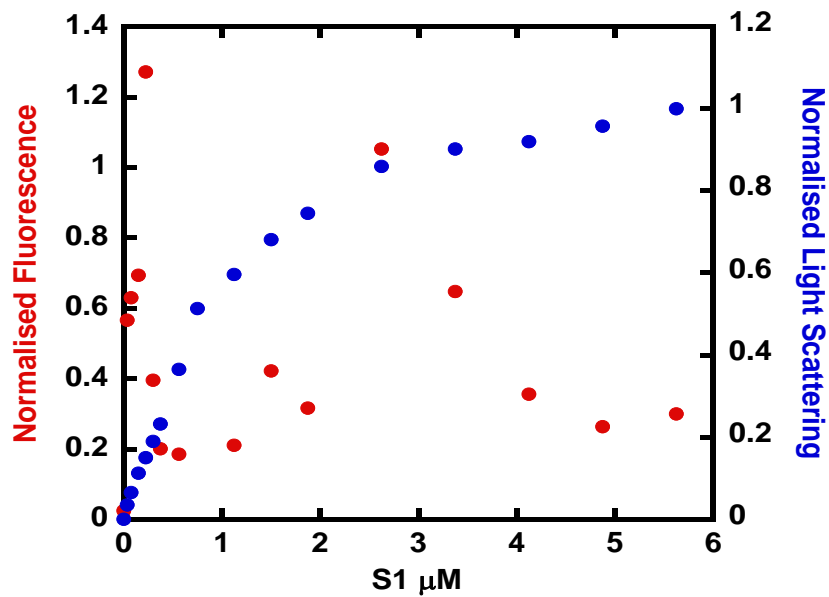


**Figure 4.7 Normalised Fluorescence and Light scattering for Actin.Tm.Tn**

The plot of pyrene iodoacetamide excimer fluorescence and corrected light scattering against S1 concentration.

## Kinetic Method

In this method, when measuring the ATP induced actin-myosin dissociation the light scattering signal decreases rapidly (due to the immediate dissociation of S1 from actin) but the excimer fluorescence is delayed until the number of S1 remaining bound is not sufficient to maintain the filament in the ON state (Geeves and Lehrer, 1994). To remove free Tm\* which will contribute to the background fluorescence but not to the change triggered by thin filament transition, we cosedimented actin.Tm.S1 at 6:1:6  $\mu\text{M}$  and the pellet were resuspended in experimental buffer. Initially, actin.Tm\*.S1 was mixed against 40 $\mu\text{M}$  ATP which causes dissociation of S1 (Figure 4.8.A). As the ATP binds to S1, the LS signal falls but the actin.Tm\* remains in the ON state as long as one or more S1 remains bound within the cooperative unit. The FL remains constant until the last S1 dissociates and then changes rapidly as the filament switches to the OFF state. The duration of the lag depends upon the size of  $n$ . Using equation  $f_{\text{on}}=1-(1-\exp(-k_{\text{LS}}t))^n$  where  $k_{\text{LS}}$  is the experimentally observed light scattering rate constant (Figure 4.8 B), we calculated a range of possible  $n$  values and compared them to the observed fluorescence transients to determine  $n$ . The experiments were repeated at higher concentrations of ATP and a value of  $n$  of 7-10 for actin.Tm was obtained at all concentrations. The value obtained from both equilibrium and kinetic studies agreed that the size of the cooperative unit is around 8 for cardiac Tm in the absence of troponin.

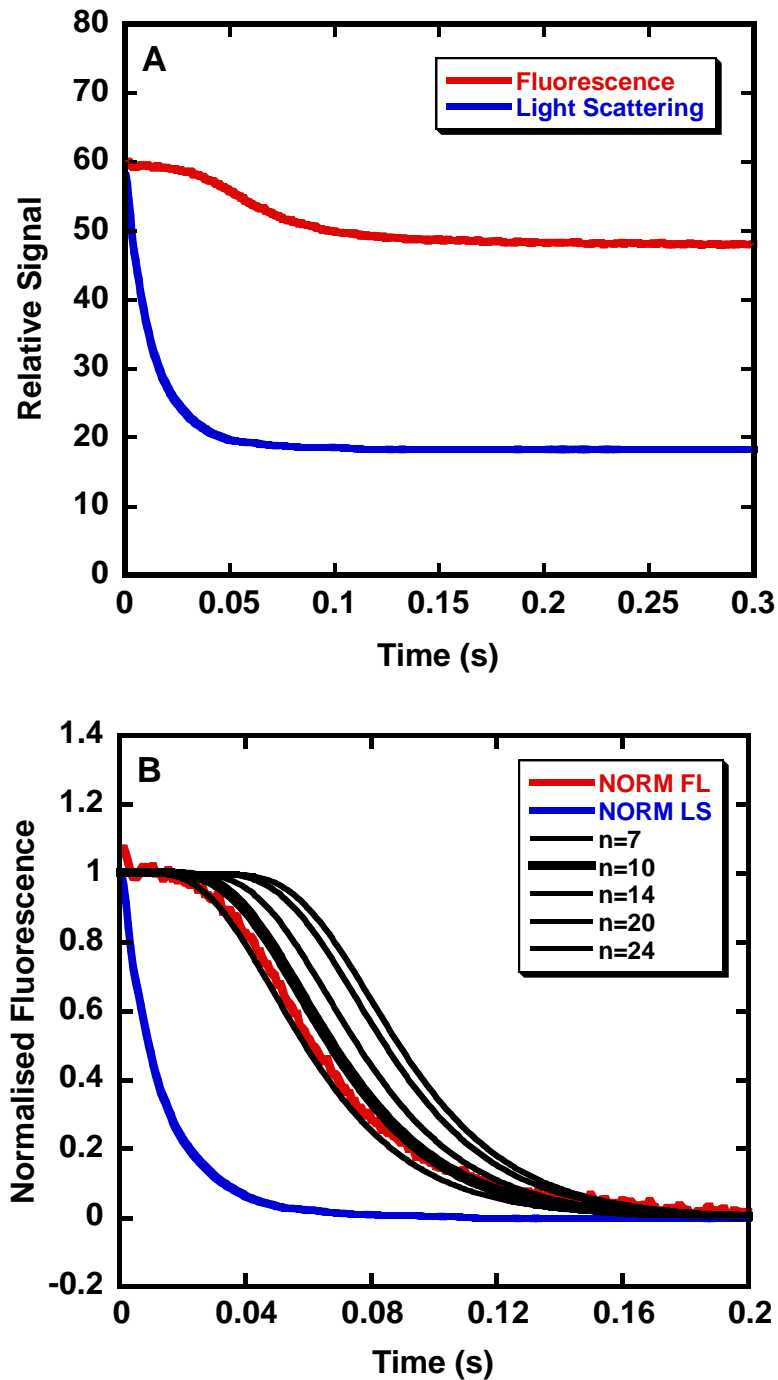


**Figure 4.8 Kinetics of ATP induced dissociation of S1 from Actin.Tm thin filament**

(A) Time courses of fluorescence and light scattering. The signals are an average of 6-8 transients (B) Normalised time courses of light scattering (blue line) and fluorescent (red line) signals when  $40\mu\text{M}$  ATP was mixed with  $6\mu\text{M}$  S1,  $6\mu\text{M}$  actin, and  $1\mu\text{M}$  Tm. The black lines are the computer generated simulation curves using  $k_{LS} = 98\text{ s}^{-1}$ . The experiments were performed in  $140\text{ mM}$  KCl,  $4\text{ mM}$   $\text{MgCl}_2$ ,  $0.2\text{ mM}$   $\text{CaCl}_2$ ,  $1\text{ mM}$  DTT,  $20\text{ mM}$  MOPS, pH 7.2.

In the presence of Tn, the signal was much smaller than for Actin.Tm thin filament as obtained in steady state fluorimetry. However, by averaging a large number of shots (9-12 shots), we reduced the noise and obtained a measureable signal change when Tn was incorporated into thin filament. Figure 4.9.B illustrates the comparison of the difference in amplitude of the fluorescence change in going from actin.Tm system (10%) to Actin.Tm in the presence of Tn (3.6%).

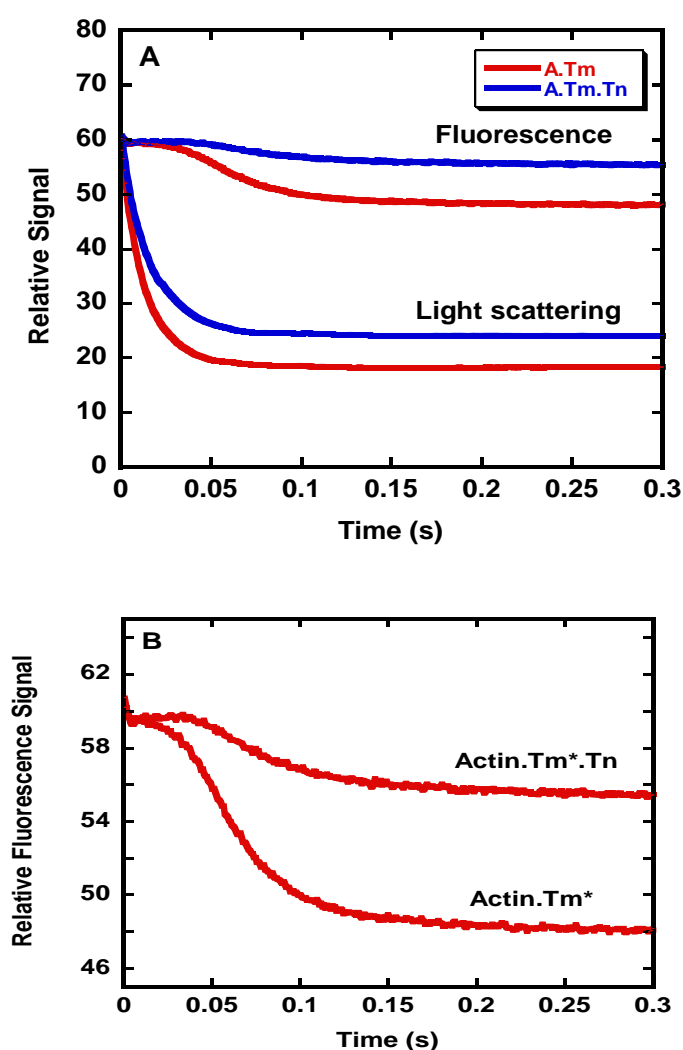


**Figure 4.9 Comparison of the amplitudes of ATP induced dissociation of S1 of A.Tm and A.Tm.Tn signals.**

*Conditions: 6  $\mu$ M actin, 1  $\mu$ M Tm, 1  $\mu$ M Tn, 6  $\mu$ M S1, 40  $\mu$ M Mg<sup>2+</sup>-ATP and 0.2 mM CaCl<sub>2</sub> in 10 mM MOPS, 140 mM KCl, 4 mM MgCl<sub>2</sub>, and 1 mM DTT 0.2 mM NaN<sub>3</sub>, pH 7.2, 25°C.*

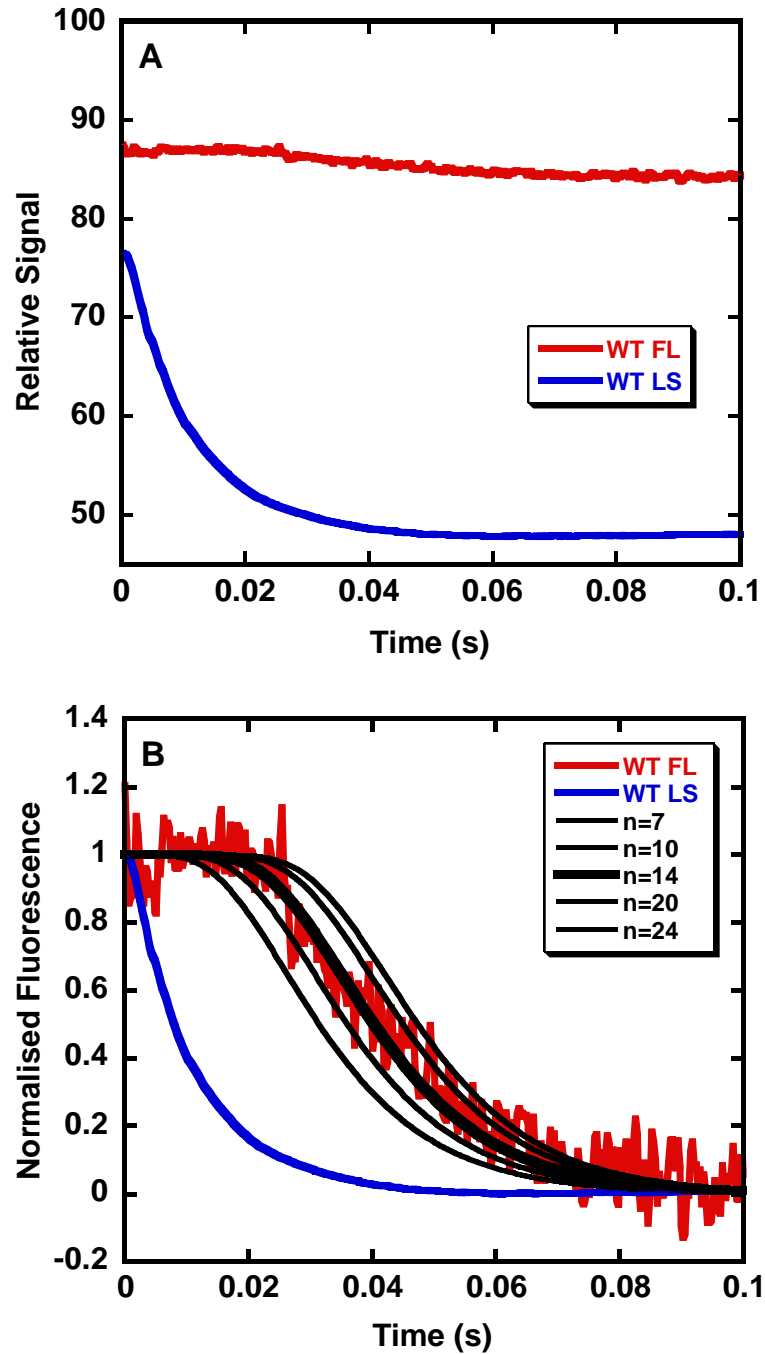
Figure 4.10- Figure 4.13 shows the superimposed fits of  $n$  values obtained for WT and 7 cTnT mutants. The cooperative unit for thin filament in the presence of wild type Tn and calcium is 10-14 in agreement with previously reported values (Maytum, Konrad et al., 2001; Maytum, Westerdorf et al., 2003). Thin filaments reconstituted with TnT R141W and S179F gave similar  $n$  values. The lag in fluorescence signal was largest for  $\Delta$ K210 (Figure 4.11B),  $\Delta$ 14 (Figure 4.13B) and  $\Delta$ 28+7 (Figure 4.13C). A greater lag suggests a larger number of actin monomers being maintained in the ON state by a single myosin S1 and therefore a bigger value of  $n$ . The simulations obtained with various  $n$  values suggest a value of  $n=20$  for thin filaments reconstituted with TnT  $\Delta$ K210, 24 for thin filaments reconstituted with TnT  $\Delta$ 14 or TnT  $\Delta$ 28+7. In contrast the fluorescence traces obtained with thin filaments reconstituted with TnT  $\Delta$ E160 showed a smaller lag and therefore a reduced size of the cooperative unit. An approximate value of  $n=5$  was determined for this mutant. These experiments were carried out a minimum of 2 times using different preparations of proteins.

Table 4.1 summarises the results from these experiments. The values obtained for  $n$  remained consistent between experiments at varying ATP concentrations.

**Table 4.1 Summary of the effect of cTnT mutations on the thin filament switching parameter  $n$**

<b>cTnT</b>	<b>Apparent cooperative unit size <math>n</math></b>	<b>No. of experiments</b>
<b>WT</b>	10-14	6
<b>TnT1-R141W</b>	10-14	6
<b>TnT2-<math>\Delta</math>K210</b>	20	5
<b>TnT1-<math>\Delta</math>E160</b>	5-6	2
<b>TnT1-S179F</b>	14	3
<b>TnT2-K273E</b>	14	3
<b>TnT2-<math>\Delta</math>14</b>	>24	2
<b>TnT2-<math>\Delta</math>28+7</b>	>24	2

The data are expressed from minimum 2 individual experiments carried out using different batches of protein preparations. Values of  $n > 20$  is not true number



**Figure 4.10 Kinetics of ATP induced dissociation of S1 from Actin.Tm.Tn thin filament (wild type)**

(A) Time courses of fluorescence and light scattering for wild type Tn. The signals are an average of 6-8 transients (B) Normalised time courses of light scattering (blue line) and fluorescent (red line) signals when  $40\mu\text{M}$  ATP was mixed with  $6\mu\text{M}$  S1,  $6\mu\text{M}$  actin,  $1\mu\text{M}$  Tm and  $1\mu\text{M}$  Tn. The black lines are the computer generated simulation curves using  $k_{LS} = 98\text{ s}^{-1}$ . The experiments were performed in  $140\text{mM}$  KCl,  $4\text{mM}$   $\text{MgCl}_2$ ,  $0.2\text{mM}$   $\text{CaCl}_2$ ,  $1\text{mM}$  DTT,  $20\text{mM}$  MOPS, pH 7.2.

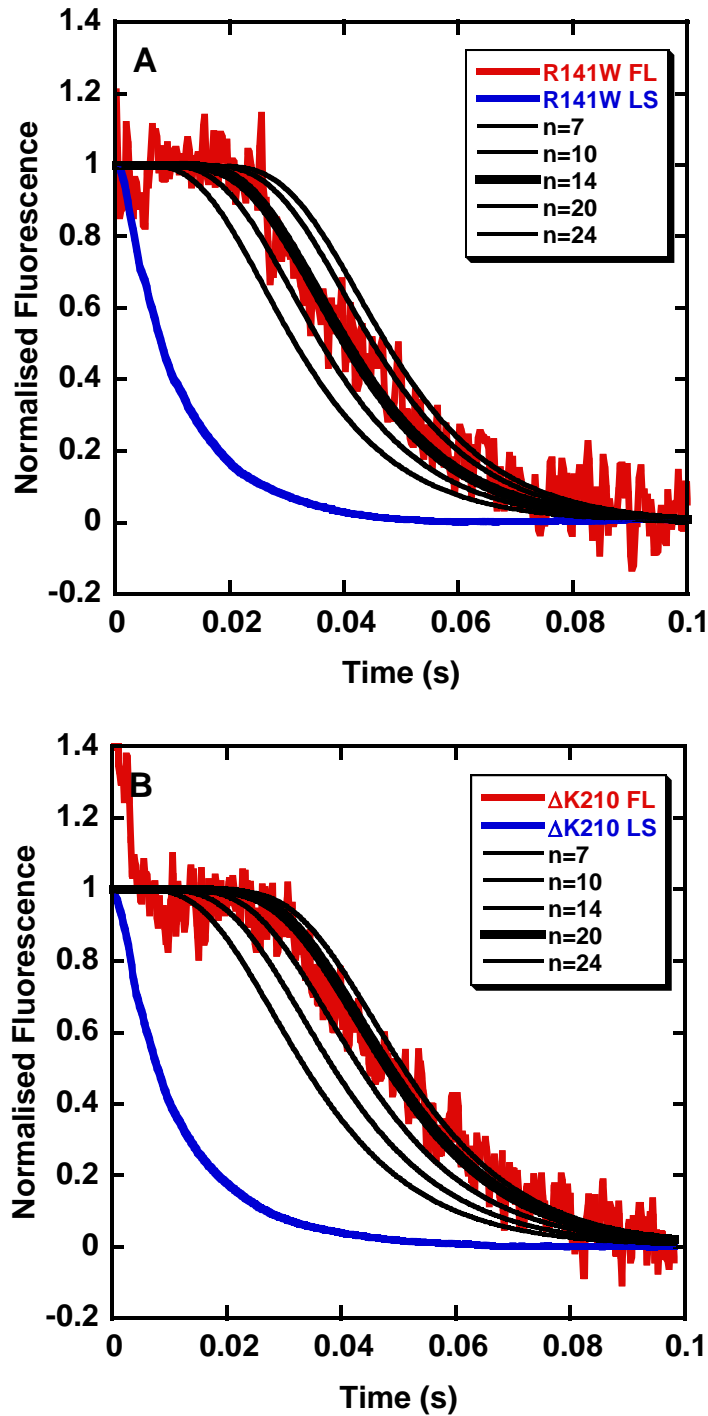


**Figure 4.11 Kinetics of ATP induced dissociation of S1 from Actin.Tm.Tn thin filament for DCM mutations**

(A) Time courses of fluorescence and light scattering for R141W Tn. The signals are an average of 6-8 transients (B) Normalised time courses of light scattering (blue line) and fluorescent (red line) signals when  $40\mu\text{M}$  ATP was mixed with  $6\mu\text{M}$  S1,  $6\mu\text{M}$  actin,  $1\mu\text{M}$  Tm and  $1\mu\text{M}$  Tn. The black lines are the computer generated simulation curves using  $k_{LS} = 94\text{ s}^{-1}$ . The experiments were performed in  $140\text{mM}$  KCl,  $4\text{mM}$   $\text{MgCl}_2$ ,  $0.2\text{mM}$   $\text{CaCl}_2$ ,  $1\text{mM}$  DTT,  $20\text{mM}$  MOPS, pH 7.2.

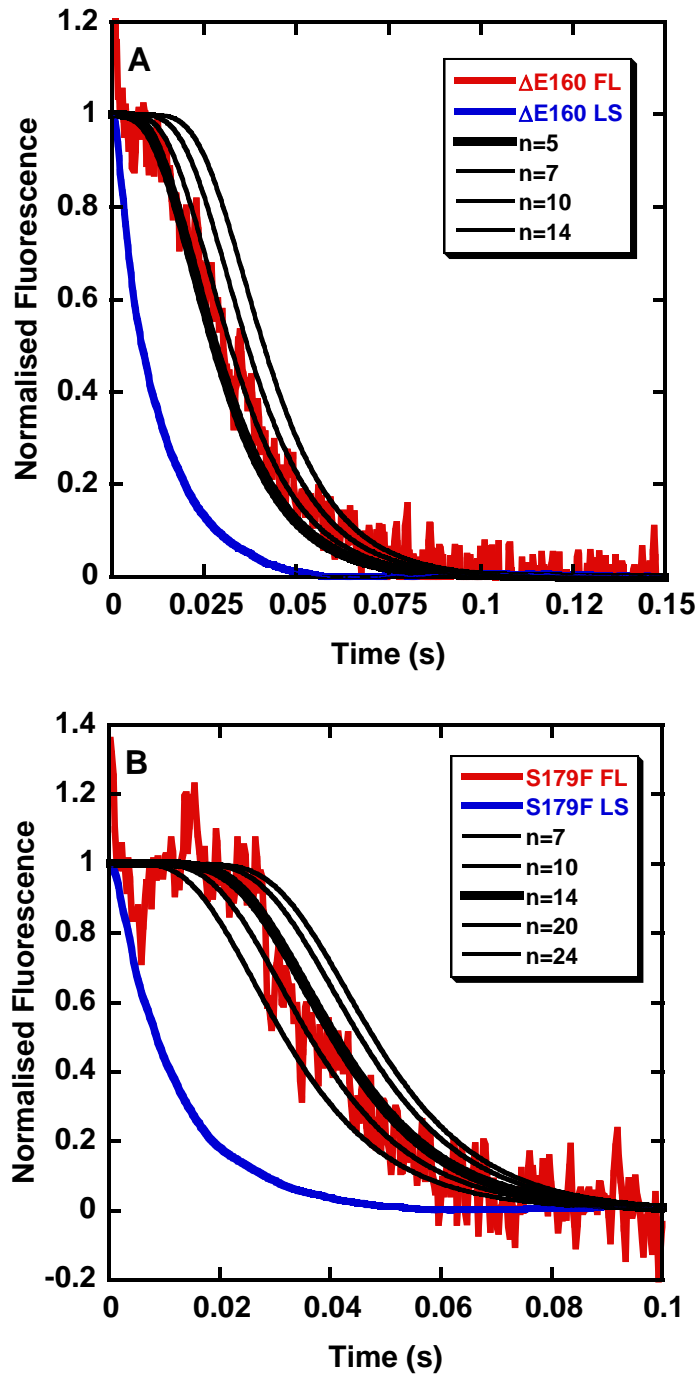


**Figure 4.12 Kinetics of ATP induced dissociation of S1 from Actin.Tm.Tn thin filament for HCM-T1 region mutation**

(A) Time courses of fluorescence and light scattering for S179F Tn. The signals are an average of 6-8 transients (B) Normalised time courses of light scattering (blue line) and fluorescent (red line) signals when  $40 \mu\text{M}$  ATP was mixed with  $6 \mu\text{M}$  S1,  $6 \mu\text{M}$  actin,  $1 \mu\text{M}$  Tm and  $1 \mu\text{M}$  Tn. The black lines are the computer generated simulation curves using  $k_{\text{LS}} = 90 \text{ s}^{-1}$ . The experiments were performed in  $140 \text{ mM}$  KCl,  $4 \text{ mM}$   $\text{MgCl}_2$ ,  $0.2 \text{ mM}$   $\text{CaCl}_2$ ,  $1 \text{ mM}$  DTT,  $20 \text{ mM}$  MOPS, pH 7.2.

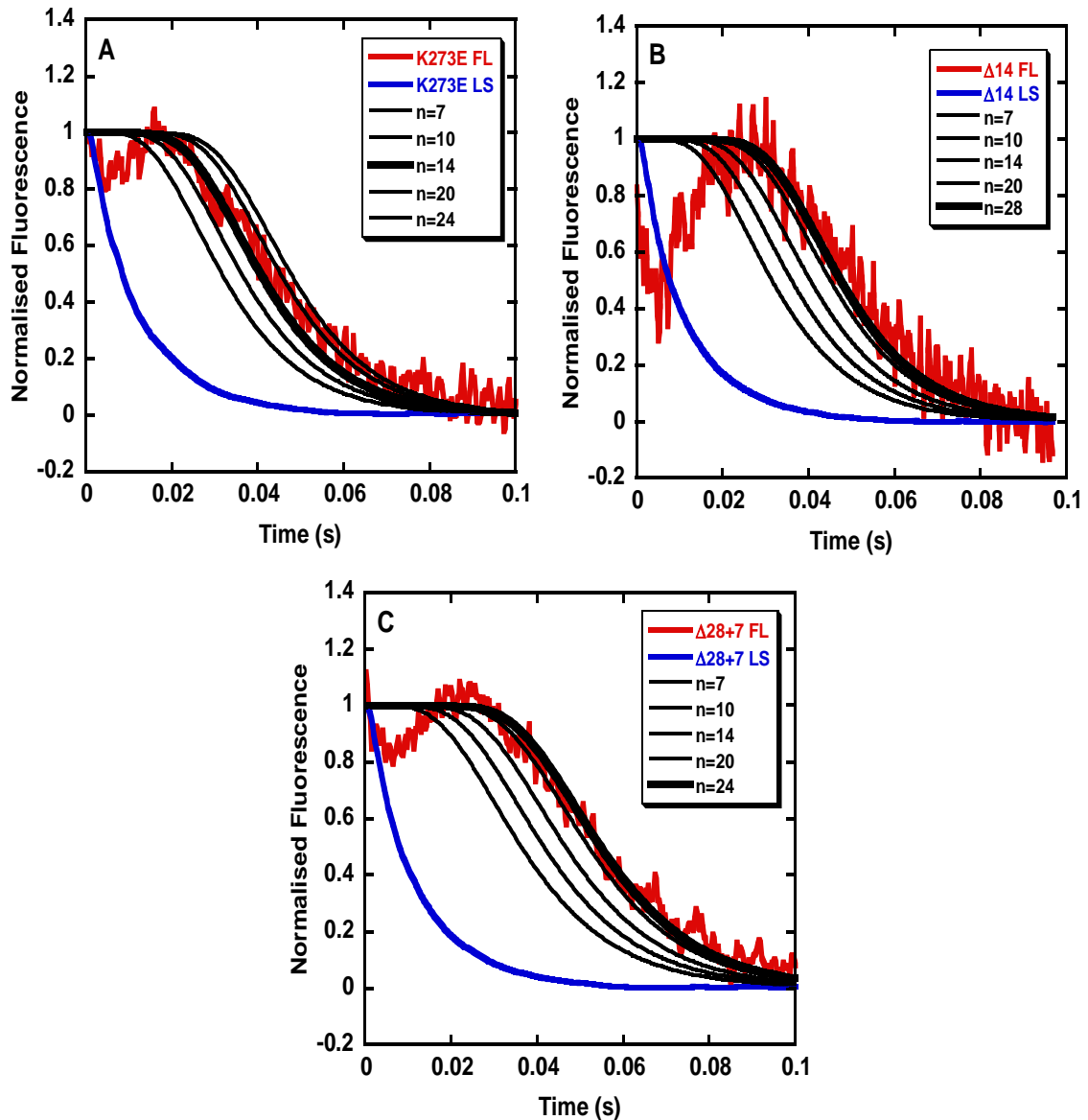


**Figure 4.13 Kinetics of ATP induced dissociation of S1 from Actin.Tm.Tn thin filament for HCM-T2 region mutations**

(A) Time courses of fluorescence and light scattering for Tn. The signals are an average of 6-8 transients (B) Normalised time courses of light scattering (blue line) and fluorescent (red line) signals when  $40\mu\text{M}$  ATP was mixed with  $6\mu\text{M}$  S1,  $6\mu\text{M}$  actin,  $1\mu\text{M}$  Tm and  $1\mu\text{M}$  Tn. The black lines are the computer generated simulation curves using  $k_{LS} = 90\text{ s}^{-1}$ . The experiments were performed in  $140\text{mM}$  KCl,  $4\text{mM}$   $\text{MgCl}_2$ ,  $0.2\text{mM}$   $\text{CaCl}_2$ ,  $1\text{mM}$  DTT,  $20\text{mM}$  MOPS, pH 7.2.

## 4.2(B) Equilibrium Constant $K_B$

### 4.2.3 Comparison of Cardiac and Skeletal Muscle Thin Filaments

As mentioned in the introduction, the blocked state is a state of muscle thin filament obtained in the absence of  $Ca^{2+}$ . It is therefore necessary to assess if different isoforms of thin filament components will affect the equilibrium constant  $K_B$ . Previous investigations have compared the effect of different isoforms of Tn (bovine heart in comparison to rabbit skeletal muscle isoforms) and concluded that there was no difference in the values of  $K_B$  between these two isoforms of Tn (Maytum et al., 1999; Reiffert et al. 1996). In this thesis we have used recombinants human cardiac Tn. Prior to carrying out stopped flow experiments to determine the effects of TnT mutations on the occupancy of B-state, the regulatory properties of cardiac versus skeletal thin filament system were compared. Cardiac thin filaments were reconstituted with cardiac isoforms of actin and Tm (obtained from sheep heart) and recombinant human cardiac Tn while skeletal muscle thin filaments were reconstituted from rabbit skeletal muscle actin, Tm and Tn.

$K_B$  is measured by comparing the kinetics of S1 binding to thin filaments at low and high  $Ca^{2+}$ . A 10 fold excess of actin was rapidly mixed with S1 and the binding event was monitored by the quenching of the fluorescence using pyrene label attached at Cys-374 of actin. Figure 4.14 shows the calcium dependence of the rate of S1 binding to actin with increasing complexity of the two systems.

For skeletal system, the observed rate constant obtained for actin alone (6 $\mu$ M) and Actin.Tm (6 $\mu$ M:1 $\mu$ M) were 20.8s<sup>-1</sup> and 15.5s<sup>-1</sup> respectively. At Actin.Tm.Tn (6  $\mu$ M:1  $\mu$ M: 1  $\mu$ M) we observed an exponential fluorescence change with  $k_{obs}$  of 12.9s<sup>-1</sup> in the presence of calcium. This suggests that the Actin.Tm.Tn+Ca<sup>2+</sup> is not in fully “on-state” as it would be expected for actin on its own. The ratio of the values of  $k_{obs}$  in the presence and absence of calcium was equal to 3.5 with a  $K_B$  (-Ca<sup>2+</sup>/+Ca<sup>2+</sup>) of 0.4.

In Figure 4.14 (B) the experiment was repeated for the cardiac thin filaments at actin concentration of 6 $\mu$ M. Values of the observed rate constant similar to those obtained with skeletal muscle thin filaments, were obtained with actin alone, actin.Tm and actin.Tm.Tn.Ca<sup>2+</sup>. However, in the absence of calcium in the cardiac system  $k_{obs}$  was 6s<sup>-1</sup>, higher than for skeletal muscle thin filaments. For cardiac thin filaments, the ratio of the values of  $k_{obs}$  in the presence and absence of calcium was equal to 2.6 and a  $K_B$ (-Ca<sup>2+</sup>/+Ca<sup>2+</sup>) of 0.61 was calculated. Our results are similar to those published previously for wild type Tn for both systems (Reiffert, Jaquet et al., 1996; Reiffert, Maytum et al., 1999; Lohmann, Westerdorf et al., 2001). The only observed difference between cardiac and skeletal muscle thin filaments was seen in the  $k_{obs}$  values obtained in the absence of Ca<sup>2+</sup>.

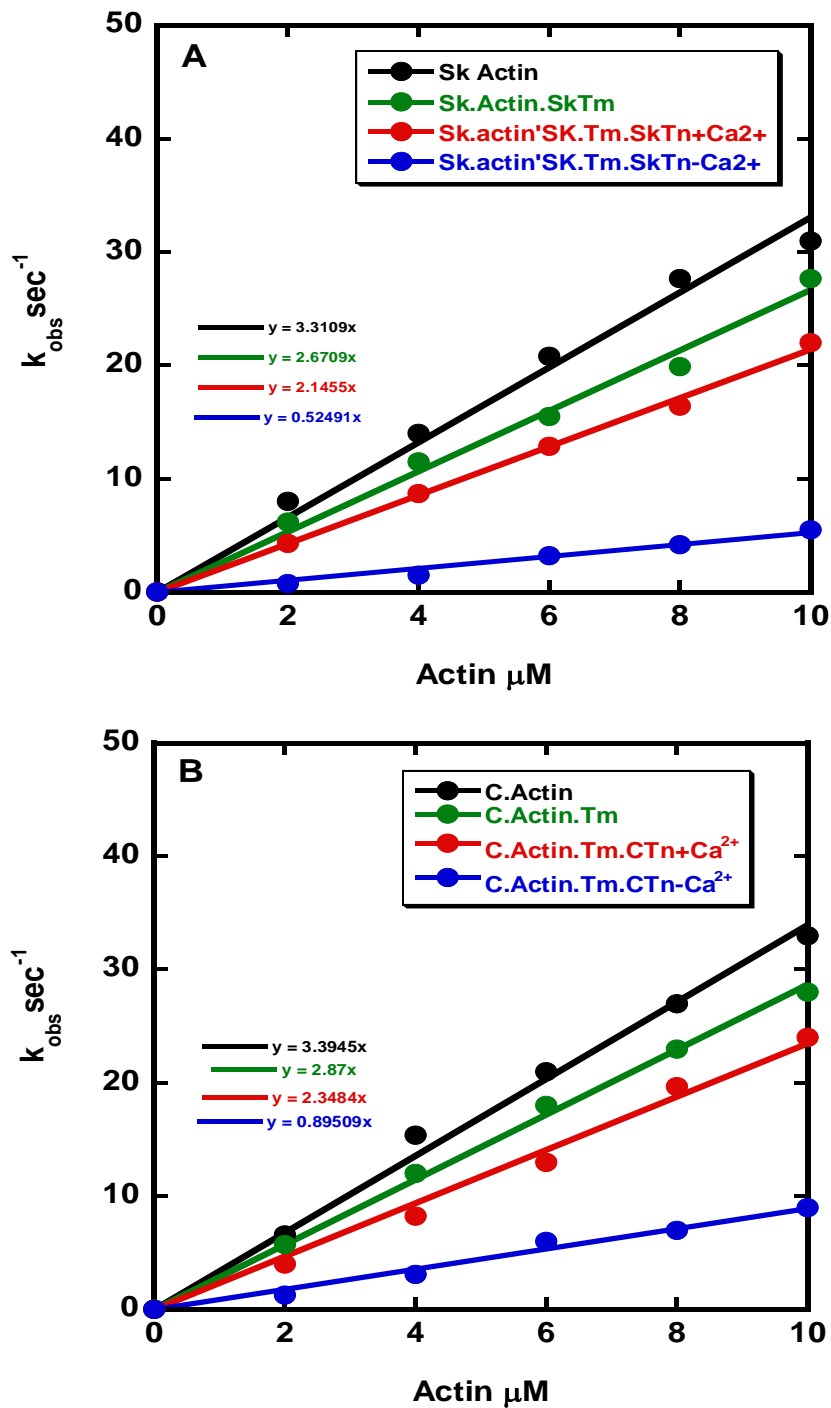


**Figure 4.14 Comparison of Cardiac versus Skeletal thin filament systems**  
 Plot of  $k_{obs}$  obtained by fitting the transients at each actin concentration to a single exponential for (A) skeletal system (B) cardiac system. Conditions: 140 mM KCl, 4 mM MgCl<sub>2</sub>, 1 mM DTT, 20 mM MOPS, pH 7.2, 0.2 mM CaCl<sub>2</sub> or 1 mM EGTA, 25°C.

#### 4.2.4 Effect of Troponin T Mutations on $K_B$ .

To detect the possible effects on the equilibrium constant  $K_B$ , the time course of kinetics of S1 binding to thin filaments were carried out for each mutations. The observed rate constants were obtained by fitting transients at increasing thin filament concentration to a single exponential for WT and all 3 groups of mutations studied. Good fits to the data suggested that the model was an accurate description of the system in the range studied.

In Figure 4.15-Figure 4.17,  $k_{obs}$  is plotted versus increasing thin filament concentration. Each of the four curves per graph represents the binding of S1 to actin alone (black curve) actin.Tm.Tn in the presence and absence of  $Ca^{2+}$  respectively (red for WT and blue for mutant). Although literature studies reported that the observed rate constant for actin alone and the Actin.Tm.Tn+ $Ca^{2+}$  are the same, in all our experiments we consistently observed a lower value for  $k_{obs}$  of S1 binding to actin in the presence of Tm.Tn and calcium in comparison to actin alone. We believe that although  $Ca^{2+}$  switches the filament from the blocked state to the closed state, a small proportion of the filament (probably less than 10%) is still in the blocked state. Hence we believe that using the  $k_{obs}$  values obtained with actin alone as a reference is more appropriate (equation 6) than using the values obtained with Tn- $Ca^{2+}$  (equation 5). The  $k_{obs}$  obtained in both the presence and absence of calcium as well as actin alone are linearly dependent upon actin concentration over the range 1-10  $\mu$ M. Table 4.2 shows the  $K_B$  values determined using both equations (5) and (6) for comparison. Experiments for WT and each mutation were carried out in parallel and performed at the same pCa values.

Apart from R141W mutation showing a slight decrease in  $K_B$  (-Ca<sup>2+</sup>/+Ca<sup>2+</sup>), the basic result of this work for DCM mutation  $\Delta$ K210 and all HCM mutations were increased  $K_B$  values. In my opinion the calculations using  $K_B$  in the presence of Ca<sup>2+</sup> is not accurate as the closed state is not fully switched on. A true reflection of the  $K_B$  values are obtained using actin curve. However, when  $K_B$  was calculated against Actin, there was no significant difference seen between WT and DCM mutations (R141W and  $\Delta$ K210) and a substantial increase in  $K_B$  was evident for all HCM mutations. In particular, HCM mutations K273E,  $\Delta$ 14 and  $\Delta$ 28+7 in the T2 region confirm loss of a blocked state.

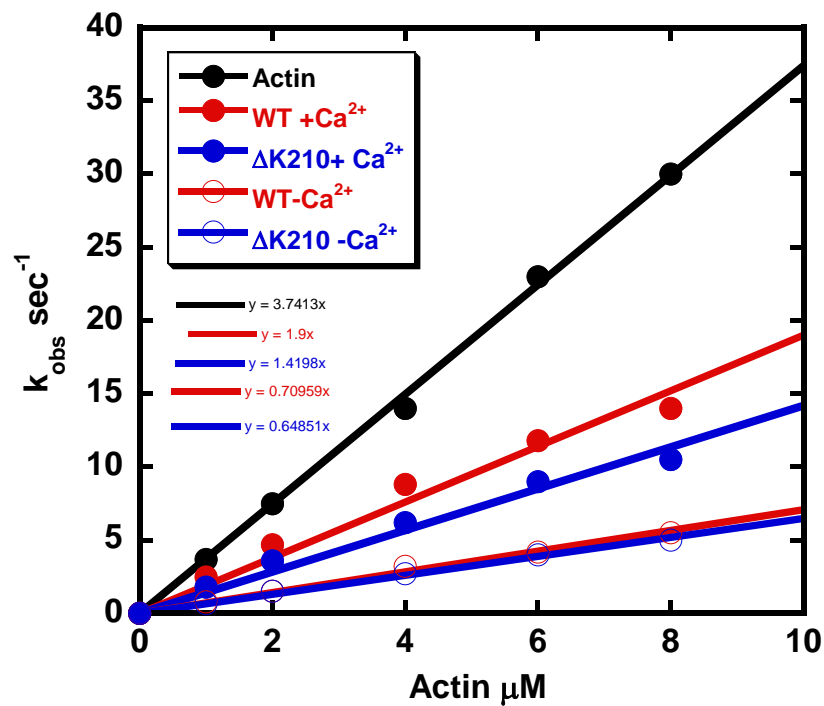
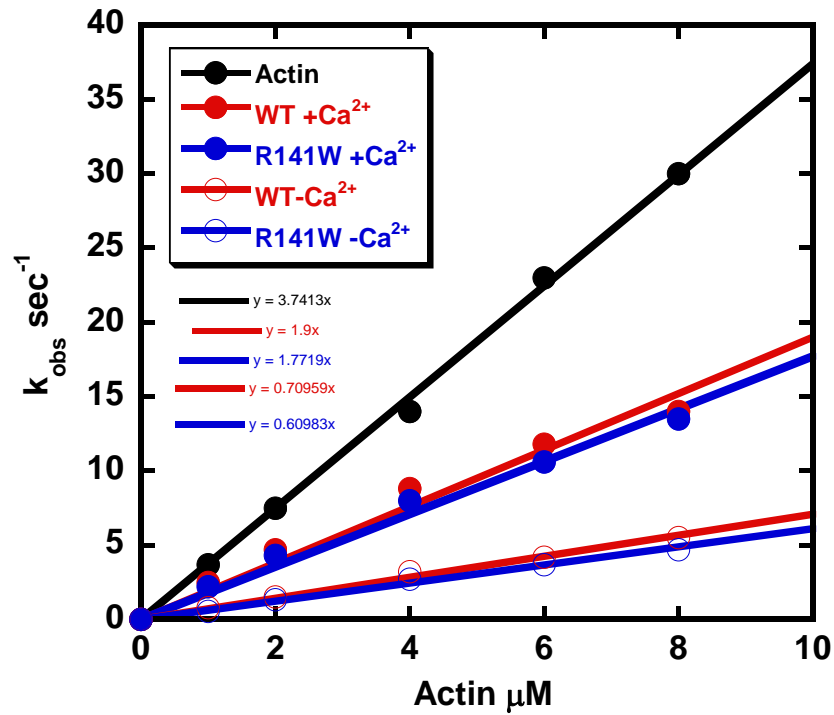


**Figure 4.15 Binding of S1 to pyrene actin in the presence and absence of Calcium for DCM mutations**

The observed rate of binding as a function of pyrene actin concentration in the presence or absence of calcium. The graphs have slopes of  $1.56 \times 10^6 \text{ M}^{-1} \cdot \text{s}^{-1}$  (+Ca<sup>2+</sup>) and  $0.52 \times 10^6 \text{ M}^{-1} \cdot \text{s}^{-1}$  (-Ca<sup>2+</sup>). Conditions: 140mM KCl, 10mM MOPS, 4mM MgCl<sub>2</sub>, 1mM DTT, 0.2mM CaCl<sub>2</sub> or 1mM EGTA, pH 7.2, at 25° C.

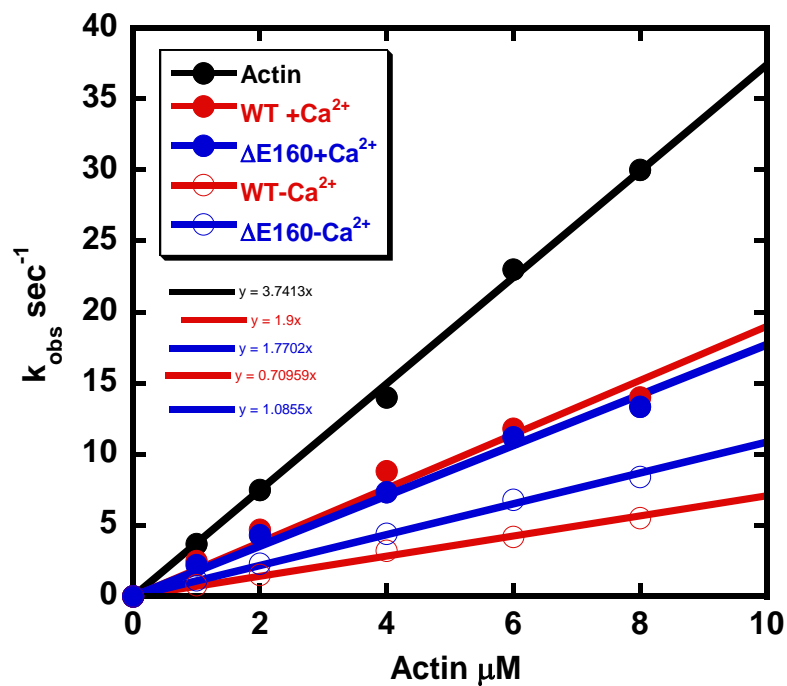


**Figure 4.16 Binding of S1 to pyrene actin in the presence and absence of Calcium for HCM-T1 mutations**

The observed rate of binding as a function of pyrene actin concentration in the presence or absence of calcium. The graphs have slopes of  $1.56 \times 10^6 \text{M}^{-1} \cdot \text{s}^{-1}$  ( $+\text{Ca}^{2+}$ ) and  $0.52 \times 10^6 \text{M}^{-1} \cdot \text{s}^{-1}$  ( $-\text{Ca}^{2+}$ ). Conditions: 140mM KCl, 10mM MOPS, 4mM  $\text{MgCl}_2$ , 1mM DTT, 0.2mM  $\text{CaCl}_2$  or 1mM EGTA, pH 7.2, at 25° C.

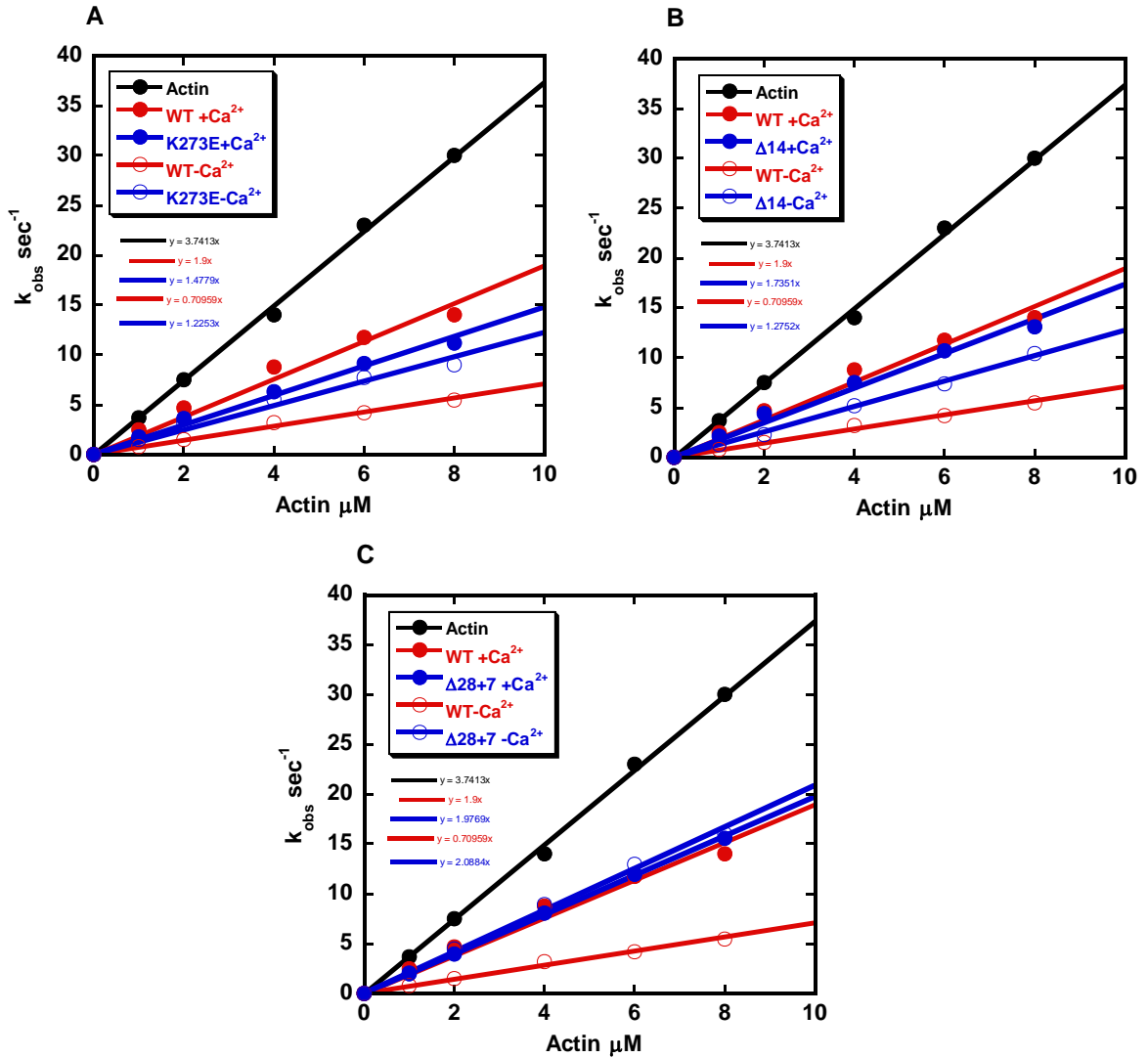


**Figure 4.17 Binding of S1 to pyrene actin in the presence and absence of Calcium for HCM T2 mutations**

The observed rate of binding as a function of pyrene actin concentration in the presence or absence of calcium. The graphs have slopes of  $1.56 \times 10^6 \text{M}^{-1} \cdot \text{s}^{-1}$  ( $+\text{Ca}^{2+}$ ) and  $0.52 \times 10^6 \text{M}^{-1} \cdot \text{s}^{-1}$  ( $-\text{Ca}^{2+}$ ). Conditions: 140mM KCl, 10mM MOPS, 4mM  $\text{MgCl}_2$ , 1mM DTT, 0.2mM  $\text{CaCl}_2$  or 1mM EGTA, pH 7.2, at 25° C.

**Table 4.2 Summary of the effect of cTnT mutations on the thin filament switching parameter  $K_B$**

cTnT	Equilibrium constant $K_B$		No. of experiments
	$-Ca^{2+}/+Ca^{2+}$	$-Ca^{2+}/Actin$	
WT	0.67±0.08	0.22±0.03	7
TnT1-R141W	0.51±0.02	0.19±0.04	7
TnT2-ΔK210	0.81±0.18	0.21±0.04	7
TnT1-ΔE160	1.58±0.02	0.39±0.02	2
TnT1-S179F	6.4±0.2	0.64±0.04	3
TnT2-K273E	4.7±0.5	0.67±0.08	4
TnT2-Δ14	2.8±0.05	0.51±0.02	6
TnT2-Δ28+7	17.5±2	1.24±0.11	2

*The numbers are expressed as mean values from a minimum of two experiments.*

## 4.3 Discussion

Cooperative transitions of thin filaments between the inhibited and activated states are important determinants of the contraction of the heart and its regulation by  $\text{Ca}^{2+}$ . Relaxation during diastole is achieved by maintaining the thin filaments in a blocked state by troponin at low  $\text{Ca}^{2+}$ . Contraction during systole is triggered by  $\text{Ca}^{2+}$  binding to troponin and subsequent switching of the thin filaments to the open state. The distribution of these states (defined by  $K_B$  and  $K_T$ , Figure 4.18) determines the level of ATP hydrolysis and force produced by the cardiac muscle. The transitions between these states are cooperative (defined by the size of the cooperative unit  $n$ ). Both the distribution of these states and thin filament cooperativity are affected by troponin. Hence it is legitimate to expect that diseases causing mutation in troponin may affect either one or more of these thin filament properties.

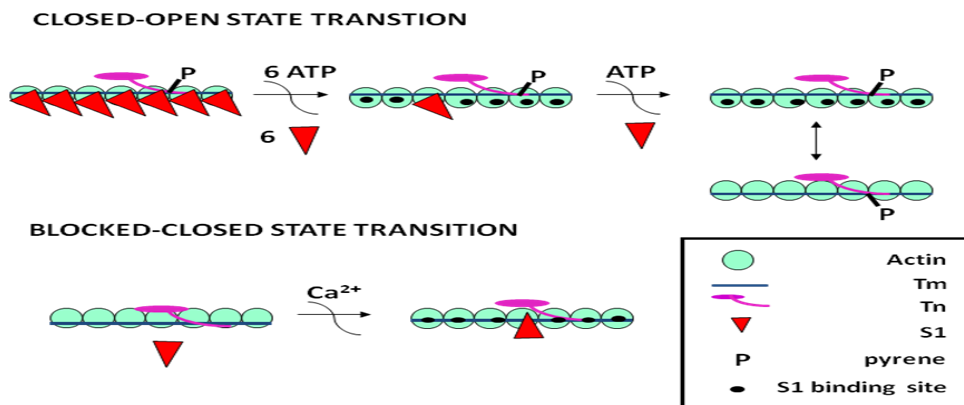


**Figure 4.18 Schematic models of thin filament switching states**

(A) size of cooperative unit ' $n$ ' (B) equilibrium constant  $K_B$ . Conditions are as follows: 10mM MOPS, 140mM KCl, 4mM  $\text{MgCl}_2$ , and 1mM DTT 0.2mM  $\text{NaN}_3$ , pH 7.2, 25°C.

The work in this chapter describes the effect of 8 cTnT mutants on two parameters  $n$  and  $K_B$  respectively.

### **4.3.1 Effect of Troponin T Mutations on the Size of the Cooperative Unit, $n$**

Cooperativity in muscle thin filaments is primarily due to Tropomyosin. Cardiac thin filament has a cooperative unit size close to the structural unit size of 7, suggesting little or no strong Tm-Tm communication. However for thin filament in the presence of Tn and calcium, the cooperative unit size is close to twice the structural unit size indicating significant Tm-Tm communication. This increased cooperativity is known to arise mainly due to the N-terminal TnT-1 fragment that binds to the Tm-Tm overlap region. Previous studies have provided estimates for  $n$  such as mechanical studies on muscle fibres were modelled as  $n=14-21$  (Moss 1992) and  $n \geq 11$  for cardiac actin.tn in the presence of calcium.

Many researchers have attempted to develop a signal to monitor the cooperative transition between the 3 states. Probes on TnI (Trybus and Taylor 1980) and actin (Criddle et al. 1985) gave very small change (less than 5%). Ischii and Lehrer reported the excimer fluorescence of Tm and studies using this probe have shown that the ON-OFF transition gave a signal change with large amplitude for actin-Tm (McKillop and Geeves 1993; Maytum et al. 1999).

It has previously been shown that, for Tm-containing actin filaments, it is possible to determine the apparent cooperative unit size,  $n$ , using the Tm excimer fluorescence probe. Data presented in this chapter confirm that both equilibrium and kinetic measurements allow an accurate determination of  $n$  for actin-tropomyosin. However in the presence of troponin the amplitude of the excimer fluorescence change upon transition between the inhibited and activated states is much smaller making the determination of  $n$  more difficult.

Equilibrium measurements of  $n$  were not successful as they rely on the incremental increase of the excimer fluorescence (a 5 % total change to be spread between 10 data points or so). The kinetic method of ATP- induced S1 dissociation proved successful for all WT and cTnT mutants (This method does not rely as much on the amplitude of the signal). Another difficulty with this method arise from the fact that for  $n > 21$ , the variation between the curves generated by different values of  $n$  (example between 21 and 28, 35...) is reduced, and the accuracy of defining  $n$  become questionable. In contrast for  $n$  values less than 7 this method is more robust (and so the differences between the obtained curves for  $n=3$  or 5 or 7 are substantial).

The results summarised in Table 4.1 showed that for  $\Delta E160$  the size of the cooperative unit  $n$  was reduced substantially from a value of  $n=14$  for WT to value of  $n=5$  which is in broad agreement with the prediction that mutations from the TnT1 region would be expected to change the size of the cooperative unit. Tn appears to not facilitate the interaction between Tm-Tn confirming that the  $\Delta E160$  mutation is in a critical region and therefore affects the binding of actin to S1. A reduction in the size of cooperative unit  $n$  is likely to lead to less activation of thin filaments and therefore to less force being produced (hypocontractile myocardium). However, ' $n$ ' remained unchanged for both R141W and S179F. An increase in cooperativity was observed for  $\Delta K210$ ,  $\Delta 14$  and  $\Delta 28+7$  to  $n \geq 20$ . These mutations have seemingly increased long range communication between neighbouring structural units. An increase in the size of cooperative unit  $n$  is likely to lead to more activation of thin filaments and therefore to more force being produced (hypercontractile myocardium). In addition increased cooperativity will lead to delayed relaxation (as shown by the

longer lag displayed in our ATP induced acto-S1 experiments). Relaxation problems are observed in patients with HCM.

### **4.3.2 Equilibrium Constant $K_B$**

The removal of  $Ca^{2+}$  during the diastole leads to the switching of thin filaments to the Blocked state. Hence the proportion of thin filament in the blocked state is an important determinant of cardiac muscle relaxation.

To monitor  $K_B$  we followed the kinetics of the binding of S1 in the presence of absence of calcium to an excess of actin. At high [actin], the observed rate constant reached a maximum value suggesting that a first order transition presumably isomerisation is rate limiting. At low [actin], the observed rate constant is linearly proportional and the gradient generated the apparent second order rate constant. The difference in the gradient obtained in the absence of  $Ca^{2+}$  to the gradient obtained for actin alone (pure actin filaments are in the fully ON state) allow the determination of  $K_B$ .

The regulatory properties of skeletal and cardiac Tn has been compared using kinetic measurements of S1 binding to reconstituted thin filament to determine the occupancy of B-state. The results were essentially the same as described in literature with the exception of the  $Tn+Ca^{2+}$  state not being in the fully open state in our studies (Maytum, Konrad et al., 2001; Maytum, Westerdorf et al., 2003). These differences in results can be described in terms of the free energy of  $Ca^{2+}$  binding being less available for switching of the system. This means the cardiac system will either be less OFF or less ON or even both at high and low calcium concentrations.

Next we investigated the effect of TnT mutations on the kinetics of S1 binding to actin thin filament to determine the occupancy of the blocked state. We found that  $K_B$  was unchanged by mutations R141W,  $\Delta$ K210 and S179F. However, an increase in  $K_B$  in the absence of  $Ca^{2+}$  was observed for K273E,  $\Delta$ E160,  $\Delta$ 14 and  $\Delta$ 28+7. This implies that these mutations cause less inhibition in the absence of  $Ca^{2+}$  and so relaxation may be compromised by these mutations.

# CHAPTER 5

Effect of TnT mutations on thin filament  
Ca<sup>2+</sup> affinity and kinetics of Ca<sup>2+</sup>  
dissociation

## **Contents**

<b>5.1</b>	<b>Introduction</b>	<b>143</b>
<b>5.2</b>	<b>Results</b>	<b>145</b>
<b>5.2 (A)</b>	<b>TnT Mutations on Ca<sup>2+</sup> Binding Properties</b>	<b>145</b>
<b>5.2 (B)</b>	<b>Effect of TnT Mutations on the Kinetics of Ca<sup>2+</sup> Dissociation</b>	<b>157</b>
<b>5.3</b>	<b>Discussion</b>	<b>191</b>

## 5.1 Introduction

Transient changes in the concentration of  $\text{Ca}^{2+}$  ions are believed to be the trigger for a cascade of protein-protein interaction alterations which lead to muscle contraction.  $\text{Ca}^{2+}$  binds TnC and the  $\text{Ca}^{2+}$  binding message is transmitted to actin via TnI and to Tm via TnT. These events ultimately lead to the activation of thin filament. The level of activation of thin filament depend on the concentration of  $\text{Ca}^{2+}$ , thin filament affinity to  $\text{Ca}^{2+}$  and the transitions from the inhibited (or blocked) state to the activated state (or open state). In functional studies including ATPase, in vitro motility assays and force measurements, thin filament activation by increasing concentration of  $\text{Ca}^{2+}$  results in a sigmoidal increase of these parameters. This is defined as  $\text{Ca}^{2+}$  sensitivity.

As stated above the multiple interactions of the Tn subunits between each other and with actin and Tm play a fundamental role in thin filament activation, it is therefore reasonable to expect that cardiomyopathy causing mutations in Tn will affect  $\text{Ca}^{2+}$  activation of thin filaments. Indeed previous investigations have suggested that modulation of  $\text{Ca}^{2+}$  sensitivity is a common functional consequence of HCM and DCM causing mutations (Robinson, Mirza et al. 2002; Mirza, Marston et al. 2005; Dyer, Jacques et al. 2009).

To elucidate the molecular mechanisms that cause the shift of the  $\text{Ca}^{2+}$  sensitivity of contractile regulation (Chapter 3) and the differences in occupancy of the blocked state in the thin filament (Chapter 4) of the TnT mutations, we aimed in this chapter to assess the effect of these mutations directly on the binding and dissociation of  $\text{Ca}^{2+}$  to the TnC subunit. This is particularly relevant

for those mutations that substantially affect the  $\text{Ca}^{2+}$  sensitivity and reduce the Hill coefficient in reconstituted systems (Redwood, Lohmann et al. 2000; Burton, Abdulrazzak et al. 2002). Changes in equilibria governing the blocked, closed and open states described by the three-state model could also be correlated to the changes seen in  $\text{pCa}_{50}$  values.

A useful biophysical approach is the use of extrinsic fluorophore attached to TnC. Cardiac TnC has two cysteine residues that can be readily alkylated by mutagenesis of a single cysteine at either position 35 (C84S) or 84 (C35S). Previous studies have reported that Cys 35 located in the non-functional  $\text{Ca}^{2+}$  binding loop I is insensitive to  $\text{Ca}^{2+}$  binding and Cys 84 located near where TnC-TnI interaction occurs reports  $\text{Ca}^{2+}$  binding to the single  $\text{Ca}^{2+}$  specific site (Dong, Wang et al. 1997). However, this was only true for uncomplexed TnC, and when incorporated into Tn complex the reversal of sensitivity to the environment was reported (Dong, Wang et al. 1997; Kobayashi and Solaro 2006).

Several previous studies have reported the  $\text{Ca}^{2+}$  dissociation kinetics in skeletal muscle using different fluorophores (Rosenfeld and Taylor 1985; Dong, Wang et al. 1997; Kobayashi and Solaro 2006). In the work presented here, we used IAANS fluorescence (at either Cys 35 and Cys 84) to measure the  $\text{Ca}^{2+}$  affinity and  $\text{Ca}^{2+}$  dissociation kinetics from  $\text{Ca}^{2+}$  specific site of TnC within the context of whole troponin complex, reconstituted thin filament and of thin filament in the presence of S1 myosin heads. To establish whether the IAANS fluorescence transients accurately reflect removal of  $\text{Ca}^{2+}$  from the  $\text{Ca}^{2+}$  specific site, Quin-2

was used as a  $\text{Ca}^{2+}$  chelator using native reconstituted thin filament proteins (Rosenfeld and Taylor 1985).

## **5.2 Results**

### **5.2 (A) TnT Mutations on $\text{Ca}^{2+}$ Binding Properties**

#### **5.2.A.1 Fluorescence Properties of IAANS-Cys 35/84 Labelled TnC**

To measure the calcium binding at the regulatory site II of cTnC in whole Tn and reconstituted thin filament selective labelling of Cys-35 and Cys-84 of cTnC with IAANS was carried out. TnC was expressed and purified with the cysteine at residue 84 mutated to serine and then modified the remaining cysteine at position 35 with IAANS (IAANS-C35-TnC). Since the concern here was to monitor the binding kinetics of the regulatory site II, it was imperative to block the sites III and IV by preincubation of the protein in buffer containing excess of  $\text{Mg}^{2+}$  (4mM) prior to experimentation. The fluorescence emission spectrum of IAANS-Cys35 TnC is relatively insensitive to  $\text{Ca}^{2+}$  (Fig. 5.1.A, blue curves). When reconstituted as a whole Tn complex the fluorescence emission at 450nm decreases to ~ 46% of that in the absence of bound  $\text{Ca}^{2+}$  (Fig. 5.1.A, green curves) and when fully reconstituted with the thin filament proteins the fluorescence decreases by ~17%. Representative data are shown in Figure 5.1 A, red curves. The large increase of the fluorescence of IAANS attached to Cys 35 observed upon  $\text{Ca}^{2+}$  binding to the Tn complex makes this label suitable to determine the  $\text{Ca}^{2+}$  affinity of the Tn complex but not for thin filaments (as the

signal from free Tn will contribute substantially to the signal obtained with thin filaments).

Ca<sup>2+</sup> binding to reconstituted thin filament can also be monitored using IAANS-C84-TnC. Herein we mutated cysteine at residue 35 to a serine and labelled cysteine at position 84 with IAANS (IAANS-Cys84). The fluorescence intensity of IAANS on Cys-84 of cTnC in Tn complex does not change significantly (less than 5% increase) and was spectrally similar to that observed with uncomplexed IAANS-Cys35-TnC upon binding Ca<sup>2+</sup> as shown in Figure 5.1.B, green curves. Hence IAANS-C84 TnC is not suitable to determine Ca<sup>2+</sup> binding affinity of the Tn complex. In contrast, when reconstituted with thin filament Ca<sup>2+</sup> binding gave a 25% decrease in the fluorescence of IAANS-C84-TnC. The absence of fluorescence change with Tn complex makes the fluorescence of IAANS-C84-TnC very suitable to determine Ca<sup>2+</sup> binding affinity of the thin filament (no interference from any excess Tn).

The calcium –induced fluorescence changes of both IAANS-labelled at Cys35 and Cys84 have shown to be coincident with the Ca<sup>2+</sup>-activated force development and pCa-ATPase activity in skinned cardiac muscle fibre (Putkey, Liu et al. 1997).

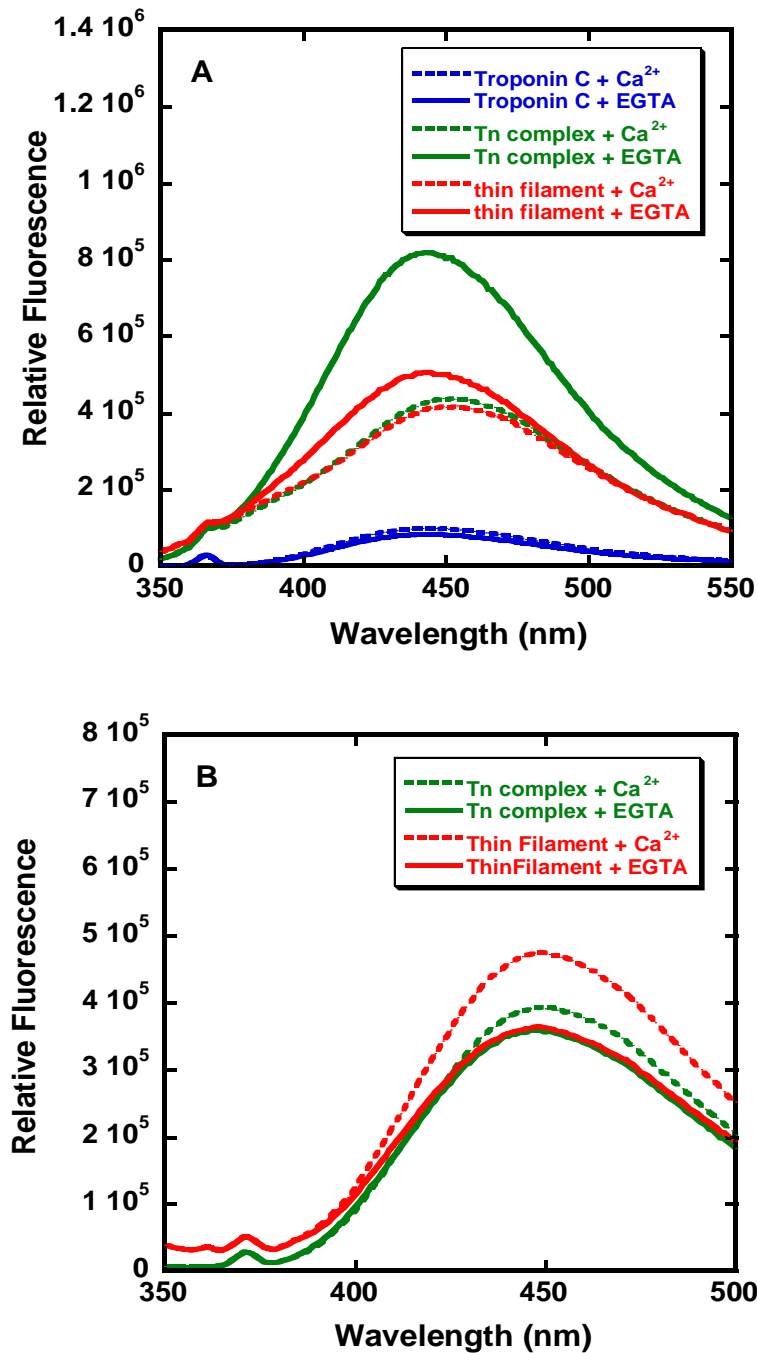


**Figure 5.1 Emission spectra of (A) IAANS attached to Cys-35 of cTnC(C84S) and (B) Cys-84 of cTnC(C35S) in various regulatory complexes.**

*The TnC subunit (blue), ternary complex (green) and the reconstituted thin filament (red) are shown. IAANS was excited at 329 nm. The conditions were 140mM KCl, 4mM MgCl<sub>2</sub>, 50mM MOPS, pH 7.0, and either 2mM EGTA (solid lines) or 0.1 mM CaCl<sub>2</sub> (dashed lines) at 25 °C.*

### 5.2.A.2 Effect of cTnT Mutations on Ca<sup>2+</sup> Affinity of the Tn Complex

The experiments reported here aims to investigate the Ca<sup>2+</sup> binding properties of Tn in complex. Ca<sup>2+</sup> binding to a single regulatory site II of TnC was monitored by the intensity change of the fluorescence emission from IAANS - Cys 35 of TnC for complex. Upon Ca<sup>2+</sup> binding to TnC, the fluorescence intensity decreases. Since the initial fluorescence values and the amplitude of fluorescence changes were slightly different between different mutants we normalised the data so that the maximum observed fluorescence change (maximum amplitude) is given a value of 1. Figure 5.2 shows the representative normalised data and Table 5.1 shows the quantitative parameters of Ca<sup>2+</sup> binding including the hill coefficient ( $n_H$ ), the pCa<sub>50</sub> and the dissociation constant ( $K_d$  calculated from the pCa<sub>50</sub>).

Initial measurements showed that the WT Tn binds Ca<sup>2+</sup> with a  $K_d = 1.86E^{-7}$  M (pCa<sub>50</sub> 6.65) in agreement with previously determined values (Li, Wang et al. 2003; Kobayashi, Dong et al. 2004; Kobayashi and Solaro 2006; Robinson, Griffiths et al. 2007).

The curves describing the fluorescence change obtained upon Ca<sup>2+</sup> binding to the Tn complexes reconstituted with DCM mutations R141W (Fig.5.2.A, blue curve) and  $\Delta$ K210 (Figure 5.2.A, red curve) are on top of the curve obtained with the WT indicating no major difference in the Ca<sup>2+</sup> binding properties of these mutant Tns. Fitting the data to the hill equation gave pCa<sub>50</sub> values very close to the wild type (pCa<sub>50</sub>=6.57 for R141W and pCa<sub>50</sub> =6.67 for  $\Delta$ K210).

Similarly, HCM-T1 mutations had essentially no effect on the  $\text{Ca}^{2+}$  binding affinity of  $\text{Ca}^{2+}$  to Tn complex. In contrast mutations located at the extreme C-terminus of TnT K273E and  $\Delta 28+7$  gave a rightward shift in the  $\text{Ca}^{2+}$  dependent fluorescence changes indicated by a decrease in the  $\text{pCa}_{50}$  values. Thus, TnT mutations in the T2 region of TnT, particularly truncated mutation  $\Delta 28+7$  bind  $\text{Ca}^{2+}$  slightly weaker compared to the WT Tn complex (Table 5.1)

All of the Tn complexes bound  $\text{Ca}^{2+}$  with a Hill coefficient  $n_H$  of  $\sim 1.0$  which indicates no cooperativity in  $\text{Ca}^{2+}$  binding to cTn as previously reported (Kobayashi and Solaro 2006). Cardiac Tn has only one  $\text{Ca}^{2+}$  specific site and so no cooperativity is expected for  $\text{Ca}^{2+}$  binding to the isolated Tn complex.

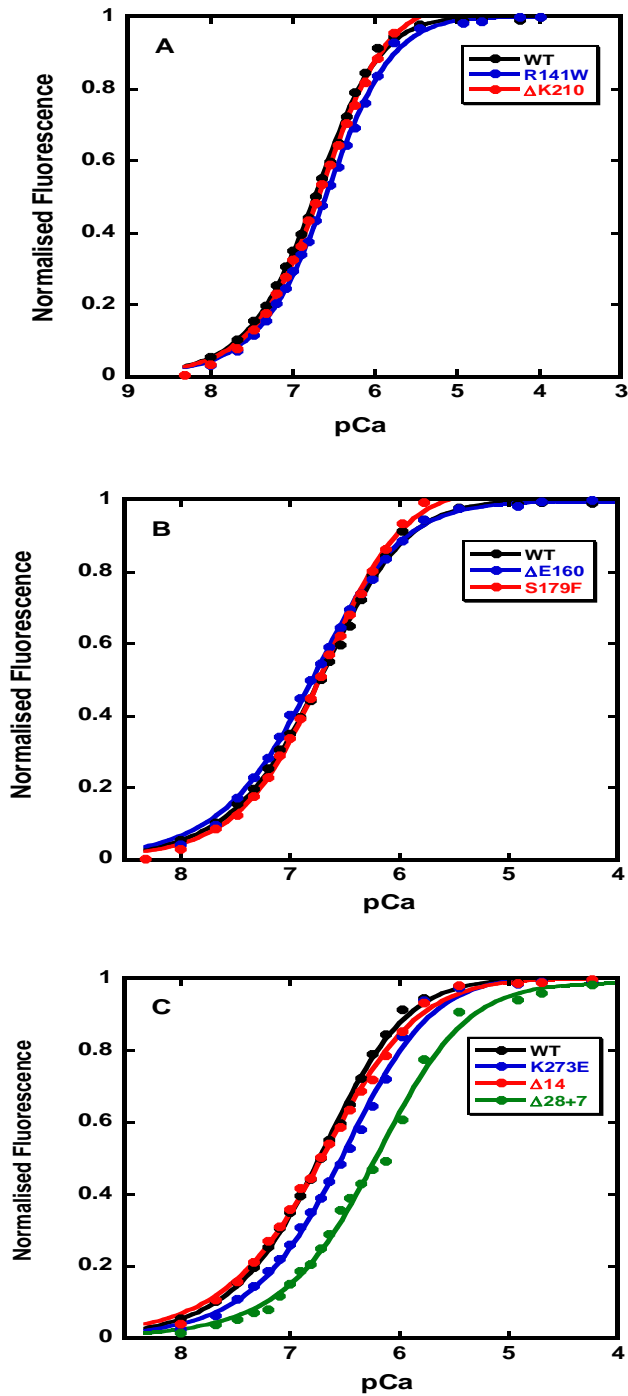


**Figure 5.2 Representative data for  $\text{Ca}^{2+}$  dependent change in relative fluorescence given by IAANS-Cys35-TnC in reconstituted Tn complex.** Relative fluorescence emission intensity change was plotted against free  $\text{Ca}^{2+}$  concentration. (A) DCM (B) T1-region HCM and (C) T2-region HCM mutations in complex. The data obtained are from two experiments and the curves are fits to the Hill equation.

**Table 5.1 Summary of the effect of cTnT mutations on the Ca<sup>2+</sup> binding properties for Tn complex using IAANS-Cys-35**

<b>cTnT</b>	<b>n<sub>H</sub></b>	<b>K<sub>d</sub></b>	<b>Tn complex pCa<sub>50</sub></b>
<b>WT</b>	1.07	1.86E-7	6.65
<b>R141W</b>	1.03	2.5E-7	6.57
<b>ΔK210</b>	1.05	2.36E-7	6.67
<b>ΔE160</b>	1.03	1.60E-7	6.70
<b>S179F</b>	1.1	1.95E-7	6.74
<b>K273E</b>	1.02	3.01E-7	6.68
<b>Δ14</b>	1.14	1.95E-7	6.75
<b>Δ28+7</b>	0.96	4.88E-7	6.31

*The numbers are expressed as mean values from two experiments*

### 5.2.A.3 Effect of Mutations in cTnT on the Ca<sup>2+</sup> Affinity of Thin Filaments:

Herein selective labelling of Cys 35 (C84S) and Cys 84(C35S) by IAANS was used for measurements of Ca<sup>2+</sup> binding to reconstituted thin filament. Since the Ca<sup>2+</sup> dependent IAANS-C35 fluorescence change of free troponin is bigger than the change obtained when Tn is incorporated in the thin filament (discussed above in section 5.2.1), it is critical to remove any excess Tn that may contribute to measurement aimed at characterising Ca<sup>2+</sup> affinity of thin filaments. To this end co-sedimentation of the Tn complexes with actin-Tm was performed before measurement of Ca<sup>2+</sup> dependent fluorescence changes.

Titration of the fluorescence change as a function of Ca<sup>2+</sup> concentration using Tn labelled at C35 position for WT produced a pCa<sub>50</sub> of 6.19 equivalent to a K<sub>d</sub> of 6.09x10<sup>-7</sup>M<sup>-1</sup>. The affinity was slightly reduced in going from Tn complex to reconstituted thin filament whereas the cooperativity increased (n<sub>H</sub> of 1.7). These data are in agreement with previous published binding affinities for WT (Kobayashi and Solaro 2006). DCM mutation R141W and ΔK210 showed small changes in pCa<sub>50</sub>. In contrast HCM associated mutations S179F, K273E and Δ14 showed a significant increase in pCa<sub>50</sub> values (Figure 5.2, Table 5.2). 2HCM mutations ΔE160 and Δ28+7 showed very small change in pCa<sub>50</sub> values. a higher hill coefficient was observed for R141W, ΔK210 and ΔE160 and decreased for S179F, K273E, Δ14 and Δ28+7.

We have also used the IAANS fluorescent probe at Cys84 to measure Ca<sup>2+</sup> affinity of reconstituted thin filament. This probe give very little change upon

Ca<sup>2+</sup> binding to free troponin and a bigger change upon Ca<sup>2+</sup> binding to troponin incorporated in thin filaments. Upon binding Ca<sup>2+</sup> to TnC, the fluorescence intensity increased and was easily monitored. WT Tn binds Ca<sup>2+</sup> with a K<sub>d</sub> of 1.58E<sup>-6</sup> M<sup>-1</sup>.( pCa<sub>50</sub> = 5.87). Thus the thin filament binds Ca<sup>2+</sup> with approximately 10-fold weaker affinity than Tn complex (Figure 5.3, Table 5.2). This is in close agreement to the previously published thin filament binding affinities (Kobayashi et al. 2006; Rosenfeld and Taylor 1985). Also the cooperativity was increased to n<sub>H</sub>=1.6 which suggests that Ca<sup>2+</sup> binding to thin filaments is cooperative.

Reconstituted Tn complexes using 2 DCM TnT mutants (R141W and ΔK210) and 6 HCM TnT mutants (ΔE160, S179F, K273E, Δ14 and Δ28+7) all showed increased Ca<sup>2+</sup> affinity. The largest effect was seen for Δ28+7 with a K<sub>d</sub> of 2.19E<sup>-7</sup> (pCa<sub>50</sub>=6.66). The hill coefficient values were all reduced in contrast to the data obtained with IANNS attached to Cys35. The reason for these discrepancies is unclear.

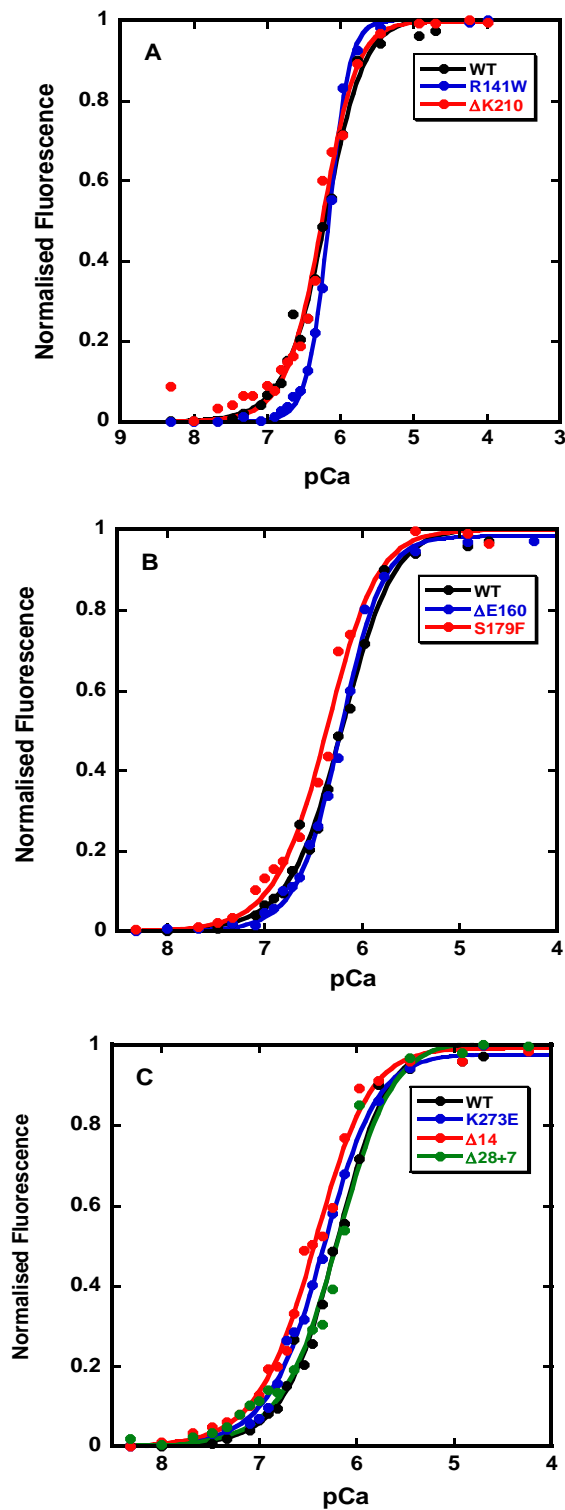


**Figure 5.3 Representative data for  $\text{Ca}^{2+}$  dependent change in relative fluorescence given by IAANS-Cys35-TnC in reconstituted thin filament.** Relative fluorescence emission intensity change was plotted against free  $\text{Ca}^{2+}$  concentration. (A) DCM (B) T1-region HCM and (C) T2-region HCM mutations in complex. The data obtained are from a single experiment and the curves are fits to the Hill equation.

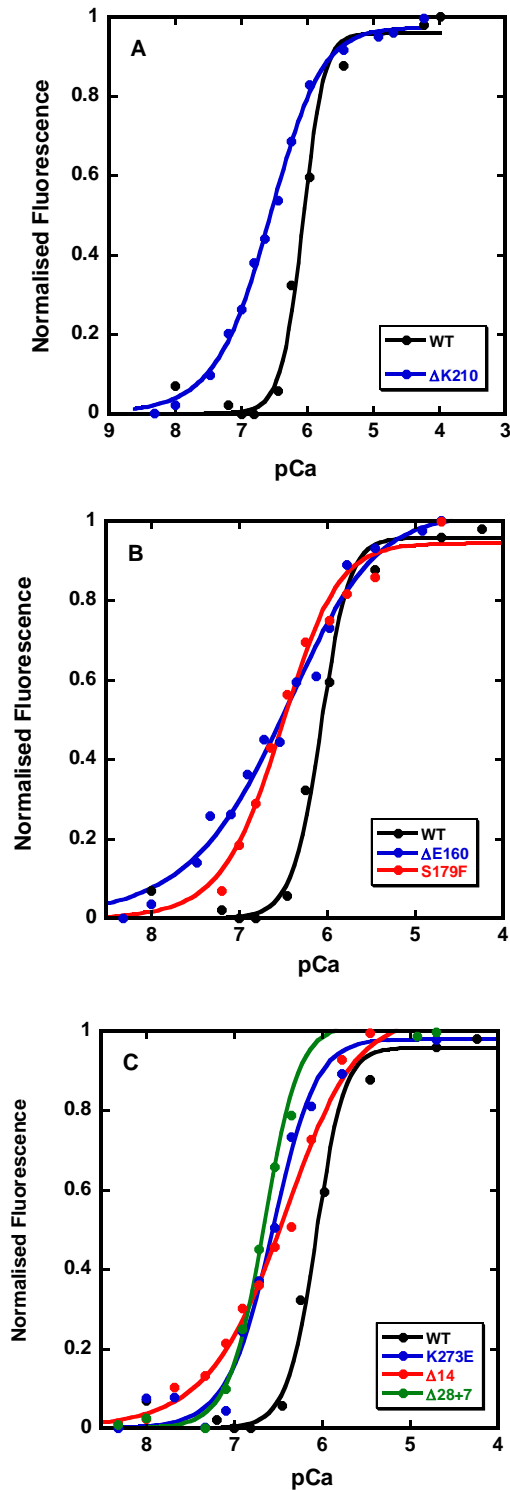


**Figure 5.4** Representative data for  $\text{Ca}^{2+}$  dependent change in relative fluorescence given by IAANS-Cys84-TnC in reconstituted thin filament. Relative fluorescence emission intensity change was plotted against free  $\text{Ca}^{2+}$  concentration. (A) DCM (B) T1-region HCM and (C) T2-region HCM mutations in complex. The data obtained are from a single experiment and the curves are fits to the Hill equation.

**Table 5.2 Summary of the effect of cTnT mutations on Ca<sup>2+</sup> binding properties for regulated thin filament**

cTnT	Cys 35			Cys 84		
	K <sub>d</sub>	pCa <sub>50</sub>	n <sub>H</sub>	K <sub>d</sub>	pCa <sub>50</sub>	n <sub>H</sub>
<b>WT</b>	6.09E-7	6.19	1.7	1.58E-6	5.87	1.6
<b>R141W</b>	6.94E-7	6.15	2.96	-	-	-
<b>ΔK210</b>	6.10E-7	6.25	2.27	2.63E-7	6.58	1.22
<b>ΔE160</b>	5.95E-7	6.22	1.92	3.16E-7	6.50	1.07
<b>S179F</b>	4.32E-7	6.36	1.6	3.02E-7	6.52	1.30
<b>K273E</b>	5.08E-7	6.34	1.4	2.69E-7	6.57	1.4
<b>Δ14</b>	3.62E-7	6.43	1.47	2.88E-7	6.45	1.2
<b>Δ28+7</b>	6.28E-7	6.20	1.47	2.19E-7	6.66	1.5

*The numbers are expressed as single experiment. Note all the mutants studied showed subtle changes in Ca<sup>2+</sup> affinities on the reconstituted thin filament.*

## **5.2 (B) Effect of TnT Mutations on the Kinetics of Ca<sup>2+</sup> Dissociation**

### **5.2.B.1 Ca<sup>2+</sup> Dissociation Kinetics of cTnT Mutations using IAANS-Cys 35**

Following Ca<sup>2+</sup> removal from the sarcoplasm of the cardiomyocytes, Ca<sup>2+</sup> dissociates from TnC bound to thin filament and it is thought that the rate of this dissociation plays an important role in cardiac muscle relaxation. It is therefore important to measure the impact of Tn mutations on the kinetics of Ca<sup>2+</sup> dissociation. We have used the same methods used to monitor Ca<sup>2+</sup> binding to TnC, namely IAANS attached either to Cys35 or Cys84.

Figure 5.5, Figure 5.6 and Figure 5.7 show the transients IAANS-Cys35 fluorescence change obtained upon chasing bound Ca<sup>2+</sup> by an excess of the Ca<sup>2+</sup> chelator EGTA. Upon Ca<sup>2+</sup> dissociation the fluorescence increases and the rate of this fluorescence increase reflect the rate of Ca<sup>2+</sup> dissociation. For the Tn complex, Ca<sup>2+</sup> dissociated from the regulatory domain of WT with a rate constant of 11.5 s<sup>-1</sup> utilising the fluorophore IAANS-Cys35 (Figure 5.5, Table 5.3) which was similar to previously reported WT hcTn under slightly different conditions (Davis, Norman et al. 2007). Figure 5.5-Figure 5.7 show that none of the mutants R141W, ΔK210, ΔE160, S179F, Δ14 and K273E affected the rate of Ca<sup>2+</sup> dissociation Δ28+7 increased Ca<sup>2+</sup> dissociation rate (4-fold) which is in correspondence to the reduced affinity observed for the Tn complex. It appears that the fluorescence change as predicted residing in the Ca<sup>2+</sup> site I minimally affects the Ca<sup>2+</sup> binding properties of the regulatory domain of Tn.

Incorporation of Tn complex into reconstituted thin filament (actin-Tm-Tn) desensitized and reduced the affinity of the regulatory N-terminal domain of TnC to  $\text{Ca}^{2+}$  ( $\text{pCa}_{50}$  from 6.65 to 6.19) as previously reported (Kobayashi and Solaro 2006; Davis, Norman et al. 2007). Consistent with these findings, we observed that IAANS-Cys35 displayed approximately 5-fold faster observed rate constant of  $\text{Ca}^{2+}$  dissociation ( $48.6\text{s}^{-1}$ ) (Figure 5.8, Table 5.3). Figure 5.8-Figure 5.10 demonstrates that the rate of  $\text{Ca}^{2+}$  dissociation from thin filaments as reported by IAANS-Cys 35 displayed marginal effects for all mutants studied except for  $\Delta 28+7$  where a two-fold increase in rate was observed ( $106.1\text{s}^{-1}$ ).

Finally cross-bridge binding has long been known to increase  $\text{Ca}^{2+}$  sensitivity of TnC in cardiac muscle (Pan and Solaro 1987; Wang and Fuchs 1994). Consistent with this effect, Figure 5.11 shows that addition of S1 reverses the thin-filament induced desensitisation 3.5 fold (Table 5.3) to  $15.9\text{s}^{-1}$ , a rate comparable with that of cardiac muscle relaxation of  $5\text{-}11\text{s}^{-1}$  at  $15^\circ\text{C}$  for WT Tn (Fitzsimons, Patel et al. 1998; Fitzsimons, Patel et al. 2001). Most mutations showed a rate constant of  $\text{Ca}^{2+}$  dissociation in the range of  $15\text{-}25\text{ s}^{-1}$  except for  $\Delta 28+7$ . This mutant showed a substantial increase in the rate constant of  $\text{Ca}^{2+}$  dissociation from thin filament in the presence of myosin heads ( $112\text{ s}^{-1}$ ) (Figure 5.11-Figure 5.13).

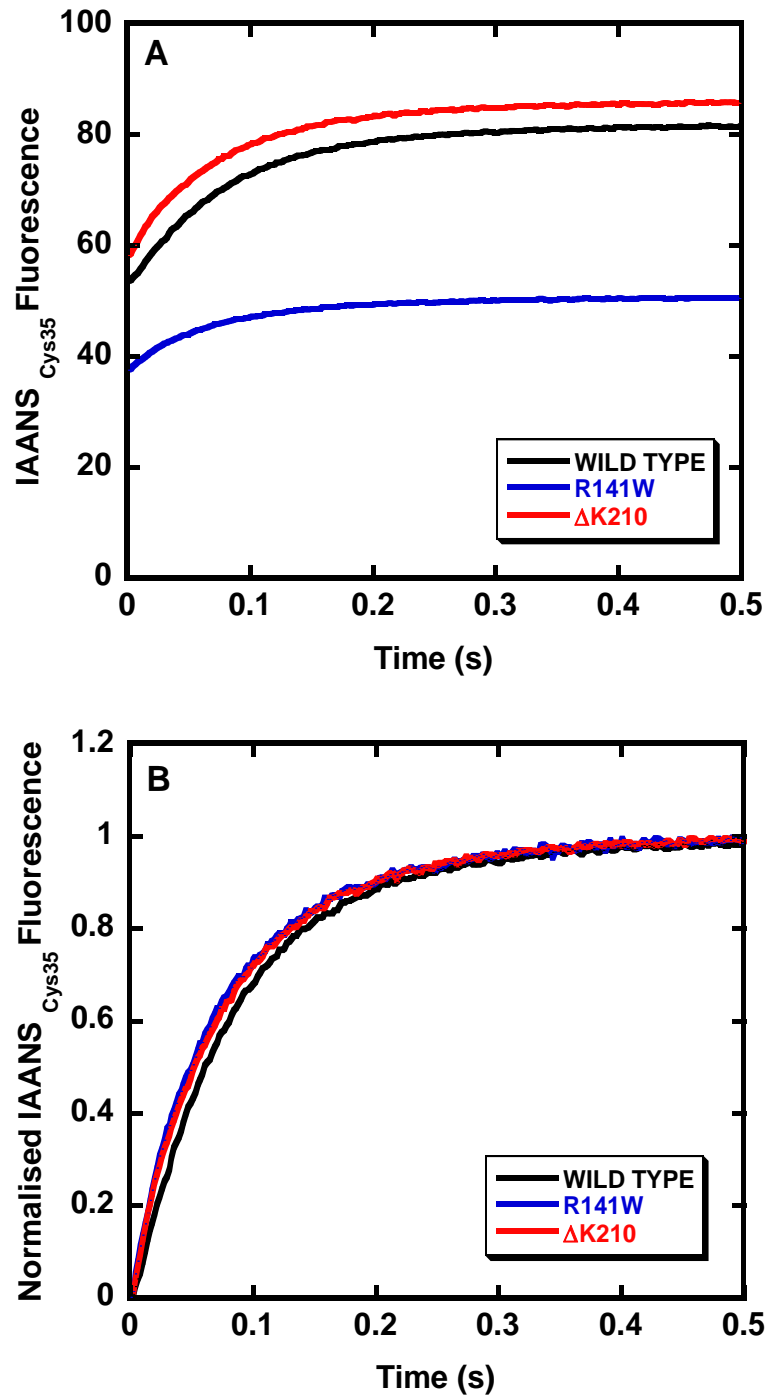


**Figure 5.5 Representative data for Ca<sup>2+</sup> dependent change in relative fluorescence of DCM mutations given by IAANS-Cys35-TnC in reconstituted Tn complex.**

(A) Stopped flow kinetic tracings obtained from mixing cTn reconstituted with cTnC mutant labeled with IAANS at Cys-35 with an equal volume of the same buffer containing an excess of the Ca<sup>2+</sup> chelator EGTA(1mM) (B) Normalised data for comparison. Buffer conditions: 140mM KCl, 4mM MgCl<sub>2</sub>, 50mM MOPS pH 7.2) containing 50μM CaCl<sub>2</sub> and 4 μM Tn.

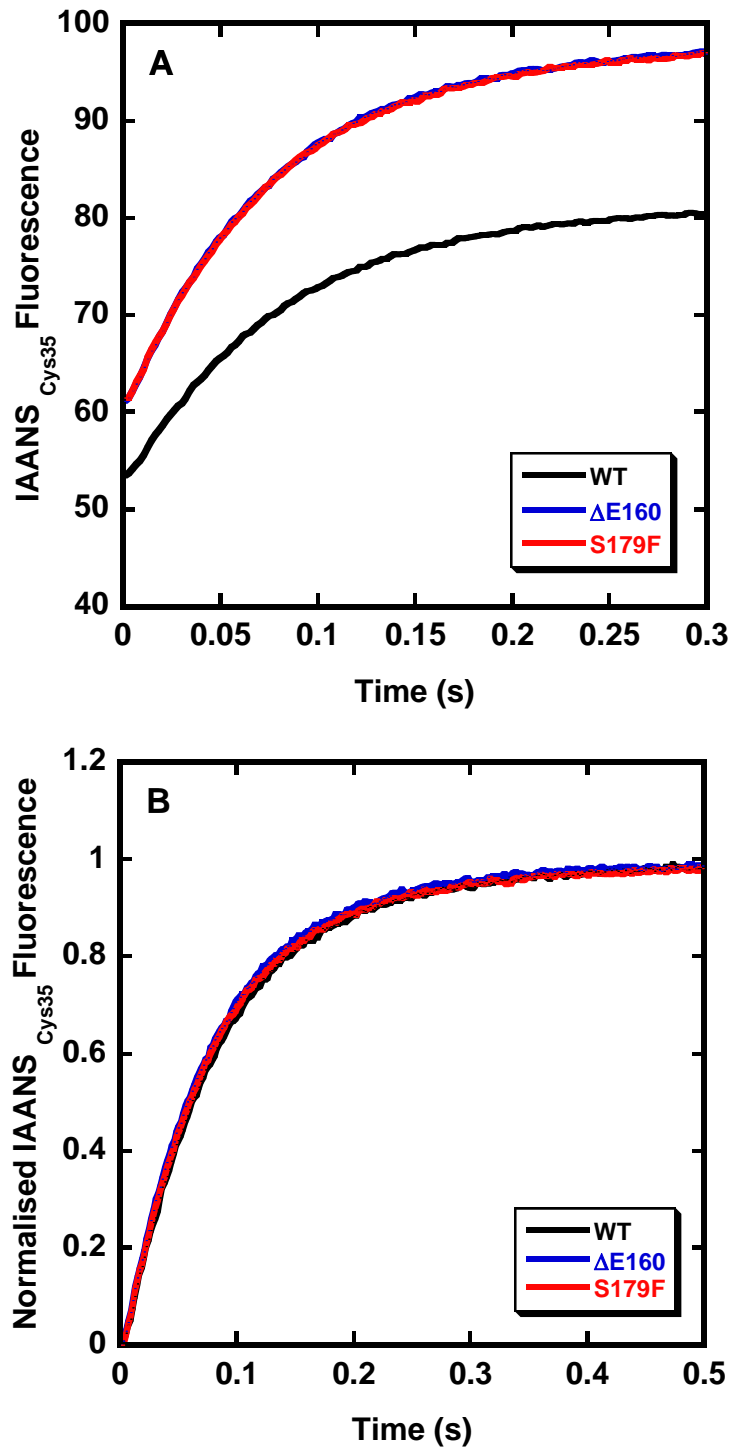


**Figure 5.6 Representative data for Ca<sup>2+</sup> dependent change in relative fluorescence of HCM-T1 mutations given by IAANS-Cys35-TnC in reconstituted Tn complex.**

(A) Stopped flow kinetic tracings obtained from mixing cTn reconstituted with cTnC mutant labeled with IAANS at Cys-35 with an equal volume of the same buffer containing an excess of the Ca<sup>2+</sup> chelator EGTA(1mM) (B) Normalised data for comparison. Buffer conditions: 140mM KCl, 4mM MgCl<sub>2</sub>, 50mM MOPS pH 7.2) containing 50μM CaCl<sub>2</sub> and 4 μM Tn.

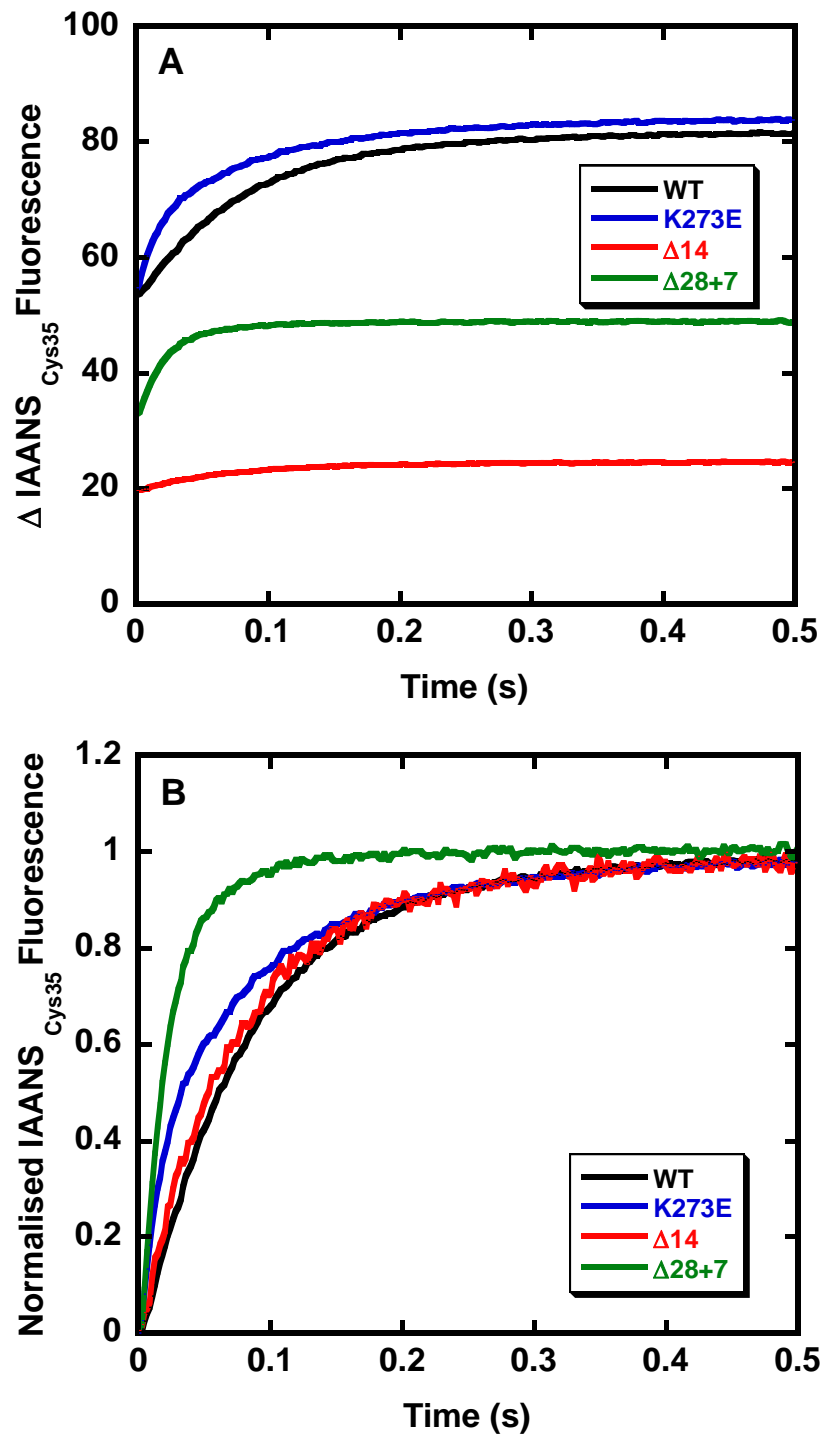


**Figure 5.7** Representative data for  $\text{Ca}^{2+}$  dependent change in relative fluorescence of HCM-T2 mutations given by IAANS-Cys35-TnC in reconstituted Tn complex.

(A) Stopped flow kinetic tracings obtained from mixing cTn reconstituted with cTnC mutant labeled with IAANS at Cys-35 with an equal volume of the same buffer containing an excess of the  $\text{Ca}^{2+}$  chelator EGTA(1mM) (B) Normalised data for comparison Buffer conditions: 140mM KCl, 4mM  $\text{MgCl}_2$ , 50mM MOPS pH 7.2) containing  $50\mu\text{M}$   $\text{CaCl}_2$  and  $4\mu\text{M}$  Tn.

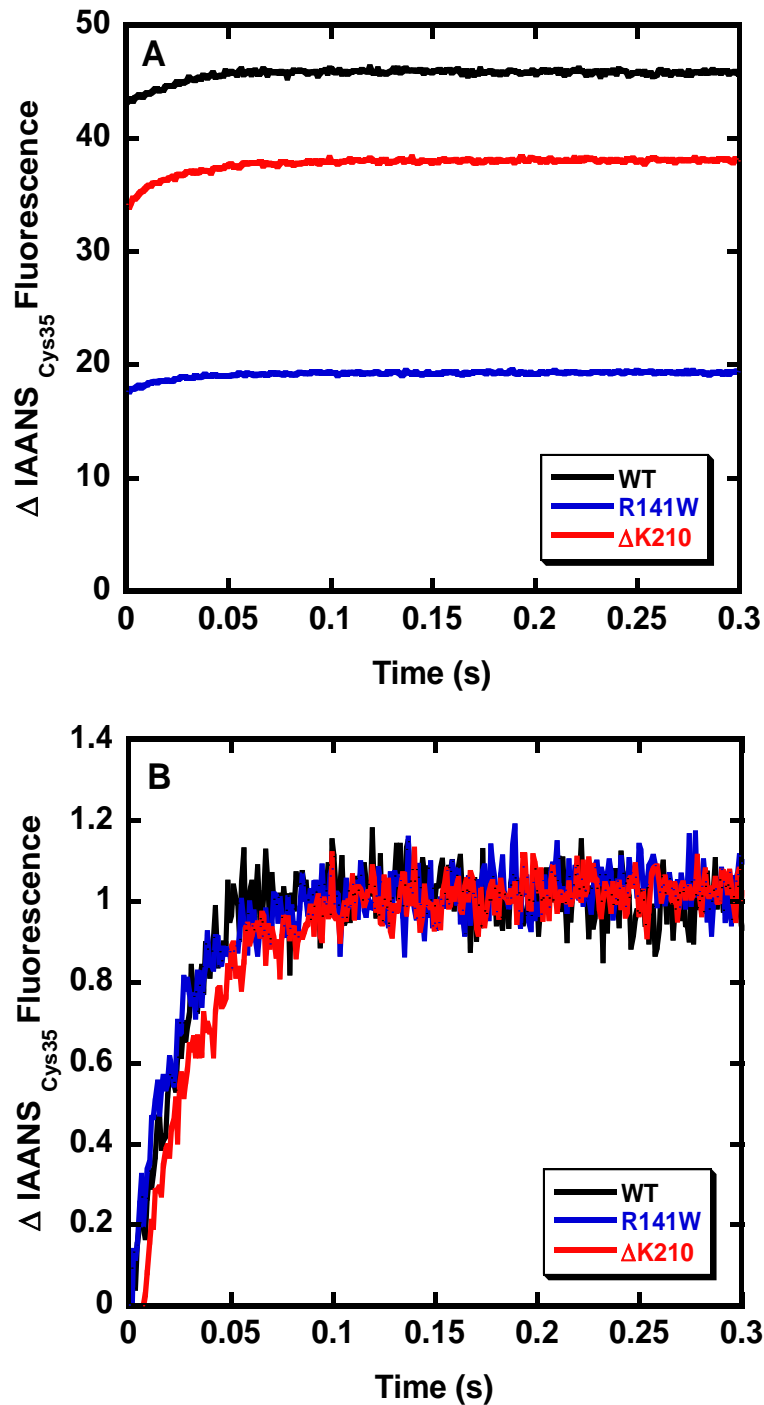


**Figure 5.8 Representative data for  $\text{Ca}^{2+}$  dependent change in relative fluorescence of DCM mutations given by IAANS-Cys35-TnC in reconstituted thin filament.**

(A) Stopped flow kinetic tracings obtained from mixing cTn reconstituted with cTnC mutant labeled with IAANS at Cys-35 with an equal volume of the same buffer containing an excess of the  $\text{Ca}^{2+}$  chelator EGTA(1mM) (B) Normalised data for comparison. Buffer conditions: 140mM KCl, 4mM  $\text{MgCl}_2$ , 50mM MOPS pH 7.2 containing  $50\mu\text{M}$   $\text{CaCl}_2$  and  $4\mu\text{M}$  Tn.

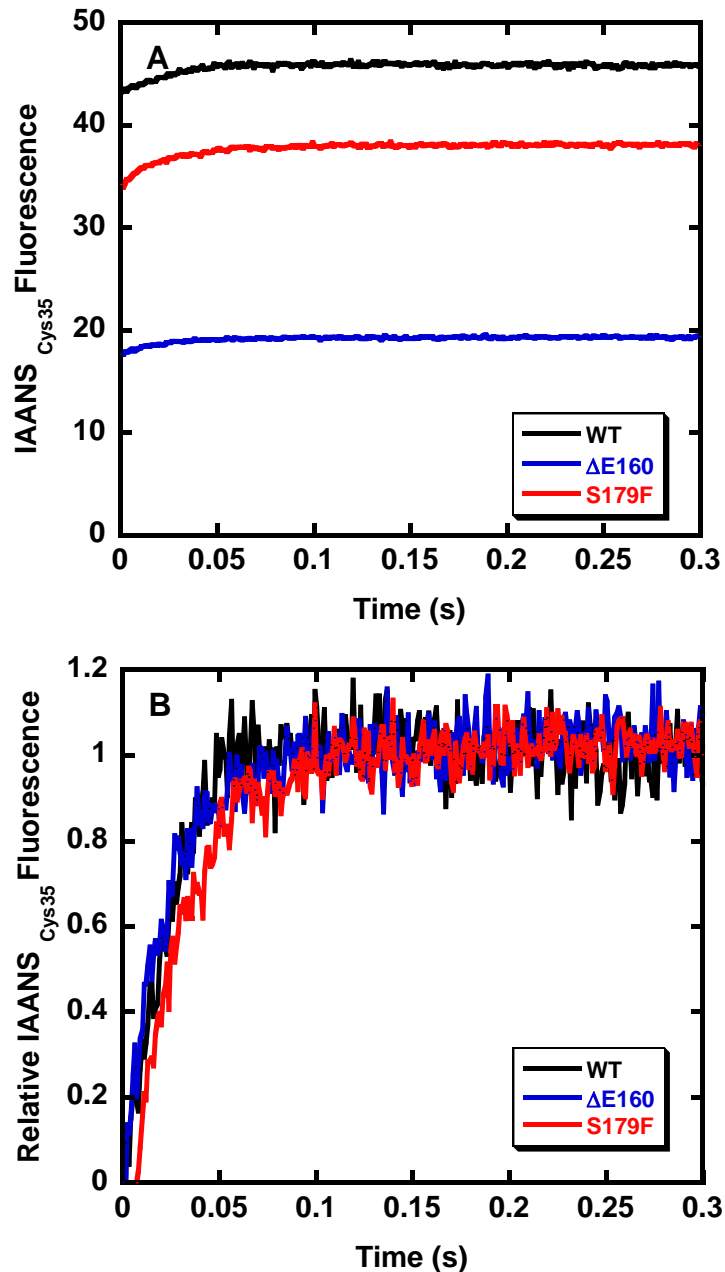


**Figure 5.9 Representative data for  $\text{Ca}^{2+}$  dependent change in relative fluorescence of HCM-T1 mutations given by IAANS-Cys35-TnC in reconstituted thin filament.**

(A) Stopped flow kinetic tracings obtained from mixing cTn reconstituted with cTnC mutant labeled with IAANS at Cys-35 with an equal volume of the same buffer containing an excess of the  $\text{Ca}^{2+}$  chelator EGTA(1mM) (B) Normalised data for comparison. Buffer conditions: 140mM KCl, 4mM  $\text{MgCl}_2$ , 50mM MOPS pH 7.2) containing  $50\mu\text{M}$   $\text{CaCl}_2$  and  $4\mu\text{M}$  Tn.

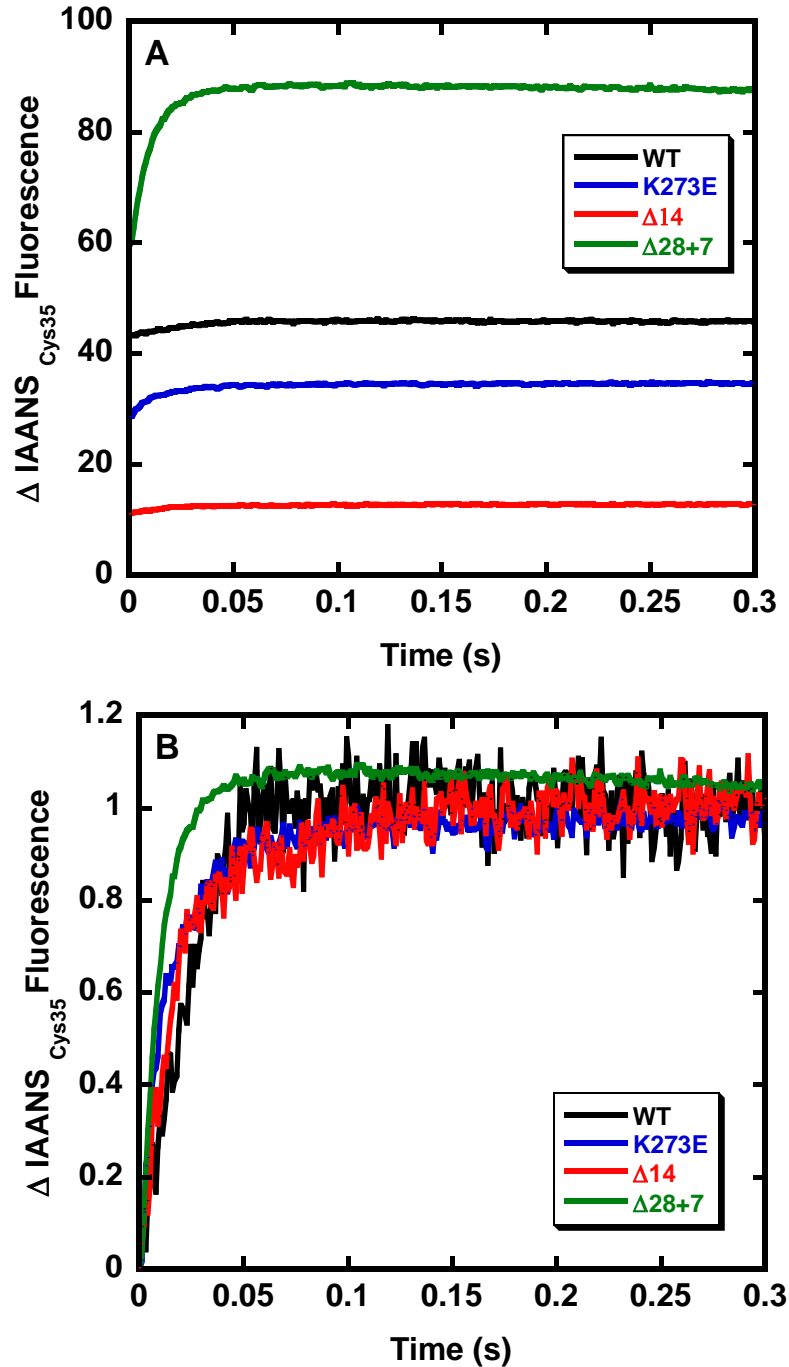


**Figure 5.10 Representative data for  $\text{Ca}^{2+}$  dependent change in relative fluorescence of HCM-T2 mutations given by IAANS-Cys35-TnC in reconstituted thin filament.**

(A) Stopped flow kinetic tracings obtained from mixing cTn reconstituted with cTnC mutant labeled with IAANS at Cys-35 with an equal volume of the same buffer containing an excess of the  $\text{Ca}^{2+}$  chelator EGTA(1mM) (B) Normalised data for comparison. Buffer conditions: 140mM KCl, 4mM  $\text{MgCl}_2$ , 50mM MOPS pH 7.2) containing 50 $\mu\text{M}$   $\text{CaCl}_2$  and 4  $\mu\text{M}$  Tn.

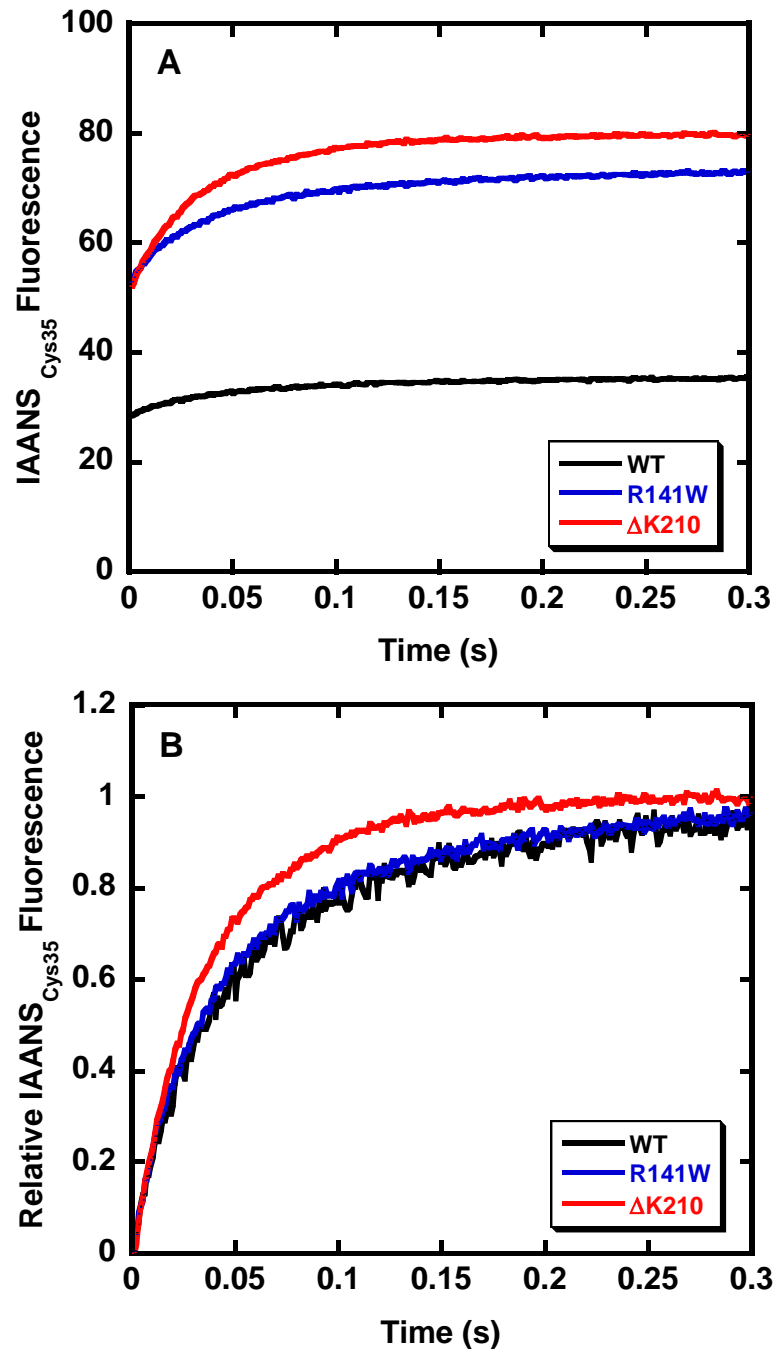


**Figure 5.11 Representative data for  $\text{Ca}^{2+}$  dependent change in relative fluorescence of DCM mutations given by IAANS-Cys35-TnC in reconstituted thin filament + S1**

(A) Stopped flow kinetic tracings obtained from mixing cTn reconstituted with cTnC mutant labeled with IAANS at Cys-35 with an equal volume of the same buffer containing an excess of the  $\text{Ca}^{2+}$  chelator EGTA(1mM) (B) Normalised data for comparison. Buffer conditions: 140mM KCl, 4mM  $\text{MgCl}_2$ , 50mM MOPS pH 7.2) containing 50 $\mu\text{M}$   $\text{CaCl}_2$  and 4  $\mu\text{M}$  Tn.

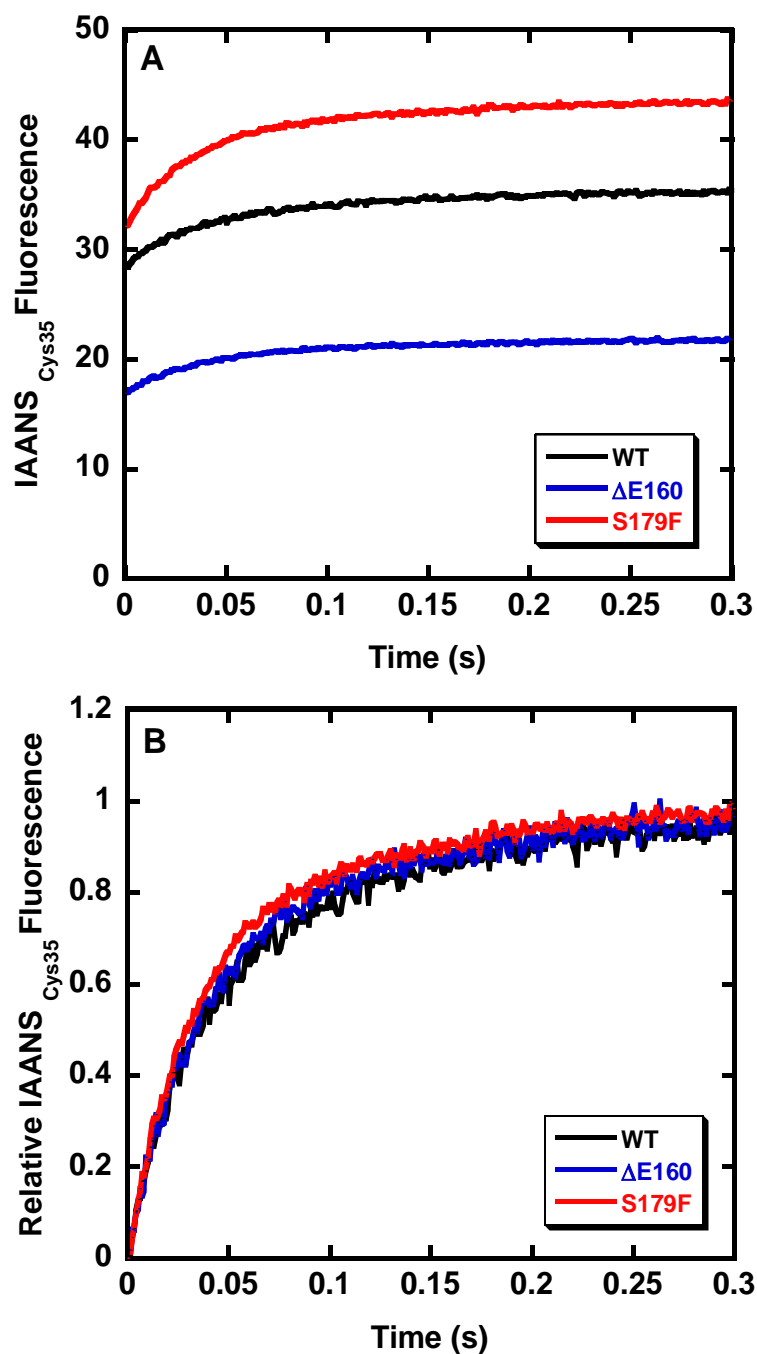


**Figure 5.12 Representative data for  $\text{Ca}^{2+}$  dependent change in relative fluorescence of HCM-T1 mutations given by IAANS-Cys35-TnC in reconstituted thin filament + S1**

(A) Stopped flow kinetic tracings obtained from mixing cTn reconstituted with cTnC mutant labeled with IAANS at Cys-35 with an equal volume of the same buffer containing an excess of the  $\text{Ca}^{2+}$  chelator EGTA(1mM) (B) Normalised data for comparison. Buffer conditions: 140mM KCl, 4mM  $\text{MgCl}_2$ , 50mM MOPS pH 7.2) containing 50 $\mu\text{M}$   $\text{CaCl}_2$  and 4  $\mu\text{M}$  Tn.

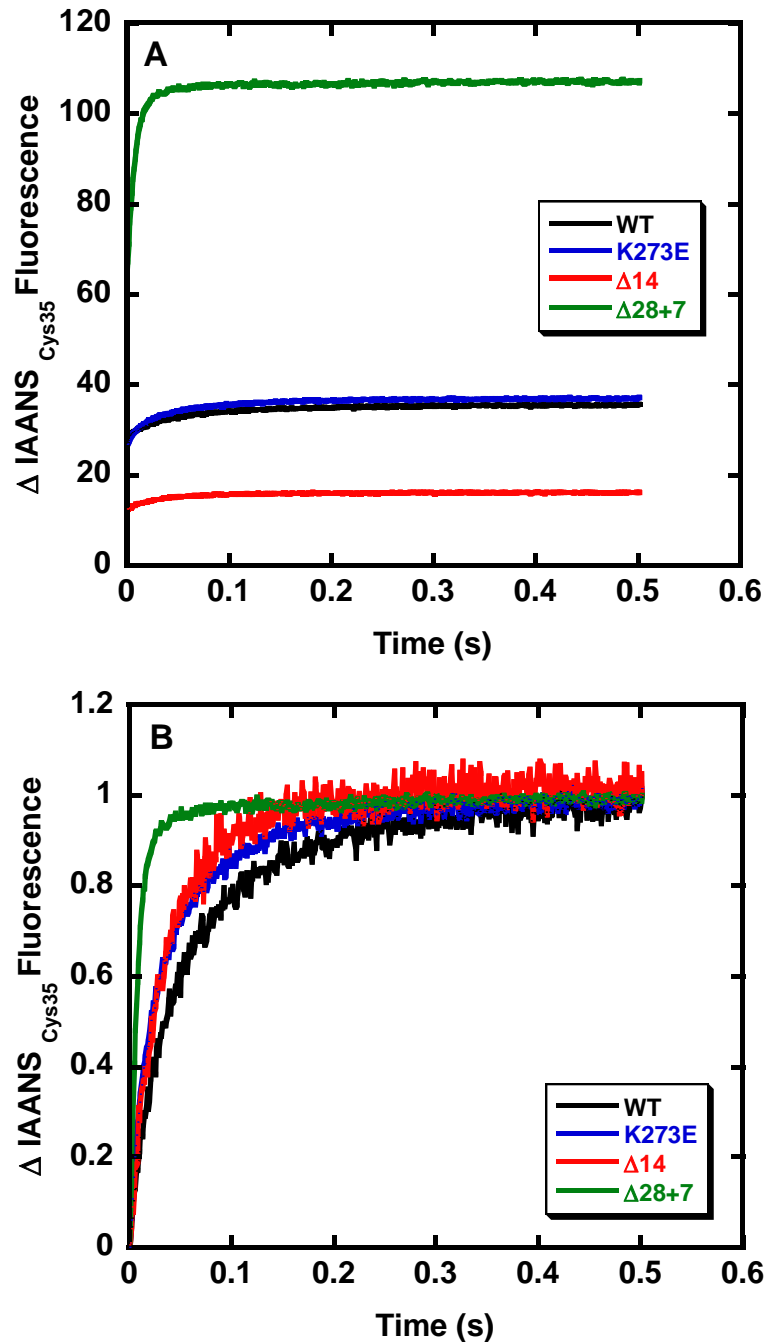


**Figure 5.13 Representative data for  $\text{Ca}^{2+}$  dependent change in relative fluorescence of HCM-T2 mutations given by IAANS-Cys35-TnC in reconstituted thin filament + S1**

(A) Stopped flow kinetic tracings obtained from mixing cTn reconstituted with cTnC mutant labeled with IAANS at Cys-35 with an equal volume of the same buffer containing an excess of the  $\text{Ca}^{2+}$  chelator EGTA(1mM) (B) Normalised data for comparison. Buffer conditions: 140mM KCl, 4mM  $\text{MgCl}_2$ , 50mM MOPS pH 7.2) containing  $50\mu\text{M}$   $\text{CaCl}_2$  and  $4\mu\text{M}$  Tn.

**Table 5.3 Summary of the effect of cTnT mutations on the Ca<sup>2+</sup> binding properties using IAANS-Cys 35**

cTnT	Tn complex		Thin Filament		Thin filament +S1	
	<i>1 exponential s<sup>-1</sup></i>	<i>amplitude</i>	<i>1 exponential s<sup>-1</sup></i>	<i>amplitude</i>	<i>1 exponential s<sup>-1</sup></i>	<i>amplitude</i>
<b>WT</b>	11.5	28.9	48.6	3	15.9	6.23
<b>R141W</b>	12.3	12.5	39.5	1.6	17.3	18
<b>ΔK210</b>	12.2	26.9	38.7	3.8	25	26.9
<b>ΔE160</b>	12.1	37.9	39.6	1.6	18	4.5
<b>S179F</b>	12.2	37.7	38.7	3.8	19.7	10.5
<b>K273E</b>	13.1	24.7	59	5.6	22.4	8.5
<b>Δ14</b>	12.4	4.9	43.2	1.5	24.9	3.3
<b>Δ28+7</b>	(40.8)	16.9	(106.1)	31	(112.2)	44.7

*The numbers are expressed as single experiment.*

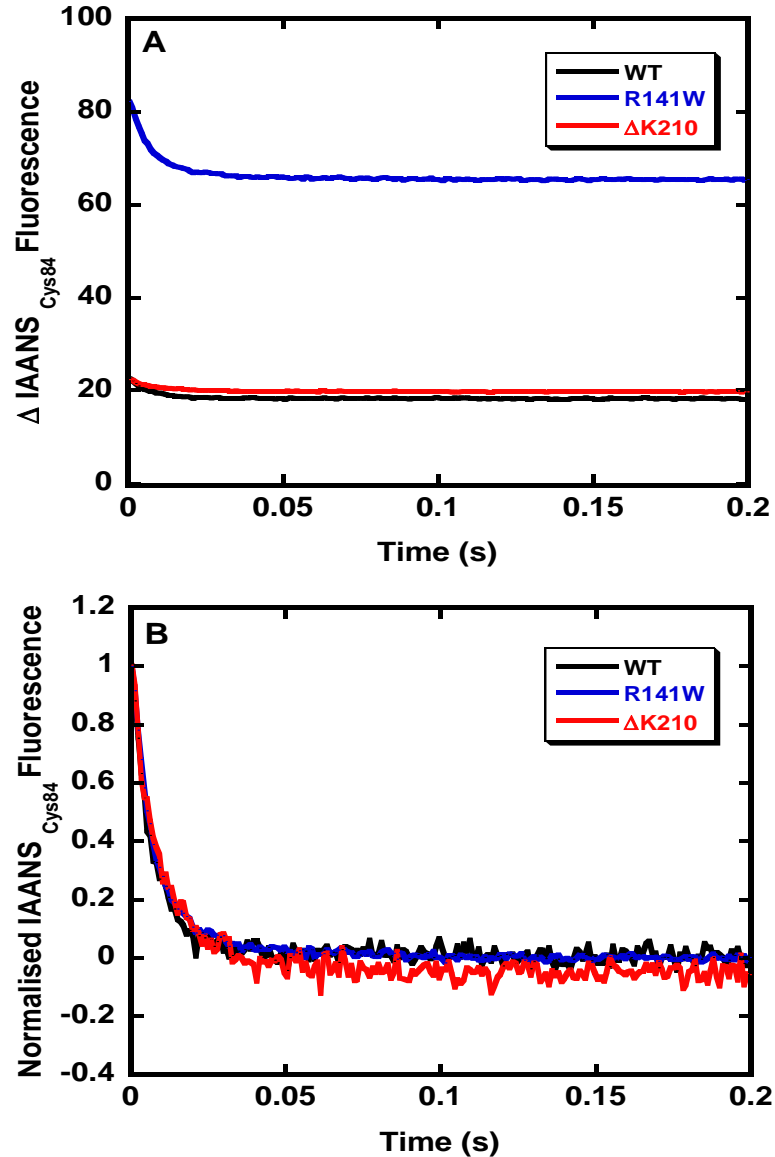
### 5.2.B.2 Ca<sup>2+</sup> Dissociation Kinetics of cTnT Mutations using IAANS-Cys 84

Figure 5.14-Figure 5.16 shows the Ca<sup>2+</sup> dependent decrease in IAANS-Cys84 fluorescence in the Tn complex. For WT Tn an observed rate constant of 75 s<sup>-1</sup> was obtained. Overall the IAANS-C84 signal was much smaller than IAANS-C35 for isolated Tn complex and thus larger errors in the calculated observed rate constants of Ca<sup>2+</sup> dissociation. The cTnT mutations showed only marginal effects on the rates of dissociation kinetics for Tn complexes (Figure 5.14-Figure 5.16, Table 5.4). S179F shows a large increase in the observed rate constant of Ca<sup>2+</sup> dissociation but this value is unlikely to be accurate due to the small signal to noise ratio.

Figure 5.17-Figure 5.19 shows the Ca<sup>2+</sup> dependent decrease in IAANS-Cys84 fluorescence in reconstituted thin filaments. With the exception of S179F all other mutants showed a consistent decrease in the observed rate constant of Ca<sup>2+</sup> dissociation which correlates well with the increased Ca<sup>2+</sup> sensitivities and apparent Ca<sup>2+</sup> affinities observed previously (Figure 5.17-Figure 5.19). Table 5.4 shows an approximately 2 fold increase in rate of Ca<sup>2+</sup> dissociation compared to the respective Tn complexes. Contrary to that observed using IAANS-Cys35,  $\Delta 28+7$  showed no drastic change in going from complex to thin filament

Incorporation of S1 into reconstituted thin filament caused a 3-fold decrease in Ca<sup>2+</sup> sensitivity in WT which corresponds to the decreased rate of dissociation observed in IAANS-Cys35 studies (Table 5.4). However, the decreased calcium sensitivities observed for all HCM and DCM mutations using IAANS-

Cys35 is not seen in this instance and the rates of dissociation of  $\text{Ca}^{2+}$  was similar to that of the WT within experimental error (Figure 5.20-Figure 5.22).



**Figure 5.14 Representative data for  $\text{Ca}^{2+}$  dependent change in relative fluorescence of DCM mutations given by IAANS-Cys84-TnC in reconstituted Tn complex.**

(A) Stopped flow kinetic tracings obtained from mixing cTn reconstituted with cTnC mutant labeled with IAANS at Cys-84 with an equal volume of the same buffer containing an excess of the  $\text{Ca}^{2+}$  chelator EGTA(1mM) (B) Normalised data for comparison. Buffer conditions: 140mM KCl, 4mM  $\text{MgCl}_2$ , 50mM MOPS pH 7.2) containing 50 $\mu\text{M}$   $\text{CaCl}_2$  and 4  $\mu\text{M}$  Tn.

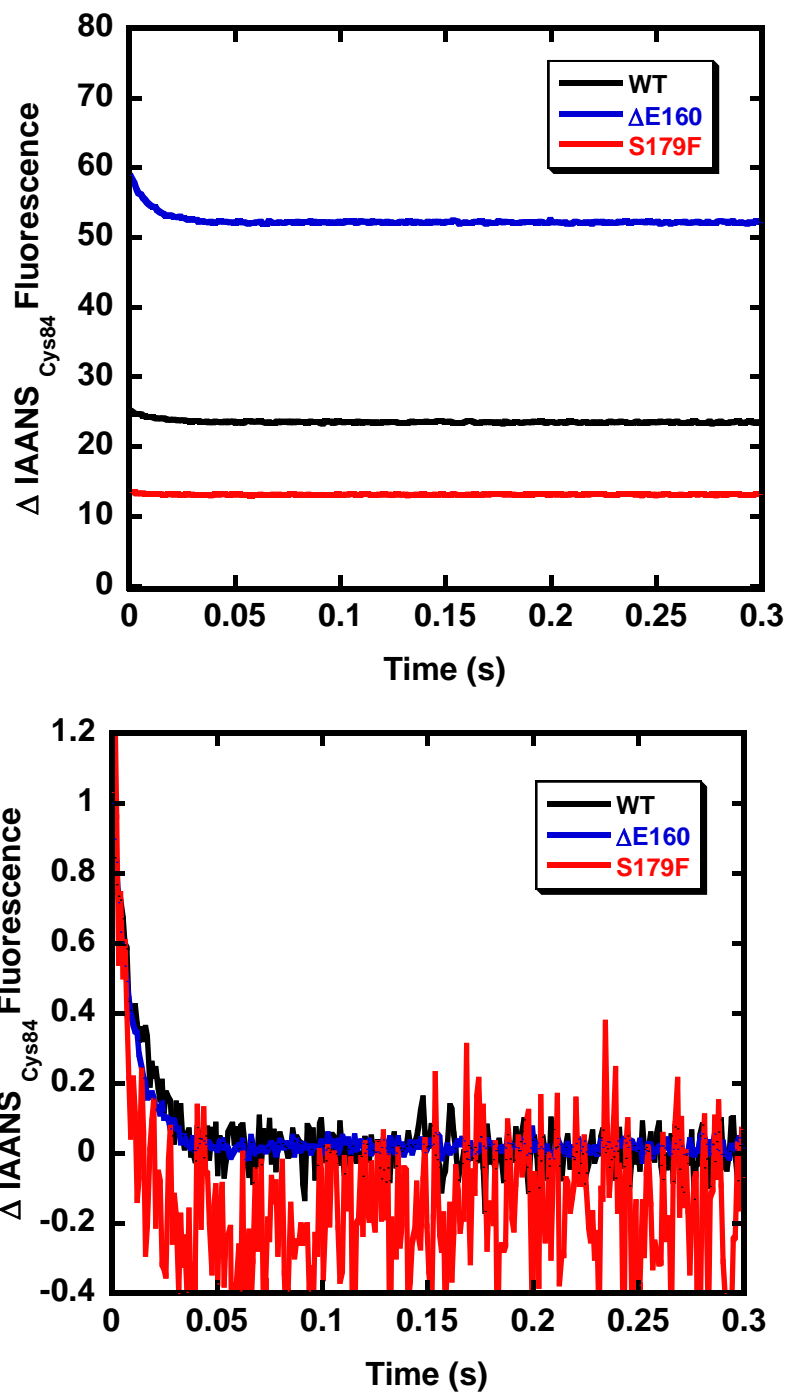


**Figure 5.15 Representative data for  $\text{Ca}^{2+}$  dependent change in relative fluorescence of HCM-T1 mutations given by IAANS-Cys84-TnC in reconstituted TnC complex.**

(A) Stopped flow kinetic tracings obtained from mixing cTn reconstituted with cTnC mutant labeled with IAANS at Cys-84 with an equal volume of the same buffer containing an excess of the  $\text{Ca}^{2+}$  chelator EGTA(1mM) (B) Normalised data for comparison. Buffer conditions: 140mM KCl, 4mM  $\text{MgCl}_2$ , 50mM MOPS pH 7.2) containing  $50\mu\text{M}$   $\text{CaCl}_2$  and  $4\mu\text{M}$  Tn.

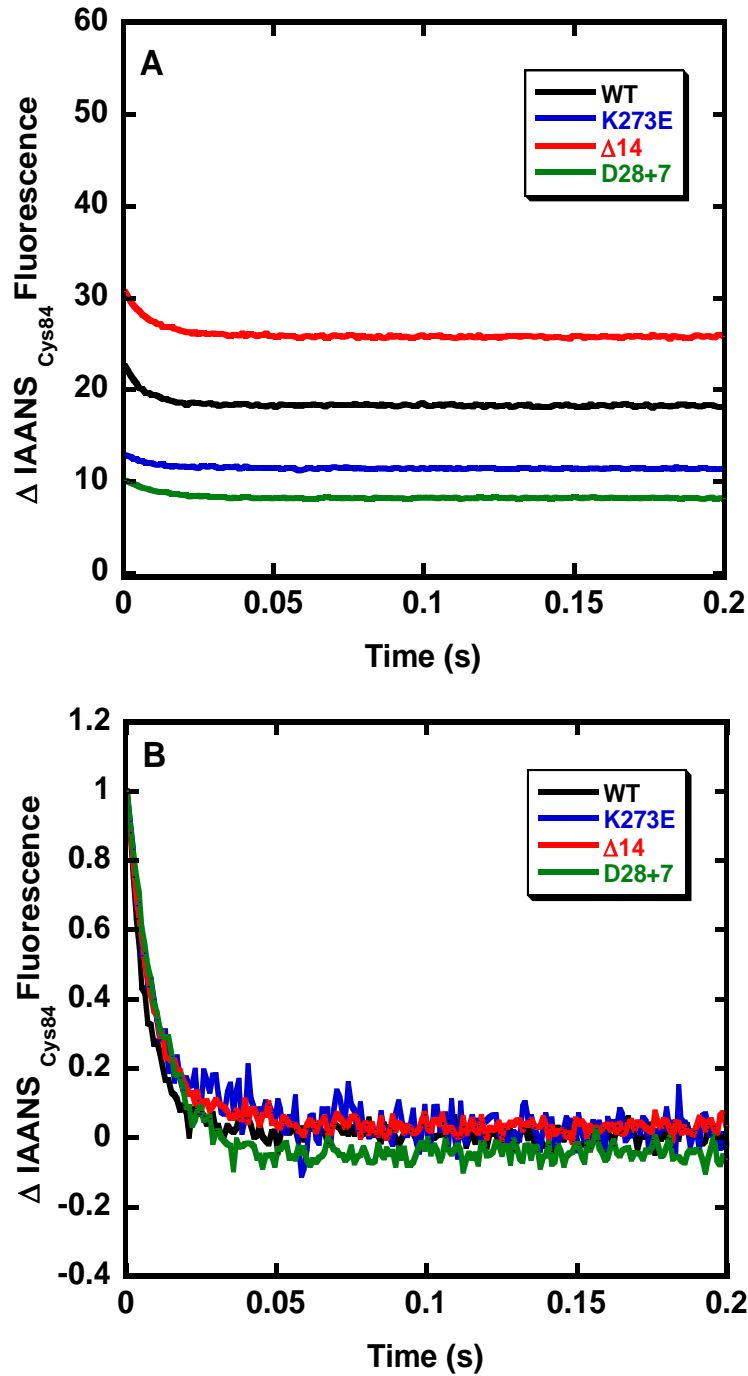


**Figure 5.16 Representative data for  $\text{Ca}^{2+}$  dependent change in relative fluorescence of HCM-T2 mutations given by IAANS-Cys84-TnC in reconstituted Tn complex.**

(A) Stopped flow kinetic tracings obtained from mixing cTn reconstituted with cTnC mutant labeled with IAANS at Cys-84 with an equal volume of the same buffer containing an excess of the  $\text{Ca}^{2+}$  chelator EGTA(1mM) (B) Normalised data for comparison Buffer conditions: 140mM KCl, 4mM  $\text{MgCl}_2$ , 50mM MOPS pH 7.2) containing 50 $\mu\text{M}$   $\text{CaCl}_2$  and 4  $\mu\text{M}$  Tn.

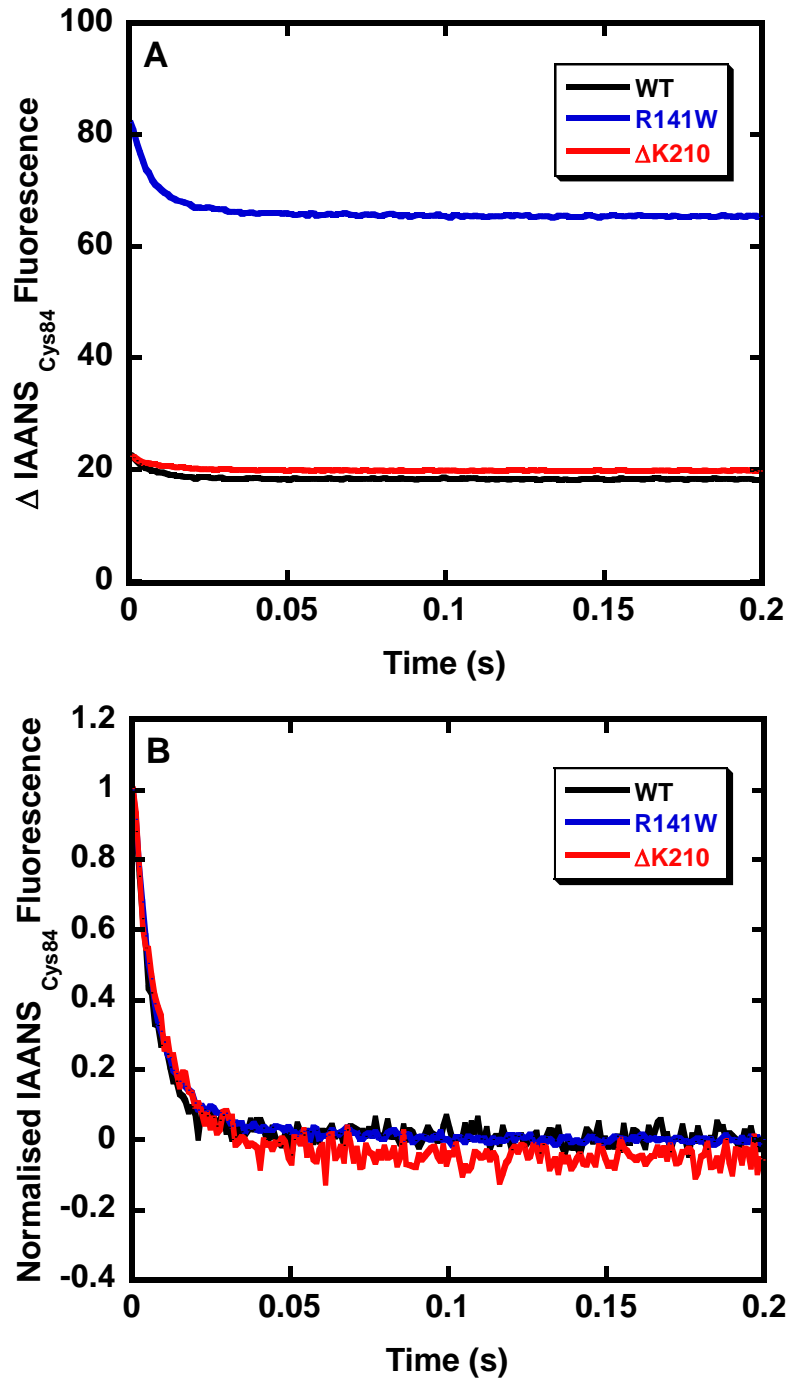


**Figure 5.17 Representative data for  $\text{Ca}^{2+}$  dependent change in relative Fluorescence of DCM mutations given by IAANS-Cys84-TnC in reconstituted thin filament.**

(A) Stopped flow kinetic tracings obtained from mixing thin filament reconstituted with cTnC mutant labeled with IAANS at Cys-84 with an equal volume of the same buffer containing an excess of the  $\text{Ca}^{2+}$  chelator EGTA(1mM) (B) Normalised data for comparison. Buffer conditions: 140mM KCl, 4mM  $\text{MgCl}_2$ , 50mM MOPS pH 7.2) containing 50 $\mu\text{M}$   $\text{CaCl}_2$  and 4  $\mu\text{M}$  Tn.

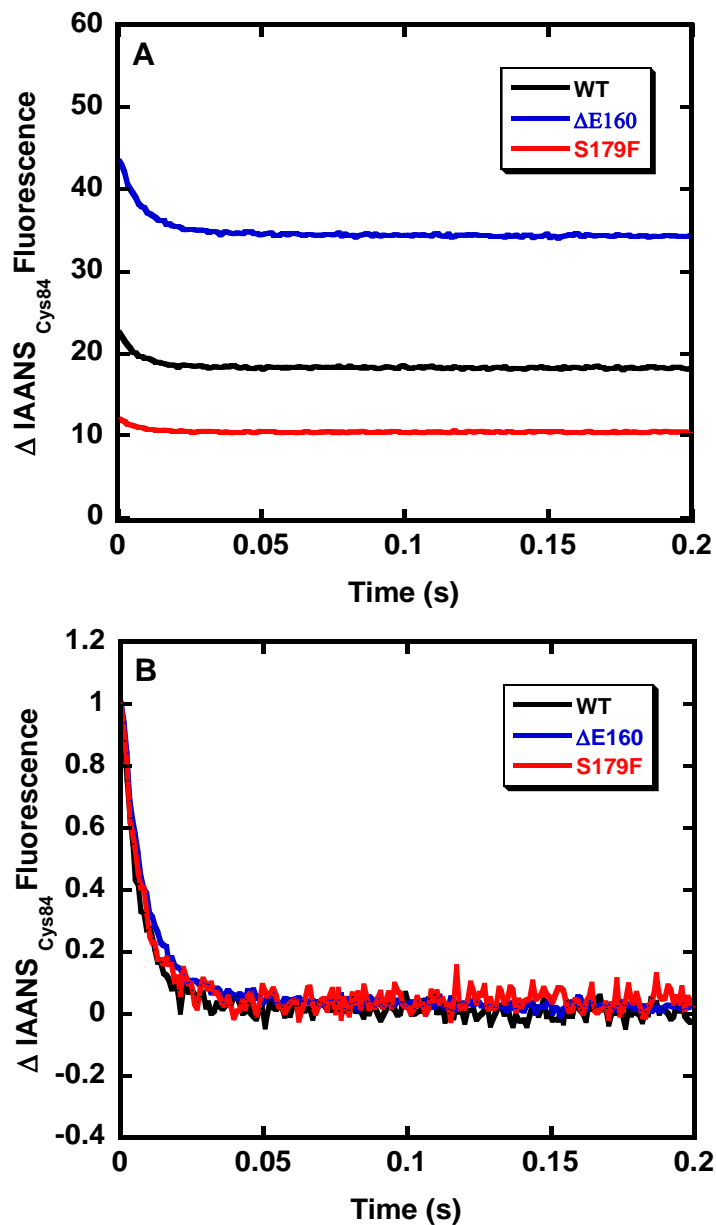


**Figure 5.18 Representative data for  $\text{Ca}^{2+}$  dependent change in relative fluorescence of HCM-T1 mutations given by IAANS-Cys84-TnC in reconstituted thin filament.**

(A) Stopped flow kinetic tracings obtained from mixing thin filament reconstituted with cTnC mutant labeled with IAANS at Cys-84 with an equal volume of the same buffer containing an excess of the  $\text{Ca}^{2+}$  chelator EGTA(1mM) (B) Normalised data for comparison. Buffer conditions: 140mM KCl, 4mM  $\text{MgCl}_2$ , 50mM MOPS pH 7.2) containing  $50\mu\text{M}$   $\text{CaCl}_2$  and  $4\mu\text{M}$  Tn.

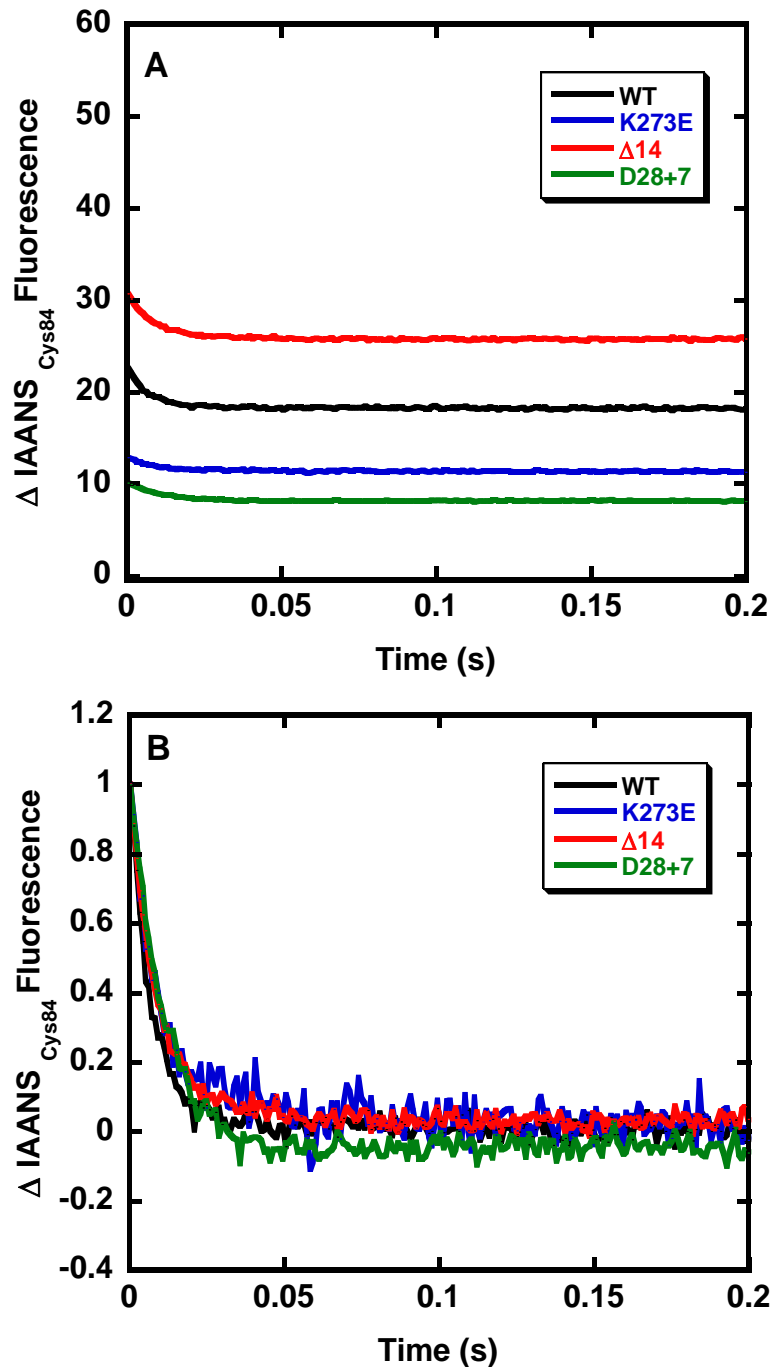


**Figure 5.19** Representative data for  $\text{Ca}^{2+}$  dependent change in relative fluorescence of HCM-T2 mutations given by IAANS-Cys84-TnC in reconstituted thin filament.

(A) Stopped flow kinetic tracings obtained from mixing thin filament reconstituted with cTnC mutant labeled with IAANS at Cys-84 with an equal volume of the same buffer containing an excess of the  $\text{Ca}^{2+}$  chelator EGTA(1mM) (B) Normalised data for comparison Buffer conditions: 140mM KCl, 4mM  $\text{MgCl}_2$ , 50mM MOPS pH 7.2) containing 50 $\mu\text{M}$   $\text{CaCl}_2$  and 4  $\mu\text{M}$  Tn.

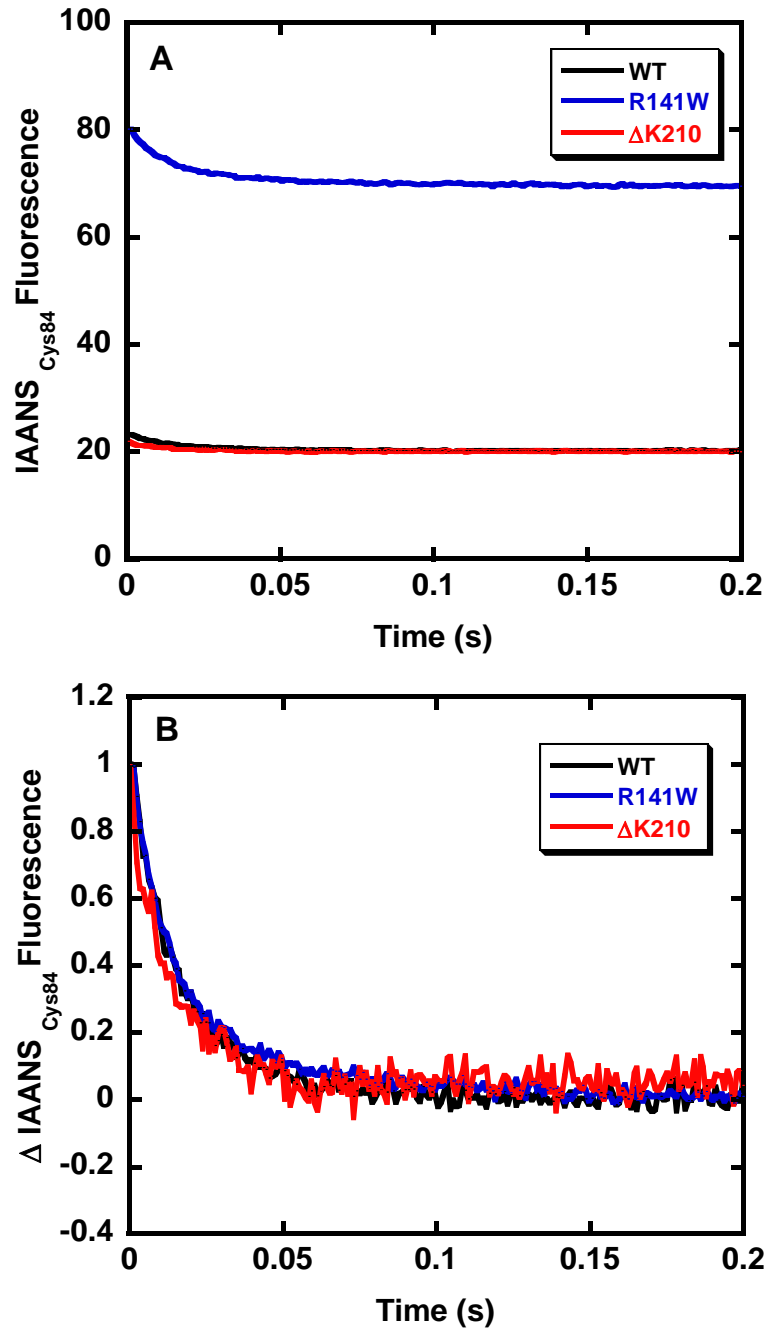


**Figure 5.20 Representative data for  $\text{Ca}^{2+}$  dependent change in relative fluorescence of DCM mutations given by IAANS-Cys84-TnC in reconstituted thin filament + S1**

(A) Stopped flow kinetic tracings obtained from mixing thin filament +S1 reconstituted with cTnC mutant labeled with IAANS at Cys-84 with an equal volume of the same buffer containing an excess of the  $\text{Ca}^{2+}$  chelator EGTA(1mM) (B) Normalised data for comparison. Buffer conditions: 140mM KCl, 4mM  $\text{MgCl}_2$ , 50mM MOPS pH 7.2) containing  $50\mu\text{M}$   $\text{CaCl}_2$  and  $4\mu\text{M}$  Tn.

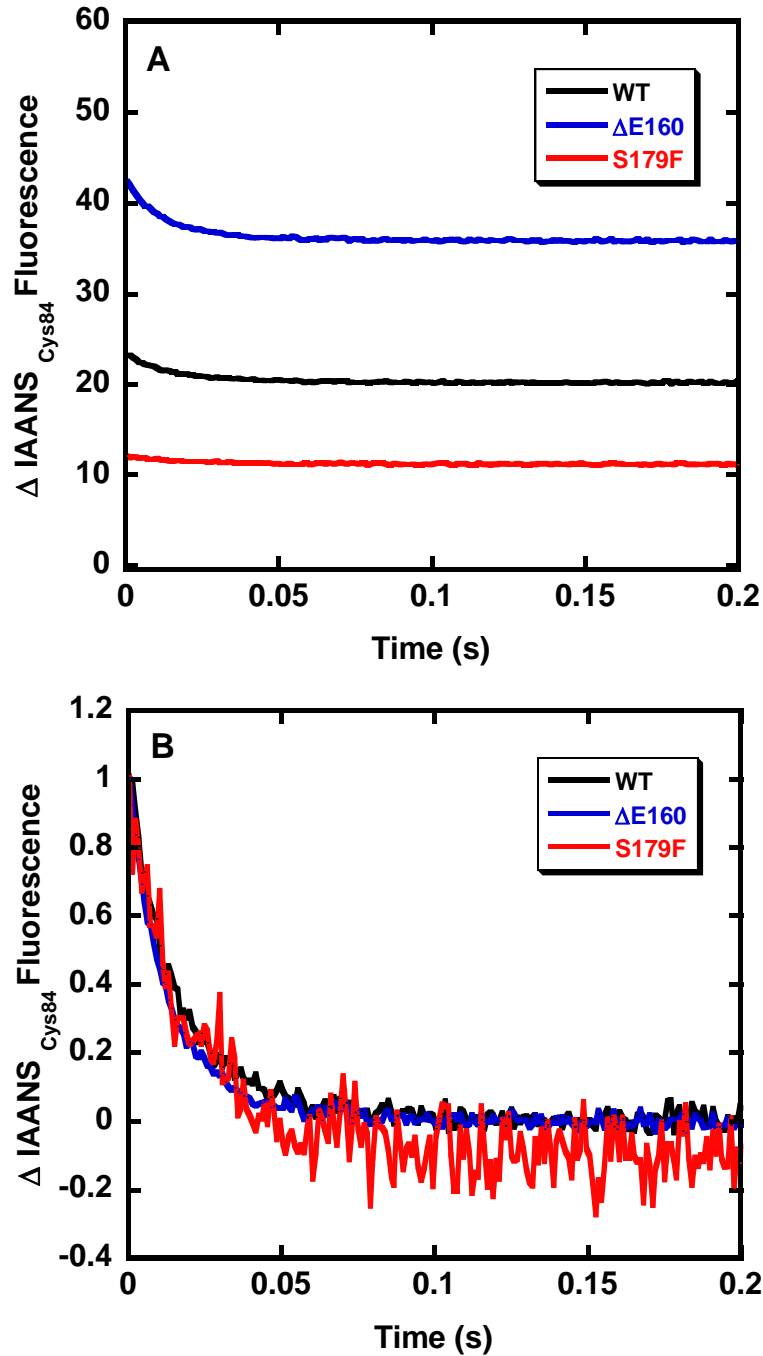


**Figure 5.21 Representative data for  $\text{Ca}^{2+}$  dependent change in relative fluorescence of HCM-T1 mutations given by IAANS-Cys84-TnC in reconstituted thin filament + S1**

(A) Stopped flow kinetic tracings obtained from mixing thin filament +S1 reconstituted with cTnC mutant labeled with IAANS at Cys-84 with an equal volume of the same buffer containing an excess of the  $\text{Ca}^{2+}$  chelator EGTA(1mM) (B) Normalised data for comparison. Buffer conditions: 140mM KCl, 4mM  $\text{MgCl}_2$ , 50mM MOPS pH 7.2) containing  $50\mu\text{M}$   $\text{CaCl}_2$  and  $4\mu\text{M}$  Tn.

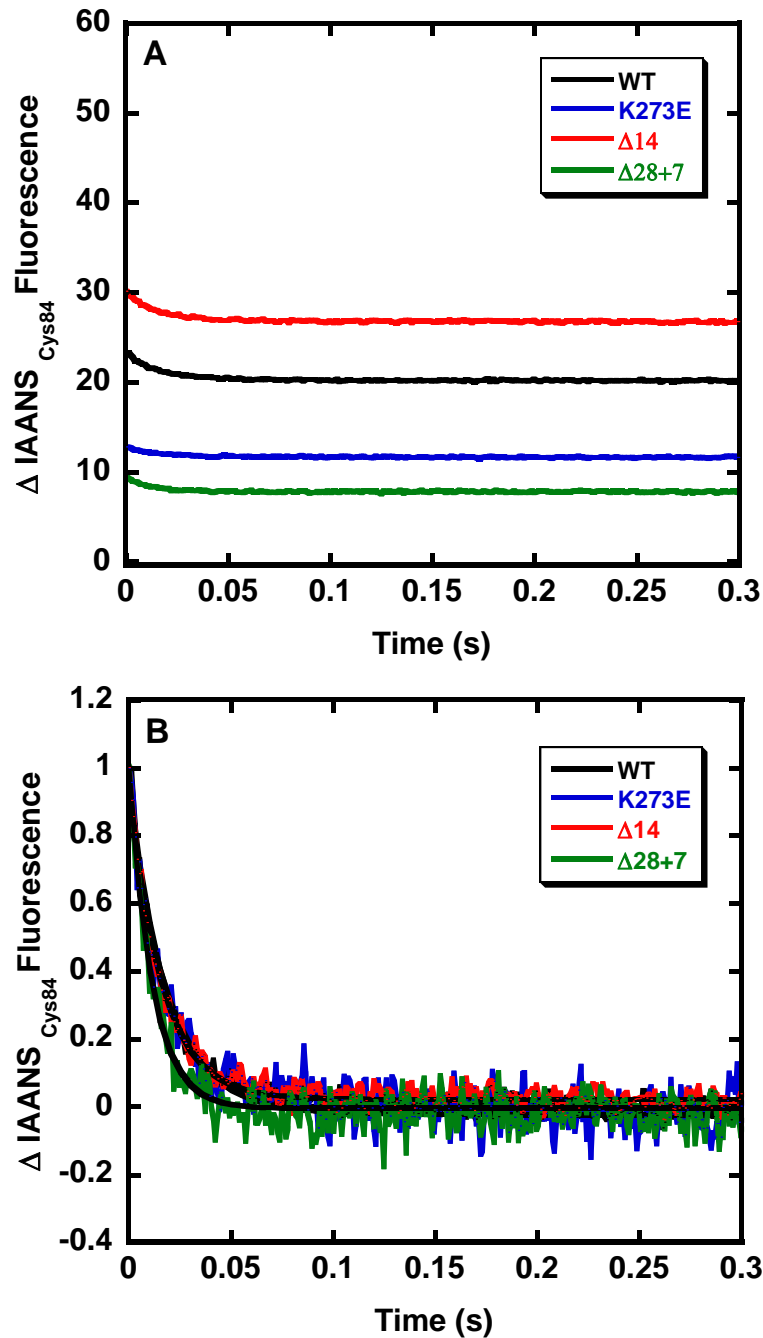


**Figure 5.22 Representative data for  $\text{Ca}^{2+}$  dependent change in relative fluorescence of HCM-T2 mutations given by IAANS-Cys84-TnC in reconstituted thin filament + S1**

(A) Stopped flow kinetic tracings obtained from mixing thin filament +S1 reconstituted with cTnC mutant labeled with IAANS at Cys-84 with an equal volume of the same buffer containing an excess of the  $\text{Ca}^{2+}$  chelator EGTA(1mM) (B) Normalised data for comparison. Buffer conditions: 140mM KCl, 4mM  $\text{MgCl}_2$ , 50mM MOPS pH 7.2 containing 50 $\mu\text{M}$   $\text{CaCl}_2$  and 4  $\mu\text{M}$  Tn.

**Table 5.4 Summary of the effect of cTnT mutations on the Ca<sup>2+</sup> binding properties using IAANS-Cys84**

cTnT	Tn complex		Thin Filament		Thin filament +S1	
	<i>1 exponential s<sup>-1</sup></i>	<i>amplitude</i>	<i>1 exponential s<sup>-1</sup></i>	<i>amplitude</i>	<i>1 exponential s<sup>-1</sup></i>	<i>amplitude</i>
<b>WT</b>	75	1.6	139	4.6	56.7	3.0
<b>R141W</b>	94.6	8	117	17.1	50.1	10.0
<b>ΔK210</b>	70.2	1.3	95.6	2.6	74.8	1.7
<b>ΔE160</b>	102	6.7	108.1	9.5	67.8	6.4
<b>S179F</b>	157	0.4	137.1	1.7	46.6	0.9
<b>K273E</b>	81.6	0.9	91.3	1.5	50.4	1.05
<b>Δ14</b>	85	2.8	106.5	5	61.6	3.3
<b>Δ28+7</b>	91.5	2.4	95.7	2.1	88.1	1.6

*The numbers are expressed as single experiment.*

### 5.2.B.3 Study of Ca<sup>2+</sup> Dissociation Kinetics of cTnT Mutations using Quin-2

Using native reconstituted Tn, the dissociation of Ca<sup>2+</sup> was measured by the increase in fluorescence on mixing with a large excess of Quin-2 fluorophore Ca<sup>2+</sup> chelator (Tsien et al. 1983). The fluorescent signal for Ca<sup>2+</sup> dissociation at 25°C is given in Figure 5.23. The curve obtained showed no lag phase but deviated from a fit to a single exponential term. In this instance, for WT the fitting procedure gave two observed rate constants of 82.3s<sup>-1</sup> and 24.2s<sup>-1</sup> with amplitudes of 30% and 70% respectively for the two terms. These amplitudes were similar to that reported previously (MacLachlan, Reid et al. 1990; Dong, Wang et al. 1997). Measurements for all of the mutations studied showed approximately equal relative amplitudes for the two terms.

No significant differences were seen for all mutations studied here except for  $\Delta 28+7$  compared to WT in all three systems (Figure 5.23-Figure 5.31). A quantitative comparison of the observed rate constants is presented in Table 5.5.

The results were comparable to measurements using IAANS-Cys 84 but were strikingly different for IAANS-Cys 35. The results indicate that the Ca<sup>2+</sup> binding measurements using IAANS-Cys 84 were not limited by slow conformational changes and actually reflected the Ca<sup>2+</sup> removal from the specific site.

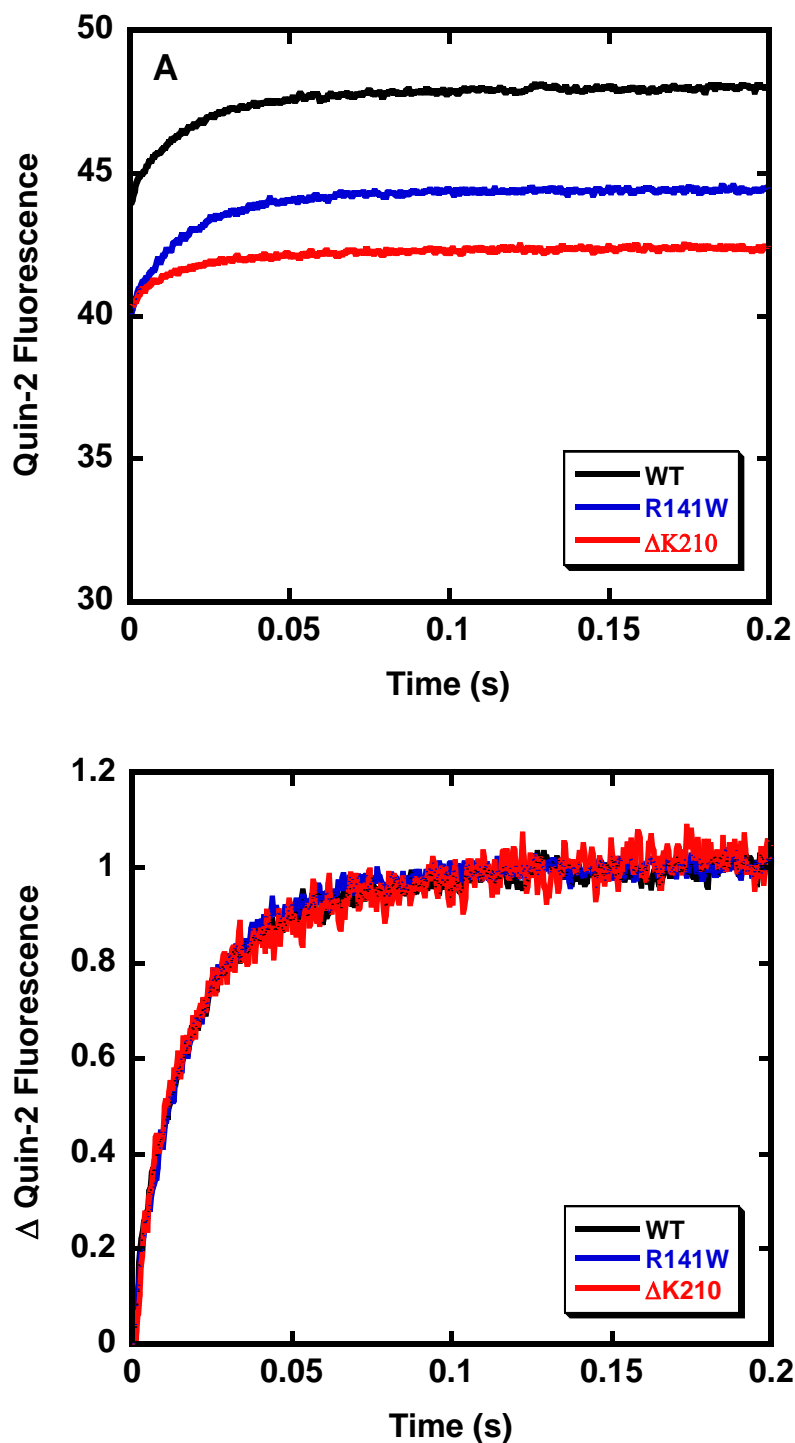


**Figure 5.23  $\text{Ca}^{2+}$  dependent change in relative fluorescence of DCM mutations given by Quin-2 in reconstituted Tn complex.**

(A) Stopped flow kinetic tracings obtained from mixing cTn with an equal volume of the same buffer containing an excess of Quin-2 (150  $\mu\text{M}$ ) (B) Normalised data for comparison. Final conditions: 140mM KCl, 4mM  $\text{MgCl}_2$ , 50mM MOPS pH 7.2) containing 50  $\mu\text{M}$   $\text{CaCl}_2$  and 4  $\mu\text{M}$  Tn.

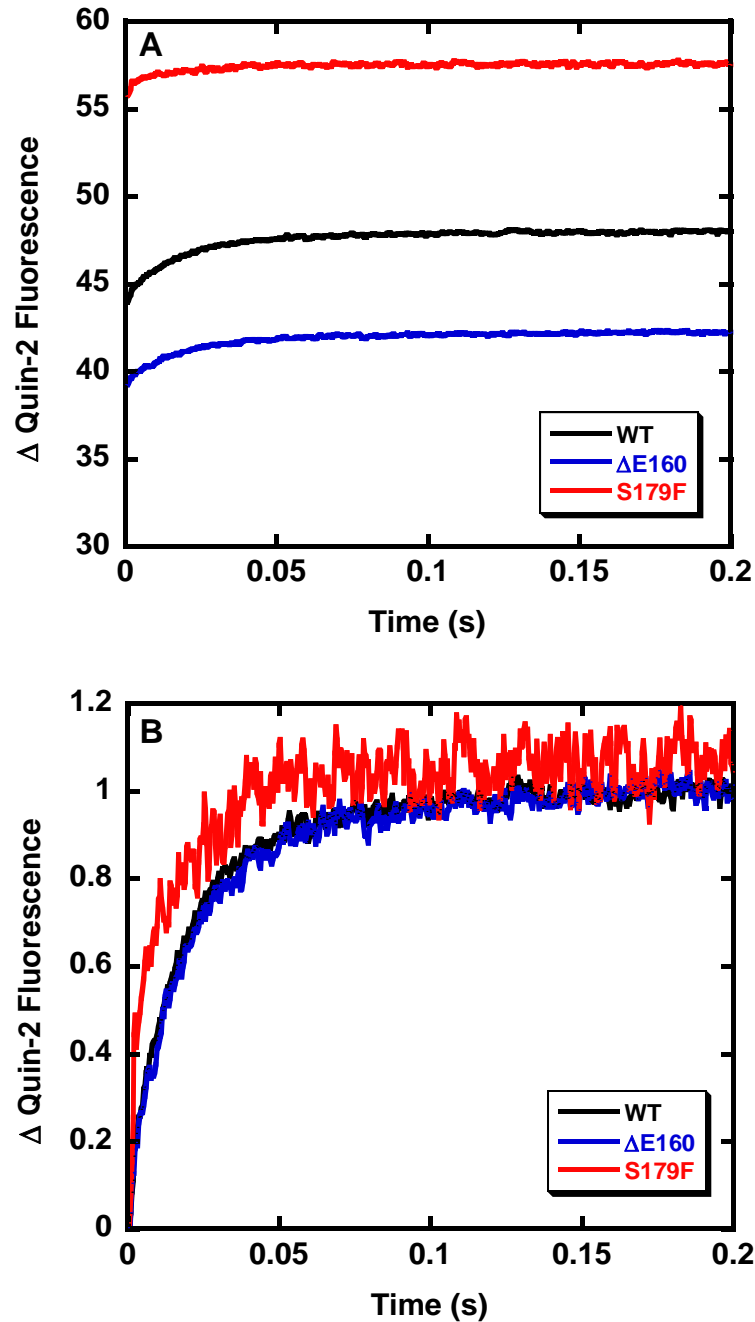


**Figure 5.24  $\text{Ca}^{2+}$  dependent changes in relative fluorescence of HCM-T1 mutations given by Quin-2 in reconstituted Tn complex.**

(A) Stopped flow kinetic tracings obtained from mixing cTn with an equal volume of the same buffer containing an excess of Quin-2(150 $\mu\text{M}$ ) (B) Normalised data for comparison. Final conditions: 140mM KCl, 4mM  $\text{MgCl}_2$ , 50mM MOPS pH 7.2) containing 50 $\mu\text{M}$   $\text{CaCl}_2$ . and 4  $\mu\text{M}$  Tn..

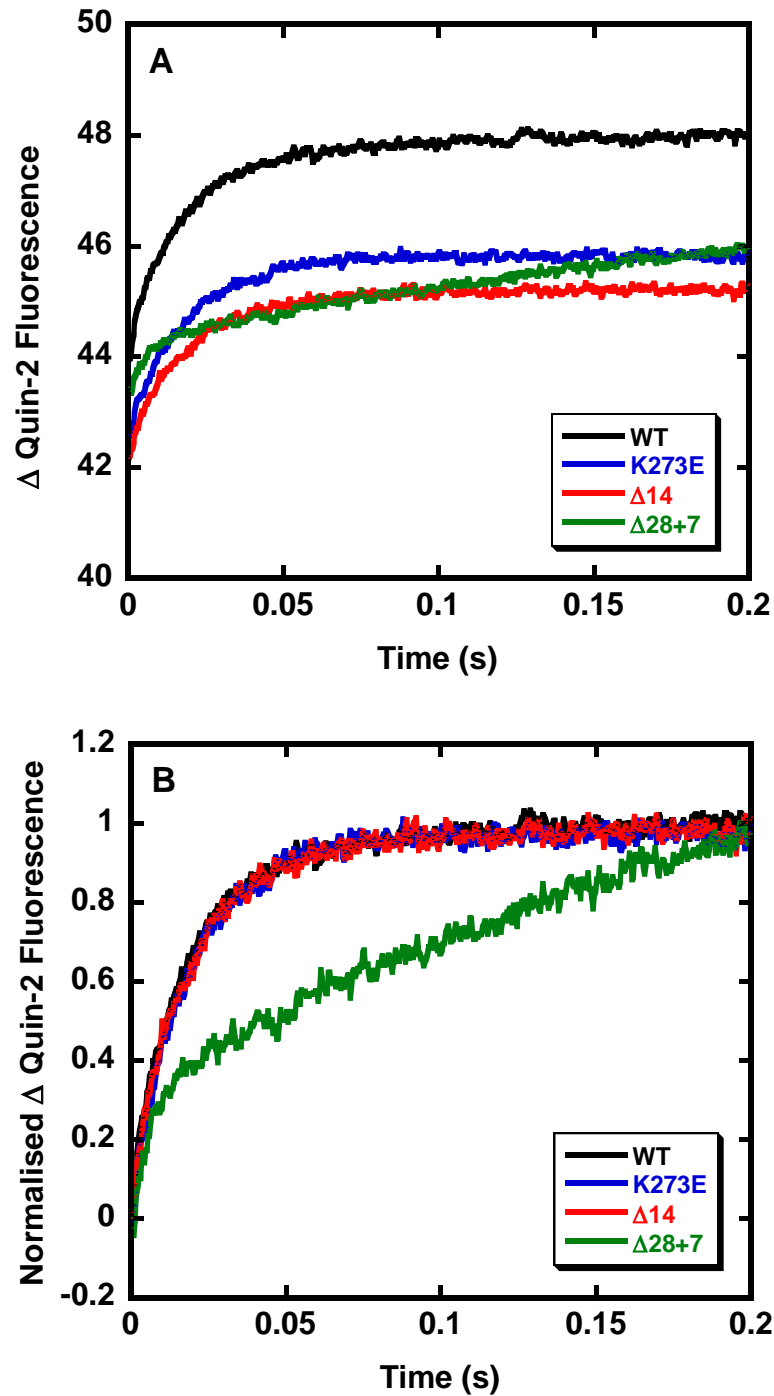


**Figure 5.25  $\text{Ca}^{2+}$  dependent change in relative fluorescence of HCM-T2 mutations given by Quin-2 in reconstituted Tn complex.**

(A) Stopped flow kinetic tracings obtained from mixing cTn with an equal volume of the same buffer containing an excess of Quin-2 (150  $\mu\text{M}$ ) (B) Normalised data for comparison. Final conditions: 140mM KCl, 4mM  $\text{MgCl}_2$ , 50mM MOPS pH 7.2) containing 50  $\mu\text{M}$   $\text{CaCl}_2$  and 4  $\mu\text{M}$  Tn.

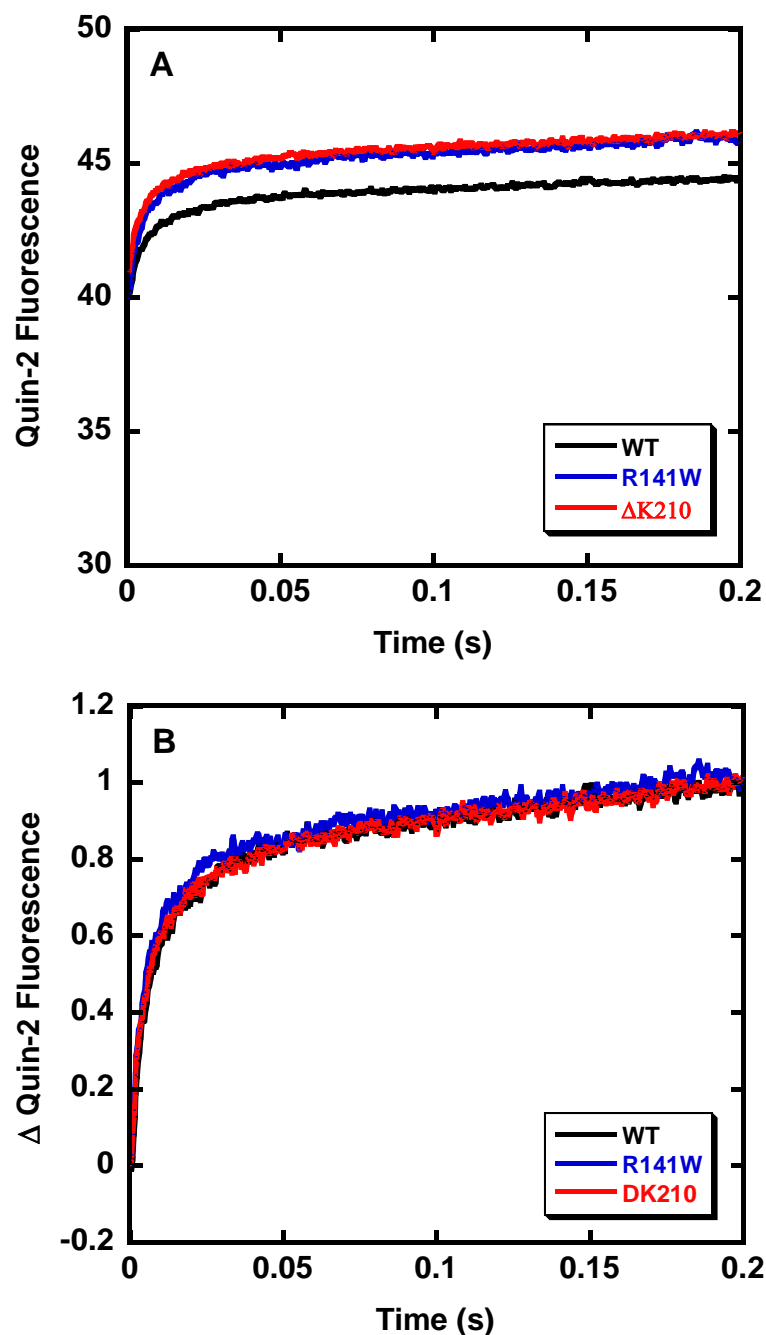


**Figure 5.26** Representative data for Ca<sup>2+</sup> dependent change in relative fluorescence of DCM mutations given by Quin-2 in reconstituted thin filament.

(A) Stopped flow kinetic tracings obtained from mixing thin filament with an equal volume of the same buffer containing an excess of Quin-2 (150 μM) (B) Normalised data for comparison. Final conditions: 140mM KCl, 4mM MgCl<sub>2</sub>, 50mM MOPS pH 7.2 containing 50 μM CaCl<sub>2</sub> and 4 μM Tn.

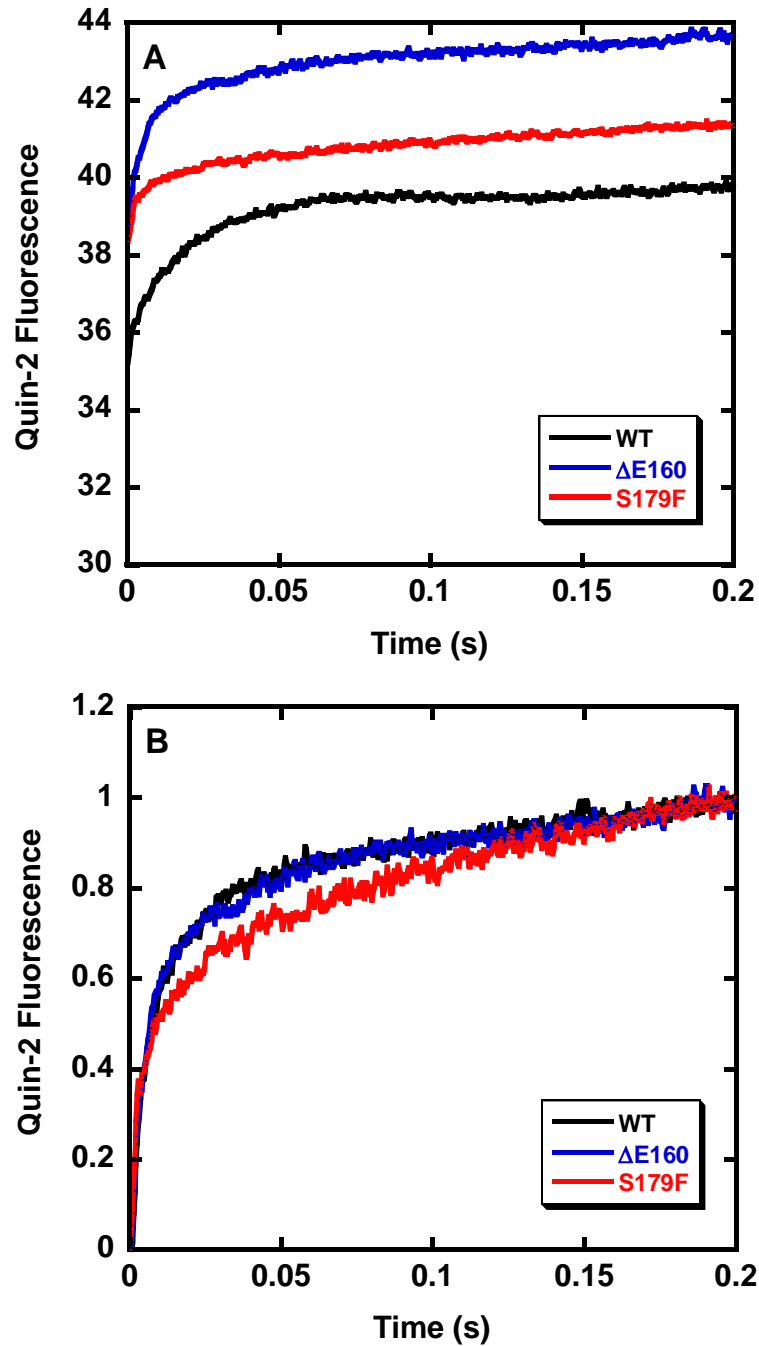


**Figure 5.27** Representative data for Ca<sup>2+</sup> dependent change in relative fluorescence of HCM-T1 mutations given by Quin-2 in reconstituted thin filament.

(A) Stopped flow kinetic tracings obtained from mixing thin filament with an equal volume of the same buffer containing an excess of Quin-2 (150 μM) (B) Normalised data for comparison. Final conditions: 140mM KCl, 4mM MgCl<sub>2</sub>, 50mM MOPS pH 7.2 containing 50 μM CaCl<sub>2</sub> and 4 μM Tn.

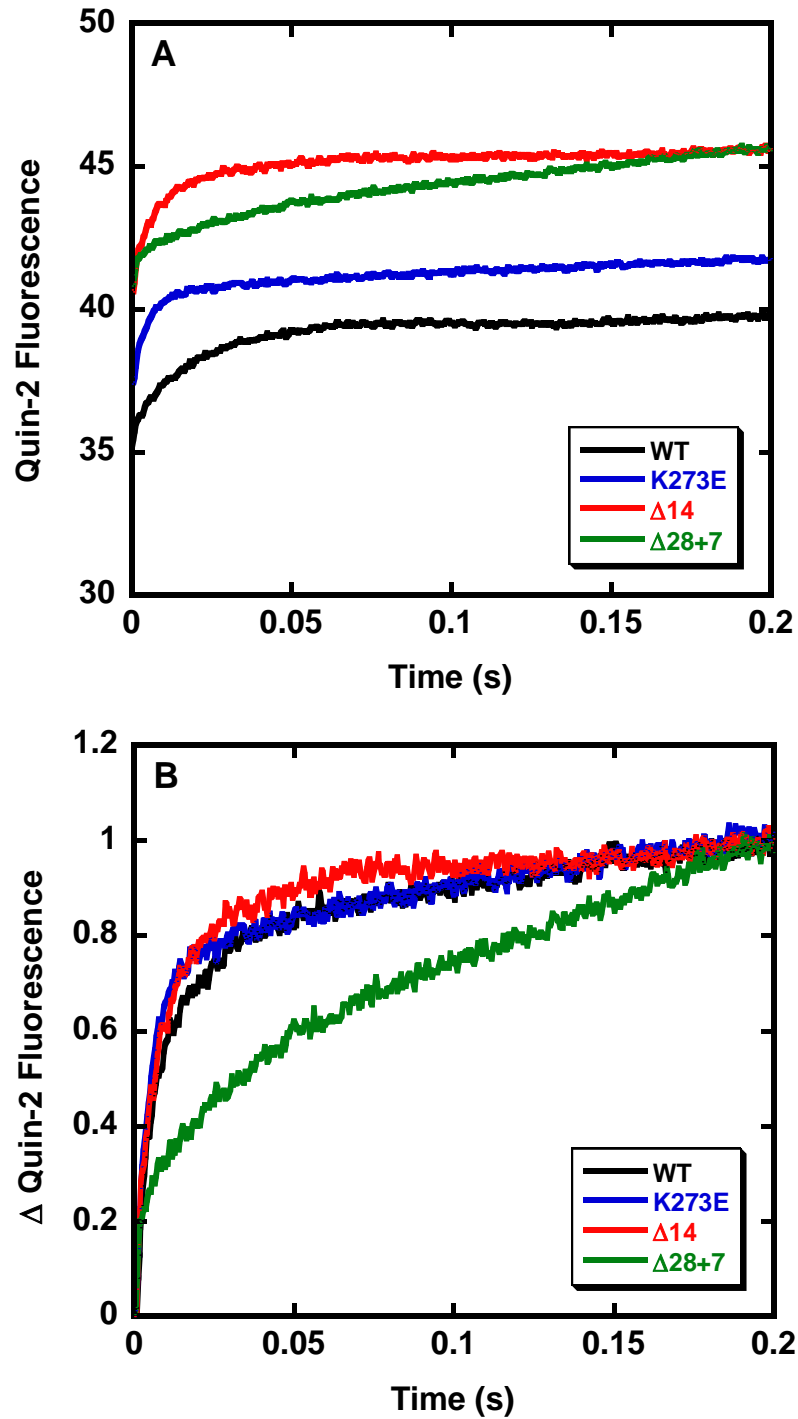


**Figure 5.28** Representative data for Ca<sup>2+</sup> dependent change in relative fluorescence of HCM-T2 mutations given by Quin-2 in reconstituted thin filament.

(A) Stopped flow kinetic tracings obtained from mixing thin filament with an equal volume of the same buffer containing an excess of Quin-2 (150 μM) (B) Normalised data for comparison. Final conditions: 140mM KCl, 4mM MgCl<sub>2</sub>, 50mM MOPS pH 7.2 containing 50 μM CaCl<sub>2</sub> and 4 μM Tn.

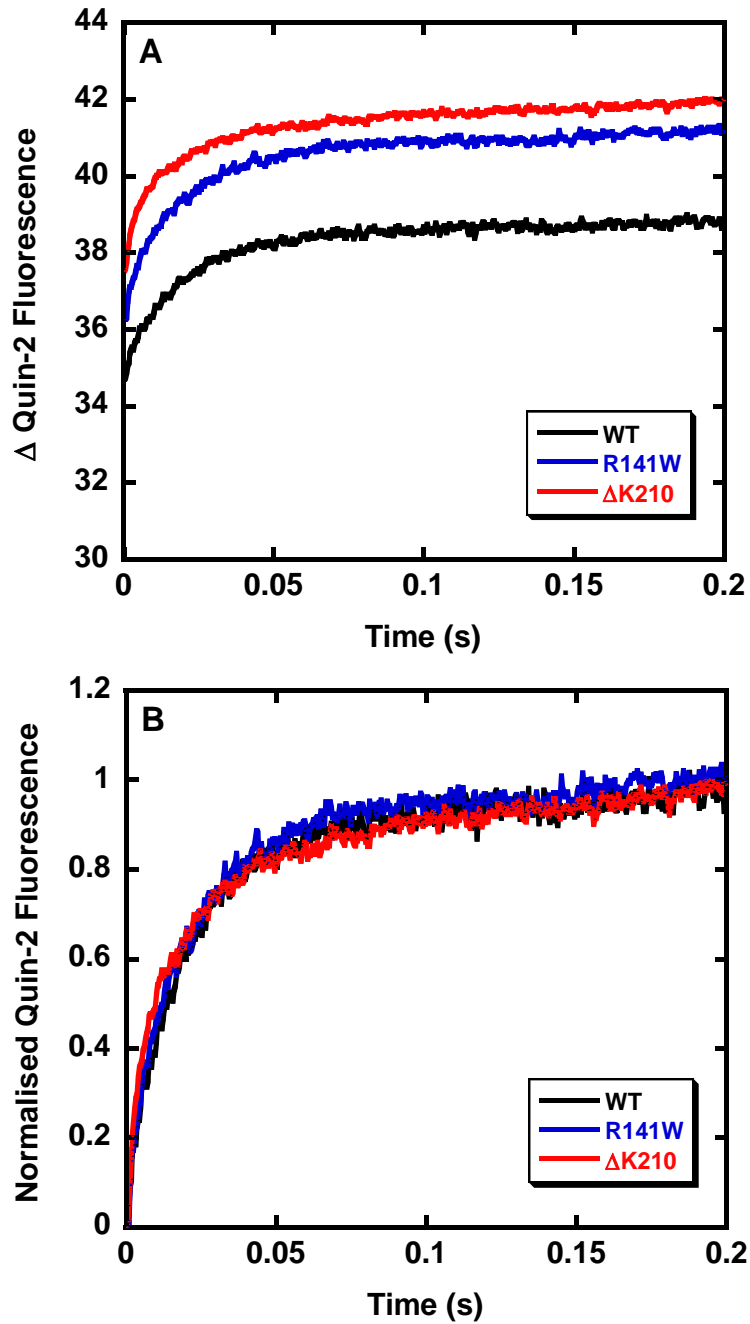


**Figure 5.29 Representative data for  $\text{Ca}^{2+}$  dependent change in relative fluorescence of DCM mutations given by Quin-2 in reconstituted thin filament + S1**

(A) Stopped flow kinetic tracings obtained from mixing thin filament+S1 with an equal volume of the same buffer containing an excess of Quin-2(150 $\mu\text{M}$ ) (B) Normalised data for comparison. Final conditions: 140mM KCl, 4mM  $\text{MgCl}_2$ , 50mM MOPS pH 7.2) containing 50 $\mu\text{M}$   $\text{CaCl}_2$ . and 4  $\mu\text{M}$  Tn.

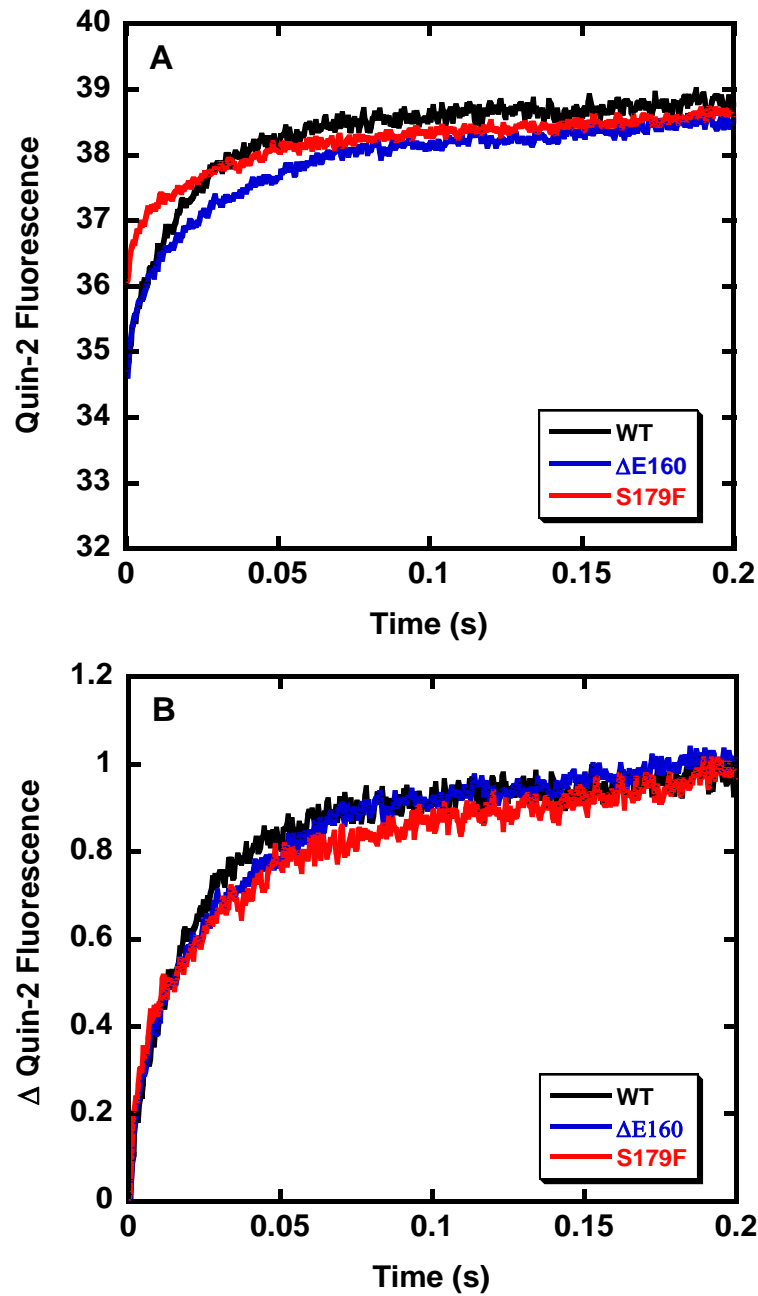


**Figure 5.30 Representative data for  $\text{Ca}^{2+}$  dependent change in relative fluorescence of HCM-T1 mutations given by Quin-2 in reconstituted thin filament + S1**

(A) Stopped flow kinetic tracings obtained from mixing thin filament+S1 with an equal volume of the same buffer containing an excess of Quin-2(150 $\mu\text{M}$ ) (B) Normalised data for comparison. Final conditions: 140mM KCl, 4mM MgCl<sub>2</sub>, 50mM MOPS pH 7.2) containing 50 $\mu\text{M}$  CaCl<sub>2</sub>. and 4  $\mu\text{M}$  Tn.

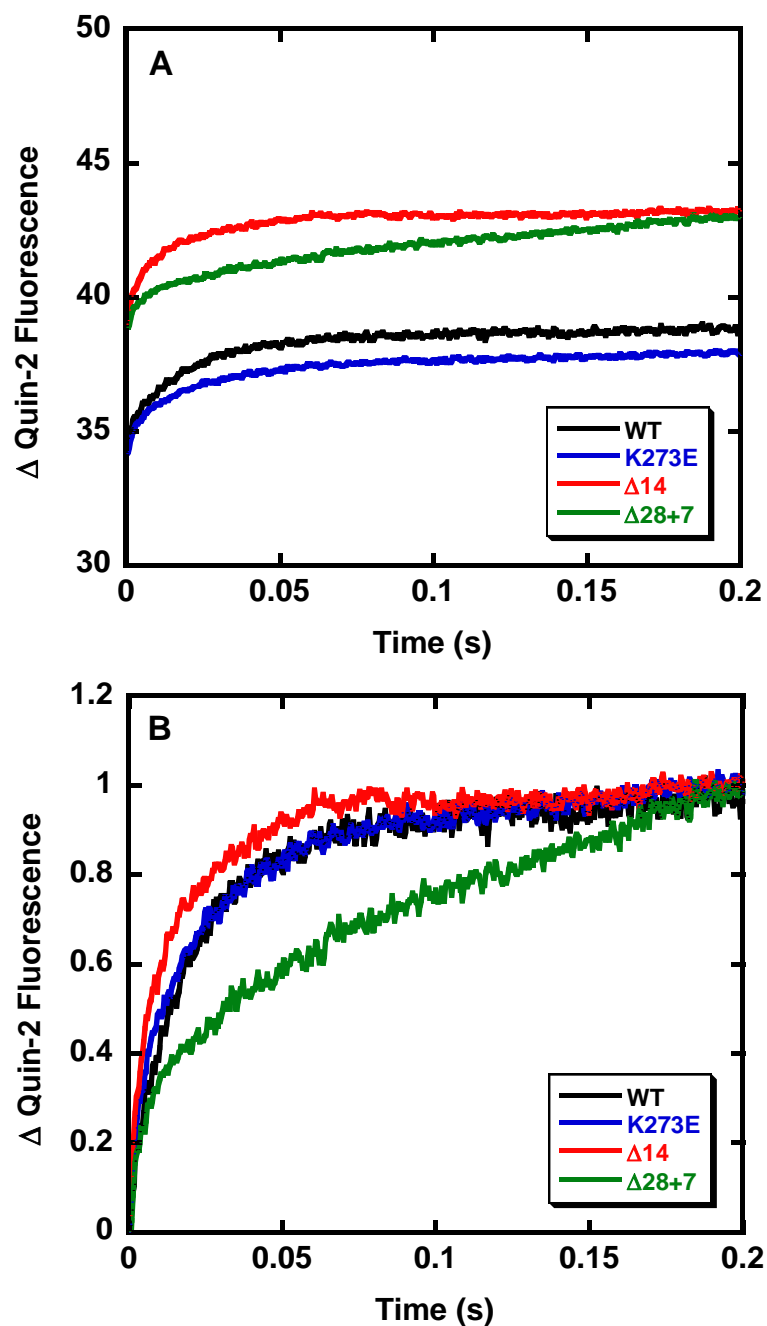


**Figure 5.31 Representative data for  $\text{Ca}^{2+}$  dependent change in relative fluorescence of HCM-T2 mutations given by Quin-2 in reconstituted thin filament + S1**

(A) Stopped flow kinetic tracings obtained from mixing thin filament+S1 with an equal volume of the same buffer containing an excess of Quin-2 ( $150\mu\text{M}$ ) (B) Normalised data for comparison. Final conditions: 140mM KCl, 4mM  $\text{MgCl}_2$ , 50mM MOPS pH 7.2 containing  $50\mu\text{M}$   $\text{CaCl}_2$ , and  $4\mu\text{M}$  Tn.

**Table 5.5 Summary of the effect of cTnT mutations on the Ca<sup>2+</sup> binding properties reconstituted Tn, thin filament and myo filament using Quin-2**

cTnT	Tn complex		Thin Filament		Thin filament +S1	
	<i>k</i> <sub>slow</sub>	<i>k</i> <sub>fast</sub>	<i>k</i> <sub>slow</sub>	<i>k</i> <sub>fast</sub>	<i>k</i> <sub>slow</sub>	<i>k</i> <sub>fast</sub>
<b>WT</b>	24.2	82.3	10.2	154.4	11.9	62.7
<b>R141W</b>	36.4	88.9	8.7	181.2	11.2	68.3
<b>ΔK210</b>	18.5	101.6	10.7	181.7	17.1	139.9
<b>ΔE160</b>	11.6	65.6	13.2	200.1	22.7	181
<b>S179F</b>	48	555	8.3	240.6	8.2	75.9
<b>K273E</b>	25.5	59.5	5.31	218.8	19.8	128.6
<b>Δ14</b>	35.5	76.9	24	173.3	35.1	123.2
<b>Δ28+7</b>	6.3	232.3	7.8	202.4	7.1	154.9

The numbers are expressed as single experiment.

## 5.3 Discussion

In this chapter we have studied the effect of TnT mutations on the  $\text{Ca}^{2+}$  affinity and  $\text{Ca}^{2+}$  dissociation kinetics of the troponin complex, the thin filament and thin filament with bound myosin heads. We used TnC, labelled with IAANS at both Cys 35 and 84, methods which were previously used extensively to investigate the equilibrium properties of  $\text{Ca}^{2+}$  binding to site II of isolated Tn complex and in Tn reconstituted with actin.Tm.

Our data described here for  $\Delta\text{K210}$  and all HCM causing mutations caused increase in  $\text{Ca}^{2+}$  affinities in thin filament without altering the  $\text{Ca}^{2+}$  affinity of the isolated Tn complex with the exception of  $\Delta\text{28+7}$  which showed reduced  $\text{Ca}^{2+}$  affinity in Tn complex and no significant change in reconstituted thin filament compared to WT. The direction of the changes to thin filament  $\text{Ca}^{2+}$  affinities using IAANS attached to Cys 84 closely matched the shifts in  $\text{Ca}^{2+}$  sensitivity studies reported in ATPase assays (Chapter 3). Thus it is possible to relate the changes in  $\text{Ca}^{2+}$  sensitivity observed for actomyosin ATPase and in vitro motility to a change in the  $\text{Ca}^{2+}$  affinity of thin filaments. An increased  $\text{Ca}^{2+}$  affinity will lead to delayed relaxation..

All HCM mutations and DCM mutant- $\Delta\text{K210}$  are present in the T1 and T2 domain of TnT and therefore could alter fundamental interactions between the components. An exception to this study was R141W residing in the N-terminal domain of TnT that showed reduced  $\text{Ca}^{2+}$  affinity in studies related to IAANS labelled at C35 showing no direct interaction with TnI and TnC. This mutation lies adjacent to the TnT-Tm overlap region and the missense mutation to

tryptophan residue may disrupt propagation of thin filament activation on  $\text{Ca}^{2+}$  binding thus reducing the affinity of subsequent Tn for  $\text{Ca}^{2+}$ .

Reduced cooperativity (reduced Hill coefficient,  $n_H$ ) was seen for all HCM mutants and DCM mutant  $\Delta\text{K210}$  in studies using IAANS-Cys84 labelled on TnC in reconstituted thin filament..

Troponin C plays a major role in intracellular  $\text{Ca}^{2+}$  buffering in cardiomyocytes (Bers 2008). Hence any significant changes in  $\text{Ca}^{2+}$  affinity may result in disturbances in intracellular  $\text{Ca}^{2+}$  handling. Intracellular  $\text{Ca}^{2+}$  is involved in many cellular processes and an altered level of intracellular  $\text{Ca}^{2+}$  resulting from mutational effects on  $\text{Ca}^{2+}$  affinity could affect a number of cellular processes and possibly explain how mutations in Tn can cause the global cardiac remodelling process observed for both DCM and HCM.

A second important point addressed in this work is the kinetic mechanism of  $\text{Ca}^{2+}$  dissociation to site II low affinity site of TnC.  $\text{Ca}^{2+}$  dissociation from troponin is important for cardiac muscle relaxation and the rate of  $\text{Ca}^{2+}$  dissociation is an important determinant of the rate of cardiac muscle relaxation.

It is of interest to compare these results for WT with work carried out by other groups to accurately reflect the changes observed in TnT mutations studied here. Previous work indicated that the environment of TnC interdomain linker consisting of residues 84-94 changes upon  $\text{Ca}^{2+}$  binding to site II (Sia, Li et al. 1997) and that IAANS labelling at either positions C35 or C84 does not affect  $\text{Ca}^{2+}$  regulation (Dong, Rosenfeld et al. 1996; Kobayashi and Solaro 2006; Robinson, Griffiths et al. 2007). The rate of  $\text{Ca}^{2+}$  dissociation kinetics for WT is in close agreement with previously reported values (Davis, Norman et al. 2007;

Davis and Tikunova 2008). These authors obtained a single rate constant of Ca dissociation using IAANS which agrees within experimental error with the values obtained. The Quin-2 experiments further confirmed Cys-84 to be directly reporting the  $\text{Ca}^{2+}$  dissociation rate from site II.

Overall our studies showed that the rate of  $\text{Ca}^{2+}$  dissociation from isolated Tn, Tn in thin filament and Tn in thin filaments decorated with myosin heads was not affected by mutation R141W,  $\Delta$ K210, S179F,  $\Delta$ E160, K273E, and  $\Delta$ 14. In contrast the rate of  $\text{Ca}^{2+}$  dissociation for  $\Delta$ 28+7 was increased when measured by IAANS-C35 but decreased when measured by Quin-2. The reason for this discrepancy remains unclear but may be due to the fact that the 2 probes measure different event. An alternative explanation is that modification of Cys35 by IAANS affects the rate constant governing  $\text{Ca}^{2+}$  dissociation from site II.

# CHAPTER 6

General Discussion

# **Contents**

<b>6.1</b>	<b>Summary of the thesis</b>	<b>196</b>
<b>6.2</b>	<b>Limitations of the studies</b>	<b>206</b>
<b>6.3</b>	<b>Future Directions</b>	<b>207</b>

This chapter presents a summary of the main findings in this thesis, and describes how the study of mutations in TnT contribute towards gaining valuable information leading to the pathological states. Limitations of the studies are then presented, and issues are discussed that could affect the interpretation of the study results. Finally, potential future research directions are explored.

## **6.1 Summary of the Thesis**

### **6.1.1 Background**

Genetic analyses over the past 20 years have revealed that inherited HCM and DCM are caused by a large number of mutations in genes of sarcomeric proteins including TnT. Defining the impact of mutations on the structure and function of these sarcomeric proteins and the resultant physiological behaviour of the sarcomere remains a substantial challenge, especially since there is a huge clinical variability ranging from sudden cardiac death at a young age (below 40 years) to mild symptoms with normal life expectancy. It is therefore important to study individual mutations in the growing interest of therapeutic intervention. It is beneficial at the biochemical level in understanding how they alter the cardiac contractile cycle and its regulation. While mutations in many genes (including myosin and tropomyosin) lead to gross morphological changes in the heart that could explain the onset of the cardiac sudden death event, mutations in troponin T are generally associated with mild or no ventricular hypertrophy yet they are associated with high incidence of sudden death. This led to the suggestion that abnormal behaviour of the cardiomyocytes (or subcellular structures such as the sarcomeres) could be at the origin of the

sudden cardiac death syndrome. Finding the biochemical changes associated with mutations in troponin T are therefore of paramount importance.

While structural studies can suggest ways in which the protein function may be affected it's only by measuring the biochemical properties directly can we understand the functional consequences of the mutations. Extensive studies by numerous groups have been carried out using steady state approaches involving force measurements, ATPase and in vitro motility assays. Although they provided useful information, they were unable to generate a comprehensive explanation of how alterations in the protein could lead to pathological states or to the disparate clinical phenotype observed with different mutations. Our approach was based on transient kinetic analysis (methods of choice for studying single steps in complex biochemical pathways).

### **6.1.2. Main Findings in the Thesis**

Among the 37 known TnT mutations, we selected 7 mutations (Table 6.1) in the 2 functional domains of TnT (T1 and T2) that were linked to both HCM and DCM. These mutations have been grouped into 3 groups:

Group 1: DCM mutations R141W and  $\Delta$ K210 in the T1 and T2 domain respectively

Group 2: HCM mutations  $\Delta$ E160 and S179F in the T1 domain

Group 3: HCM mutations K273E, truncated  $\Delta$ 14 and  $\Delta$ 28+7 in the T2 domain

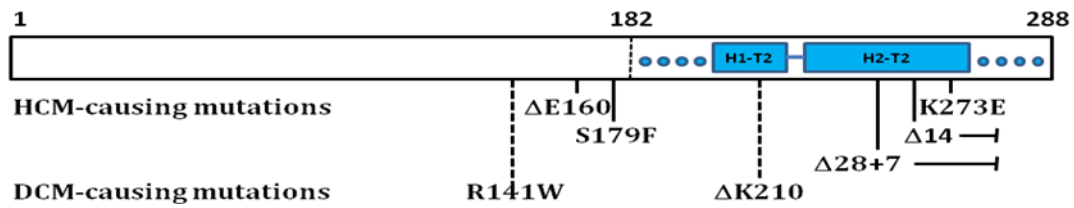


**Figure 6.1 Position of HCM and DCM causing mutations in TnT sequence**

### **Functional consequences of DCM associated mutations (Group 1)**

We studied DCM associated deletion mutation ( $\Delta K210$ ) and missense mutation (R141W). CD analysis revealed that both R141W and  $\Delta K210$  TnT mutations caused no changes in the secondary structure in agreement with previous findings (Venkatraman, Harada et al. 2003). Thus these mutations do not seem to have affected the overall fold of TnT and the Tn complex. Analysis of their binding to the thin filaments by co-sedimentation showed that their incorporation in thin filaments was not affected. Overall these structural investigations suggest that these mutant proteins are incorporated normally in the sarcomeres within the cardiomyocytes. This warrants functional investigations.

We detected no change in the parameters studied ( $n$ ,  $K_B$ ,  $Ca^{2+}$  affinity and rate constant of  $Ca^{2+}$  dissociation) for R141W. Hence this mutant does not seem to affect cooperativity along thin filament. This is consistent with the finding that this mutation does not affect the Hill coefficient of  $Ca^{2+}$  activation of actomyosin ATPase (our data, see Table 6.1) or force measurement (Venkatraman et al 2003). We and other groups (Venkatraman, Harada et al. 2003; Mirza, Marston et al. 2005) have reported a distinct pattern of depressed maximal actomyosin ATPase and depressed contraction (Knock out studies by Morimoto's lab). This could be due to an inhibition of the transition from the closed to the open state

( $K_T$ ), a parameter that we have not measured in this work. R141W involves loss of positive charge and lies in the N-terminal T1 region of TnT. It is in the region of large  $\alpha$ -helical content and has been shown to bring to Tm that extends over the junction between adjacent Tm-Tm interactions. This could potentially affect the Tm-TnT binding and TnT interactions with TnI and TnC (Cabral-Lilly et al.1997).

$\Delta$ K210, however, gave an increase in the size of the cooperative unit  $n$  to 20. An increase in the size of cooperative unit  $n$  is likely to lead to more activation of thin filaments and therefore to more force being produced (hypercontractile myocardium). In addition increased cooperativity will lead to delayed relaxation (as shown by the longer lag displayed in our ATP induced acto-S1 experiments).  $Ca^{2+}$  affinity for  $\Delta$ K210 was increased. In contrast no significant changes were observed for the distribution of inhibited and activated states ( $K_B$ ) and for the observed rate constant of calcium dissociation from TnC.

$\Delta$ K210 is located in helix 1 which is not in proximity to TnI and TnC and has been suggested by Malnic et al. 1998 to interact with Tm and actin in the absence of  $Ca^{2+}$  and is released upon  $Ca^{2+}$  binding. This could explain the altered  $Ca^{2+}$  activation observed with this mutant.

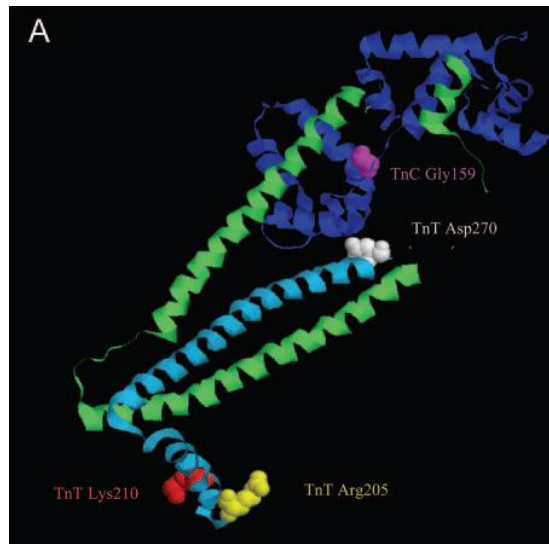


**Figure 6.2 Location of  $\Delta K210$  mutation in Tn structure**

*Partial ribbon structure of Tn (PDB 1J1D) determined by X-ray diffraction. TnC is blue, TnI is green and TnT is cyan. The site of  $\Delta K210$  is shown as a space filling in red. (Takeda et al 2003)*

**Functional abnormalities induced by HCM associated mutations in TnT1 (Group 2)**

This group consisted of a deletion mutation ( $\Delta E160$ ) and a missense mutation (S179F) associated with HCM. Using steady state ATPase we found no significant differences in the maximal activation and inhibition of the actomyosin ATPase but an increased  $Ca^{2+}$  sensitivity of the actomyosin ATPase for both mutations. This in agreement with previous findings that these mutations increase  $Ca^{2+}$  sensitivity of force without significant changes to the maximum force levels (Szczesna et al. 2000; Harada and Potter 2004). No significant difference in  $\alpha$ -helical content for S179F compared to WT was found; however  $\Delta E160$  showed a marked increase in  $\alpha$ -helical content. This in not surprising since residues 80-180 for cTnT which included  $\Delta E160$  and S179F mutations have been identified to be highly  $\alpha$ -helical (Hinkle et al. 1999).

Analysis of thin filaments switching revealed that both mutations increased KB in the absence of  $\text{Ca}^{2+}$ . This means that in the absence of  $\text{Ca}^{2+}$ , thin filaments are not switched to the blocked state to the same level as for the WT. A decreased population in the blocked state is likely to interfere with the relaxation of cardiomyocytes. Relaxation abnormalities (defined as diastolic dysfunction) are a common abnormality in HCM. The effect on cooperativity was different between the 2 mutations. The size of the cooperative unit  $n$  was unchanged for S179F but was substantially reduced for  $\Delta\text{E160}$ . A reduction in the size of cooperative unit  $n$  is likely to lead to less activation of thin filaments and therefore to less force being produced (hypocontractile myocardium). Figure 6.3 illustrates the interaction of TnT (160–193) with the C-terminal domain of TnC mapped using NMR chemical shift mapping techniques (Blumenschein et al. 2001).

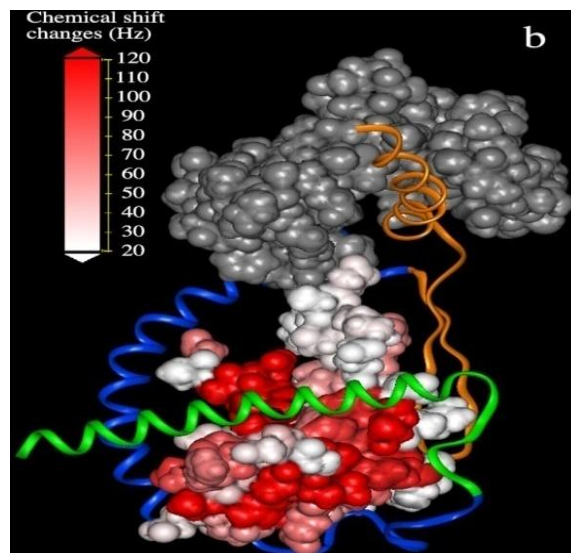


**Figure 6.3 Molecular surface mapping of TnT-(160–193) binding site in the C domain of TnC**

*TnT-(160–193) coloured in blue binding to whole TnC (shown as a surface). The region of TnI corresponding to the peptide TnI-(1–40) is coloured in green, while the region corresponding to TnI-(96–139) is coloured in orange.*

### **Functional consequences of mutations in the C-terminal region of TnT (Group 3)**

This group consisted of a missense mutation (K273E) and two truncation mutations ( $\Delta 14$  and  $\Delta 28+7$ ) associated with HCM. Steady state ATPase studies showed reduced maximal activation and inhibition for  $\Delta 14$  and  $\Delta 28+7$ . In contrast K273E mutation caused a significant increase in ATPase activation but behaved similarly to WT in actomyosin inhibitory assays. All mutations in this group showed increased  $\text{Ca}^{2+}$  sensitivity.

Truncation of the extreme C-terminus increased cooperativity along thin filament (higher  $n$  values obtained for  $\Delta 14$  and  $\Delta 28+7$  in comparison to the WT) but remained the same as for WT for K273E.

The equilibrium constant  $K_B$  was increased for all 3 mutations which explains the reduced inhibitory activity seen for  $\Delta 14$  and  $\Delta 28+7$  in the ATPase assays.  $\text{Ca}^{2+}$  dissociation kinetic studies showed a reduced rate of calcium dissociation for  $\Delta 28+7$  compared to WT.

Our data are broadly in agreement with previous findings. A reduced activation of the actomyosin ATPase and severely reduced inhibition were reported for both  $\Delta 14$  and particularly  $\Delta 28+7$  (Mukherjea et al. 1999). Both truncated mutations showed a marked  $\text{Ca}^{2+}$  sensitising effect. The maximum force was depressed by  $\Delta 28+7$  mutation (Nakaura et al. 1999). Using in situ troponin exchange technique, all the mutations in this group showed increase in  $\text{Ca}^{2+}$  sensitivity on skinned fibre force development without significantly changing the maximum force level (Szczesna et al. 2000; Harada and Potter 2004).

The main findings that support our hypothesis are dependent on the significance of experiments performed on each mutation summarised in Table 6.1. In order to determine the relative significance of the results, statistical significance of each data set using p-values was employed. The p-value figures used to determine the colour-coded significance levels in Table 6.1 has been outlined in Appendix E.

In general, experiments performed on Group 1 mutations showed no apparent changes in the parameters studied except for  $\Delta$ K210 which showed a significantly reduced ATPase as well as an increase in the size of the cooperative unit  $n$ . The significance level of ' $n$ ' was based on repetitive experimentation and not on p-value measurements.

In Group 2, an important observation was that  $\Delta$ E160 showed a marked increase in  $\alpha$ -helical content and thermal stability. These experiments were statistically very significant. The size of the cooperative unit  $n$  was unchanged for S179F but was substantially reduced for  $\Delta$ E160. The equilibrium constant  $K_B$  was increased for both and these figures were considered to be extremely statistically significant.

A reduced activation of the actomyosin ATPase and severely reduced inhibition was reported for the two truncated Group 3 mutations. the  $\alpha$ -helical content,  $n$ , and  $K_B$  were all increased compared to WT and were considered to be statistically significant for both mutations. Although K273E mutation caused a no significant change in ATPase and ' $n$ ', these experiments were only considered to be significantly reduced in the  $\alpha$ -helical content as well as thermal stability.  $K_B$  was increased for K273E showing extreme significance level.

Overall the data reported in this thesis suggests that it is the functional changes caused by mutations that are critical in developing the disease and not the specific location of the mutation.

**Table 6.1 Summary of General Findings**

TnT	ATPase Activity		Circular Dichroism			n*	K <sub>B</sub> -Ca <sup>2+</sup> /Actin
	Activation	Inhibition	α-Helical Content TnT	α-Helical Content Tn Complex	Thermal Stability of Tn Complex		
R141W	↔	↔	↔	↔	↔	↔	↔
ΔK210	↓	↔	↔	↔	↔	↑	↔
ΔE160	↔	↔	↑	↑	↑	↓	↑
S179F	↔	↔	↔	↔	↔	↔	↑
K273E	↔	↔	↑	↓	↓	↔	↑
Δ14	↓	↓	↑	↑	↔	↑	↑
Δ28+7	↓	↓	↑	↑	↔	↑	↑

\* The significance of the 'n' parameter data set is based on the repetitive of experimentation and not as per p-values

**KEY – p value significance**

Not Significant

Extremely Significant



0.9999 - 0.1010	not statistically significant	
0.0989 - 0.0512	not quite statistically significant	
0.0500 - 0.0102	statistically significant	
0.0099 - 0.0010	very statistically significant	
> 0.0010	extremely statistically significant	

## 6.2 Limitations of the Studies

Two issues could affect the outcome of this thesis:

1) The nature of the isoform of the proteins used in our assays (skeletal versus cardiac, human versus sheep and rabbit). Conditions were kept as close to physiological conditions as we could by using human cardiac sequence recombinant Tn and cardiac tissue purified actin and Tm from sheep heart muscle. However, S1 was obtained from rabbit skeletal muscle.

2) Measurements in our experiments used 100% mutant yet *in vivo* these mutations are expressed up to 50% (in general between 5 and 20%) since HCM and DCM are known to be autosomal dominant diseases (One copy of the gene is normal and one copy is defective).

Literature studies have shown that the relative amount WT to mutant proteins affects the molecular changes often in a highly unpredictable way. For example,  $\Delta K210$  has been shown to increase  $Ca^{2+}$  sensitivity (in experiments using 100% mutant) or decrease of  $Ca^{2+}$  sensitivity (if the experiment used 50% of wildtype:mutant) (Robinson et al. 2002). Therefore the molecular defect is likely to be affected not only by the nature of the mutation but also by the level of expression. Investigation of the functional properties of these mutations at the physiological ratio of mutant to wildtype should be performed.

## 6.3 Future Directions

In this thesis we have focused on investigating the effect of TnT mutations on thin filaments properties. However, the mutations could affect secondary mechanism of cardiac adaptation to physiological or pathological conditions.

There has been compelling evidence demonstrating post translational modifications of cardiac Tn play an important role in modulating cardiac function (Solaro, Varghese et al. 2002; Kobayashi and Solaro 2005). Mutations in TnT could change the effect of these post-translational modifications. Analysis of cardiac myofibrils isolated from  $\Delta$ K210 hearts have shown to alter the phosphorylation propensity of key sarcomeric proteins. Molecular modelling of cTnT- $\Delta$ K210 structure reveals changes in the electrostatic environment of cTnT helix (residues 203–224) that could lead to a more basic environment around Thr203, which may affect PKC-dependent phosphorylation of TnT (Sfichi-Duke, Garcia-Cazarin et al. 2010). Hence studying the effect of mutations in association with post-translational modification could reveal interesting findings.

Another example of secondary mechanism that can affect cardiac function is acidosis observed during brief ischemic conditions (Dorn and Force 2005).

It has been reported that a decrease in  $\text{Ca}^{2+}$  sensitivity of actomyosin ATPase and force is a protective mechanism that allow the heart to tolerate mild ischemic conditions (Solaro et al., 2002b). Mutations in TnT (particularly, those that affect  $\text{Ca}^{2+}$  sensitivity) could interfere with this natural means of cardio protection from mild ischemia. Hence studying the effect of these mutations in this context could provide valuable insight.

# APPENDICES

# Appendix A

## Antibiotics stock solutions

(Working concentration: 1  $\mu$ L/mL)

**Ampicillin (Amp):** Stock of 100mg/ml

1 g Ampicillin

q.s to 10 ml with sterile ddwater (sddH<sub>2</sub>O)

Filter sterilise using a 0.22 micron unit

Aliquot and stored at -20°C

**Kanamycin (Kan):** Stock of 30mg/ml

0.3 g Kanamycin

q.s to 10 ml with sterile ddwater (sddH<sub>2</sub>O)

Filter sterilise using a 0.22 micron unit

Aliquot and stored at -20°C

**Chloramphenicol (CM):** Stock of 25mg/ml

0.25 g Chloramphenicol

q.s to 10 ml with absolute ethanol

Filter sterilise using a 0.22 micron unit

Aliquot and stored at -20°C

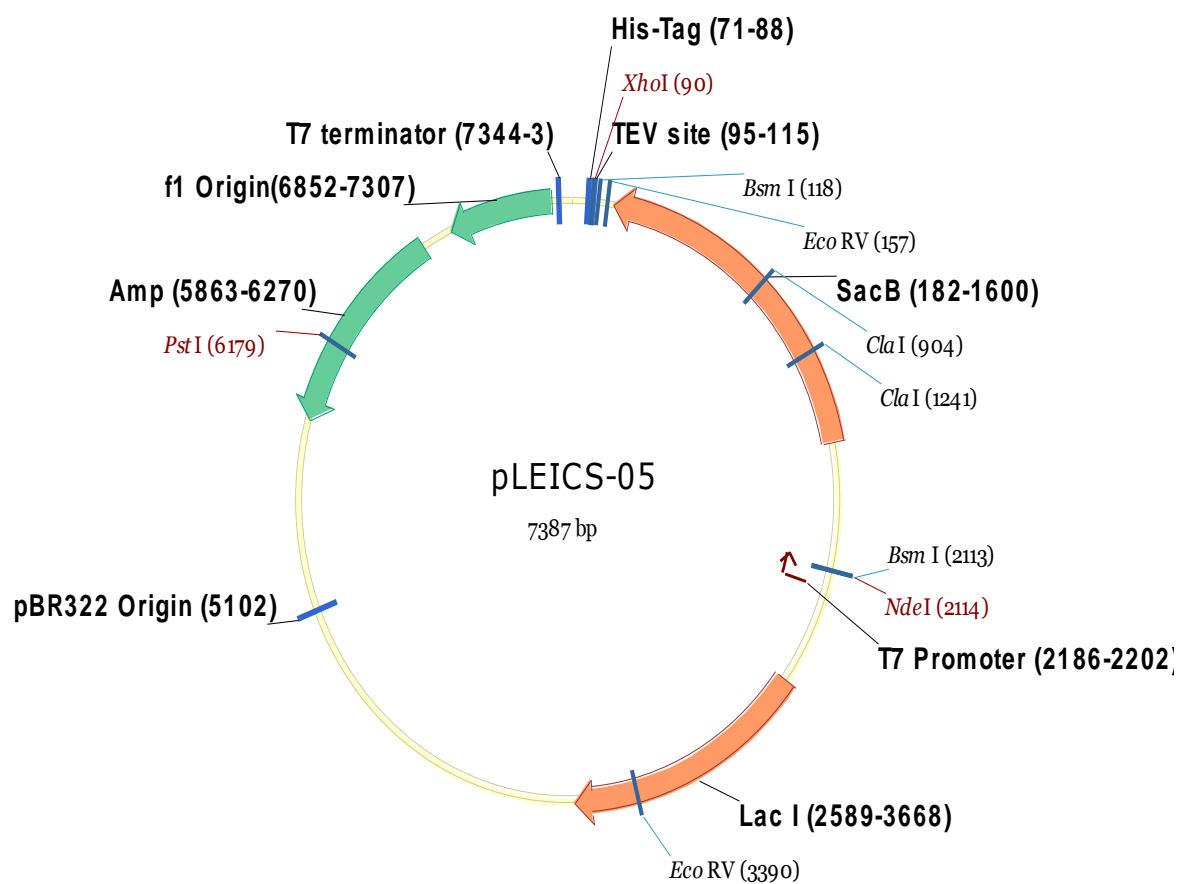
# Appendix B

## Procedure for Gel Preparation using ProtoGel

Reagents used	Volume for 12% Separating Gel (10ml)	Volume of 4% Stacking Gel (10ml)
De-ionised water	3.29	6.1
10% SDS	0.1	0.1
ProtoGel	4.0	1.3
1.5M Tris-HCl, pH 8.8	2.5	-
0.5M Tris-HCl, pH 6.8	-	2.5
10% Ammonium persulphate	0.1	0.05
TEMED	0.01	0.01

# Appendix C

## Expression vector of hcTnT



# Appendix D

## Primer sequences used in cloning WT and mutant TnT

Primer	Primer sequence 5' to 3'
WT	FOR* AGGAGATATACATATGTCTGACATAGAAGAGGTGGTGGGA REV GAAGTACAGGTTCTCTCATTTCAGCGCCCGGTGACTTTA
R141W	FOR CGGGCCGAGCAGCAGCGCATCTGGAATGAGCGGGAGAAGGAGCGG REV CCGCTCCTTCTCCCGCTCATTCCAGATGCGCTGCTGCTCGGCCCG
$\Delta$ K210	FOR CTGAGCGGGAAAAGAAGAAGATTCTGGCTGAGAGGAGGAAGGT REV ACCTTCCTCCTCTCAGCCAGAATCTTCTTCTTTCCCGCTCAG
$\Delta$ E160	FOR GAGAGGGCTCGACGAGAGGAGGAGAACAGGAGG REV CCTCCTGTTCTCCTCCTCTCGTCGAGCCCT TCTTC
S179F	FOR CGGAAGAAGAAGGCTTTGTTCAACATGATGCATTTTGGG REV AAAATGCATCATGTTGAACAAAGCCTTCTTCTT
K273E	FOR AGGATCAACGATAACCAGGAAGTCTCCAAGACCCGCGGG REV CCCGCGGGTCTTGGAGACTTCCTGGTTATCGTTGAT
$\Delta$ 14	REV GAAGTACAGGTTCTCTCAGACTTTCTGGTTATCGTT
$\Delta$ 28+7	REV AAGTACAGGTTCTCTCAGCCTTCGCGCGGATCCTGCAGCTCATATTTCT

For= Forward primer and Rev= reverse primer

# Appendix E

## Significance levels of experiments expressed as p-values

TnT	ATPase Activity		Circular Dichroism			n*	K <sub>B</sub> - Ca <sup>2+</sup> /Actin
	Activation	Inhibition	α-Helical Content TnT	α-Helical Content Tn Complex	Thermal Stability of Tn Complex		
<b>R141W</b>	0.0824	0.7751	0.5786	0.0956	0.4418	6	0.4533
<b>ΔK210</b>	< 0.0001	0.8864	0.7210	0.4367	0.0690	5	0.8026
<b>ΔE160</b>	0.1910	0.7751	< 0.0001	0.0009	0.0064	2	< 0.0001
<b>S179F</b>	0.4774	0.1263	0.6171	0.0668	0.6832	3	< 0.0001
<b>K273E</b>	0.0660	0.7389	0.0033	0.0002	0.0043	3	< 0.0001
<b>Δ14</b>	< 0.0001	0.0020	< 0.0001	0.0014	0.1531	2	< 0.0001
<b>Δ28+7</b>	0.0032	< 0.0001	< 0.0001	0.0038	0.1531	2	< 0.0001

\* The significance of the 'n' parameter data set is based on the repetitive of experimentation, not on as per p-value

### p value range

p value = 0.9999 - 0.1010:	not statistically significant
p value = 0.0989 - 0.0512:	not quite statistically significant
p value = 0.0500 - 0.0102:	statistically significant
p value = 0.0099 - 0.0010:	very statistically significant
p value = > 0.0010:	extremely statistically significant

# REFERENCES

Alahyan, M., M. R. Webb, S. B. Marston and M. El-Mezgueldi. (2006). "The mechanism of smooth muscle caldesmon-tropomyosin inhibition of the elementary steps of the actomyosin ATPase." *J Biol Chem* 281(28): 19433-19448.

Ashrafian, H. and H. Watkins (2007). "Reviews of translational medicine and genomics in cardiovascular disease: new disease taxonomy and therapeutic implications cardiomyopathies: therapeutics based on molecular phenotype." *J Am Coll Cardiol* 49(12): 1251-1264.

Ashrafian, H., C. Redwood, E. Blair and H. Watkins. (2003). "Hypertrophic cardiomyopathy: a paradigm for myocardial energy depletion." *Trends Genet* 19(5): 263-268.

Bacchiocchi, C., P. Graceffa and S. Lehrer(2004). "Myosin-induced movement of alphaalpha, alphabeta, and betabeta smooth muscle tropomyosin on actin observed by multisite FRET." *Biophys J* 86(4): 2295-2307.

Bagshaw, C. R. (1994). "The molecular mechanism of muscle contraction: 40 years after the sliding filament hypothesis. Christ's College, Cambridge, England, 17-21 September 1994." *Journal of Muscle Research and Cell motility* 15(6): 701-702.

Baudenbacher, F., T. Schober, J. R, Pintom V. Y. Sidorov, F. Hilliard, R. J. Solaro, J. D. Potter and B. C. Knollman. (2008). "Myofilament Ca<sup>2+</sup> sensitization causes susceptibility to cardiac arrhythmia in mice." *Journal of Clinical Investigation* 118(12): 3893-3903.

Bers, D. M. (2008). "Calcium cycling and signaling in cardiac myocytes." *Annu Rev Physiol* 70: 23-49.

Bharadwaj, S., S. Hitchcock-DeGregori, A. Thorburn and G. L. Prasad. (2004). "N terminus is essential for tropomyosin functions: N-terminal modification disrupts stress fiber organization and abolishes anti-oncogenic effects of tropomyosin-1." *Journal of Biological Chemistry* 279(14): 14039-14048.

Blumenschein, T. M., B. P. Tripet, R. S. Hodges and B. D Sykes. (2001). "Mapping the interacting regions between troponins T and C. Binding of TnT

and TnI peptides to TnC and NMR mapping of the TnT-binding site on TnC." *Journal of Biological Chemistry* 276(39): 36606-36612.

Bonne, G., L. Carrier, J. Bercovici, C. Cruaud, P. Richard, B. Hainque, M. Gautel, S. Labeit, M. James, J. Beckmann, et al(1995). "Cardiac myosin binding protein-C gene splice acceptor site mutation is associated with familial hypertrophic cardiomyopathy." *Nature Genetics* 11(4): 438-440.

Bonne, G., L. Carrier, P. Richard, B. Hainque and K. Schwartz. . (1998). "Familial hypertrophic cardiomyopathy: from mutations to functional defects." *Circulation Research* 83(6): 580-593.

Bottinelli, R., D. A. Coviello, C. S. Redwood, M. A. Pellegrino, B. J. Maron, P. Spirito, H. Watkins and C. Reggiani. (1998). "A mutant tropomyosin that causes hypertrophic cardiomyopathy is expressed in vivo and associated with an increased calcium sensitivity." *Circulation Research* 82(1): 106-115.

Burton, D., H. Abdulrazzak, A. Knott, K. Elliott, C. Redwood, H. Watkins, S. Marston and C. Ashley. (2002). "Two mutations in troponin I that cause hypertrophic cardiomyopathy have contrasting effects on cardiac muscle contractility." *Biochem J* 362(Pt 2): 443-451.

Cabral-Lilly, D., L. S. Tobacman, J. P. Mehegan, C. Cohen. (1997). "Molecular polarity in tropomyosin-troponin T co-crystals." *Biophys J* **73**(4): 1763-1770.

Chandra, M., V. L. Rundell, J. C. Tardiff, L. A. Leinwand, P. P. De Tomb and R. J. Solaro. (2001). "Ca(2+) activation of myofilaments from transgenic mouse hearts expressing R92Q mutant cardiac troponin T." *Am J Physiol Heart Circ Physiol* 280(2): H705-713.

Chang, A. N., M. S. Parvatiyar and J. D. Potter. (2008). "Troponin and cardiomyopathy." *Biochem Biophys Res Commun* 369(1): 74-81.

Chen, R., T. Tsuji, F. Ichida, K. R. Bowles, X. Yu, S. Watanabe, K. Hirono, S. Tsubata, Y. Hamamichi, J. Ohta, et al. (2002). "Mutation analysis of the G4.5 gene in patients with isolated left ventricular noncompaction." *Mol Genet Metab* 77(4): 319-325

- Cheng, T. O. (2005). "Frequency of cardiac troponin I mutations in families with hypertrophic cardiomyopathy in China." *J Am Coll Cardiol* 46(1): 180-181; author reply 181.
- Cohn, J. N., R. Ferrari and N. Sharpe. (2000). "Cardiac remodeling--concepts and clinical implications: a consensus paper from an international forum on cardiac remodeling. Behalf of an International Forum on Cardiac Remodeling." *J Am Coll Cardiol* 35(3): 569-582.
- Craig, R. and W. Lehman (2001). "Crossbridge and tropomyosin positions observed in native, interacting thick and thin filaments." *J Mol Biol* 311(5): 1027-1036.
- Criddle, A. H., M. A. Geeves and T. Jeffries. (1985). "The use of actin labelled with N-(1-pyrenyl)iodoacetamide to study the interaction of actin with myosin subfragments and troponin/tropomyosin." *Biochemical Journal* 232: 343-349.
- Crilley, J. G., E. A. Boehm, E. Blair, B. Rajagopalan, A. M. Blamire, P. Styles, W. J. McKenna, I. Ostman-Smith, K. Clarke and H. Watkins. (2003). "Hypertrophic cardiomyopathy due to sarcomeric gene mutations is characterized by impaired energy metabolism irrespective of the degree of hypertrophy." *J Am Coll Cardiol* 41(10): 1776-1782.
- Davis, J. P. and S. B. Tikunova (2008). "Ca(2+) exchange with troponin C and cardiac muscle dynamics." *Cardiovascular Research* 77(4): 619-626.
- Davis, J. P., C. Norman, T. Kobayashi, R. J. Solaro, D. R. Swartz and S. B. Tikunova. (2007). "Effects of thin and thick filament proteins on calcium binding and exchange with cardiac troponin C." *Biophys J* 92(9): 3195-3206.
- Dong, W. J., C. K. Wang, A. M. Gordon, S. S. Rosenfeld and H. C. Cheung. (1997). "A kinetic model for the binding of Ca<sup>2+</sup> to the regulatory site of troponin from cardiac muscle." *Journal of Biological Chemistry* 272(31): 19229-19235.
- Dong, W. J., C. K. Wang, A. M. Gordon and H. C. Cheung. (1997). "Disparate fluorescence properties of 2-[4'-(iodoacetamido)anilino]-naphthalene-6-sulfonic acid attached to Cys-84 and Cys-35 of troponin C in cardiac muscle troponin." *Biophys J* 72(2 Pt 1): 850-857.

Dong, W., S. S. Rosenfeld, C. K. Wang, A. M. Gordon and H. C. Cheung. (1996). "Kinetic studies of calcium binding to the regulatory site of troponin C from cardiac muscle." *Journal of Biological Chemistry* 271(2): 688-694.

Doolan, A., M. Tebo, J. Ingles, L. Nguyen, T. Tsoutsman, L. Lam, C. Chiu, J. Chung, R. G. Weintraub and C. Semsarian. (2005). "Cardiac troponin I mutations in Australian families with hypertrophic cardiomyopathy: clinical, genetic and functional consequences." *Journal of Molecular and Cellular Cardiology* 38(2): 387-393.

Dorn, G. W., 2nd and T. Force (2005). "Protein kinase cascades in the regulation of cardiac hypertrophy." *J Clin Invest* 115(3): 527-537.

Dorn, G. W., 2nd, J. Robbins, P. H. Sugden. (2003). "Phenotyping hypertrophy: eschew obfuscation." *Circ Res* 92(11): 1171-1175.

Dyer, E. C., A. M. Jacques, A. C. Hoskins, D. G. Ward, C. E. Gallon, A. E. Messer, J. P. Kaski, M. Burch, J. C. Kentish and S. B. Marston. (2009). "Functional analysis of a unique troponin c mutation, GLY159ASP, that causes familial dilated cardiomyopathy, studied in explanted heart muscle." *Circ Heart Fail* 2(5): 456-464.

Elliott, P. M., L. D'Cruz and W. J. McKenna. (1999). "Late-onset hypertrophic cardiomyopathy caused by a mutation in the cardiac troponin T gene." *New England Journal of Medicine* 341(24): 1855-1856.

Farah, C. S. and F. C. Reinach (1995). "The troponin complex and regulation of muscle contraction." *FASEB J.* 9: 755-767.

Fatkin, D., M. E. Christe, O. Aristizabal, B. K. McConnell, S. Srinivasan, F. J. Schoen, C. E. Seidman, D. H. Turnbull and J. G. Seidman. (1999). "Neonatal cardiomyopathy in mice homozygous for the Arg403Gln mutation in the alpha cardiac myosin heavy chain gene." *Journal of Clinical Investigation* 103(1): 147-153.

Fiset, C. and W. R. Giles (2008). "Cardiac troponin T mutations promote life-threatening arrhythmias." *Journal of Clinical Investigation*.

- Fitzsimons, D. P., J. R. Patel and R. L. Moss. (1998). "Role of myosin heavy chain composition in kinetics of force development and relaxation in rat myocardium." *J Physiol* 513 ( Pt 1): 171-183.
- Fitzsimons, D. P., J. R. Patel and R. L. Moss. (2001). "Cross-bridge interaction kinetics in rat myocardium are accelerated by strong binding of myosin to the thin filament." *J Physiol* 530(Pt 2): 263-272.
- Foth, B. J., M. C. Goedecke and D. Soldati. (2006). "New insights into myosin evolution and classification." *Proc Natl Acad Sci U S A* 103(10): 3681-3686.
- Franz, W. M., M. Muller, O. J. Muller, R. Hermann, T. Rothmann, M. Cremer, R. D. Cohn, T. Voit and H. A. Katus. (2000). "Association of nonsense mutation of dystrophin gene with disruption of sarcoglycan complex in X-linked dilated cardiomyopathy." *Lancet* 355(9217): 1781-1785.
- Franz, W. M., O. J. Muller and H. A. Katus. (2001). "Cardiomyopathies: from genetics to the prospect of treatment." *Lancet* 358(9293): 1627-1637.
- Fraser, I. D. and S. B. Marston (1995). "In vitro motility analysis of actin-tropomyosin regulation by troponin and calcium. The thin filament is switched as a single cooperative unit." *Journal of Biological Chemistry* 270(14): 7836-7841.
- Fujino, N., M. Shimizu, H. Ino, M. Yamaguchi, T. Yasuda, M. Nagata, T. Konno and H. Mabuchi. (2002). "A novel mutation Lys273Glu in the cardiac troponin T gene shows high degree of penetrance and transition from hypertrophic to dilated cardiomyopathy." *American Journal of Cardiology* 89(1): 29-33.
- Geeves, M. A. and D. J. Halsall (1987). "Two step ligand binding and cooperativity. A model to describe the cooperative binding of myosin subfragment 1 to regulated actin." *Biophysical Journal* 52: 215-220.
- Geeves, M. A. and S. S. Lehrer (1994). "Dynamics of the muscle thin filament regulatory switch: the size of the cooperative unit." *Biophys J* 67(1): 273-282.
- Geisterfer-Lowrance, A. A., M. Christe, D. A. Conner, J. S. Ingwall, F. J. Schoen, C. E. Siedman and J. G. Seidman. (1996). "A mouse model of familial hypertrophic cardiomyopathy." *Science* 272(5262): 731-734.

Geisterfer-Lowrance, A. A., S. Kass, G. Tanigawa, H. Vosberg, W. McKenna, C. E. Seidman and J. G. Seidman. (1990). "A molecular basis for familial hypertrophic cardiomyopathy: a beta cardiac myosin heavy chain gene missense mutation." *Cell* 62(5): 999-1006.

Gerull, B., M. Gramlich, J. Atherton, M. McNabb, K. Trombitas, S. Sasse-Klassen, J. G. Seidman, C. Seidman, H. Granzier, S. Labeit, et. al. (2002). "Mutations of TTN, encoding the giant muscle filament titin, cause familial dilated cardiomyopathy." *Nature Genetics* 30(2): 201-204.

Gomes, A. V. and J. D. Potter (2004). "Molecular and cellular aspects of troponin cardiomyopathies." *Ann N Y Acad Sci* 1015: 214-224.

Gomes, A. V., J. Liang and J. D. Potter. (2005). "Mutations in human cardiac troponin I that are associated with restrictive cardiomyopathy affect basal ATPase activity and the calcium sensitivity of force development." *Journal of Biological Chemistry* 280(35): 30909-30915.

Gordon, A. M., E. Homsher and M. Regnier (2000). "Regulation of contraction in striated muscle." *Physiol Rev* 80(2): 853-924.

Grunig, E., J. A. Tasman, H. Kucherer, W. Franz, W. Kubler and H. A. Katus. (1998). "Frequency and phenotypes of familial dilated cardiomyopathy." *J Am Coll Cardiol* 31(1): 186-194.

Gulati, J., A. Babu and H. Su. (1992). "Functional delineation of the Ca(2+)-deficient EF-hand in cardiac muscle, with genetically engineered cardiac-skeletal chimeric troponin C." *Journal of Biological Chemistry* 267(35): 25073-25077.

Gunning, P. W., G. Schevzov, A. J. Kee and E. C Hardeman. (2005). "Tropomyosin isoforms: divining rods for actin cytoskeleton function." *Trends Cell Biol* 15(6): 333-341.

Haim, T. E., C. Dowell, T. Diamanti, J. Scheuer and J. C. Tardiff. (2007). "Independent FHC-related cardiac troponin T mutations exhibit specific alterations in myocellular contractility and calcium kinetics." *J Mol Cell Cardiol* 42(6): 1098-1110.

- Harada, K. and J. D. Potter (2004). "Familial hypertrophic cardiomyopathy mutations from different functional regions of troponin T result in different effects on the pH and Ca<sup>2+</sup> sensitivity of cardiac muscle contraction." *Journal of Biological Chemistry* 279(15): 14488-14495.
- Harada, K., F. Takahashi-Yanaga, M. Reiko, M. Sachio and I. Ohtsuki. (2000). "Functional consequences of the deletion mutation deltaGlu160 in human cardiac troponin T." *J Biochem* 127(2): 263-268.
- Hasenfuss, G., L. Mulieri, B. J. Leavitt, P. D. Allen, J. R. Haerberle and N. R. Alpert. (1992). "Alteration of contractile function and excitation-contraction coupling in dilated cardiomyopathy." *Circulation Research* 70: 1225-1232.
- Head, J. G., M. D. Ritchie and M. A. Geeves. (1995). "Characterisation of the equilibrium between blocked and closed states of muscle thin filaments." *European Journal of Biochemistry* 227: 694-699.
- Hershberger, R. E., S. B. Parks, J. D. Kushner, L. Duanxiang, S. Ludwigsen, P. Jakobs, D. Nauman, D. Burgess, J. Partain and M. Litt. (2008). "Coding sequence mutations identified in MYH7, TNNT2, SCN5A, CSR3, LBD3, and TCAP from 313 patients with familial or idiopathic dilated cardiomyopathy." *Clin Transl Sci* 1(1): 21-26.
- Herzberg, O. and M. N. James (1988). "Refined crystal structure of troponin C from turkey skeletal muscle at 2.0 Å resolution." *J Mol Biol* 203(3): 761-779.
- Hill, L. E., J. P. Mehegan, C. A. Butters and L. S. Tobacman. (1992). "Analysis of troponin-tropomyosin binding to actin. Troponin does not promote interactions between tropomyosin molecules." *Journal of Biological Chemistry* 267(23): 16106-16113.
- Hill, T. L., E. Eisenberg and L. Greene. (1980). "Theoretical model for the cooperative equilibrium binding of myosin subfragment 1 to the actin-troponin-tropomyosin complex." *Proc Natl Acad Sci U S A* 77(6): 3186-3190.
- Hill, T. L., E. Eisenberg and J. M. Chalovich. (1981). "Theoretical models for cooperative steady-state ATPase activity of myosin subfragment-1 on regulated actin." *Biophys J* 35(1): 99-112.

- Hinkle, A., A. Goranson, C. A. Butters and L. S. Tobacman. (1999). "Roles for the troponin tail domain in thin filament assembly and regulation. A deletional study of cardiac troponin T." *J Biol Chem* **274**(11): 7157-7164.
- Ho, C. Y., H. M. Lever, R. DeSanctis, C. F. Farver, J. G. Seidman and C. E. Seidman. (2000). "Homozygous mutation in cardiac troponin T: implications for hypertrophic cardiomyopathy." *Circulation* 102(16): 1950-1955.
- Hoffmann, B., H. Schmidt-Traub, A. Perrot, K. J. Osterzeil and R. Geßner. (2001). "First mutation in cardiac troponin C, L29Q, in a patient with hypertrophic cardiomyopathy." *Hum Mutat* 17(6): 524.
- Holmes, K. C., D. Popp, W. Gebhard and W. Kabsch. (1990). "Atomic model of the actin filament." *Nature* 347: 44-49.
- Homsher, E., B. Kim, A. Bobkova and L. S. Tobacman. (1996). "Calcium regulation of thin filament movement in an in vitro motility assay." *Biophys J* 70(4): 1881-1892.
- Houdusse, A., M. L. Love, R. Dominguez, Z. Grabarek and C. Cohen. (1997). "Structures of four Ca<sup>2+</sup>-bound troponin C at 2.0 Å resolution: further insights into the Ca<sup>2+</sup>-switch in the calmodulin superfamily." *Structure* 5(12): 1695-1711.
- Huxley, H. E. (1958). "The contraction of muscle." *Sci Am* 199(5): 67-72 passim.
- Ichida, F., S. Tsubata, K. R. Bowles, N. Haneda, K. Uese, T. Miyawaki, W. J. Dreyer, J. Messina, H. Li, N. E. Bowles and J. A. Towbin. (2001). "Novel gene mutations in patients with left ventricular noncompaction or Barth syndrome." *Circulation* 103(9): 1256-1263.
- Ischii, Y. and S. S. Lehrer (1987). "Fluorescence probe studies of the state of tropomyosin in reconstituted muscle thin filaments." *Biochemistry* 26: 4922-4925.

- Ishii, Y. and S. S. Lehrer (1990). "Excimer fluorescence of pyrenyliodoacetamide-labeled tropomyosin: a probe of the state of tropomyosin in reconstituted muscle thin filaments." *Biochemistry* 29(5): 1160-1166.
- Kabsch, W., H. G. Mannherz, D. Suck, E. F. Pai and K. C. Holmes (1990). "Atomic structure of actin:DNase I complex." *Nature* 347: 37-44.
- Kamisago, M., S. D. Sharma, S. R. DePalma, S. Solomon, P. Sharma, B. McDonough, L. Smoot, M. P. Mullen, P. K. Woolf, E. D. Wigle, et al (2000). "Mutations in sarcomere protein genes as a cause of dilated cardiomyopathy." *New England Journal of Medicine* 343(23): 1688-1696.
- Kataoka, A., C. Hemmer and P. B. Chase . (2007). "Computational simulation of hypertrophic cardiomyopathy mutations in troponin I: influence of increased myofilament calcium sensitivity on isometric force, ATPase and  $[Ca^{2+}]_i$ ." *J Biomech* 40(9): 2044-2052.
- Keeling, P. J., Y. Gang, H. Seo, S. E. Bent, V. Murday, A. L. P. Caforio and W. J. McKenna (1995). "Familial dilated cardiomyopathy in the United Kingdom." *Br Heart J* 73(5): 417-421.
- Kimura, A., H. Harada, J. Park, H. Nishi, M. Satoh, M. Takahashi, S. Hiroi, T. Sasaoka, N. Ohbuchi, T. Nakamura, et al. (1997). "Mutations in the cardiac troponin I gene associated with hypertrophic cardiomyopathy." *Nature Genetics* 16(4): 379-382.
- Klabunde, R.E. (2005). "Electrical activity of the heart". *Cardiovascular physiology concepts* . Lippincott Williams & Wilkins. ISBN 0-7817-5030-X.
- Knollmann, B. C., P. Kirchhof, S. G. Sirenko, H. Degen, A. E. Greene, T. Schober, J. C Mackow, L. Fabritz, J. D Potter and M, Morad (2003). "Familial hypertrophic cardiomyopathy-linked mutant troponin T causes stress-induced ventricular tachycardia and  $Ca^{2+}$ -dependent action potential remodeling." *Circulation Research* 92(4): 428-436.
- Kobayashi, T. and R. J. Solaro (2005). "Calcium, thin filaments, and the integrative biology of cardiac contractility." *Annu Rev Physiol* 67: 39-67.

- Kobayashi, T. and R. J. Solaro (2006). "Increased Ca<sup>2+</sup> affinity of cardiac thin filaments reconstituted with cardiomyopathy-related mutant cardiac troponin I." *Journal of Biological Chemistry* 281(19): 13471-13477.
- Kobayashi, T., L. Jin and P. P. de Tombe. (2008). "Cardiac thin filament regulation." *Pflugers Arch* 457(1): 37-46.
- Kobayashi, T., W. J. Dong, E. M. Burkart, H. C Cheung and R. J. Solaro. (2004). "Effects of protein kinase C dependent phosphorylation and a familial hypertrophic cardiomyopathy-related mutation of cardiac troponin I on structural transition of troponin C and myofilament activation." *Biochemistry* 43(20): 5996-6004.
- Kouyama, T. and K. Mihashi (1981). "Fluorimetry study of N-(1-pyrenyl)iodoacetamide-labelled F-actin. Local structural change of actin protomer both on polymerization and on binding of heavy meromyosin." *Eur J Biochem* 114(1): 33-38.
- Laemmli, U. K. (1970). "Cleavage of structural proteins during the assembly of the head of bacteriophage T4." *Nature* 227: 680-685.
- Lehman, W., V. Hatch, V. Korman, M. Rosol, L. Thomas, R. Maytum, M. A. Geeves, J. E. Van Eyk, L. S. Tobacman and R. Craig. (2000). "Tropomyosin and actin isoforms modulate the localization of tropomyosin strands on actin filaments." *J Mol Biol* 302(3): 593-606.
- Lehrer, S. S., N. L. Golitsina and M. A. Geeves. (1997). "Actin-tropomyosin activation of myosin subfragment 1 ATPase and thin filament cooperativity. The role of tropomyosin flexibility and end-to-end interactions." *Biochemistry* 36(44): 13449-13454.
- Lehrer, S. S. and M. A. Geeves (1998). "The muscle thin filament as a classical cooperative/allosteric regulatory system." *J. Mol. Biol.* 277: 1081-1089.
- Li, D., G. Z. Czernuszewicz, O Gonzalez, T. Tapscott, A. Karibe, J. Durand, R. Brugada, R. Hill, J. M. Gregoritch, J. L. Anderson, et al. (2001). "Novel cardiac troponin T mutation as a cause of familial dilated cardiomyopathy." *Circulation* 104(18): 2188-2193.

- Li, M. X., S. M. Gagne, S. Tsuda, C. M. Kay, L. B. Smillie and B. D. Sykes. (1995). "Calcium binding to the regulatory N-domain of skeletal muscle troponin C occurs in a stepwise manner." *Biochemistry* 34(26): 8330-8340.
- Li, M. X., X. Wang, D. A. Lindhout, N. Buscemi, J. E. Van Eyk and B. D. Sykes. (2003). "Phosphorylation and mutation of human cardiac troponin I differentially destabilize the interaction of the functional regions of troponin I with troponin C." *Biochemistry* 42(49): 14460-14468.
- Li, M. X., X. Wang and B. D. Sykes. (2004). "Structural based insights into the role of troponin in cardiac muscle pathophysiology." *Journal of Muscle Research and Cell motility* 25(7): 559-579.
- Li, Y., S. Mui, J. H. Brown, J. Strand, L. Reshetnikova, L. S. Tobacman and C. Cohen. (2002). "The crystal structure of the C-terminal fragment of striated-muscle alpha-tropomyosin reveals a key troponin T recognition site." *Proc Natl Acad Sci U S A* 99(11): 7378-7383.
- Lohmann, K., B. Westerdorf, R. Maytum, M. A. Geeves and K. Jaquet. (2001). "Overexpression of human cardiac troponin in Escherichia coli: its purification and characterization." *Protein Expr Purif* 21(1): 49-59.
- Lombardi, R., A. Bell, V. Senthil, J. Sidhu, M. Nosedà, R. Roberts and A. J. Marian. (2008). "Differential interactions of thin filament proteins in two cardiac troponin T mouse models of hypertrophic and dilated cardiomyopathies." *Cardiovascular Research* 79(1): 109-117.
- Lowry, O. H., N. J. Rosebrough, A. L. Farr and R. J. Randall. (1951). "Protein measurements with Folin phenol reagent." *J.Biol.Chem.* 193: 265-275.
- Lu, Q. W., S. Morimoto, K. Harada, C-K. Du, F. Takahashi-Yanaga, Y. Miwa, T. Sasaguri and I. Ohtsuki. (2003). "Cardiac troponin T mutation R141W found in dilated cardiomyopathy stabilizes the troponin T-tropomyosin interaction and causes a Ca<sup>2+</sup> desensitization." *Journal of Molecular and Cellular Cardiology* 35(12): 1421-1427.
- M. EL-Mezgueldi & C.R. Bagshaw. (2008) "The Myosin Family: Biochemical

and kinetic properties." In *Myosins: a superfamily of molecular motors* (ed. Colluccio, L.M.) Springer, pp 55-93.

MacLachlan, L. K., D. G. Reid, R. C Mitchell, C. J. Salter and S. J. Smith. (1990). "Binding of a calcium sensitizer, bepridil, to cardiac troponin C. A fluorescence stopped-flow kinetic, circular dichroism, and proton nuclear magnetic resonance study." *Journal of Biological Chemistry* 265(17): 9764-9770.

MacLean-Fletcher, S. and T. D. Pollard (1980). "Identification of a factor in conventional muscle actin preparations which inhibits actin filament self-association." *Biochem Biophys Res Commun* 96(1): 18-27.

Malnic, B., C. S. Farah and F. C Reinach. (1998). "Regulatory properties of the NH<sub>2</sub>- and COOH-terminal domains of troponin T. ATPase activation and binding to troponin I and troponin C." *Journal of Biological Chemistry* 273(17): 10594-10601.

Margossian, S. S. and S. Lowey (1982). "Preparation of myosin and its subfragments from rabbit skeletal muscle." *Methods Enzymol* 85 Pt B: 55-71.

Marian, A. J., G. Zhao, Y. Seta, R. Roberts and Q. Yu. (1997). "Expression of a mutant (Arg92Gln) human cardiac troponin T, known to cause hypertrophic cardiomyopathy, impairs adult cardiac myocyte contractility." *Circulation Research* 81(1): 76-85.

Maron, B. J., W. C. Roberts, H. A. McAllister, D. R. Rosing and S. E. Epstein. (1980). "Sudden death in young athletes." *Circulation* 62(2): 218-229.

Maytum, R., B. Westerdorf, K. Jaquet and M. A. Geeves. (2003). "Differential regulation of the actomyosin interaction by skeletal and cardiac troponin isoforms." *Journal of Biological Chemistry* 278(9): 6696-6701.

Maytum, R., M. Konrad, S. S. Lehrer and M. A. Geeves. (2001). "Regulatory properties of tropomyosin effects of length, isoform, and N-terminal sequence." *Biochemistry* 40(24): 7334-7341.

- Maytum, R., S. S. Lehrer and M. A. Geeves. (1999). "Cooperativity and switching within the three-state model of muscle regulation." *Biochemistry* 38(3): 1102-1110.
- McConnell, B. K., K. A. Jones, D. Fatkin, L. H. Arroyo, R. T. Lee, O. Aristizabal, D. H. Turnbull, D. Georgakopoulos, D. Kass, M. Bond, et al. (1999). "Dilated cardiomyopathy in homozygous myosin-binding protein-C mutant mice." *Journal of Clinical Investigation* 104(9): 1235-1244.
- McKenna, W. J. and A. J. Camm (1989). "Sudden death in hypertrophic cardiomyopathy. Assessment of patients at high risk." *Circulation* 80(5): 1489-1492.
- McKillop, D. F. A. and M. A. Geeves (1993). "Regulation of the interaction between actin and myosin subfragment-1: evidence for three states of the thin filament." *Biophys.J.* 65: 693-701.
- Mesnard, L., D. Logeart, S. Taviaux, S. Diriong, J. J. Mercadier and F. Samson (1995). "Human cardiac troponin T: cloning and expression of new isoforms in the normal and failing heart." *Circulation Research* 76(4): 687-692.
- Mestroni, L., C. Rocco, D. Gregori, D. Sinagra, A. Di Lenarda, S. Miocic, M. Vatta, B. Pinamonti, F. Muntoni, A. L. P. Caforio, et al. (1999). "Familial dilated cardiomyopathy: evidence for genetic and phenotypic heterogeneity. Heart Muscle Disease Study Group." *J Am Coll Cardiol* 34(1): 181-190.
- Michels, V. V., P. P. Moll, F. A. Miller, A. J. Tajik, J. S. Chu, D. J. Driscoll, J. C. Burnett, R. J. Rodeheffer, J. H. Chesebro and H. D. Tazelaar. (1992). "The frequency of familial dilated cardiomyopathy in a series of patients with idiopathic dilated cardiomyopathy." *New England Journal of Medicine* 326(2): 77-82.
- Miki, M., H. Hai, K. Saeki, Y. Shitaka, K-I. Sano, Y. Maeda and T. Wakabayashi. (2004). "Fluorescence resonance energy transfer between points on actin and the C-terminal region of tropomyosin in skeletal muscle thin filaments." *J Biochem* 136(1): 39-47.

Miles, A. J. and B. A. Wallace (2006). "Synchrotron radiation circular dichroism spectroscopy of proteins and applications in structural and functional genomics." *Chem Soc Rev* 35(1): 39-51.

Miller, T., D. Szczesna, P. R. Housmans, J. Zhao, F. de Freitas, A. V. Gomes, L. Culbreath, J. McCue, Y. Wang, Y. Xu, et al. (2001). "Abnormal contractile function in transgenic mice expressing a familial hypertrophic cardiomyopathy-linked troponin T (I79N) mutation." *Journal of Biological Chemistry* 276(6): 3743-3755.

Mirza, M., S. Marston, R. Willott, C. Ashley, J. Mogensen, W. McKenna, P. Robinson, C. Redwood and H. Watkins. (2005). "Dilated cardiomyopathy mutations in three thin filament regulatory proteins result in a common functional phenotype." *Journal of Biological Chemistry* 280(31): 28498-28506.

Mogensen, J., A. Bahl, T. Kubo, N. Elanko, R. Taylor and W. J. McKenna. (2003). "Comparison of fluorescent SSCP and denaturing HPLC analysis with direct sequencing for mutation screening in hypertrophic cardiomyopathy." *J Med Genet* 40(5): e59.

Mogensen, J., I. C. Klausen, A. K. Pedersen, H. Egeblad, P. Bross, T. A. Kruse, N. Gregersen, P. S. Hansen, U. Baandrup and A. D. Borglum. (1999). "Alpha-cardiac actin is a novel disease gene in familial hypertrophic cardiomyopathy." *Journal of Clinical Investigation* 103(10): R39-43.

Mogensen, J., R. T. Murphy, T. Shaw, A. Bahl, C. Redwood, H. Watkins, M. Burke, P. M. Elliott and W. J. McKenna. (2004). "Severe disease expression of cardiac troponin C and T mutations in patients with idiopathic dilated cardiomyopathy." *J Am Coll Cardiol* 44(10): 2033-2040.

Montgomery, D. E., J. C. Tardiff and M. Chandra. (2001). "Cardiac troponin T mutations: correlation between the type of mutation and the nature of myofilament dysfunction in transgenic mice." *J Physiol* 536(Pt 2): 583-592.

Moolman, J. C., V. A. Corfield, B. Posen, K. Ngumbela, C. Seidman, P. A Brink, H. Watkins. (1997). "Sudden death due to troponin T mutations." *J Am Coll Cardiol* 29(3): 549-555.

Morimoto, S. (2008). "Sarcomeric proteins and inherited cardiomyopathies." *Cardiovascular Research* 77(4): 659-666.

Morimoto, S., F. Yanaga, R. Minakami and I. Ohtsuki. (1998). "Ca<sup>2+</sup>-sensitizing effects of the mutations at Ile-79 and Arg-92 of troponin T in hypertrophic cardiomyopathy." *American Journal of Physiology* 275(1 Pt 1): C200-207.

Morimoto, S., H. Nakaura, F. Yanaga and I. Ohtsuki.(1999). "Functional consequences of a carboxyl terminal missense mutation Arg278Cys in human cardiac troponin T." *Biochem Biophys Res Commun* 261(1): 79-82.

Morimoto, S., Q. W. Lu, K. Harada, F. Takahashi-Yanaga, R. Minakami, M. Ohta, T. Sasaguri, I. Ohtsuki. (2002). "Ca(2+)-desensitizing effect of a deletion mutation Delta K210 in cardiac troponin T that causes familial dilated cardiomyopathy." *Proc Natl Acad Sci U S A* 99(2): 913-918.

Moss, R. L. (1992). "Ca<sup>2+</sup> regulation of mechanical properties of striated muscle. Mechanistic studies using extraction and replacement of regulatory proteins." *Circ Res* 70(5): 865-884

Mukherjea, P., L. Tong, J. G. Seidman, C. E. Seidman and S. E. Hitchcock-DeGregori. (1999). "Altered regulatory function of two familial hypertrophic cardiomyopathy troponin T mutants." *Biochemistry* 38(40): 13296-13301.

Murakami, K., M. Stewart, K. Nozawa, K. Tomii, H. Kudou, N. Igarashi, Y. Shirakihara, S. Wakatsuki, T. Yasunaga and T. Wakayabashi. (2008). "Structural basis for tropomyosin overlap in thin (actin) filaments and the generation of a molecular swivel by troponin-T." *Proc Natl Acad Sci U S A* 105(20): 7200-7205.

Nakajima-Taniguchi, C., H. Matsui, S. Nagata, T. Kishimoto and K. Yamauchi-Takahara. (1995). "Novel missense mutation in alpha-tropomyosin gene found in Japanese patients with hypertrophic cardiomyopathy." *Journal of Molecular and Cellular Cardiology* 27(9): 2053-2058.

Nakaura, H., S. Morimoto, F. Yanaga, M. Nakata, H. Nishi, T. Imaizumi and I. Ohtsuki. (1999). "Functional changes in troponin T by a splice donor site

mutation that causes hypertrophic cardiomyopathy." *American Journal of Physiology* 277(2 Pt 1): C225-232.

Ohtsuki, I. and S. Morimoto (2008). "Troponin: regulatory function and disorders." *Biochem Biophys Res Commun* 369(1): 62-73.

Oleszczuk, M., I. M. Robertson, M. X. Li and B. D. Sykes. (2010). "Solution structure of the regulatory domain of human cardiac troponin C in complex with the switch region of cardiac troponin I and W7: the basis of W7 as an inhibitor of cardiac muscle contraction." *Journal of Molecular and Cellular Cardiology* 48(5): 925-933.

Olson, T. M., N. Y. Kishimoto, F. G. Whitby and V. V. Michels. (2001). "Mutations that alter the surface charge of alpha-tropomyosin are associated with dilated cardiomyopathy." *Journal of Molecular and Cellular Cardiology* 33(4): 723-732.

Olson, T. M., V. V. Michels, S. N. Thibodeau, Y-S. Tai and M. T. Keating. (1998). "Actin mutations in dilated cardiomyopathy, a heritable form of heart failure." *Science* 280(5364): 750-752.

Opie, L. H., P. J. Commerford, B. J. Gersh and M. A. Pfeffer. (2006). "Controversies in ventricular remodelling." *Lancet* 367(9507): 356-367.

Otterbein, L. R., P. Graceffa and R. Dominquez. (2001). "The crystal structure of uncomplexed actin in the ADP state." *Science* 293(5530): 708-711.

Pan, B. S. and R. J. Solaro (1987). "Calcium-binding properties of troponin C in detergent-skinned heart muscle fibers." *Journal of Biological Chemistry* 262(16): 7839-7849.

Pearlstone, J. R. and L. B. Smillie (1983). "Effects of troponin-I plus-C on the binding of troponin-T and its fragments to alpha-tropomyosin. Ca<sup>2+</sup> sensitivity and cooperativity." *Journal of Biological Chemistry* 258(4): 2534-2542.

Pearlstone, J. R., M. R. Carpenter, P. Johnson and L. B. Smillie . (1976). "Amino-acid sequence of tropomyosin-binding component of rabbit skeletal muscle troponin." *Proc Natl Acad Sci U S A* 73(6): 1902-1906.

Perry, S. V. (1998). "Troponin T: genetics, properties and function." *Journal of Muscle Research and Cell motility* 19(6): 575-602.

Poetter, K., H. Jiang, S. Hassanzadeh, S. R. Master, A. Chang, M. C. Dalakas, I. Rayment, J. R. Sellers, L. Fananapazir and N. D. Epstein. (1996). "Mutations in either the essential or regulatory light chains of myosin are associated with a rare myopathy in human heart and skeletal muscle." *Nature Genetics* 13(1): 63-69.

Pollard, T. D. (1990). "Actin." *Curr Opin Cell Biol* 2(1): 33-40.

Potter, J. D. (1982). "Preparation of troponin and its subunits." *Methods in Enzymology*. 85: 241-263.

Potter, J. D., Z. Sheng, B-S. Pan and J. Zhao. (1995). "A direct regulatory role for troponin T and a dual role for troponin C in the Ca<sup>2+</sup> regulation of muscle contraction." *Journal of Biological Chemistry* 270(6): 2557-2562.

Purcell, I. F., W. Bing, S. B. Marston. (1999). "Functional analysis of human cardiac troponin by the in vitro motility assay: comparison of adult, foetal and failing hearts." *Cardiovascular Research* 43(4): 884-891.

Putkey, J. A., W. Liu, S. Ahmed, M. Zhang, J. D. Potter and W. G. L. Kerrick. (1997). "Fluorescent probes attached to Cys 35 or Cys 84 in cardiac troponin C are differentially sensitive to Ca<sup>2+</sup>-dependent events in vitro and in situ." *Biochemistry* 36(4): 970-978.

Rayment, I., W. R. Rypniewski, K. Schmidt-Base, R. Smith, D. R. Tomchick, M. M. Benning, D. A. Winkelmann, G. Wesenberg and H. M. Holden. (1993). "Three-dimensional structure of myosin subfragment-1: a molecular motor." *Science* 261(5117): 50-58.

Redwood CS, Moolman-Smook JC, Watkins H. Properties of mutant contractile proteins that cause hypertrophic cardiomyopathy. *Res* 1999;44:20 – 36. *Cardiovasc*

Redwood, C., K. Lohmann, W. Bing, G. M. Esposito, K. Elliott, H. Abdulrazzak, A. Knott, I. Purcell, S. Marston and H. Watkins. (2000). "Investigation of a

truncated cardiac troponin T that causes familial hypertrophic cardiomyopathy: Ca(2+) regulatory properties of reconstituted thin filaments depend on the ratio of mutant to wild-type protein." *Circulation Research* 86(11): 1146-1152.

Reiffert, S. U., K. Jaquet, L. M. G. Heilmeyer Jr, M. D. Ritchie and M. A. Geeves. (1996). "Bisphosphorylation of cardiac troponin I modulates the Ca(2+)-dependent binding of myosin subfragment S1 to reconstituted thin filaments." *FEBS Lett* 384(1): 43-47.

Reiffert, S., R. Maytum, M. Geeves, K. Lohmann, T. Greis, M. Bluggel, H. E Meyer, L. M. G. Heilmeyer and K. Jaquet. (1999). "Characterization of the cardiac holotroponin complex reconstituted from native cardiac troponin T and recombinant I and C." *Eur J Biochem* 261(1): 40-47.

Richard, P., P. Charron, L. Carrier, C. Ledeuil, T. Cheav, C. Pichereau, A. Benaiche, R. Isnard, O. Dubourg, M. Burban. (2003). "Hypertrophic cardiomyopathy: distribution of disease genes, spectrum of mutations, and implications for a molecular diagnosis strategy." *Circulation* 107(17): 2227-2232.

Richardson, P., W. McKenna, M. Bristow, B. Maisch, B. Mautner, J. O'Connell, E. Olsen, G. Thiene, J. Goodwin, I. Gyarfaz, et al (1996). "Report of the 1995 World Health Organization/International Society and Federation of Cardiology Task Force on the Definition and Classification of cardiomyopathies." *Circulation* 93(5): 841-842.

Robinson, P., M. Mirza, A. Knott, H. Abdulrazzak, R. Willott, S. Marston, H. Watkins and C. Redwood. (2002). "Alterations in thin filament regulation induced by a human cardiac troponin T mutant that causes dilated cardiomyopathy are distinct from those induced by troponin T mutants that cause hypertrophic cardiomyopathy." *Journal of Biological Chemistry* 277(43): 40710-40716.

Robinson, P., P. J. Griffiths, H. Watkins and C. S. Redwood. (2007). "Dilated and hypertrophic cardiomyopathy mutations in troponin and alpha-tropomyosin have opposing effects on the calcium affinity of cardiac thin filaments." *Circulation Research* 101(12): 1266-1273.

Rosenfeld, S. S. and E. W. Taylor (1985). "Kinetic studies of calcium binding to regulatory complexes from skeletal muscle." *Journal of Biological Chemistry* 260(1): 252-261.

Rust, E. M., F. P. Albayya, and J. M. Metzger(1999). "Identification of a contractile deficit in adult cardiac myocytes expressing hypertrophic cardiomyopathy-associated mutant troponin T proteins." *Journal of Clinical Investigation* 103(10): 1459-1467.

Sadayappan, S., N. Finley, J. W. Howarth, H. Osinka, R. Klevitsky, J. N. Lorenz, P. R. Rosevear and J. Robbins. (2008). "Role of the acidic N' region of cardiac troponin I in regulating myocardial function." *Faseb J* 22(4): 1246-1257.

Satoh, M., M. Takahashi, T. Sakamoto, M. Hiroe, F. Marumo and A. Kimura. (1999). "Structural analysis of the titin gene in hypertrophic cardiomyopathy: identification of a novel disease gene." *Biochem Biophys Res Commun* 262(2): 411-417.

Schaertl, S., S. S. Lehrer and M. A. Geeves. (1995). "Separation and characterization of the two functional regions of troponin involved in muscle thin filament regulation." *Biochemistry* 34(49): 15890-15894.

Seidman, J. G. and C. Seidman (2001). "The genetic basis for cardiomyopathy: from mutation identification to mechanistic paradigms." *Cell* 104(4): 557-567.

Sfichi-Duke, L., M. L. Garcia-Cazarin, C. A. Sumandea, G. A. Sievert, W. Balke, D. Zhan, S. Morimoto and M. P. Sumandea. (2010). "Cardiomyopathy-causing deletion K210 in cardiac troponin T alters phosphorylation propensity of sarcomeric proteins." *J Mol Cell Cardiol* 48(5): 934-942.

Sheng, H. Z., Q. J. Shan, X. Wu and K. J. Cao. (2008). "[Cardiac troponin I gene mutation (Asp127Tyr) in a Chinese patient with hypertrophic cardiomyopathy]." *Zhonghua Xin Xue Guan Bing Za Zhi* 36(12): 1063-1065.

Shimizu, M., H. Ino, T. Yasuda, N. Fujino, K. Uchiyama, T. Mabuchi, T. Konno, T. Kaneda, T. Fujita, E. Masuta, et al. (2005). "Gene mutations in adult Japanese patients with dilated cardiomyopathy." *Circ J* 69(2): 150-153.

Sia, S. K., M. X. Li, L. Spyrapopolous, S. M. Gagne, W. Liu, J. A. Putley and B. D. Sykes. (1997). "Structure of cardiac muscle troponin C unexpectedly reveals a closed regulatory domain." *Journal of Biological Chemistry* 272(29): 18216-18221.

Sin, I. L., R. Fernandes and D. Mercola. (1978). "Direct identification of the high and low affinity calcium binding sites of troponin-C." *Biochem Biophys Res Commun* 82(4): 1132-1139.

Sleep, J. A. and R. L. Hutton (1978). "Actin mediated release of ATP from a myosin-ATP complex." *Biochemistry* 17(25): 5423-5430.

Slupsky, C. M. and B. D. Sykes (1995). "NMR solution structure of calcium-saturated skeletal muscle troponin C." *Biochemistry* 34(49): 15953-15964.

Solaro, R.J., B.M. Wolska, G. Arteaga, A. F. Martin, P. Buttrick and P. de Tombe . (2002b), "Modulation of Thin Filament Activity in Long and Short term regulation of Cardiac Function", *Molecular Control Mechanisms in Striated Muscle Contraction*, R.J.Solaro, R.L.Moss, eds, Kluwer Academic Publishers, Netherlands, pp 291-327.

Solaro, R. J. (2007). "Translational medicine with a capital T, troponin T, that is." *Circulation Research* 101(2): 114-115.

Solaro, R. J. and H. M. Rarick (1998). "Troponin and tropomyosin: proteins that switch on and tune in the activity of cardiac myofilaments." *Circulation Research* 83(5): 471-480.

Solaro, R. J., J. Varghese, A. J. Marian and M. Chandra. (2002). "Molecular mechanisms of cardiac myofilament activation: modulation by pH and a troponin T mutant R92Q." *Basic Res Cardiol* 97 Suppl 1: I102-110.

Solaro, R. J., P. Rosevear and T. Kobayashi. (2008). "The unique functions of cardiac troponin I in the control of cardiac muscle contraction and relaxation." *Biochem Biophys Res Commun* 369(1): 82-87.

- Spudich, J. A. (1994). "How molecular motors work." *Nature* 372(6506): 515-518.
- Spudich, J. A. and S. Watt (1971). "The regulation of rabbit skeletal muscle contraction." *Journal of Biological Chemistry* 246: 4866-4871.
- Squire, J. M. and E. P. Morris (1998). "A new look at thin filament regulation in vertebrate skeletal muscle." *FASEB Journal* 12: 761-771.
- Stehle, R., B. Iorga and G. Pfitzer. (2007). "Calcium regulation of troponin and its role in the dynamics of contraction and relaxation." *Am J Physiol Regul Integr Comp Physiol* 292(3): R1125-1128.
- Sumandea, M. P., W. G. Pyle, T. Kobayashi, P. de Tombe and R. J. Solaro. (2003). "Identification of a functionally critical protein kinase C phosphorylation residue of cardiac troponin T." *J Biol Chem* 278(37): 35135-35144.
- Suomalainen, A., A. Paetau, H. Leinonen, A. Majander, P. Peltonen and H. Somer. (1992). "Inherited idiopathic dilated cardiomyopathy with multiple deletions of mitochondrial DNA." *Lancet* **340**(8831): 1319-1320.
- Sweeney, H. L., A. J. Straceski, L. A. Leinwand, B. A. Tikunov and L. Faust. (1994). "Heterologous expression of a cardiomyopathic myosin that is defective in its actin interaction." *J Biol Chem* 269(3): 1603-1605.
- Sweeney, H. L., H. S. Feng, Z. Yang and H. Watkins. (1998). "Functional analyses of troponin T mutations that cause hypertrophic cardiomyopathy: insights into disease pathogenesis and troponin function." *Proc Natl Acad Sci U S A* 95(24): 14406-14410.
- Szczesna, D., R. Zhang, J. Zhao, M. Jones, G. Guzman and J. D. Potter. (2000). "Altered regulation of cardiac muscle contraction by troponin T mutations that cause familial hypertrophic cardiomyopathy." *Journal of Biological Chemistry* 275(1): 624-630.
- Takeda, S., A. Yamashita, K. Maeda and Y. Maeda. (2003). "Structure of the core domain of human cardiac troponin in the Ca(2+)-saturated form." *Nature* 424(6944): 35-41.

- Tardiff, J. C., S. M. Factor, B. D. Tompkins, T. E. Hewett, B. M. Palmer, R. L. Moore, S. Schwartz, J. Robbins and L. A. Leinwand. (1998). "A truncated cardiac troponin T molecule in transgenic mice suggests multiple cellular mechanisms for familial hypertrophic cardiomyopathy." *J Clin Invest* 101(12): 2800-2811.
- Tardiff, J. C., T. E. Hewett, B. D. Palmer, C. Olsson, S. M. Factor, R. L. Moore, J. Robbins and L. A. Leinwand . (1999). "Cardiac troponin T mutations result in allele-specific phenotypes in a mouse model for hypertrophic cardiomyopathy." *Journal of Clinical Investigation* 104(4): 469-481.
- Tausky, H. H. and E. Schorr (1953). "A microscopic method for the determination of inorganic phosphorus." *J. Biol. Chem.* 202: 675-685.
- Taylor, E. W. and R. W. Lymn (1972). "Enzyme kinetics and the mechanism of muscle contraction." *Muscle Biol* 1: 47-69.
- Teare, D. (1958). "Asymmetrical hypertrophy of the heart in young adults." *Br Heart J* 20(1): 1-8.
- Thierfelder, L., C. MacRae, H. Watkins, J. Tomfohrde, M. Williams, W. McKenna, K. Bohm, G. Noeske, M. Schlepper, A. Bowcock, et al. (1993). "A familial hypertrophic cardiomyopathy locus maps to chromosome 15q2." *Proc Natl Acad Sci U S A* 90(13): 6270-6274.
- Thierfelder, L., H. Watkins, C. McRae, R. Lamas, W. McKenna, H-P. Vosberg, J. G. Seidman and C. E. Seidman (1994). "Alpha-tropomyosin and cardiac troponin T mutations cause familial hypertrophic cardiomyopathy: a disease of the sarcomere." *Cell* 77(5): 701-712.
- Tobacman, L. S. (1996). "Thin filament-mediated regulation of cardiac contraction." *Annu Rev Physiol* 58: 447-481.
- Tobacman, L. S., D. Lin, C. Butters, C. Landis, N. Back, D. Pavlovi and E. Homsher. (1999). "Functional consequences of troponin T mutations found in hypertrophic cardiomyopathy." *Journal of Biological Chemistry* 274(40): 28363-28370.

- Tobacman, L. S., M. Nihli, C. Butters, M. Heller, V. Hatch, R. Craig, W. Lehman and E. Homsher. (2002). "The troponin tail domain promotes a conformational state of the thin filament that suppresses myosin activity." *Journal of Biological Chemistry* 277(31): 27636-27642.
- Torricelli, F., F. Girolami, I. Olivetto, L. Passerini, S. Frusconi, D. Vargiu, P. Richard and F. Cecchi. (2003). "Prevalence and clinical profile of troponin T mutations among patients with hypertrophic cardiomyopathy in tuscan." *American Journal of Cardiology* 92(11): 1358-1362.
- Towbin, J. A. and N. E. Bowles (2002). "The failing heart." *Nature* 415(6868): 227-233.
- Trybus, K. M. and E. W. Taylor (1980). "Kinetic studies of the cooperative binding of subfragment 1 to regulated actin." *Proc Natl Acad Sci U S A* 77(12): 7209-7213.
- Tsien, R. Y. 1983. Intracellular measurement of ion activities, *Annu. Rev. Biophys. Bioeng.* 12:91-116.
- Van Driest, S. L., V. C. Vasile, S. R. Ommen, M. L. Will, A. J. Tajik, B. J. Gersh, and M. J. Ackerman. (2004). "Myosin binding protein C mutations and compound heterozygosity in hypertrophic cardiomyopathy." *J Am Coll Cardiol* 44(9): 1903-1910.
- Varnava, A. M., P. M. Elliott, C. Baboonian, F. Davison, M. J. Davies and W. J. McKenna. (2001). "Hypertrophic cardiomyopathy: histopathological features of sudden death in cardiac troponin T disease." *Circulation* 104(12): 1380-1384.
- Varnava, A., C. Baboonian, F. Davison, L. de Cruz, P. M. Elliott, M. J. Davies and W. J. McKenna. (1999). "A new mutation of the cardiac troponin T gene causing familial hypertrophic cardiomyopathy without left ventricular hypertrophy." *Heart* 82(5): 621-624.
- Venkatraman, G., K. Harada, A. V. Gomes, W. G. L. Kerrick and J. D. Potter. (2003). "Different functional properties of troponin T mutants that cause dilated cardiomyopathy." *Journal of Biological Chemistry* 278(43): 41670-41676.

- Vikstrom, K. L. and L. A. Leinwand (1996). "Contractile protein mutations and heart disease." *Curr Opin Cell Biol* 8(1): 97-105.
- Vinogradova, M. V., D. B. Stone, G. G. Malanina, C. Karatzaferi, R. Cooke, R. A. Mendelson and R. J. Fletterick. (2005). "Ca(2+)-regulated structural changes in troponin." *Proc Natl Acad Sci U S A* 102(14): 5038-5043.
- Wang, Y. P. and F. Fuchs (1994). "Length, force, and Ca(2+)-troponin C affinity in cardiac and slow skeletal muscle." *American Journal of Physiology* 266(4 Pt 1): C1077-1082.
- Watkins, H., C. E. Seidman, J. G. Seidman, H. S. Feng and H. L. Sweeney. (1996). "Expression and functional assessment of a truncated cardiac troponin T that causes hypertrophic cardiomyopathy. Evidence for a dominant negative action." *Journal of Clinical Investigation* 98(11): 2456-2461.
- Watkins, H., D. Conner, L. Thierfelder, J. A. Jarcho, C. MacRae, W. J. McKenna, B. J. Maron, J. G. Seidman and C. E. Seidman. (1995). "Mutations in the cardiac myosin binding protein-C gene on chromosome 11 cause familial hypertrophic cardiomyopathy." *Nature Genetics* 11(4): 434-437.
- Watkins, H., W. J. McKenna, L. Thierfelder, H. J. Suk, R. Anan, A. O'Donoghue, P. Spirito, A. Matsumori, C. S. Moravec, J. G. Seidman and C. E. Seidman. (1995). "Mutations in the genes for cardiac troponin T and alpha-tropomyosin in hypertrophic cardiomyopathy." *New England Journal of Medicine* 332(16): 1058-1064.
- Weber, A. and S. Winicur (1961). "The role of calcium in the superprecipitation of actomyosin." *Journal of Biological Chemistry* 236: 3198-3202.
- Weeds, A. G. and R. S. Taylor (1975). "Separation of subfragment-1 isoenzymes from rabbit skeletal muscle myosin." *Nature* 257(5521): 54-56.
- Whitby, F. G. and G. N. Phillips, Jr. (2000). "Crystal structure of tropomyosin at 7 Angstroms resolution." *Proteins* 38(1): 49-59.
- Wolff, M. R., S. H. Buck, S. W. Stoker, M. L. Greaser and R. M. Mentzer. (1996). "Myofibrillar calcium sensitivity of isometric tension is increased in

human dilated cardiomyopathies: role of altered beta-adrenergically mediated protein phosphorylation." *J Clin Invest* 98(1): 167-176.

Yanaga, F., S. Morimoto and I. Ohtsuki. (1999). "Ca<sup>2+</sup> sensitization and potentiation of the maximum level of myofibrillar ATPase activity caused by mutations of troponin T found in familial hypertrophic cardiomyopathy." *Journal of Biological Chemistry* 274(13): 8806-8812.

Zot, A. S., J. D. Potter and W. L. Strauss. (1987). "Isolation and sequence of a cDNA clone for rabbit fast skeletal muscle troponin C. Homology with calmodulin and parvalbumin." *Journal of Biological Chemistry* 262(32): 15418-15421.